Best

Available

Copy

U.S. DEPARTMENT OF COMMERCE
National Technical Information Service

AD-A024 724

SEAWORTHINESS CHARACTERISTICS OF A SMALL WATERPLANE AREA TWIN HULL (SWATH IV)

PART II

DAVID W. TAYLOR NAVAL SHIP RESEARCH
AND DEVELOPMENT CENTER

MAY 1976

148143

SPD 620-02

DAVID W. TAYLOR
NAVAL SHIP RESEARCH AND DEVELOPMENT CENTER

Bethesda, Maryland 20084

SEAWORTHINESS CHARACTERISTICS OF A SMALL WATERPLANE AREA TWIN HULL (SWATH IV) PART II

by

James A. Kallio

and

Joseph J. Ricci

APPROVED FOR PUBLIC RELEASE: DISTRIBUTION UNLIMITED

SHIP PERFROMANCE DEPARTMENT

The Preliminary Draft of this Report was prepared prior to the Directive on use of the metric system. In the interest of time and economics, no conversion to metric unit has been made.

MAY 1976

SPD 620-02

SEAWORTHINESS CHARACERTISTICS OF A SMALL
WATERPLANE AREA TWIN HULL (SWATH IV) PART II

UNCLASSIFIED

SECURITY CLASSIFICATION OF THIS PAGE (When Data Entered)

REPORT DOCUMENTATION PAGE

READ INSTRUCTIONS BEFORE COMPLETING FORM

1. REPORT NUMBER
SPD 620-02

2. GOVT ACCESSION NO.

3. RECIPIENT'S CATALOG NUMBER

4. TITLE (and Subtitle)
Seaworthiness Characteristics of a Small Waterplane Area Twin Hull (SWATH IV) Part II

5. TYPE OF REPORT & PERIOD COVERED

6. PERFORMING ORG. REPORT NUMBER

7. AUTHOR(s)
James A. Kallio and Joseph J. Ricci

8. CONTRACT OR GRANT NUMBER(s)

9. PERFORMING ORGANIZATION NAME AND ADDRESS
Ship Performance Department
David W. Taylor Naval Ship Research and Development Center

10. PROGRAM ELEMENT, PROJECT, TASK AREA & WORK UNIT NUMBERS

11. CONTROLLING OFFICE NAME AND ADDRESS

12. REPORT DATE
May 1976

13. NUMBER OF PAGES
210

14. MONITORING AGENCY NAME & ADDRESS(if different from Controlling Office)

15. SECURITY CLASS. (of this report)
UNCLASSIFIED

15a. DECLASSIFICATION/DOWNGRADING SCHEDULE

16. DISTRIBUTION STATEMENT (of this Report)
Approved for Public Release: Distribution Unlimited

17. DISTRIBUTION STATEMENT (of the abstract entered in Block 20, if different from Report)

18. SUPPLEMENTARY NOTES

19. KEY WORDS (Continue on reverse side if necessary and identify by block number)
SWATH, Loads, Motions, Waves

20. ABSTRACT (Continue on reverse side if necessary and identify by block number)
Experiments were conducted with a model of a small waterplane area twin hull craft in both the Maneuvering and Seakeeping Facility and Carriage 2 of the David W. Taylor Naval Ship Research and Development Center to determine loads and motions at various headings and speeds. Data were obtained in both regular and random seaways.

DD FORM 1 JAN 73 1473 EDITION OF 1 NOV 65 IS OBSOLETE
S/N 0102-014-6601

UNCLASSIFIED

SECURITY CLASSIFICATION OF THIS PAGE (When Data Entered)

MAJOR DTNSRDC ORGANIZATIONAL COMPONENTS

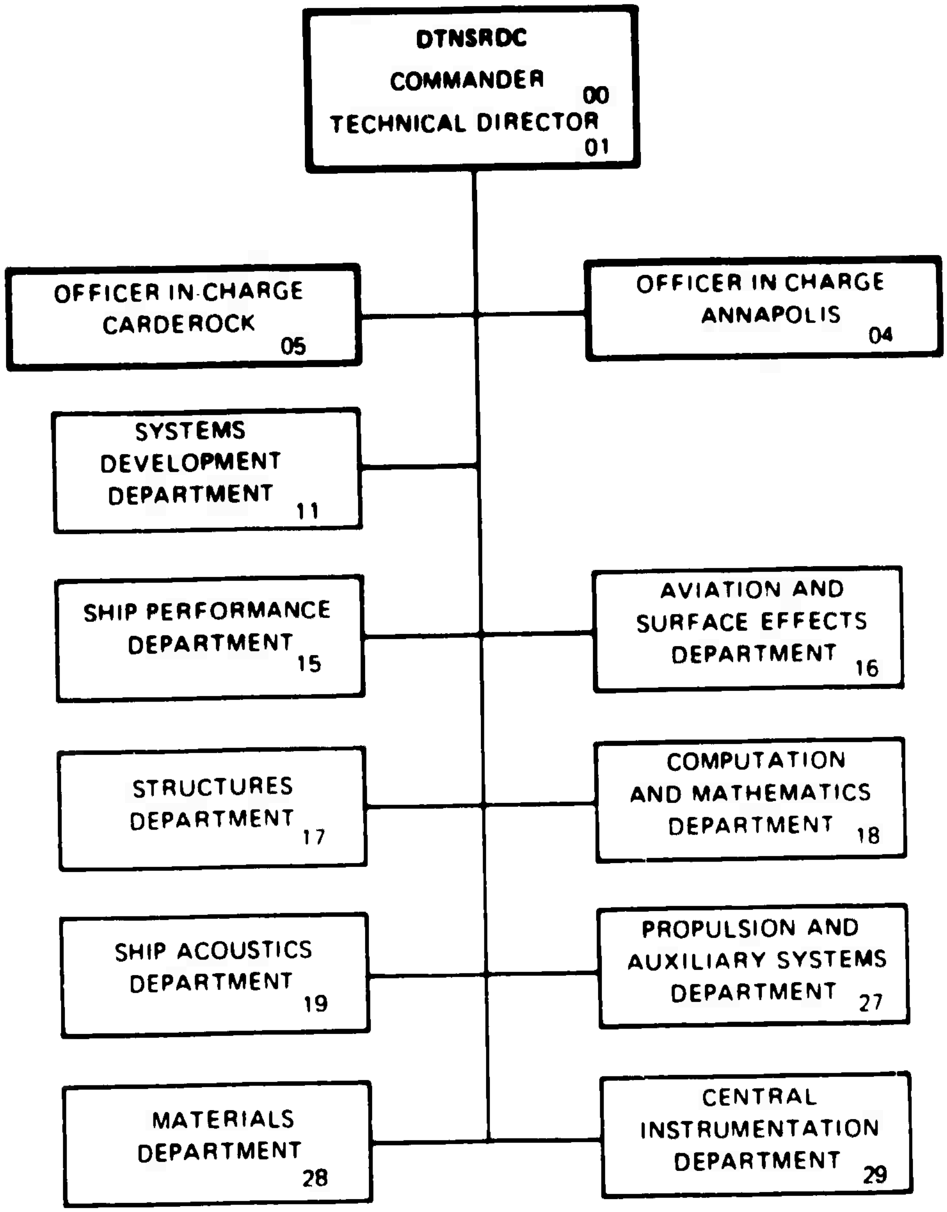

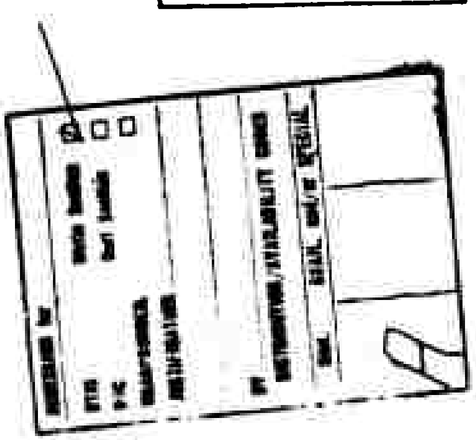

NDW-NSRDC 3960/46 (REV. 8-71)
GPO 888-234

TABLE OF CONTENTS

LIST OF TABLES

LIST OF FIGURES

LIST OF FIGURES (Cont'd)

LIST OF FIGURES (Cont'd)

LIST OF FIGURES (Cont'd)

LIST OF FIGURES (Cont'd)

LIST OF FIGURES (Cont'd)

LIST OF FIGURES (Cont'd)

LIST OF FIGURES (Cont'd)

LIST OF FIGURES (Cont'd)

ABSTRACT

Experiments were conducted with a model of a small waterplane area twin hull craft in both the Manuevering and Seakeeping Facility and Carriage 2 of the David Taylor Model Basin, of the David W. Taylor Naval Ship Research and Development Center (DTNSRDC) to determine motions and loads at various headings and speeds. Data were obtained in both regular and random seaways.

ADMINISTRATIVE INFORMATION

This project was funded by the Systems Development Department Advanced Concepts Office, DTNSRDC, under work unit 1170-026.

INTRODUCTION

An extensive experimental program was conducted on a small waterplane area twin hull craft represented by a 20.4 scale model, DTNSRDC Model 5287, designated as SWATH IV. Experiments were conducted in head, beam, stern quartering and following regular and random seaways at speeds corresponding to full scale speeds of 0, 10, 20 and 32 knots. These experiments were conducted with the model free running, without restraint, in six degrees of freedom (6 DOF). Measurements were made of the seaway, the SWATH IV pitch, heave, roll and relative motion near the bow, as well as absolute vertical motion near the forward and aft strut ends, both port and starboard. In addition, loads on the bridging structure due to relative hull motions were measured by means of an instrumented flexure. Pressures due to wave impacting were also measured at various locations along the bridging structure between the two hulls. Investigations were made of the effect of draft on the motions, loads and impact pressures at various headings and speeds; the effect of transverse metacentric height ($\overline{GM}_t$) in beam seas; and the effect of various appendages in head and following seas at the heaviest displacement. Figure 1 presents the matrix of SWATH IV configurations investigated.

This report presents results of all experiments conducted on the SWATH IV model and is an extension of the work reported in Reference 1*.

---

*References are listed on page 35.

DESCRIPTION OF MODEL AND TEST EQUIPMENT

The model used in this investigation is the same model used to evaluate the cambered-hull effect on resistance and propulsion of a SWATH type craft reported in Reference 2. Abberviated body lines and plans are presented in Figures 2 and 3. Since propeller diameter did not markedly affect craft performance in the study of Reference 2, and since propellers 3217 and 3218 were readily available, they were used during the present series of experiments.

Propulsion was provided by two five horsepower D.C. motors, one housed in each hull. The two hulls were connected by a combination of block gages and flexure beams equipped with strain gages to permit measurement of moments and forces on the bridging structure.

These were attached to the hulls above the struts at approximately Stations 6 and 14. A plywood bridging structure, split down the centerline, was also attached to the model at the location shown in Figure 4. Diaphram type pressure transducers were distributed along the length and on the bow section of this structure, in accordance with Figure 5, in order to measure impact pressures. No attempt was made to scale the rigidity of this structure. Since the model was free running, controllable rudders were necessay to maintain course. Figure 4 shows the location and size of these rudders. Each rudder was controlled by a steering servo located on its particular hull. In an attempt to improve ship motions and maintain vertical plane stability (pitch) for some conditions, a variety of appendages was attached either to the lower hulls or struts during the experiments.

For example, during calm water experiments at the 32 ft draft, bare hull condition it was found that vertical plane instability existed somewhere between 20 and 32 knots full scale. Therefore, a fixed horizontal fin was attached inboard at the stern of each hull to provide stabilization for the 32 ft draft, 32 knot condition. Figures 6 and 7 indicate the location, size and shape of the fins used.

Once the bare hull configuration responses were characterized, certain other appendages were added in an attempt to improve the ship motions at the 32 ft draft. Heave "blisters" were installed at the location shown in Figure 8. These consisted of molded fiberglass bolt-on sections attached both inboard and outboard on each strut above the waterline. These blisters were constructed such that they doubled the strut thickness over the nominal at a given longitudinai position in an effort to introduce some heave damping. Since the blisters were located at the 36 ft waterline and above, they were only effective in wave conditions where height of the wave profile exceeded 36 feet.

In an effort to introduce additional heave damping, 4 ft by 102 ft bilge keels were added both inboard and outboard at 9 feet above the base line on each hull at the longitudinal location shown in Figure 9.

Table 1 presents SWATH IV ship particulars for the 28, 30 and 32 ft draft bare hull configurations while Table 2 presents SWATH IV ship particulars for all hull configurations investigated

DESCRIPTION OF MEASUREMENTS AND INSTRUMENTATION

As mentioned previously, the SWATH IV experiments were conducted with the model self propelled and free running, without restraint, in all six degrees of freedom. Tethering lines, required for acceleration and deceleration of the model, and motor power cables and transducer signal cables were the only connections between the model and carriage. These lines and cables were slack during data collection and did not affect model responses.

Model speed was controlled manually and was regulated in accordance with preset carriage speed. Thus the model was kept fairly stationary with respect to the carriage and model speed was relatively constant. However, during some head sea conditions with severe impacting, and during some following sea conditions there was considerable surge motion.

Course was maintained by means of yaw and sway signal inputs to rudder servo control devices on each hull. Since mechanical rudder coupling and different servo characteristics could affect the relative force measurements between the two hull, the rudder servos were electronically coupled to ensure nearly identical rudder motions. Heave, surge and relative motion at the bow as well as wave height were measured by ultrasonic displacement transducers. Heave was measured at Station 10 on the centerline, surge near Station 19 on the centerline and relative bow motion 1.5 ft (full scale) aft of Station 0 on the centerline.

Pitch, roll and yaw were measured by vertical gyroscopes mounted near Station 10 on the bridging structure. Absolute vertical motions at the bow and stern were measured with vertical accelerometers at Station 4 (port and starboard) and Station 16, (port and starboard), respectively.

The only mechanical connection between the two hulls was a combination of modular force gages and flexured, strain gaged beams. Sufficient space was left between the two halves of the wood bridging structure to permit the hulls to move relative to each other without debasing the measurement of forces and moments between the hulls. This block gage-beam arrangement enabled the measurement of six loads used to calculate the five relative forces and moments due to relative motions between the hulls. These assemblies were centered about the centerline and 112 ft (full-scale) aft of the FP (near the LCG). The neutral axis of the bending moment flexure was 60.6 ft above the base line. The following are the five relative forces and moments derived from block gage-beam assemblies:

Transverse Vertical Bending Moment: the moment that tends to produce relative roll between hulls

Torsional Moment: the moment that tends to produce relative pitch between hulls

Yawing Moment: the moment that tends to produce relative yaw between hulls

Vertical Shear Force: the force that tends to produce relative heave between hulls

Transverse Force: the force that tends to produce relative sway between hulls

Although the bridging structure did not necessarily represent that of a prototype, it did provide a means of determining the order of magnitude of impact pressure which a prototype might experience in various seaways. No attempt was made to scale the bridging structure to simulate the vibratory characteristics of a prototype. Impact pressures on this structure were measured by strain-gaged diaphragm type pressure transducers located as shown in Figure 5. These gages, designed and manufactured at DTNSRDC, were rated at 0 to 15 psi with a flat response to 1500 hz and a natural frequency of at least 25,000 hz, and thus were more than adequate to measure the impacting phenomena.

EXPERIMENTAL PROCEDURE

The basic goals of this experimental investigation were to first characterize both calm water and seaway responses of the SWATH IV bare hull configuration at the 28, 30 and 32 ft drafts and then to add appendages as necessary to try to improve motion responses. A limited number of experiments was also conducted to determine the effect of transverse metacentric height on the transverse vertical bending moment. For each of the three drafts listed in Table 1, a series of calm water runs was made to determine running trim, sinkage and natural periods of pitch, heave and roll at the various speeds. Trim moments were produced by moving ballast in order to maintain an approximate zero running trim in calm water at both the 20 and 32 knot speeds. The model maintained fairly even keel trim at 10 knots for all three bare hull draft conditions so no shift in ballast was required from the zero speed, zero trim condition.

Once the trim moments were established, calm water runs were conducted during which the model was force pulsed manually near its natural frequency in either pitch, heave or roll at the various speeds in order to determine motion decay curves and natural periods. In many cases at 20 and 32 knot speeds, the motion was so highly damped that the determination of the natural heave and pitch periods was difficult or impossible by this means.

Experiments were then conducted in regular and long crested irregular waves at the various headings and speeds for the 28, 30 and 32 ft draft bare hull conditions (See Figure 1). Nominal wave steepness ($2\zeta_A/\lambda$) ranged from about 1/60 to 1/100 during these experiments. However, some motions became quite severe at the longer wave lengths due to the large natural periods of motions. In these cases the steepnesses were decreased to around 1/130 to prevent swamping of the model. In addition, some experiments were conducted in near synchronous wave conditions at several steepnesses in order to provide a linearity check on the motions.

Irregular wave experiments were also conducted at various headings and speeds in order to obtain statistical data on motions, loads and frequency of impacting on the bridging structure. For each condition about 150 samples of peak-to-peak motions were obtained since experience has shown that realistic inferences about the population may be made from this sample size. However, not all sample sizes in some following sea conditions were this large. The Sea States 4, 5, and 6 indicated in Figure 1 correspond to fully developed seas with significant wave heights of 7, 10 and 15 ft respectively.

A limited number of experiments was conducted in both regular and random beam seas at the 28 ft draft with two different $\overline{GM}_t$'s and at the 32 ft draft, to determine the effect of $\overline{GM}_t$ and draft on roll motion and transverse vertical bending moment. Investigations of the effects of motion damping devices were carried out with the 32 ft draft configuration. Calm water experiments for the 32 ft draft bare hull configuration indicated vertical plane (pitch) instability existed somewhere between 20 and 32 knots because the model would not accelerate up to 32 knots and maintain a near zero running trim. The horizontal stabilizer fin, described earlier, was therefore attached inboard at the stern on each hull. Calm water bare hull trim moments due to shifting ballast were maintained and calm water running trim was adjusted to near zero by chaning the fin angle of attack. (In other words, ballast weight trim moment was held constant throughout these investigations). Experiments in only regular and in random head and following seas were conducted with these fins. One condition was investigated with a smaller fin in head regular and random seas only.

Heave blisters were investigated in calm water and in head and following regular and random waves. The damping effects of bilge keels were obtained in calm water and in head regular and random waves only. As seen in Table 2, the nominal calm water ballast trim moment for 20 knots had to be increased in order to acquire a zero running trim for the conditions with bilge keels.

DATA COLLECTION AND REDUCTION

During the experiments, the transducer signals were amplified and recorded in analog form on paper strip chart (including an oscillograph for impacts) and analog magnetic tape. The system for measuring impacts provided a flat response to 1500 hz, which is more than adequate for the phenomena studied. The analog tape data were digitized and then analyzed by the CDC 6400 computer program.

Calm water running trim, sinkage and natural period oscillation data were read from strip chart records.

Reduction of regular wave data produced Fourier transform coefficients for the fundamental frequency of the wave height signal and corresponding coefficients of the other signals. Mean offsets, amplitudes and phases for each of the signals were then determined. Phases were calculated relative to the wave as it passed the nominal LCG of the model (112 ft aft of the forward strut edge), with a positive phase defining the response leading the wave. Mean offsets of surge and sway signals were used to correct for model surge and sway away from its zero position relative to the fixed wave height probe.

Data obtained in random waves were analyzed in both the time and frequency domains. This analysis yields mean values, power spectra, histograms and Fourier transforms as well as statistical information about the time histories. Only significant double amplitudes, the average of the one-third highest peak-to-peak fluctuations, are presented in this report. Impact pressure data obtained in random waves was extracted manually from strip chart records. Absolute motion spectra for bow (port and starboard) and stern (port and starboard) motions were obtained by integrating the acceleration spectra at these respective locations.

PRESENTATION AND DISCUSSION OF RESULTS

Due to the large volume of data and the numerous variations in model configurations, the data in this report is presented in segments as shown below:

Regular Waves - Bare Hull, 28 ft Draft

Regular Waves - Bare Hull, 30 ft Draft

Regular Waves - Bare Hull, 32 ft Draft

Random Waves - Bare Hull

Regular Waves - $\overline{GM}_t$ Effect in Beam Seas, 28 ft Draft

Regular Waves - Large $\overline{GM}_t$, 28 ft Draft

Regular Head Seas - Hull with Appendages, 32 ft Draft

Regular Following Seas - Hull with Appendages, 32 ft Draft

Random Waves - Hull with Appendages, 32 ft Draft

The results of calm water experiments are presented in tabular form in Table 2. This table indicates the amount of trim moment needed for zero running trim for each particular speed and model configuration.

For the configurations with fins the fin angle indicated is the angle of attack on the fin necessary to give near zero running trim (positive fin angle means leading edge up). Natural periods derived from calm water oscillation experiments are shown in the last three columns.

The regular wave data in this report are presented as a function of wave length to ship length ratio, λ/L, and the motions and loads are nondimensionalized in accordance with the scheme shown in Table 3, as requested by the sponsor. The observations made during the discussion of regular wave data refer to the maximum dimensionless response and not to the response to any particular wave length. Phases are also presented but not discussed.

REGULAR WAVES - BARE HULL, 28 ft DRAFT

Figures 10 through 35 present results in dimensionless form of experiments in regular waves for the 28 ft draft, nominal $\overline{GM}_t$ craft configuration at various speeds and headings. It is necessary to indicate that since the model for this experiment possessed a bridging structure, impacting did occur during some experiments in near synchronous wave conditions. This is important because the magnitude of the motions at these conditions may have been attenuated by the bridging structure impacting the wave.

There is little speed effect at the 28 ft draft on maximum dimensionless heave amplitude in head seas (Figure 10). In beam seas, heave is largest at 0 knots and decreases as speed increases to 10 knots, with little speed effect above 10 knots. In stern and following seas, heave is largest at 0 knots and decreases as speed increases to 10 knots. There is no stern or following sea data above 10 knots.

There is little heading effect on maximum dimensionless heave amplitude at 0 knots. At 10 knots heave decreases as heading is changed from head to beam seas, with little heading effect as heading changes from beam to stern and stern to following seas. At 20 and 32 knots, heave is largest in head seas and decreases as heading changes to beam seas.

Dimensionless relative bow motion amplitude (Figure 12) varies only slightly with speed up to 32 knots in head seas, and in stern and following seas there is virtually no variation up to 10 knots, the maximum speed for which data was obtained at these headings. In beam seas, relative bow motion is largest at 0 knots and decreases as speed increases to 10 knots, with little speed effect above 10 knots. At 0 knots, relative bow motion is about the same in head and beam seas and decreases as heading changes to stern and following seas. At 10 knots, heave is largest in head seas, minimum in beam seas and about the same in both stern and following seas. At 20 and 32 knots relative bow motion decreases as heading changes from head to beam seas.

Figure 14 shows that in head seas pitching motion decreases as speed increases from zero to 10 knots, but increases again as speed increases from 10 to 32 knots where it is about the same order of magnitude as at zero speed. There is little pitching motion at any speed in beam seas. In both stern and following seas pitch motion decreases as speed increases from 0 to 10 knots. There is no data in quartering and following seas at 20 and 32 knots. At 0 and 10 knots, pitch motion decreases as heading changes from head to beam but increases as heading changes from beam to quartering and from quartering to following seas. Note that at 0 and 10 knots pitch is about the same in following and head seas. At 20 and 32 knots, pitch motion decreases as heading changes from head to beam seas.

Figure 16 shows little roll motion in head and following seas at any of the speeds examined. In beam seas roll motion decreases as speed increases from 0 to 10 knots, with little speed effect above 10 knots. In stern quartering seas roll motion data is insufficient to draw conclusions. At 0 knots, the largest roll motion occurs in beam seas while at 10 knots roll motion is largest in stern quartering seas. At 20 and 32 knots roll motion increases as heading changes from head to beam seas. There is no data at 20 and 32 knots in quartering and following seas.

Dimensionless absolute motions near the bow (Figures 18 and 20) increases slightly in magnitude as speed increases up to 20 and 32 knots in head seas. In beam seas the largest absolute bow motion occurs at zero speed. For the underway speeds they are approximately the same. There is no data for 20 and 32 knots in quartering and following seas. At 0 knots there is little heading effect on the maximum magnitude of absolute bow motion. At 10 knots absolute bow motion is largest in head seas and decreases as the heading becomes beam seas. At 10 knots, the maximum absolute bow motion is generally about the same in beam, quartering and following seas for a particular hull. At both 20 and 32 knots, absolute bow motion is largest in head seas and decreases as the heading becomes beam seas.

Dimensionless absolute motion near the stern (Figures 22 and 24) varies only slightly in magnitude with speed in head seas. In beam, quartering and following seas, absolute stern motion decreases as speed increases from 0 to 10 knots. In beam seas the absolute stern motion varies little as speed increases from 10 to 32 knots. There is no data at 20 and 32 knots in quartering and following seas. At 0 knots, there is little heading effect on maximum absolute stern motion. At 10 knots the maximum absolute stern motion is generally about the same in beam, quartering and following seas for a particular hull. At both 20 and 32 knots, absolute stern motion is largest in head seas and decreases as heading becomes beam seas.

In general, absolute motions near the stern (Figures 22 and 24) are larger than those near the bow (Figures 18 and 20) for corresponding speeds and headings. Also note that motion of the starboard hull is larger than that of the port hull in beam seas at 10 and 20 knots and in quartering seas at 10 knots. This would suggest that the roll axis is not on the centerline but to the port of the centerline. Recent experiments on a 2900 ton developmental SWATH design, along with motion pictures of the experiments, bear this out.

Figure 26 which presents dimensionless transverse force at various speeds and headings, shows there is little speed effect on maximum magnitude in head seas; at 10 thru 32 knots there is only a slight increase in magnitude over the zero knot condition. In beam seas the transverse force is largest at 10 knots and about the same magnitude at 0, 20 and 32 knots. There is very little speed effect in quartering seas up to 10 knots. In following seas side force is largest, through still small, at 10 knots. There is no data for 20 and 32 knots in quartering and following seas. At 0 and 10 knots the transverse force is largest in quartering seas and in beam seas still significantly larger than at the other headings. At 20 and 32 knots the magnitude of the side force is about the same in head and beam seas.

Dimensionless vertical shear force, presented in Figure 28, in head seas is very small at all speeds. In beam seas the vertical shear force is largest at 0 knots and remains about the same for 10 through 32 knots. In quartering seas, the vertical shear force increases from 0 to 10 knots. There is virtually no speed effect on vertical shear force in following seas up to 10 knots. There is no data in quartering and following seas at 20 and 32 knots. At 0 knots, vertical shear force is largest in beam seas and very small at the other headings. At 10 knots vertical shear is very small in head and following seas and about the same in beam and quartering seas. At 20 and 32 knots, the vertical shear is largest in beam seas.

Nondimensional transverse bending moment, presented in Figure 30, is very small in head seas up to 20 knots and increases slightly as speed increases to 32 knots. In beam seas transverse vertical bending moment decreases as speed increases from 0 to 10 knots and increases again at 20 and 32 knots. In quartering seas, bending moment decreases as speed increases from 0 to 10 knots. In following seas, bending moment is very small at 0 and 10 knots. There is no data at 20 and 32 knots for quartering and following seas. At 0 and 10 knots, bending moment is slightly larger in quartering seas than in beam seas and is very small in head and following seas. At 20 and 32 knots, bending moment is much larger in beam seas than in head seas.

Dimensionless torsional moment, Figure 32, is very small in head seas up through 20 knots and increases as speed increases from 20 to 32 knots. In beam seas, the torsional moment is very small throughout the speed range. In quartering seas, torsional moment increases slightly as speed increases from 0 to 10 knots. In following seas, torsional moment is very small at both 0 and 10 knots. There is no data in quartering and following seas at 20 and 32 knots. At 0 and 10 knots, torsional moment is very small at all headings except quartering seas where it is fairly large. At 20 knots torsional moment is small in both head and beam seas. At 32 knots, the torsional moment is considerably larger in head seas than in beam seas.

Dimensionless yaw moment, Figure 34, is negligible for all speeds in head and following seas. The yaw moment in beam and quartering seas is about the same for all speeds. There is no data in quartering and following seas at 20 and 32 knots. At 0 and 10 knots, the yaw moment is about the same in beam and quartering seas and larger than in head and following seas. At 20 and 32 knots, yaw moment is much larger in beam seas than in head seas.

It should be noted here that the large side forces (Figure 26), vertical shear forces (Figure 28), transverse bending moment (Figure 30), and torsional moment (Figure 32) depicted by some of the data spots in head seas at 32 knots may be due to wave impacting on the bridging structure.

REGULAR WAVES - BARE HULL, 30 ft DRAFT

Figures 36 and 37 present results of experiments in regular head seas at 20 knots for the 30 ft draft, nominal $\overline{GM}_t$ craft configuration. Figure 36 shows dimensionless absolute motions near the bow and stern, both port and starboard. Absolute motions near the stern (Station 16) are larger than those near the bow (Station 4) as was the case at the 28 ft draft.

Figure 37 presents yaw, torsional and transverse bending moments and transverse and vertical shear forces.

REGULAR WAVES - BARE HULL, NOMINAL $\overline{GM}_t$, 32 ft DRAFT

Figures 38 through 63 present motions and loads and their phases obtained during experiments in regular waves at speeds of 0, 10 and 20 knots in head, beam and following seas for the 32 ft draft, bare hull, nominal $\overline{GM}_t$ craft configuration.

In Figure 38, which presents dimensionless heave motions, the limited amount of data in head seas suggests that heave motion follows the trend at the 28 ft draft (Figure 10). In beam seas there is insufficient data to form conclusions. In following seas heave is largest at 0 knots and decreases as speed increases to 20 knots. For all speeds the trends observed at the 28 ft draft concerning heading effect on heave motion appear to be the same at the 32 ft draft. There is no beam sea data at 20 knots.

Nondimensional relative bow motion magnitude for the 32 ft draft presented in Figure 40, generally follows the same trend observed at the 28 ft draft (Figure 12) in terms of speed and heading effect. In following seas there is a significant increase in maximum relative bow motion as speed increases from 0 to 20 knots. At 20 knots relative bow motion appears to be larger in following than in head seas.

Dimensionless pitch and roll motion at the 32 ft draft presented in Figures 42 and 44, although sparse in head and beam seas, seems to follow the trends observed at the 28 ft draft.

Dimensionless absolute motions near the bow and stern for the 32 ft draft presented in Figures 46 to 52, appear to follow the trends observed at the 28 ft draft (Figures 18 - 24). Note that in following seas the magnitude of the absolute stern motion decreases significantly as speed increases from 0 to 20 knots (Figures 50 and 52).

Dimensionless moments and forces at the 32 ft draft, presented in Figures 54 - 62 appear to follow the trends observed at the 28 ft draft with one exception. Figure 30 indicates that in beam seas at the 28 ft draft the transverse vertical bending moment decreases as speed increases from 0 to 10 knots and Figure 58 shows that this may not be the case at the 32 ft draft.

Figure 64 presents results of linearity experiments in regular waves for both the 28 and 32 ft draft bare hull configurations. These experiments were conducted with the regular wave length near heave synchronism for the particular speed. Figure 64a shows dimensionless pitch, heave and relative bow motion results from experiments in head seas at various speeds. Generally, the motion responses remain linear with wave height for pitch and relative bow motion at all speeds and for heave only at 0 knots.

Figure 64b, which presents results of linearity experiments for the 28 and 32 ft draft bare hull configurations at zero speed in following seas, indicatesthat nondimensional motion responses are nonlinear except for pitch at the 28 ft draft.

RANDOM WAVES - BARE HULL

A discussion on the applicatility of using a finite number of random sea spectral formulations which can be generated in a tank to predict motion responses in the "real ocean" is appropriate at this time.

Figure 65 presents wave height spectra for Sea States 4, 5 and 6 generated during experiments on SWATH IV. They may not exactly duplicate theorectical Pierson-Moskowitz idealized spectra; they are, however, realistic and do contain sufficient energy in the frequency range to excite the present model and elicit motion responses.

Since a craft may be required to operate in a wide range of ocean environments, caution must be exercised in using responses determined from experiments in a finite number of wave spectral formulations (as is the case for random seas generated in a tank). To establish design criteria, the responses should be examined in various seas which the craft will encounter during its lifetime. Since it is physically impossible to generate all these spectra in a tank, the following approach is taken: Establish the response amplitude operator [defined as $(\text{motion amplitude}/\text{wave amplitude})^2$] either by analytical means or by experiments in regular or random waves and predict the responses in any desired sea condition. A basic assumption underlying this prediction technique is that the craft behaves as a linear system. Also, if it is desired to predict statistics such as significant values or most probable maxima, the probability density function governing the phenomenon must be known or established.

In general, it is not sufficient to represent a seaway by designating its average wave height alone. There could be many sea conditions with the same statistical average wave height and yet have quite different spectral density (energy) distribution with respect to wave frequency. If a craft has small inherent damping such as SWATH ships have, the motion amplitude would be large when the craft is excited at or near its resonant frequency. Assume two sea conditions with identical significant wave heights but considerably different spectra density distributions such that seaway A (as shown below), has its peak energy near the craft natural frequency while seaway B has its maximum energy displaced from the craft natural frequency.

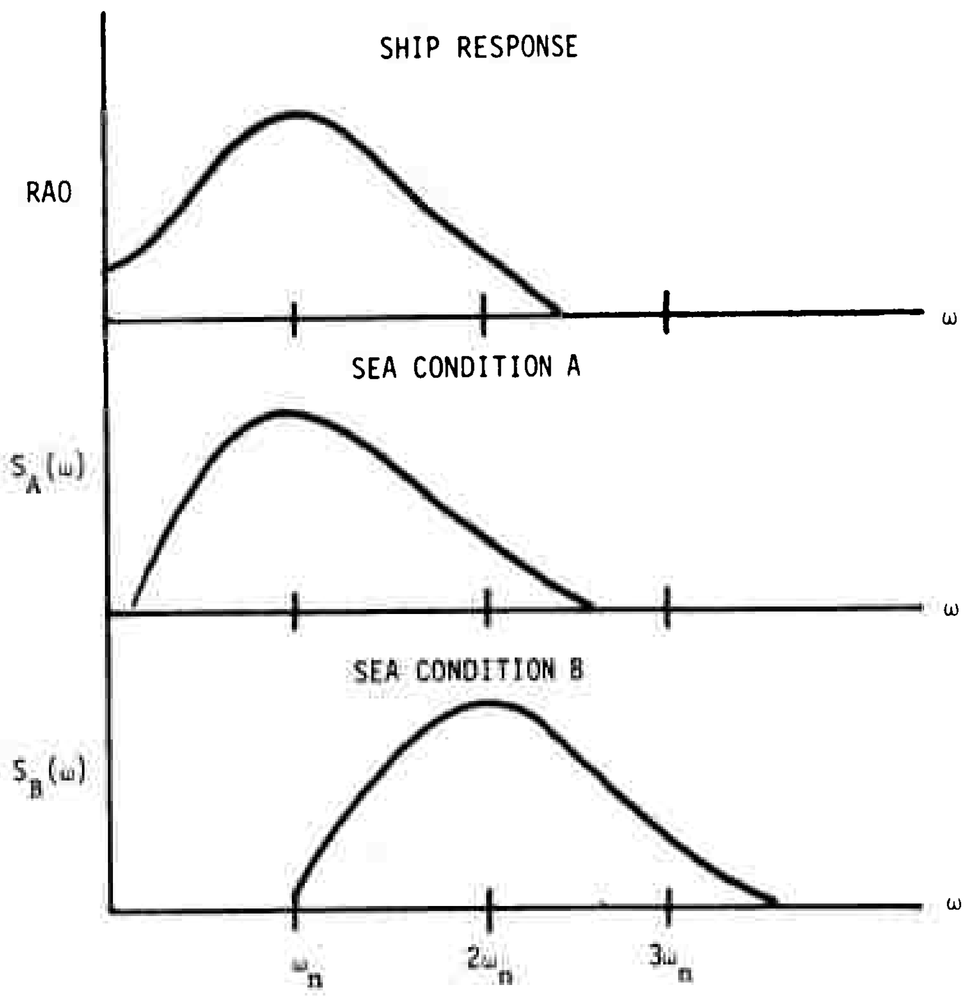

Here we have

$$\int_0^\infty S_A(\omega)\, d\omega = \int_0^\infty S_B(\omega)\, d\omega$$

but

$$E_A >> E_B$$

where $E_A = \int_0^\infty RAO(\omega) \quad S_A(\omega) d\omega$ and $E_B = \int_0^\infty RAO(\omega) \quad S_B(\omega) d\omega$

The significant motion amplitude, $M_{1/3}$, assuming a Rayleigh distribution function, is obtained by

$$(M_{1/3})_A = 2\sqrt{E_A} >> (M_{1/3})_B = 2\sqrt{E_B}$$

which clearly demonstrates that the craft would experience larger significant motions in sea condition A than in sea condition B.

In the present case, the principle of linear superposition was applied to experimentally-obtained RAO's and utilized in conjunction with 305 available ocean spectra measured at Station India in the North Atlantic Ocean. The assumptions were made that the SWATH craft behaved as a linear system and that the probability density function of the peak-to-peak excursions followed a Rayleigh probability distribution law. The calculated responses were then compared to those obtained from experiments conducted in tank generated waves.

Regular wave data obtained during experiments on the 28 ft draft bare hull and the 32 ft draft with large fins craft configurations were used to demonstrate motion prediction techniques in random waves (See Figures 65A and 65B). The results shown in the cross symbols in Figures 65A and 65B were obtained in the following manner:

Significant heave or relative bow motion (RBM) amplitude

$$= 2.0 \sqrt{\int_0^\infty R(\omega) \quad S(\omega) d\omega}$$

where

$R(\omega)$ = response amplitude operator

$$= \left[\frac{\text{Heave (or RBM Amplitude)}}{\text{Wave Amplitude}}\right]^2$$

$S(\omega)$ = wave spectrum from Station India[2]

ω = wave frequency, rad/sec

The solid lines in the figures are obtained by using the Pierson-Moskowitz spectra:

$$S(\omega) = \frac{A}{\omega^5} \quad e^{(-\frac{B}{\omega^4})}$$

where $A = 0.0081(g)^2$ (g = gravitational acceleration)

$B = 33.56/(h_{1/3})^2$

$h_{1/3}$ = significant wave height in feet

It is seen in Figure 65A that the experimentally obtained values of significant heave and relative bow motion lie at the upper limit of the data calculated using the Station India wave spectra. This is because the sea spectra chosen for the model experiments (Figure 65) has maximum energy in a frequency range near the heave natural frequency.

Data presented in Figure 65B show results of experiments and calculations for the 32 ft draft configuration with large fins. These data show that experimental results obtained in the random tank generated waves agree quite well with results calculated using the Station India spectra. The reason that the motions for the large fin case are not as large as the bare hull case should be due to the difference in the frequency distribution of the RAO's compared to the bare hull case. The difference in heave and pitch natural frequencies of the craft as well as the peak motion amplitudes and the shape of the RAO's all contributed to this effect.

It is clear from these two figures that the motion data obtained from the random wave experiments should be used as a general qualitative measure of the motion magnitude experienced by a craft in a seaway of a given significant wave height, but not necessarily a representative average for any sea condition having the same significant wave height. The main objective of the random wave experiments should be rather to check the linearity assumption utilized to obtain the statistics of motion amplitudes the craft experiences in random seaways.

Figures 66 through 76 present results of experiments in random waves for 28, 30 and 32 ft. draft bare hull craft configurations at various speeds and headings. Data are presented in terms of significant double amplitudes (average of 1/3 highest peak to peak values) of motions and loads as a function of significant wave height.

Figure 66 presents significant double amplitudes of heave and relative bow motions. In general, heave and relative bow motion tend to be linear with significant wave height up to about 20 ft. Where there is sufficient data, it also appears there is little or no draft effect on heave or relative bow motions. For a given speed, heave and relative bow motion tend to be larger in head seas than at other headings.

Significant double amplitudes of pitch and roll, presented in Figure 67, appear fairly linear with wave height up to about 20 ft. There is very little speed effect on pitch in head seas while in following seas pitch is largest at 10 knots. In head seas pitch motion is lowest for the 30 ft draft at 10 and 32 knots. At 10 and 20 knots for the 32 ft draft pitch motion is significantly larger in following than in head seas.

Figure 67 also presents significant double amplitudes of roll motion. The large roll indicated by data points in head and following seas is probably rudder induced. In beam seas roll is very large at 0 knots and decreases as speed increases to 10 knots for both the 28 ft and 32 ft drafts. There appears to be no draft effect on roll motion in beam seas.

Figure 68 presents significant double amplitudes of absolute motion near the bow. At all headings there is little speed effect on the absolute bow motion. There is very little draft effect on absolute motion at any heading or speed. For a given speed the absolute bow motions are generally about the same for all headings.

Figure 69 presents significant double amplitudes of absolute motion near the stern. In head seas the absolute stern motion increases with speed and is largest at 20 and 32 knots, although at 32 knots the stern motion is somewhat smaller for the 30 ft draft in a given sea state. In beam seas the stern motion is largest at zero speed. In following seas there is little speed effect on stern motion. Throughout the speed range investigated the stern motion is largest in head seas.

Figure 70, which presents significant double amplitude of side force, shows that there is very little speed or draft effect on side force in either head or following seas. In beam seas the transverse force is largest at 10 knots. In beam seas there is no appreciable draft effect on transverse force. At zero and 20 knots the effect of heading on transverse force is very small while at 10 knots the transverse force is much larger in beam seas than in either head or following seas.

Figure 71 presents significant double amplitudes of vertical shear forces. For the various speeds and headings there is very little draft effect on vertical shear force. At all headings there is no appreciable speed effect on vertical shear force. For all drafts and speeds the vertical shear force is much larger in beam seas than in either head or following seas while the difference in head and following seas is small.

Figure 72 presents significant double amplitudes of transverse vertical bending moment. In both head and following seas there is no draft or speed effect on transverse bending moment. In beam seas the transverse bending moment for both drafts decreases as speed increases. Throughout the speed range investigated, the transverse bending moment is about the same magnitude in both head and following seas while it is very much larger in beam seas than in either head or following seas.

Figure 73 presents significant double amplitudes of torsional moment. There appears to be little draft or speed effect while for a given speed torsional moment appears to be smaller in following seas than in head or beam seas.

The large torsional moments in head seas are probably due to bow impact at the higher wave heights. In following seas the large excursions in surge and the large torsional moments indicated by the data are due to the craft being restrained by restraining ropes.

Figure 74 presents significant double amplitudes of yaw moment. In both head and following seas there is no effect of draft or speed on yaw moment. In beam seas the available data indicates the yaw moment may be slightly lower at 20 knots than at the other two speeds. For all speeds the yaw moment is significantly higher in beam seas than in either head or following seas.

Figures 75 and 76 present impact pressure data obtained during experiments at the 32 ft draft bare hull configuration in a following Sea State 6 at 10 knots. These figures indicate that the stern experienced the greatest frequency and severest impact (see Figure 75 Gage #8). Note however (Figure 76), that for about 80% of the impacts on gage 8 the pressure magnitude was less than 5 psi while on gage 1 about 40% of the impacts had pressure magnitudes between 5 and 10 psi. It is pointed out however, that the sample sizes are somewhat small and experience has shown that for cases when the sample size of impact pressures is less than about 50, caution should be used in drawing conclusions from the data.

REGULAR WAVES - $\overline{GM}_t$ EFFECT IN BEAM SEAS, 28 ft DRAFT

Figures 77 through 85 present dimensionless motion and force data obtained during experiments in regular beam seas for the 28 ft draft bare hull craft configuration with both nominal and large $\overline{GM}_t$.

Figures 77 and 81 indicate that the craft with the larger $\overline{GM}_t$ experiences smaller roll at both 0 and 10 knots. These figures also show that heave, relative bow motion and roll decrease significantly as the speed increases from 0 to 10 knots.

Figures 79 and 81, which present dimensionless absolute motions near the bow and stern, indicate that the craft with the larger $\overline{GM}_t$ has about the same absolute motion as the craft with nominal $\overline{GM}_t$ at 0 and 10 knots. Absolute bow and stern motions decrease as speed increases from 0 to 10 knots for both $\overline{GM}_t$ craft configurations.

Figures 83 and 85 present dimensionless forces and moments for the craft with nominal and large $\overline{GM}_t$ respectively. There is no $\overline{GM}_t$ effect on transverse force at either 0 or 10 knots.

The vertical shear force for both $\overline{GM}_t$ craft configuration decreases with speed from zero to 10 knots. There is no $\overline{GM}_t$ effect on either yaw or torsional moment at 0 or 10 knots. Transverse vertical bending moment for the craft with nominal $\overline{GM}_t$ decreases as speed increases from 0 to 10 knots while it remains about the same at 0 and 10 knots for the craft with large $\overline{GM}_t$.

REGULAR WAVES - LARGE $\overline{GM}_t$, 28 ft DRAFT

Figures 86 through 111 present results of experiments conducted in beam and quartering regular waves with the 28 ft draft, bare hull, large $\overline{GM}_t$ craft configuration.

Figure 86, which presents nondimensional heave, shows that heave decreases as speed increases from 0 to 10 knots in both beam and quartering seas. There is little effect on heave for either 0 or 10 knots as bending is changed for quartering to beam seas. Heave for the craft with large $\overline{GM}_t$ is about the same as for the craft with nominal $\overline{GM}_t$ at 0 and 10 knots in bean and quartering seas (See Figure 10).

Figure 88 presents dimensionless relative bow motion and shows a decrease in motion as speed increases from 0 to 10 knots in both beam and quartering seas. It also shows that relative bow motion is about the same for both heading at both 0 and 10 knots. The craft with large $\overline{GM}_t$ experiences less severe relative bow motion than the craft with nominal $\overline{GM}_t$ in beam seas at 0 knots and in quartering seas at 0 and 10 knots (see Figure 12).

Figure 90 presents nondimensional pitch and shows no speed effect on pitch motion in beam seas while pitch decreases as speed increases from 0 to 10 knots in quartering seas. Pitch is more severe in quartering than in beam seas at either 0 or 10 knots. The craft with large $\overline{GM}_t$ experiences larger pitch motion than the craft with nominal $\overline{GM}_t$ only at 0 knots in quartering seas (See Figure 14).

Figure 92, which presents dimensionless roll, shows that roll motion decreases as speed increases from 0 to 10 knots in beam seas, but is about the same for the two speeds in quartering seas. At zero knots roll is about the same in both beam and quartering seas while at 10 knots roll in beam seas is much less than in quartering seas. The craft with large $\overline{GM}_t$ experiences less severe roll in beam seas than does the craft with nominal $\overline{GM}_t$ at both 0 and 10 knots. In quartering seas the craft with large $\overline{GM}_t$ experiences larger motions at 0 knots than the craft with nominal $\overline{GM}_t$ (see Figure 16).

Figures 94 through 101 present dimensionless absolute motions of both hulls near the bow and stern in regular beam and quartering seas. These figures show that absolute motions decrease as speed increases from 0 to 10 knots in beam seas while in quartering seas there is little speed effect. Also, there is very little heading effect on maximum absolute motion at 0 or 10 knots in beam and quartering seas. The craft with large $\overline{GM}_t$ experiences less severe motions than does the craft with nominal $\overline{GM}_t$ in beam and quartering seas at 0 knots (see Figures 18 through 25).

Figure 102 presents dimensionless transverse force. This figure shows that transverse force increases in beam seas as speed increases from 0 to 10 knots. At 0 and 10 knots the transverse force is significantly larger in quartering seas than in beam seas. The craft with large $\overline{GM}_t$ experiences about the same magnitude of transverse force as does the craft with nominal $\overline{GM}_t$ in beam and quartering seas at 0 and 10 knots (see Figure 26).

Figure 104 presents nondimensional vertical shear force experienced by the craft at 0 and 10 knots in beam and quartering seas. Vertical shear force decreases as speed increases form 0 to 10 knots in beam seas while there is no speed effect in quartering seas. Vertical shear forces are largest at 0 knots in beam seas and largest at 10 knots in quartering seas. The craft with large $\overline{GM}_t$ experiences smaller vertical shear forces than the craft with nominal $\overline{GM}_t$ in beam and quartering seas at 0 and 10 knots except in quartering seas at 0 knots. (See Figure 28)

Figure 106, which presents dimensionless transverse vertical bending moment, shows that transverse bending moment decreases as speed increases from 0 to 10 knots in both beam and quartering seas. Also transverse bending moment is significantly less severe in quartering than in beam seas at both 0 and 10 knots. The craft with large $\overline{GM}_t$ experiences larger transverse bending moments than the craft with nominal $\overline{GM}_t$ in beam seas at 0 and 10 knots but the opposite is true for the craft operating in quartering seas (see Figure 30).

Figure 108, which presents nondimensional torsional moment, shows neither speednor heading effect on torsional moment in beam or quartering seas at 0 and 10 knots. The craft with larger GM_t experiences less severe torsional moment than does the craft with nominal GM_t in quartering seas at 0 and 10 knots (see Figure 32).

Figure 110 presents nondimensional yaw moment for the craft operating in beam and quartering seas at 0 and 10 knots. Yaw moment decreases as speed increases from 0 to 10 knots in both beam and quartering seas. There is also very little GM_t effect on yaw moment in beam and quartering seas at 0 and 10 knots (see Figure 34).

REGULAR HEAD SEAS - HULL WITH APPENDAGES, 32 ft DRAFT

Figures 112 through 135 present results of experiments in head regular seas at various speeds for the craft at 32 ft draft with various appendages.

Figure 112, which presents nondimensional heave, shows the bilge keels are the most effective of the three appendage configurations at 0 and 20 knots.

Figure 114 presents dimensionless relative bow motion and shows that the bilge keels are more effective than the other appendages at 0 and 20 knots. The blisters appear to be ineffective in reducing either heave or relative bow motion at any speed.

Figure 116, which presents dimensionless pitch, shows that pitch motion at 20 knots for the large fin craft configuration is much less than for the other appendage configuration.

Figures 118 through 125 present dimensionless absolute motion of both hulls near the bow and stern. These figures show that the bilge keels are most effective in reducing absolute bow and stern motions at 0 and 20 knots while the large fins produce a slight decrease in motion at 20 knots but also produce an increase in motion at 0 knots. The addition of heave blisters provides no reduction of bow or stern motion.

Figures 126 through 135 present dimensionless transverse force, vertical bending moment, torsional moment, and yaw moment. There is no appreciable speed or appendage effect on the above forces and moments in head seas for the speed range investigated.

Figure 136 presents results of linearity experiments conducted in head sea for the 32 ft draft configuration both with and without appendages.

REGULAR FOLLOWING SEAS - HULL WITH APPENDAGES, 32 ft DRAFT

Figures 137 through 160 present results of experiments in following regular waves of various speeds for the craft at the 32 ft draft with and without appendages.

Figure 137 presents dimensionless heave and shows a reduction in motion as craft speed increases form 0 to 20 knots for the bare hull and blister configuration. However, heave increases as speed increases from

20 to 32 knots for the craft configuration with large fins, which is opposite to the trend seen in head seas (see Figure 112).

Figure 139, which presents nondimensional relative bow motion, shows that relative bow motion increases as speed increases from 0 to 20 knots for the bare hull configuration. There is no speed effect on relative bow motion from 20 to 32 knots for the craft with large fins. Relative bow motion for the bare hull craft and craft with large fins at 20 knots is larger in following seas than in head seas (Figure 114). Relative bow motion is less with the blisters at 0 knots and slightly less with the large fins at 20 knots compared to the motion of the bare hull configuration.

Figure 141 presents dimensionless pitch and indicates that pitch increases as speed increases from 0 to 20 knots for the bare hull craft. There appears to be no speed effect on the pitch for the craft with large fins of blisters. There is only a slight reduction in pitch due to the addition of blisters and little effect on pitch due to the large fins at 20 knots. Note that there is substantial increase in pitch motion in following seas compared to head seas, with and without appendages (see Figure 116).

Figures 143 through 150 present dimensionless absolute motions for both hulls near the bow and stern. These figures indicate little speed effect on absolute bow motion for the bare hull craft while there is a decrease in absolute stern motion as speed increases from 0 to 32 knots for the bare hull configuration. At 0 and 20 knots the largest absolute bow motion is experienced by the bare hull craft. At 0 and 20 knots there is little appendage effect on absolute stern motion. In general, absolute bow and stern motions are significantly larger in head seas than in following seas for corresponding speed and appendage configuration (see Figures 118 through 125).

Figures 151 through 160 present dimensionless transverse force, vertical shear force, transverse vertical bending moment, torsional moment and yaw moment. There is no appreciable speed or appendage effect on these forces and moments in following seas for the speeds investigated.

RANDOM WAVES - HULL WITH APPENDAGES, 32 ft DRAFT

Figures 161 through 169 present results of experiments in random waves for the craft at the 32 ft draft with various appendages at various speeds and headings. Data are presented as significant double amplitudes of motions and forces as a function of significant wave height.

Figure 161 presents significant double amplitudes of heave and relative bow motion. In head seas the craft with large fins experiences the least severe heave except at 0 knots where the craft with bilge keels has the least severe heave. Heave is greatest in head seas for the craft with blister at 0 and 32 knots. In following seas the large fins are not effective in reducing motion at 20 knots while the blisters increase heave motion at 0 and 20 knots compared to bare hull motion.

At 0 knots bare hull craft heave motion is about the same at all headings. Heave for the craft with blisters is slightly larger in following than in head seas.

At 20 knots the craft with large fins and the craft with blisters experience significantly larger heave in following seas than in head seas. At 32 knots the craft with large fins appears to experience much larger heave in following seas than in head seas.

Figure 161 also presents significant double amplitudes of relative bow motion experienced by the craft with and without appendages at various speeds and headings. Relative bow motion in head seas for the craft with blisters is unaffected by speed.

In following seas relative bow motion for the bare hull craft increases appreciably as speed increases from 10 to 20 knots. Relative bow motion in following seas at 20 knots is lower for the craft with large fins than for the bare hull craft.

At 20 knots relative bow motion for all craft configurations is larger in following than in head seas.

Figure 162 presents significant double amplitudes of pitch for the craft with and without appendages, operating at various headings and speeds. In head seas pitch for the craft with blisters and the craft with bilge keels is unaffected by speed. Pitch for the craft with large fins operating in head seas decreases as speed increases. The small pitch at 32 knots for the craft with blister and small fins is probably due more to the small fins than blisters.

In following seas pitch for the bare hull craft increases significantly as speed increases from 0 to 10 knots and is about the same at 10 and 20 knots.

At 10 knots bare hull craft pitch decreases from head to beam seas but increases very significantly in following seas. At 20 knots pitch motion for all craft configurations is much larger in following seas than in head seas, and at 32 knots for the craft with large fins.

Figure 162 also presents significant double amplitudes of roll for the craft with and without appendages operating at various speeds and headings. In head seas and following seas the large roll motion was probably rudder induced. In beam seas roll for the bare hull craft decreases slightly as speed increases from 0 to 10 knots.

Figures 163 and 164 present significant double amplitudes of absolute motion near the bow and near the stern respectively. At 20 and 32 knots the large fins are most effective in reducing absolute bow and stern motion in head seas. Absolute bow motion for the bare hull craft in head seas decreases slightly as speed increases while motion for the craft with large fins decreases dramatically as speed increases. The large decrease in absolute bow and stern motion between 20 and 32 knots for the craft with blisters and small fins operating in head seas is probably due more to the small fins then the blisters.

In following seas the absolute bow and stern motions at 20 and 32 knots are lowest for the craft with large fins.

At 0 knots the absolute bow and stern motions for the bare hull craft tend to be of the same magnitude in both head and following seas and lower in beam seas than in either head or following seas. At zero speed the absolute bow motion of the craft with blisters decreases as heading changes from head to following seas while the opposite is true of the absolute stern motion.

At 20 knots absolute bow motion for the craft with blisters and the craft with large fins is slightly larger in following than in head seas while absolute stern motion for the same two craft configuration follows an opposite trend. At 32 knots the craft with large fins has larger absolute bow motion and smaller absolute stern motion in following seas than in head seas.

Figure 165 presents significant double amplitudes of transverse force experienced by the craft with and without appendages operating at various speeds and headings. The large values of transverse force in head and following seas are probably rudder induced (see roll in Figure 162).

Significant double amplitudes of vertical shear force experienced by the craft with and without appendages at various speeds and headings are presented in Figure 166. Generally, these forces are low in head and following seas. In beam seas there is a slight decrease in vertical shear force as speed increases from 0 to 10 knots.

Figure 167 presents significant double amplitudes of transverse vertical bending moment for the craft with and without appendages operating at various speeds and headings. The large bending moment for the bare hull craft in head seas at 20 knots is probably rudder induced (see roll in Figure 162). In beam seas the transverse bending moment is very large at 0 knots and decreases as speed increases from 0 to 10 knots.

Figure 168 presents significant double amplitudes of torsional moment experienced by the craft with and without appendages operating at various speeds and headings. The large values of torsional moment in head seas may be due to asymmetrical wave impact on the bow while the large torsional moment in following seas is probably caused by the model being restrained in surge during the experiments. In beam seas torsional moment increases slightly as speed increases from 0 to 10 knots.

Figure 169 presents significant double amplitudes of yaw moment experienced by the craft with and without appendages at various speeds and headings. In head and following seas there is no appendage or speed effect on yaw moment. In beam seas for the bare hull craft there is very little speed effect on yaw moment.

REFERENCES

1. Kallio, James A. and Ricci, J.J., "Seaworthiness Characteristics of a Small Waterplane Area Twin Hull (SWATH IV) Part I" NSRDC SPD Research and Department Report No. SPD 620-01, August 1975

2. Lin, A.C.M., et al, "Prediction of Resistance and Propulsion Characteristics for a Small Waterplane Area Twin Hull (SWATH) Form presented by Model 5287," NSRDC Evaluation Report No. 396-H-08, December 1972.

SWATH IV

	HEAD SEAS (180°)															
	REGULAR WAVES				RANDOM WAVES											
					SEA STATE 4				SEA STATE 5				SEA STATE 6			
SHIP SPEED, KNOTS -	0	10	20	32	0	10	20	32	0	10	20	32	0	10	20	32
BARE HULL 28 ft Draft Nominal GM_t	△	△	■	■					■	△	△	■	■	■	■	■
BARE HULL 28 ft Draft Large GM_t																
BARE HULL 30 ft Draft Nominal GM_t			■									■		■	■	■
BARE HULL 32 ft Draft Nominal GM_t	△	△	■		△	△			△	△	△		△	△	■	
LARGE FIN 32 ft Draft	■		■	■							■	■	■		■	■
SMALL FIN 32 ft Draft				■												■
BLISTERS 32 ft Draft	■		■	■							■	■	■		■	■
BILGE KEELS 32 ft Draft	■		■										■		■	

	BEAM SEAS (90°)															
	REGULAR WAVES				RANDOM WAVES											
					SEA STATE 4				SEA STATE 5				SEA STATE 6			
SHIP SPEED, KNOTS -	0	10	20	32	0	10	20	32	0	10	20	32	0	10	20	32
BARE HULL 28 ft Draft Nominal GM_t	△	△	△	△					△	△	△		△	△	△	
BARE HULL 28 ft Draft Large GM_t	△	△														
BARE HULL 30 ft Draft Nominal GM_t																
BARE HULL 32 ft Draft Nominal GM_t	△	△			△	△			△	△				△		
LARGE FIN 32 ft Draft																
SMALL FIN 32 ft Draft																
BLISTERS 32 ft Draft																
BILGE KEELS 32 ft Draft																

	STERN QUARTERING SEAS (45°)											
	REGULAR WAVES				RANDOM WAVES							
					SEA STATE 5				SEA STATE 6			
SHIP SPEED, KNOTS -	0	10	20	32	0	10	20	32	0	10	20	32
BARE HULL 28 ft Draft Nominal GM_t	△	△										
BARE HULL 28 ft Draft Large GM_t	△	△										
BARE HULL 30 ft Draft Nominal GM_t												
BARE HULL 32 ft Draft Nominal GM_t												
LARGE FIN 32 ft Draft												
SMALL FIN 32 ft Draft												
BLISTERS 32 ft Draft												
BILGE KEELS 32 ft Draft												

	FOLLOWING SEAS (0°)															
	REGULAR WAVES				RANDOM WAVES											
					SEA STATE 4				SEA STATE 5				SEA STATE 6			
SHIP SPEED, KNOTS -	0	10	20	32	0	10	20	32	0	10	20	32	0	10	20	32
BARE HULL 28 ft Draft Nominal GM_t	△	△							△	△			△	△		
BARE HULL 28 ft Draft Large GM_t																
BARE HULL 30 ft Draft Nominal GM_t																
BARE HULL 32 ft Draft Nominal GM_t	△	■	■		△	△			△	△	■		△	■	■	
LARGE FIN 32 ft Draft			■	■								■			■	
SMALL FIN 32 ft Draft																
BLISTERS 32 ft Draft	■		■						■		■		■			
BILGE KEELS 32 ft Draft																

Figure 1 - Matrix of SWATH IV Experimental Conditions

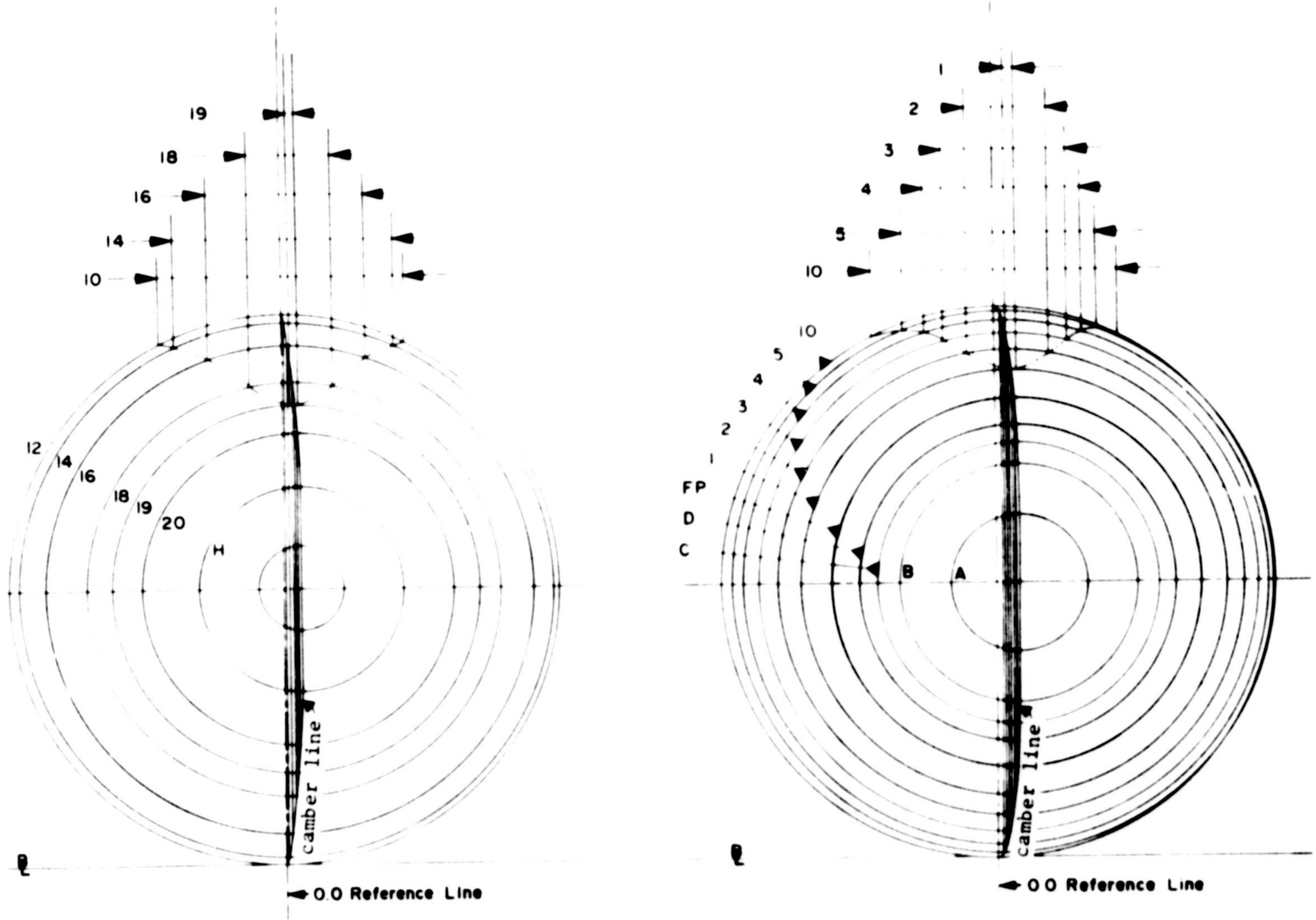

Figure 2 - Abbreviated Body Plan for SWATH IV Represented by Model 5287

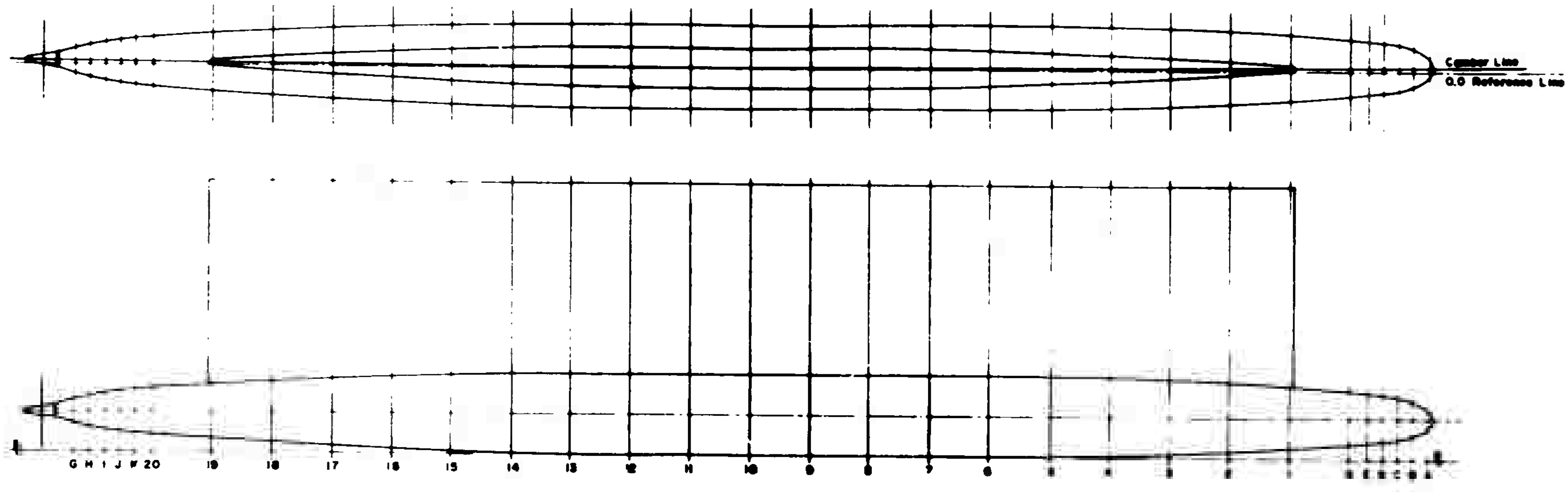

SWATH IV
MODEL 5287

Figure 3 - Abbreviated Lines and Profile for SWATH IV Represented by Model 5287

Bridging Structure and Rudder on SWATH IV

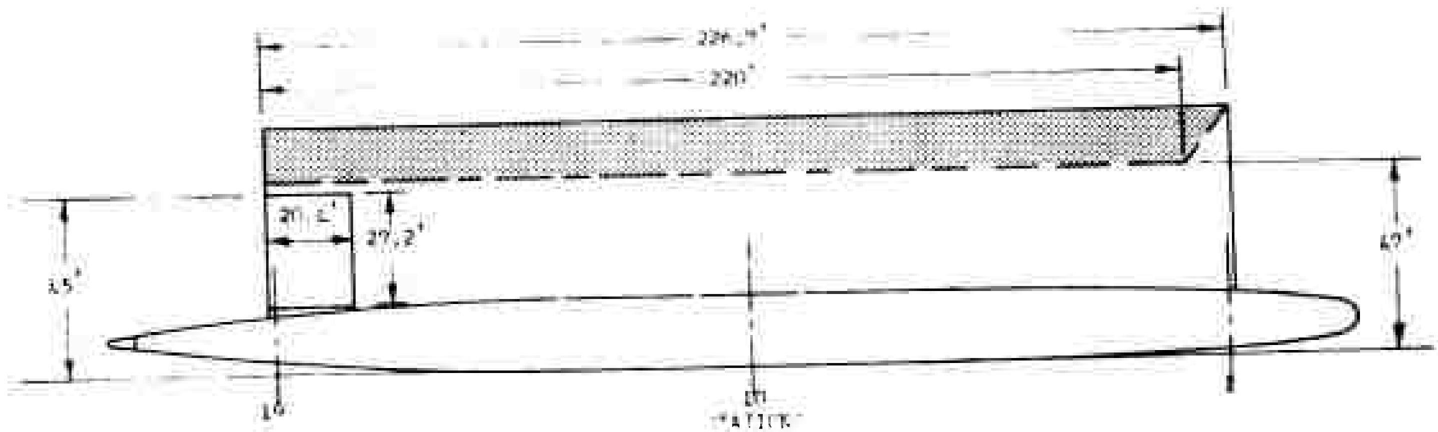

Figure 4 - Bridging Structure and Rudder Size and Location on SWATH IV

SWATH IV

Pressure Gage Locations

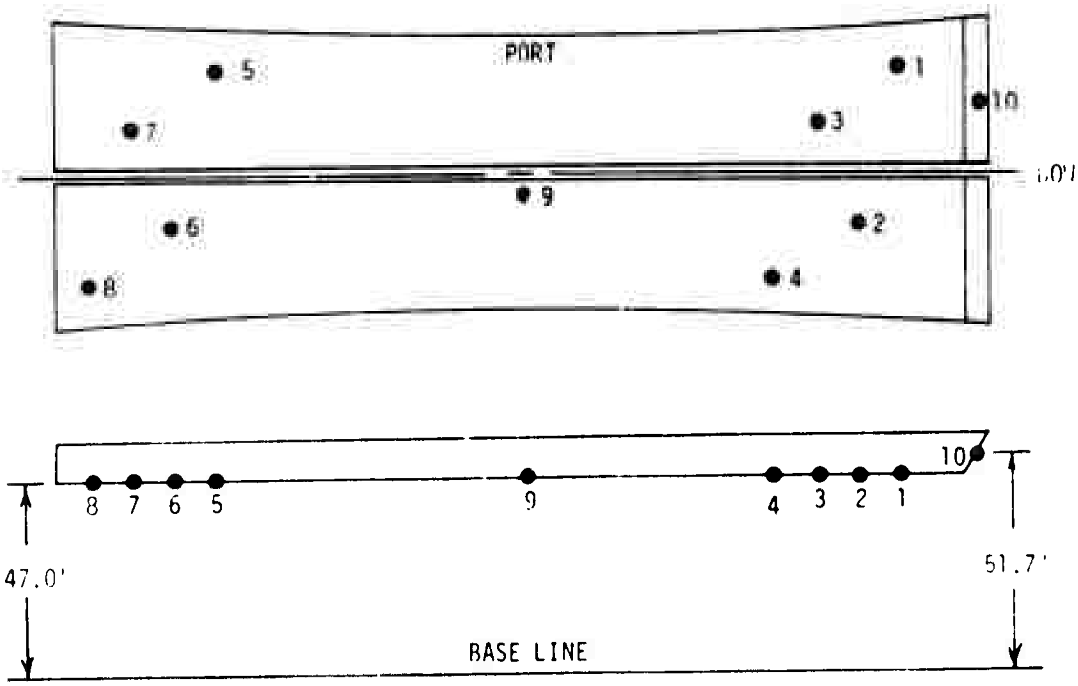

Gage No.	Distance Aft of Fwd. Strut Edge (ft.)	Distance Off Centerline (ft.)	Distance Above Base Line (ft.)
1	22.85	25.5 Port	47
2	33.05	11.9 Stbd.	47
3	43.25	11.9 Port	47
4	53.45	25.5 Stbd.	47
5	187.75	25.5 Port	47
6	197.95	11.9 Stbd.	47
7	208.15	11.9 Port	47
8	218.35	25.5 Stbd	47
9	112.95	5.1 Stbd.	47
10	2.45	17.0 Port	51.7

Figure 5 - Pressure Gage Locations on SWATH IV Bridging Structure

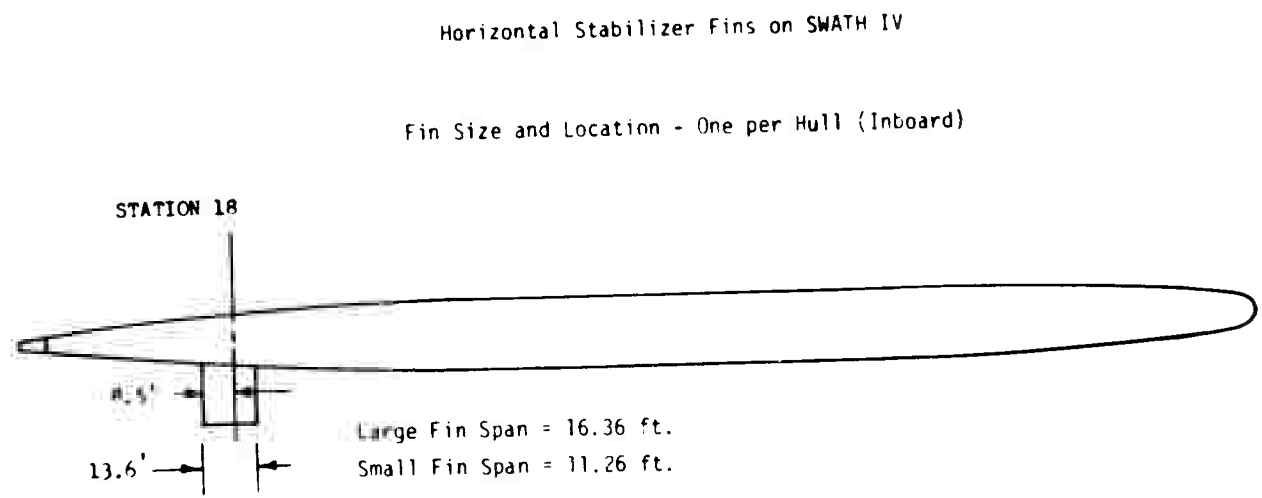

Figure 6 - Schematic Showing Fin Size and Location on SWATH IV

Horizontal Stabilizer Fin Offsets

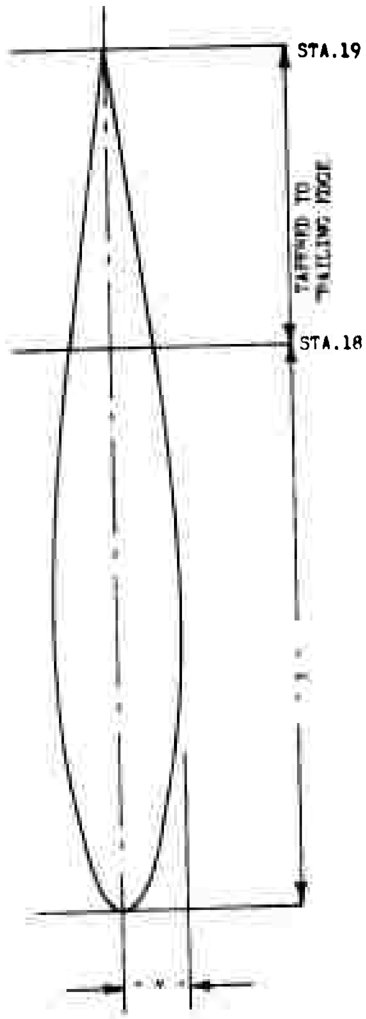

TABLE OF FIN OFFSETS		
STATION NO.	" X " (FEET)	" Y " (FEET)
1	.068	.165
2	.102	.199
3	.170	.250
4	.340	.343
5	.680	.476
6	1.020	.576
7	1.360	.658
8	2.040	.787
9	2.720	.882
10	3.400	.950
11	4.080	.994
12	4.760	1.018
13	5.100	1.017
14	6.120	.983
15	6.800	.926
16	7.480	.852
17	8.160	.763
18	8.840	.665
19	13.600	.000
LEADING EDGE RADIUS = .216 FEET		

Figure 7 - Schematic and Offsets for SWATH IV Horizontal Stabilizer Fins

Heave Blisters on SWATH IV

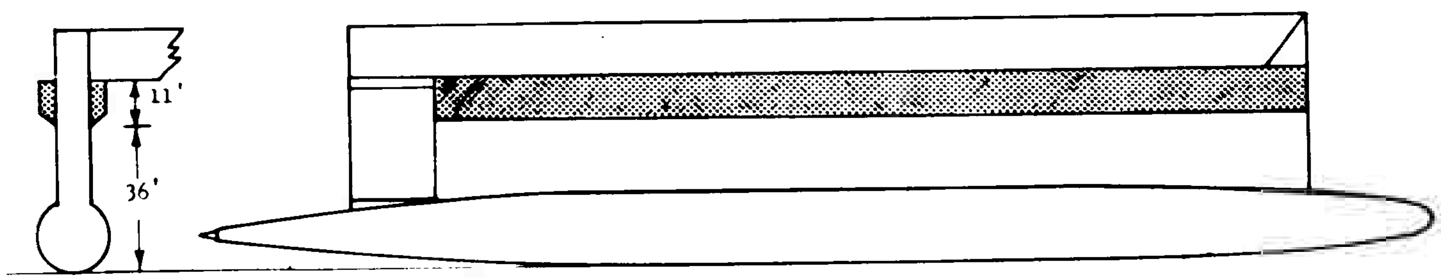

Note - Strut width with blisters is twice nominal strut width.

Figure 8 - Schematic Showing Blister Size and Location on SWATH IV

Bilge Keels on SWATH IV

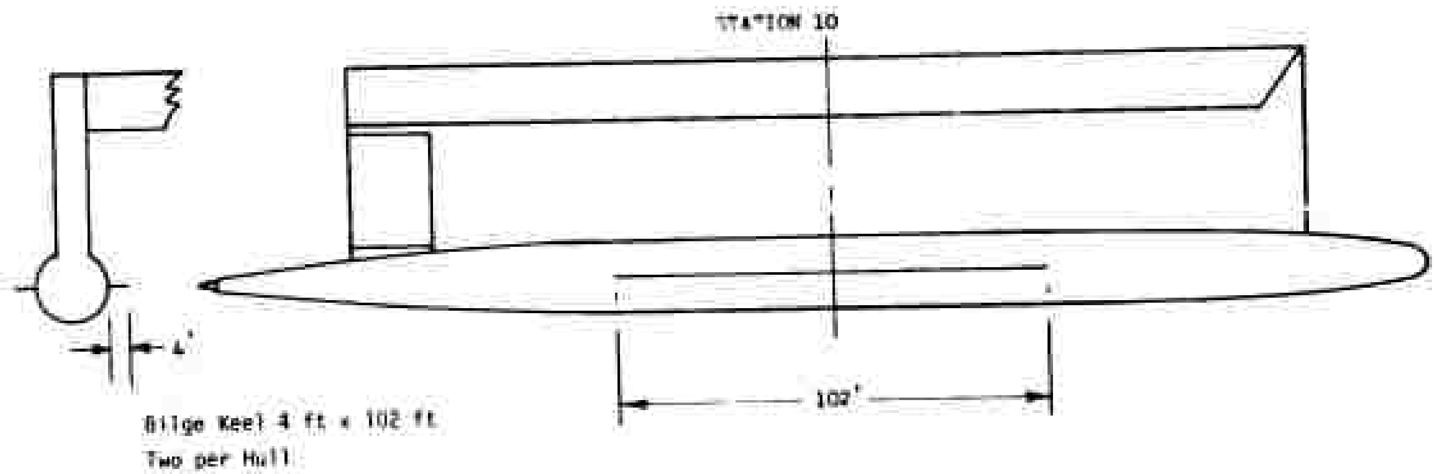

Figure 9 - Schematic Showing Bilge Keel Size And Location on SWATH IV

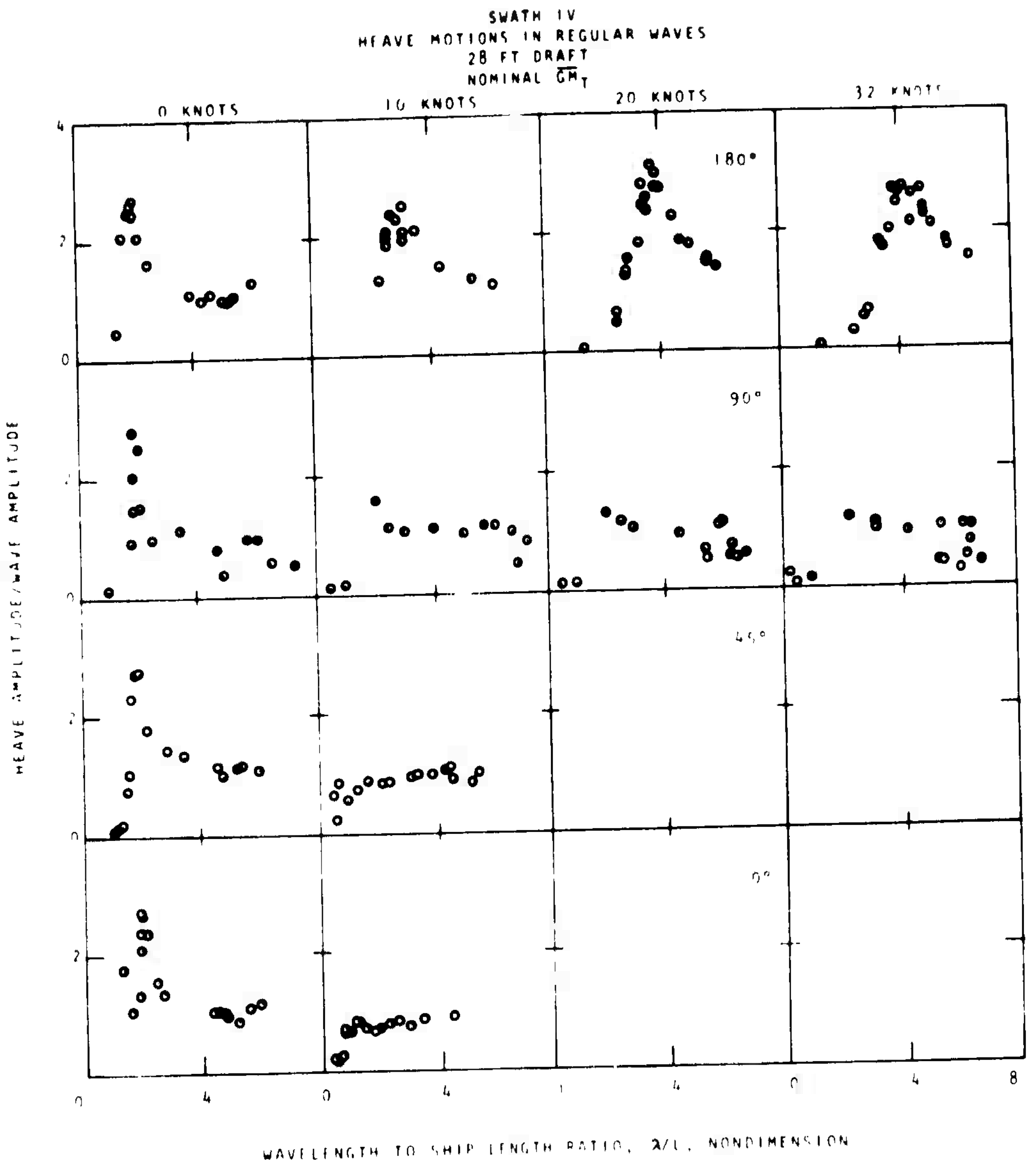

Figure 10 - Dimensionless Heave in Regular Waves, 28 ft Draft, Nominal $\overline{GM}_t$

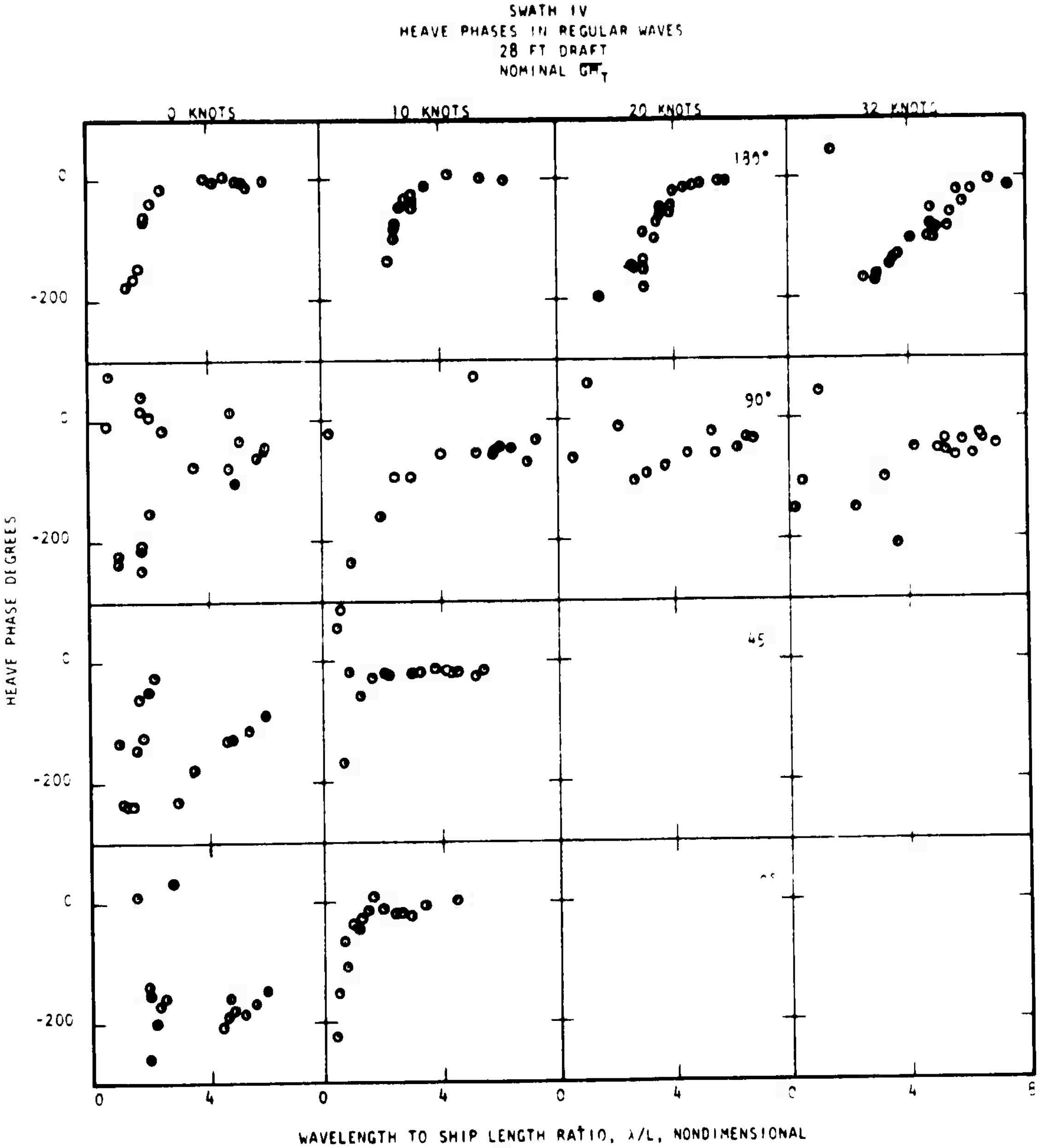

Figure 11 - Heave Phase in Regular Waves, 28 ft Draft, Nominal $\overline{GM}_t$

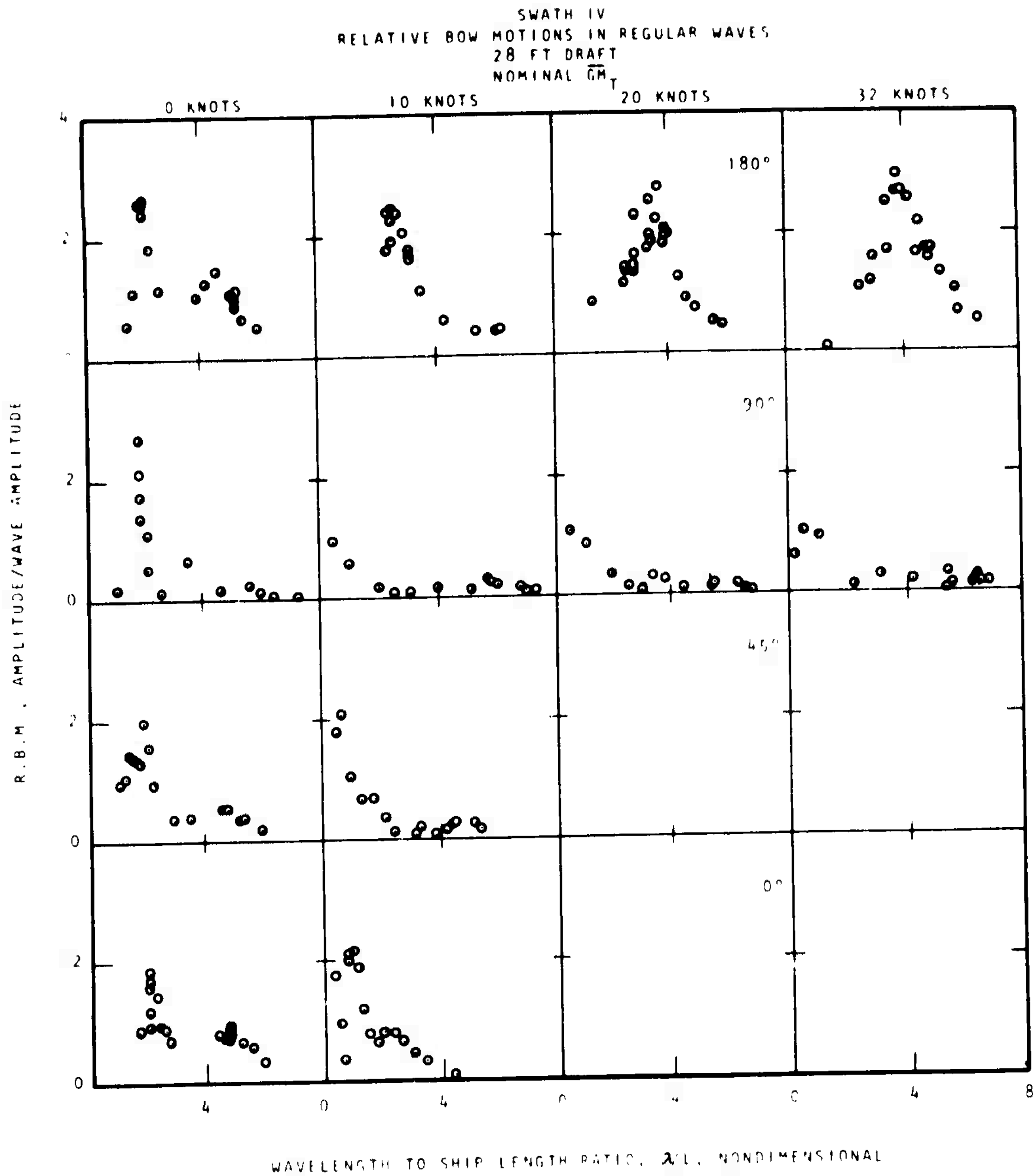

Figure 12 - Dimensionless Relative Bow Motion in Regular Waves, 28 ft Draft, Nominal $\overline{GM}_t$

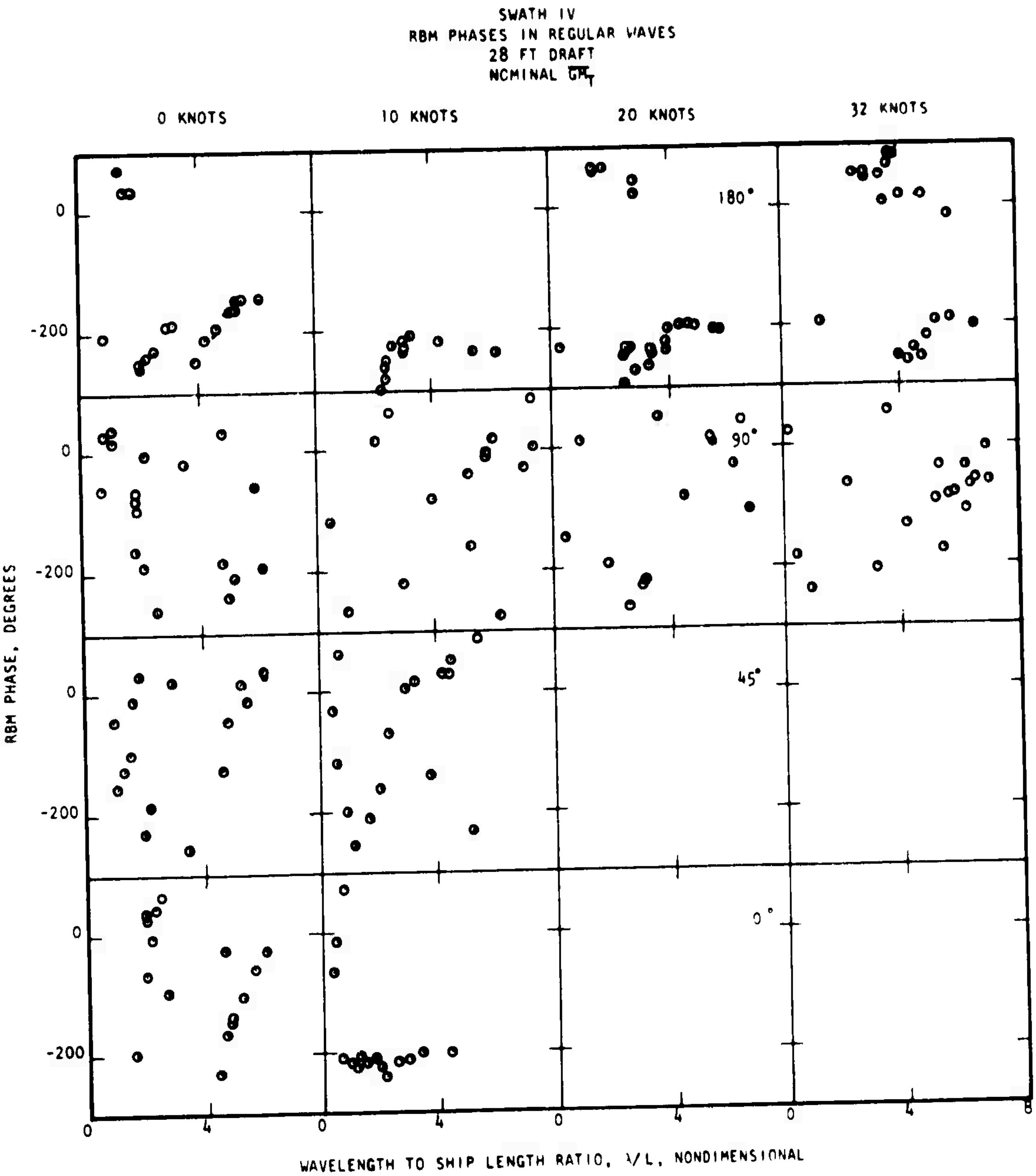

Figure 13 - Relative Bow Motion Phase in Regular Waves, 28 ft Draft, Nominal $\overline{GM}_t$

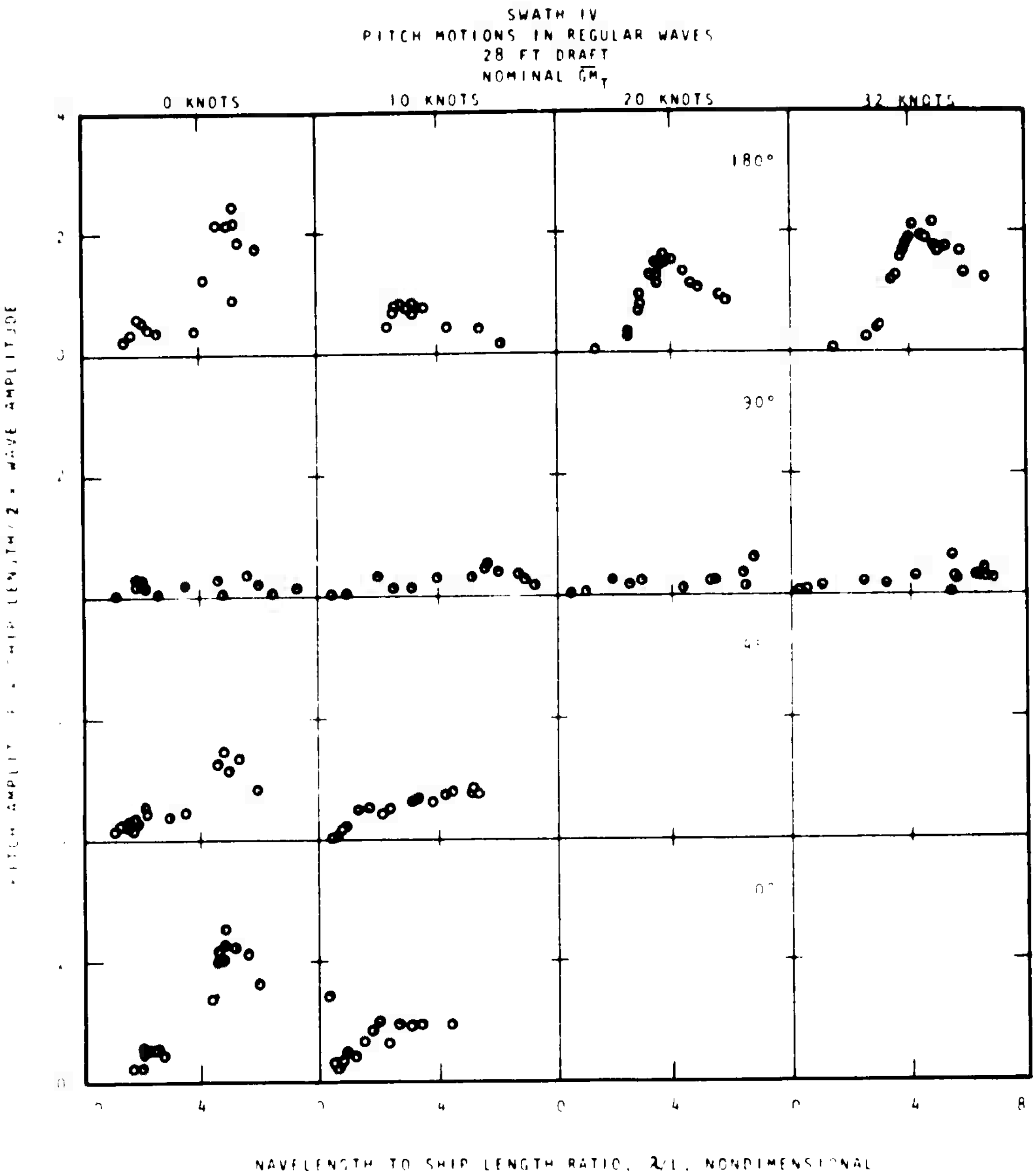

Figure 14 - Dimensionless Pitch in Regular Waves, 28 ft Draft, Nominal $\overline{GM}_t$

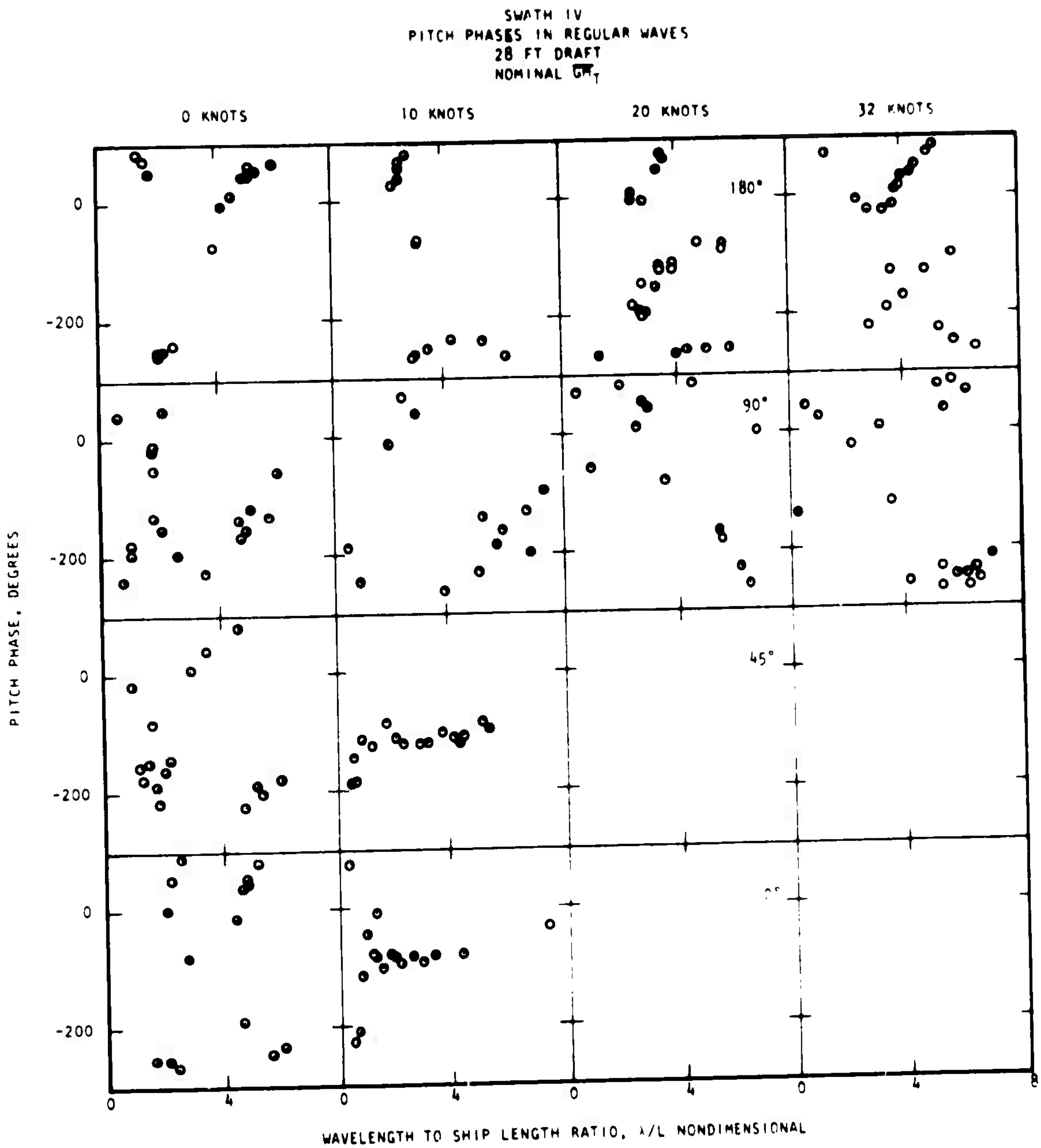

Figure 15 - Pitch Phase in Regular Waves, 28 ft Draft, Nominal $\overline{GM}_t$

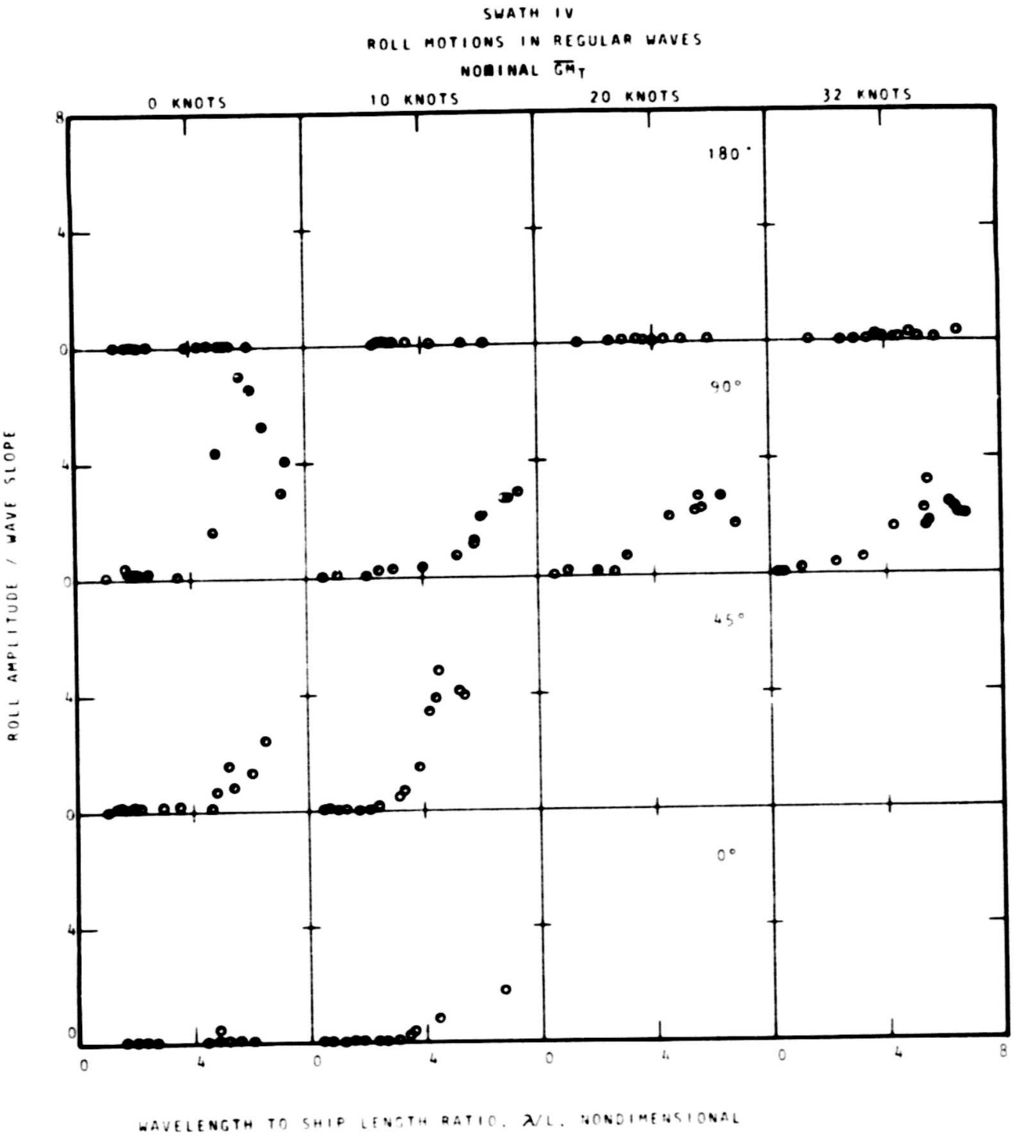

Figure 16 - Dimensionless Roll in Regular Waves, 28 ft Draft, Nominal $\overline{GM}_t$

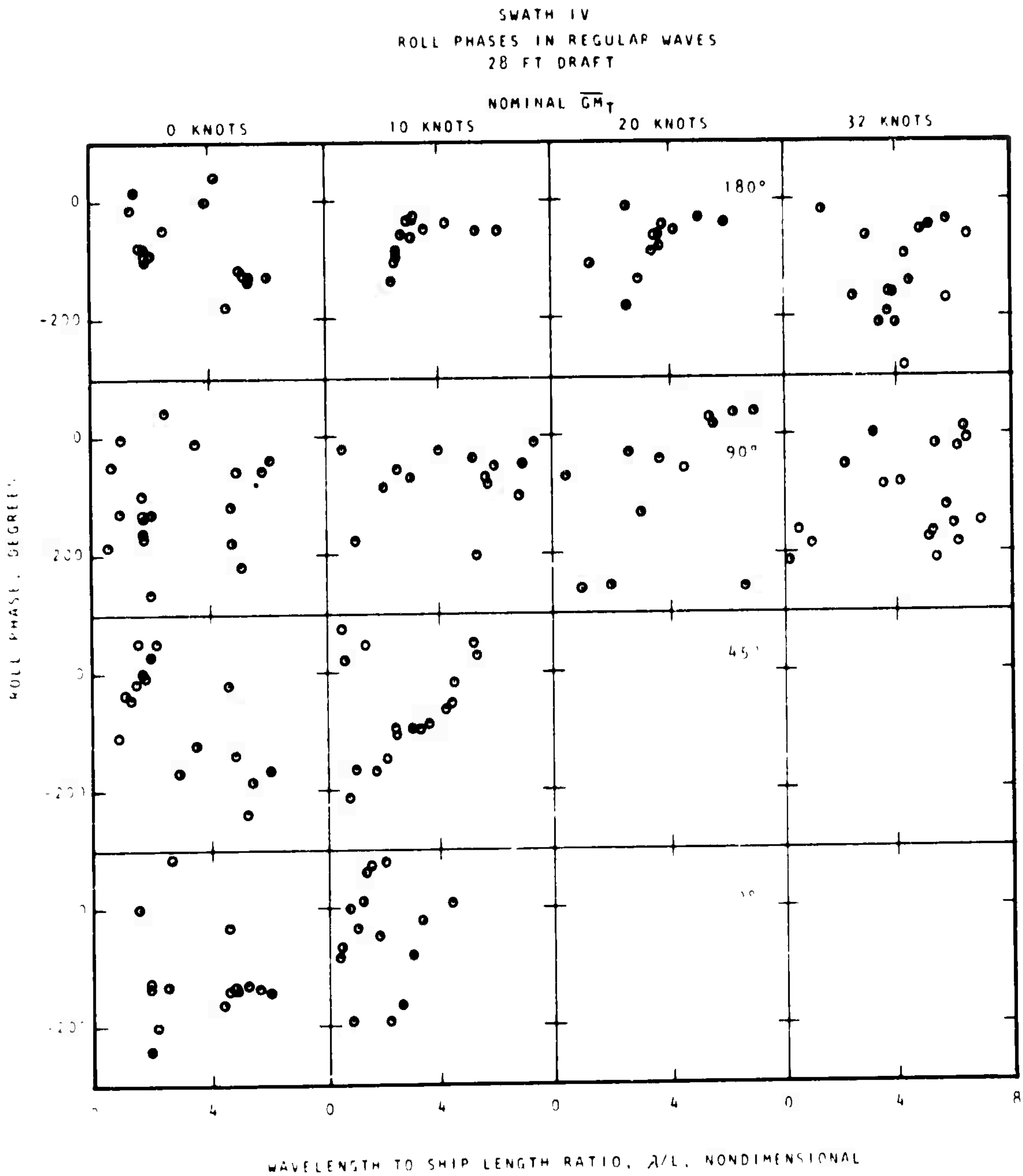

Figure 17 - Roll Phase in Regular Waves, 28 ft Draft, Nominal $\overline{GM}_t$

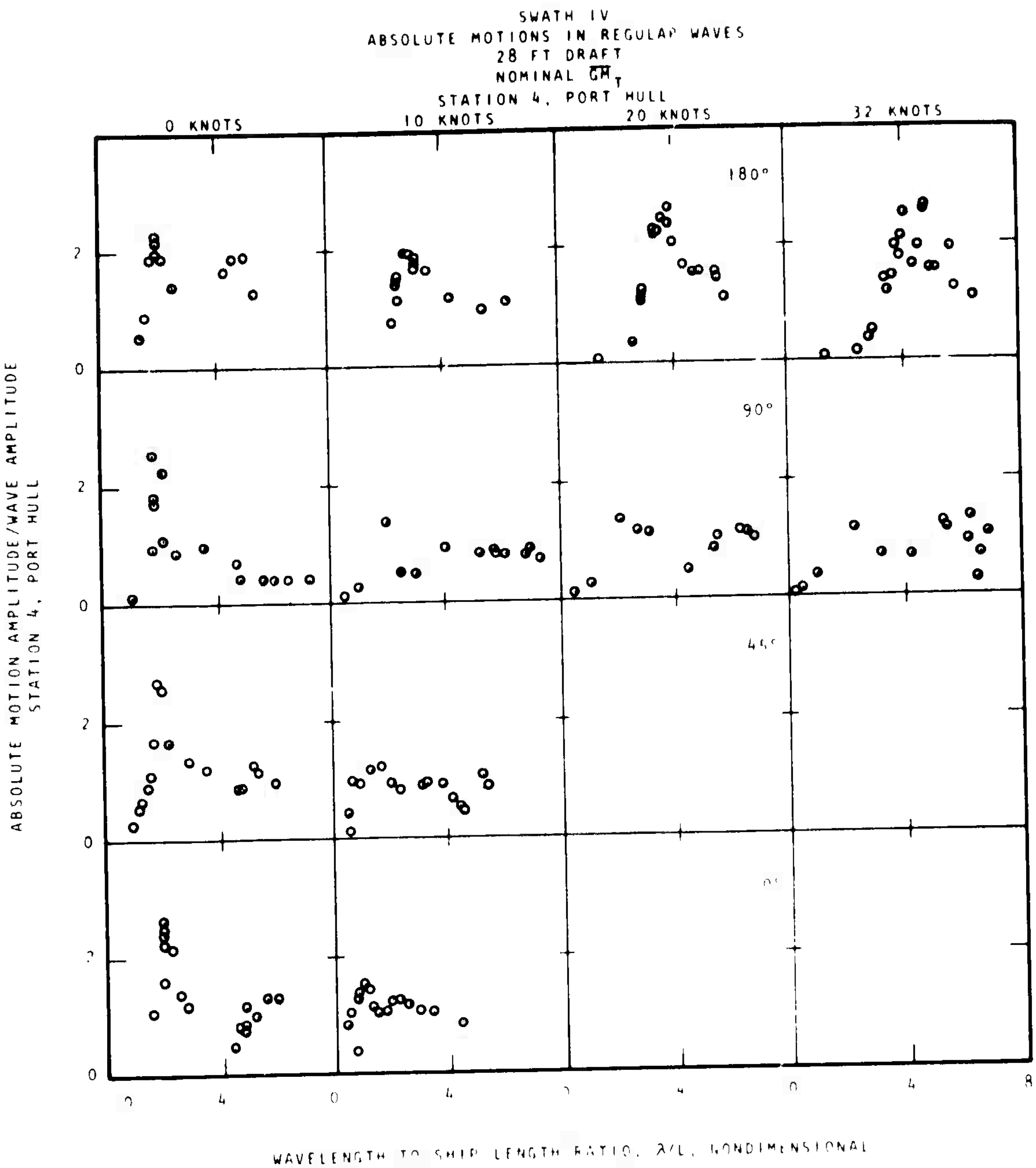

Figure 18 - Dimensionless Absolute Motion in Regular Waves, Forward Port, 28 ft Draft, Nominal $\overline{GM}_t$

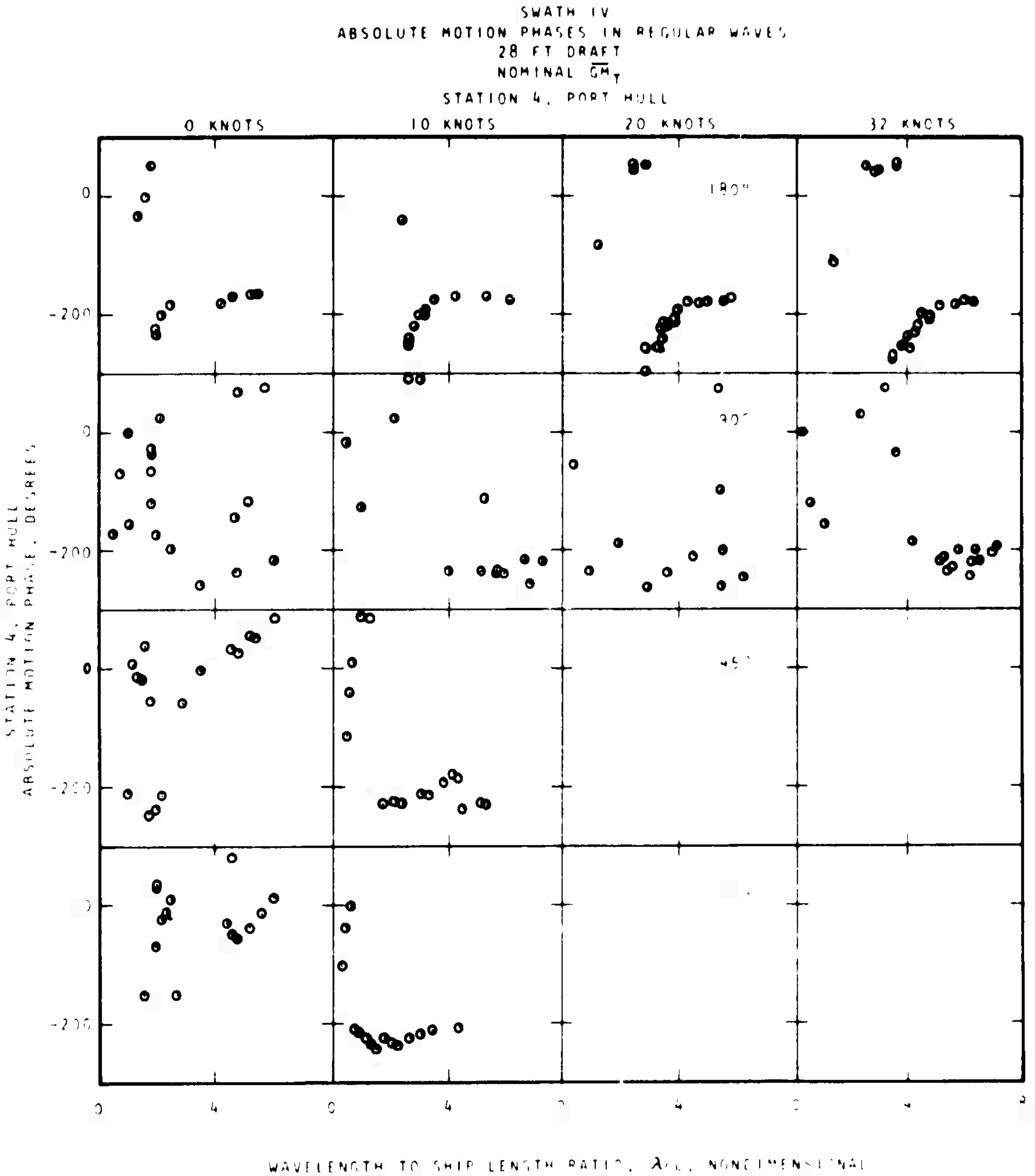

Figure 19 - Absolute Motion Phase in Regular Waves, Forward Port, 28 ft Draft, Nominal $\overline{GM}_t$

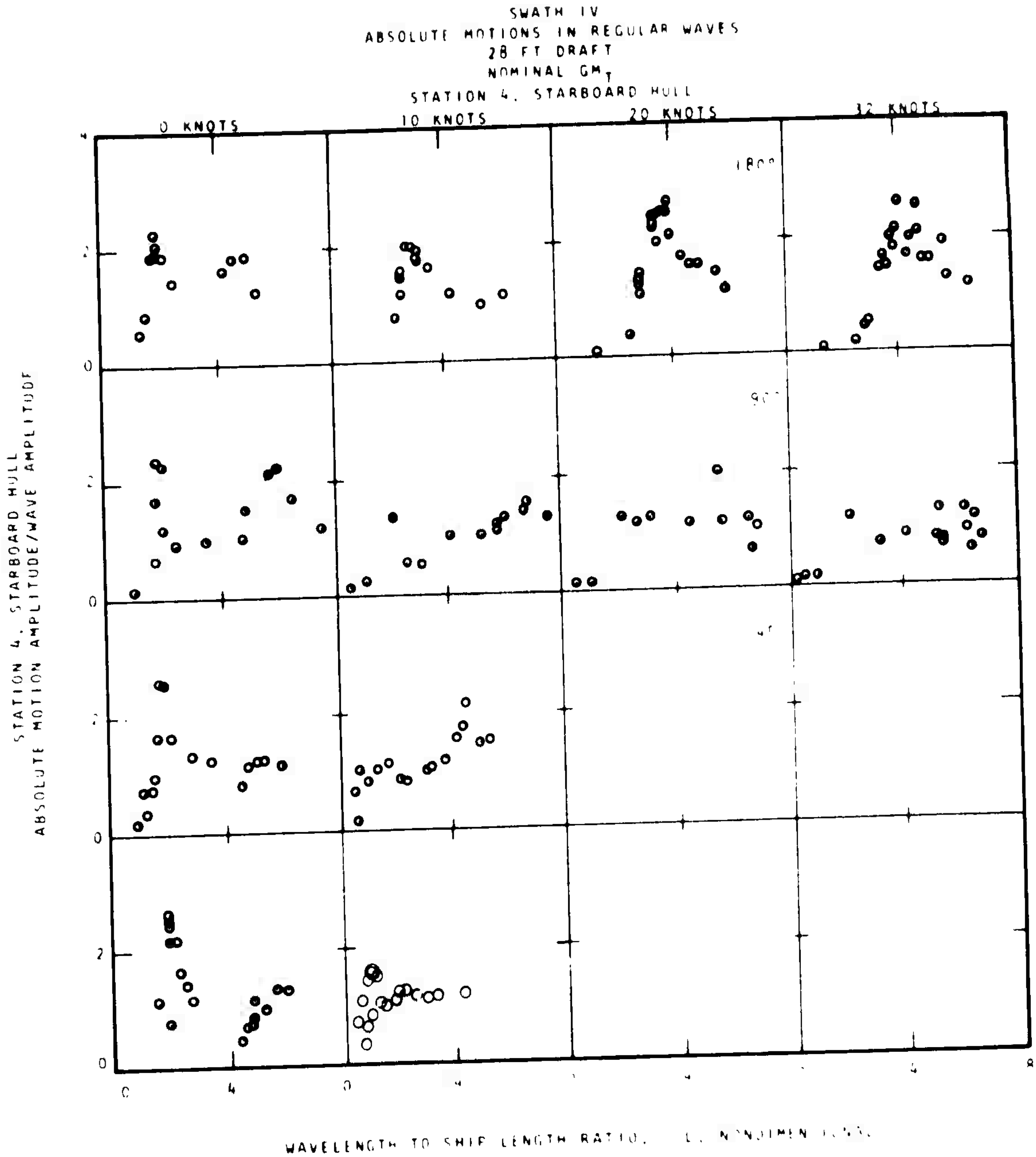

Figure 20 - Dimensionless Absolute Motion in Regular Waves, Forward Starboard, 28 ft Draft, Nominal $\overline{GM}_t$

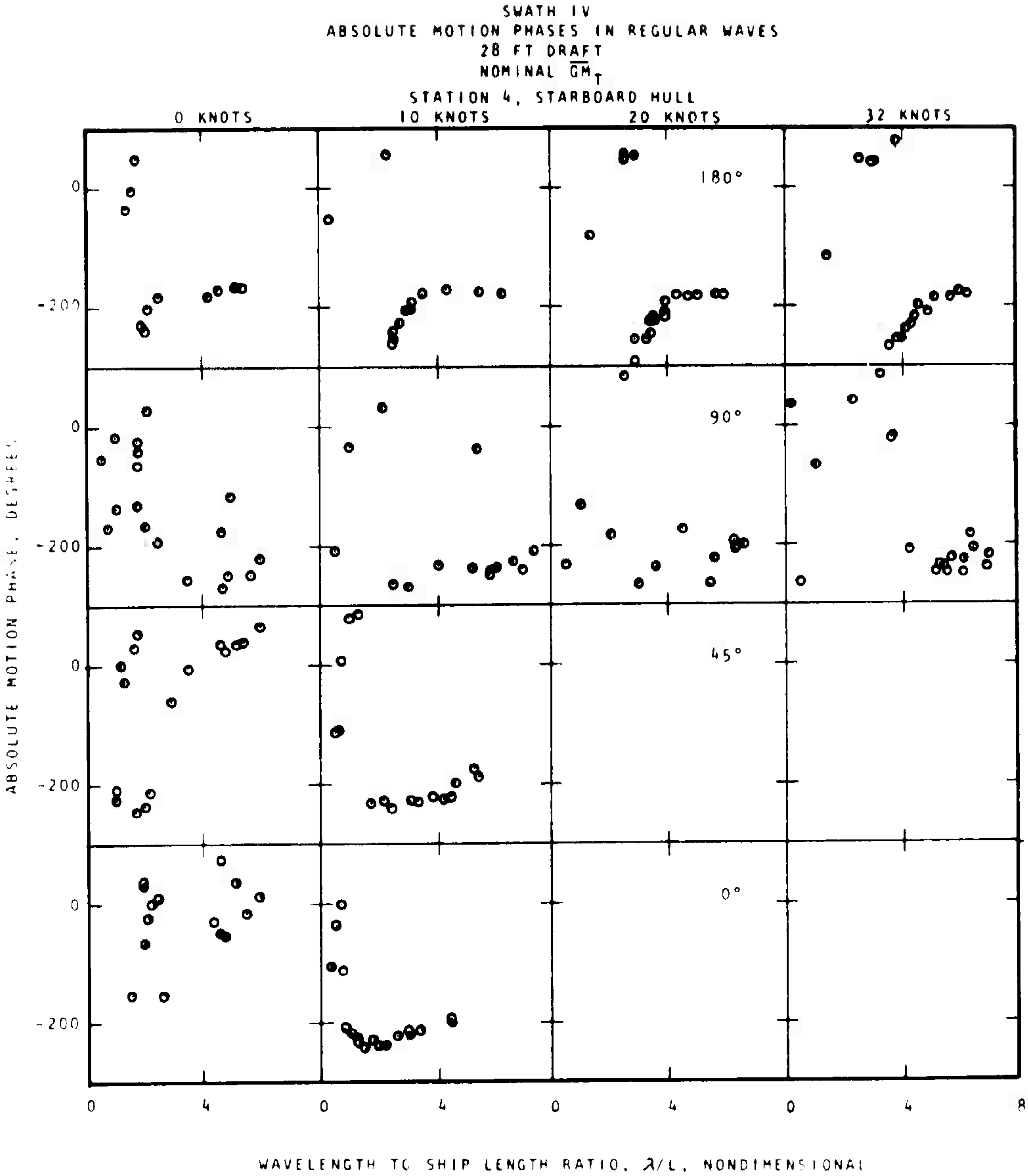

Figure 21 - Absolute Motion Phase in Regular Waves, Forward Starboard, 28 ft Draft, Nominal $\overline{GM}_t$

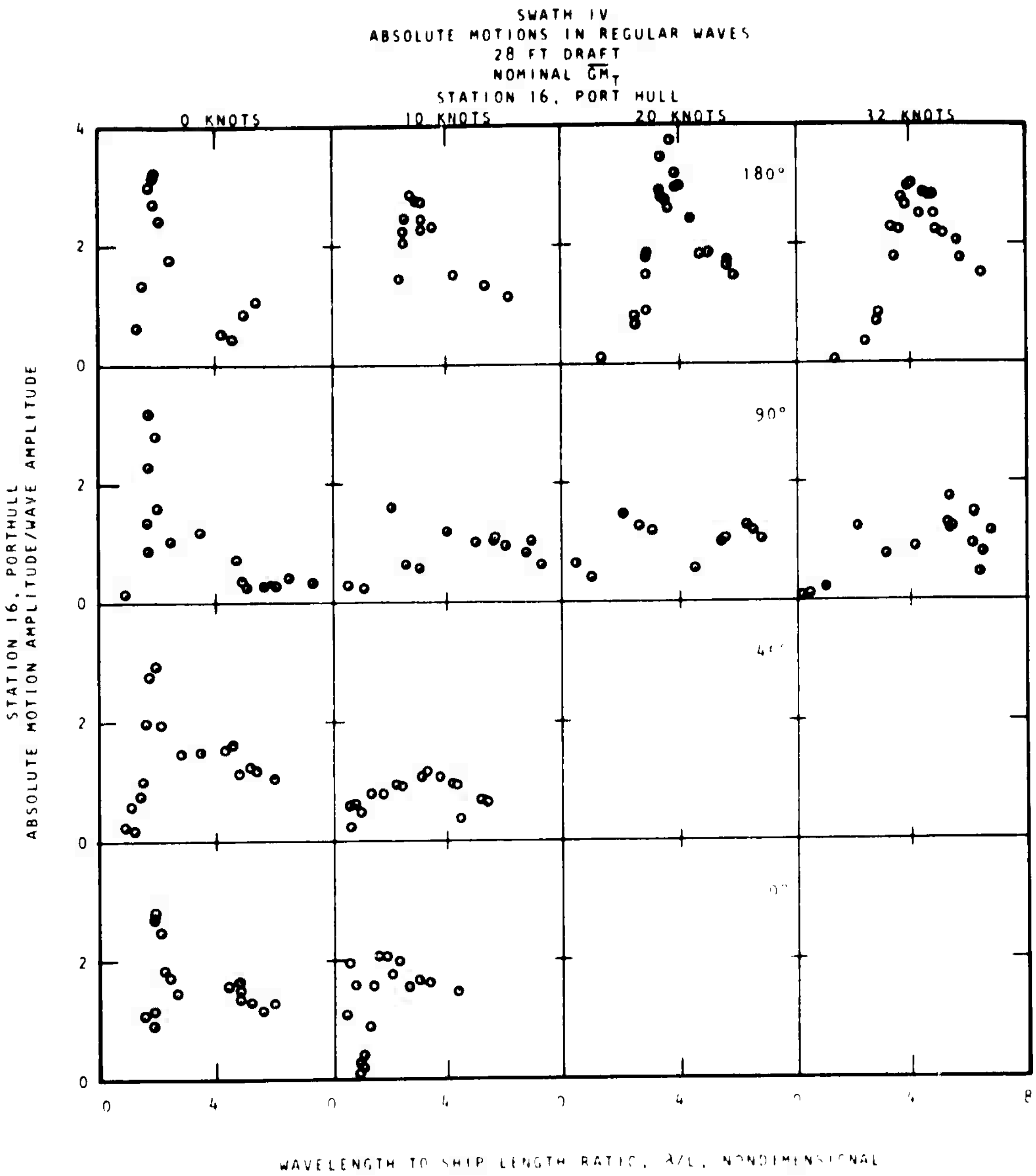

Figure 22 - Dimensionless Absolute Motion in Regular Waves,
Aft Port, 28 ft Draft, Nominal $\overline{GM}_t$

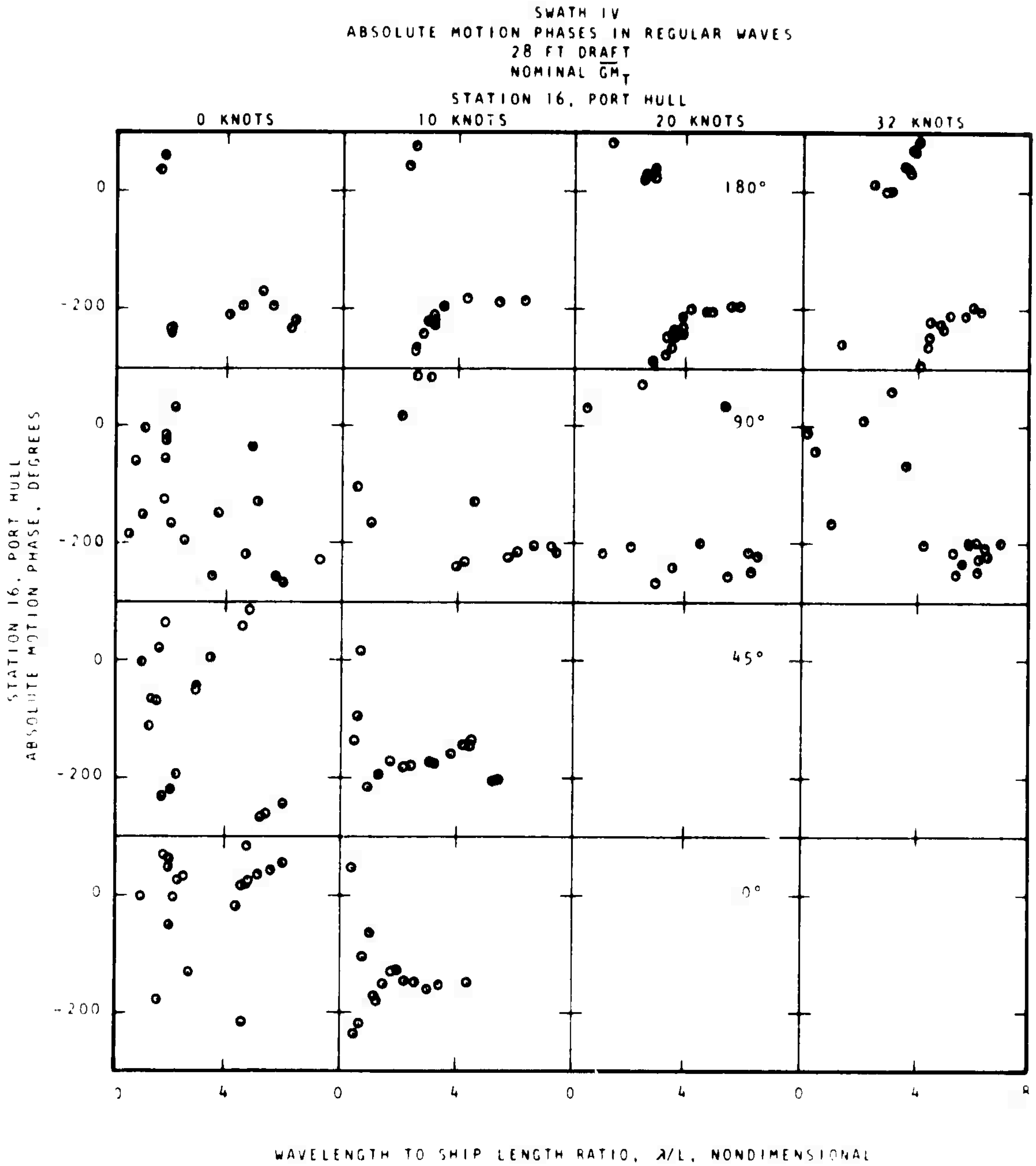

Figure 23 - Absolute Motion Phase in Regular Waves, Aft Port, 28 ft Draft, Nominal $\overline{GM}_t$

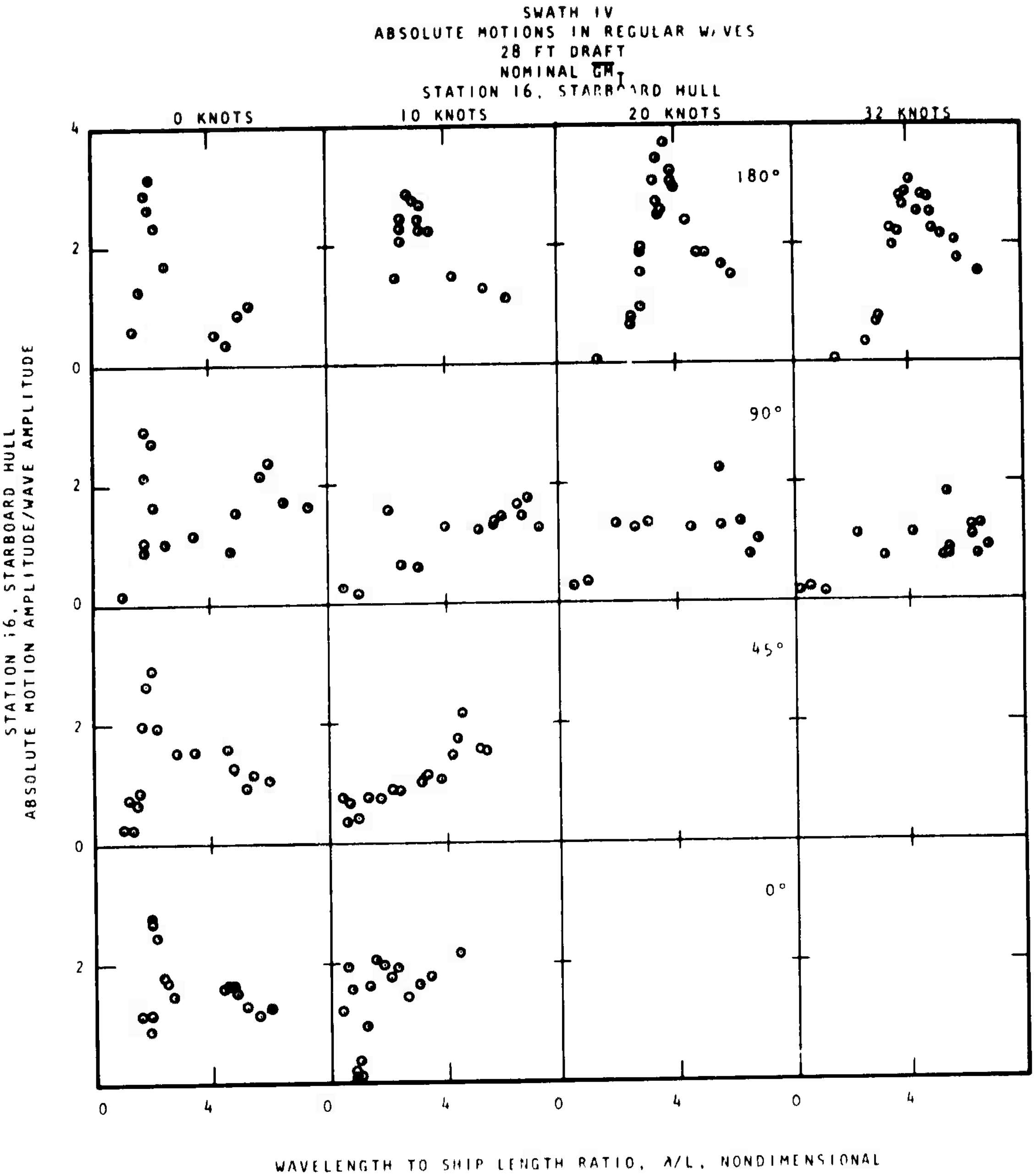

Figure 24 - Dimensionless Absolute Motion in Regular Waves, Aft Starboard, 28 ft Draft, Nominal $\overline{GM}_t$

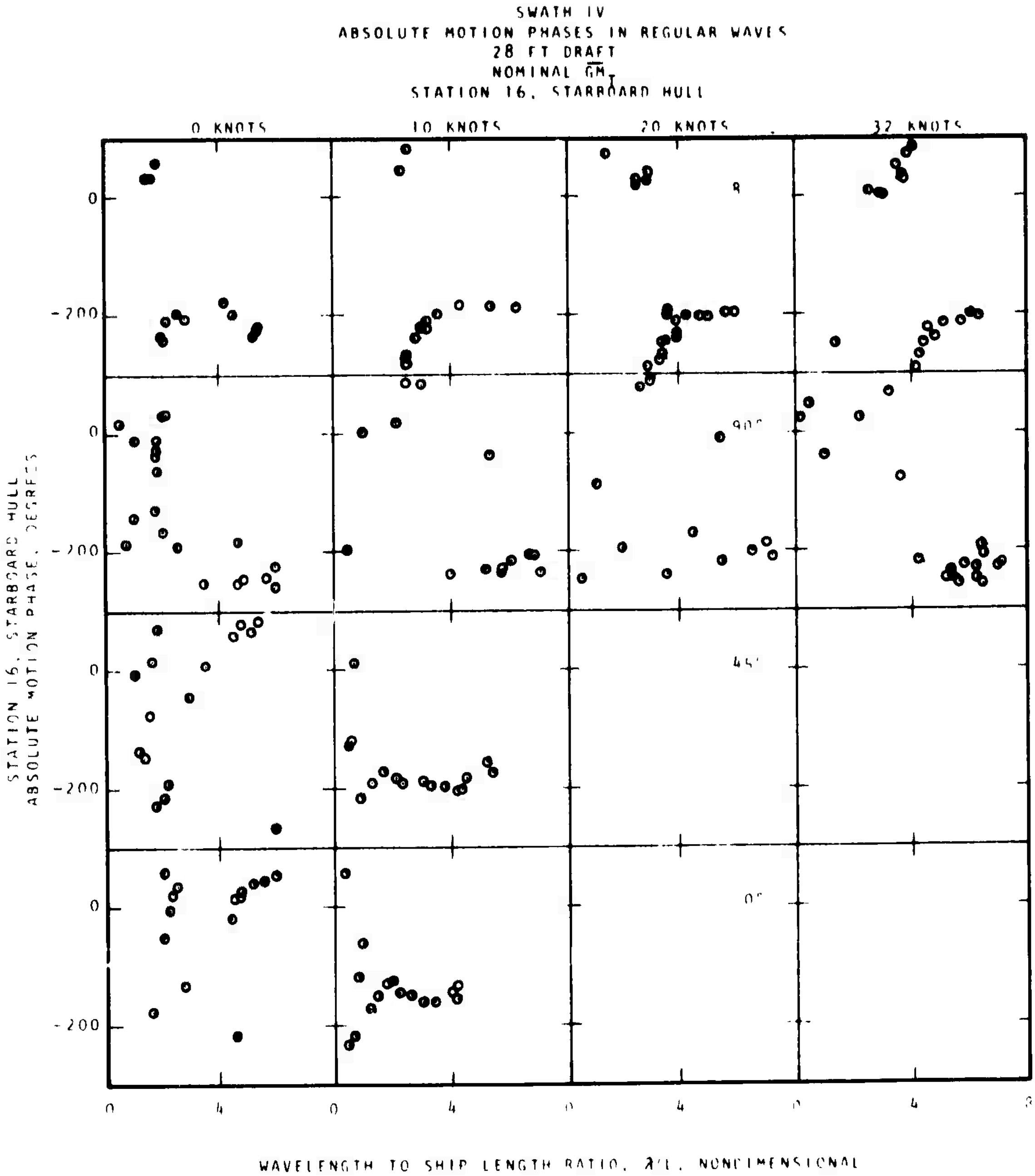

Figure 25 - Absolute Motion Phase in Regular Waves, Aft Starboard, 28 ft Draft, Nominal $\overline{GM}_t$

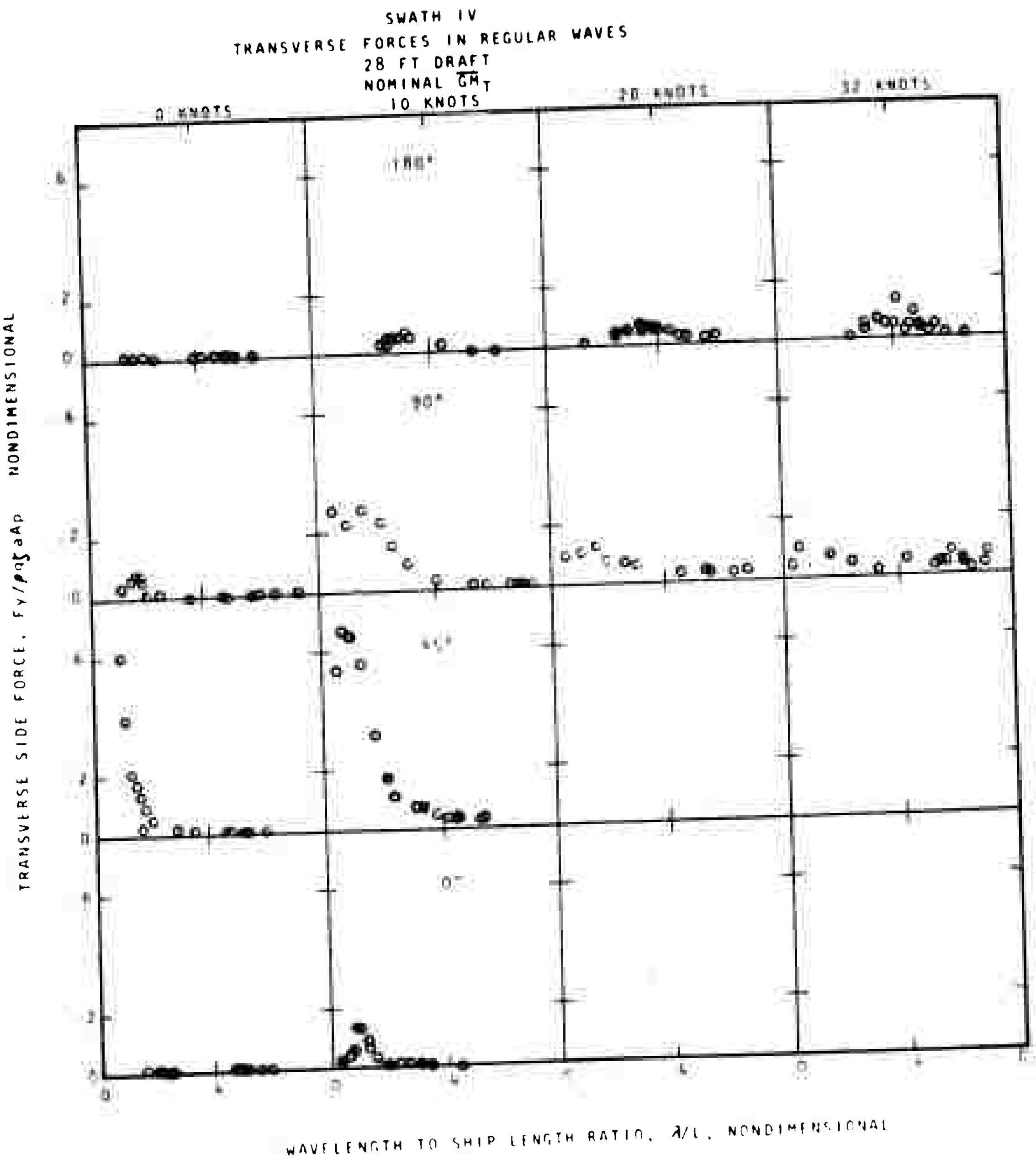

Figure 26 - Dimensionless Transverse Force in Regular Waves, 28 ft Draft, Nominal $\overline{GM}_t$

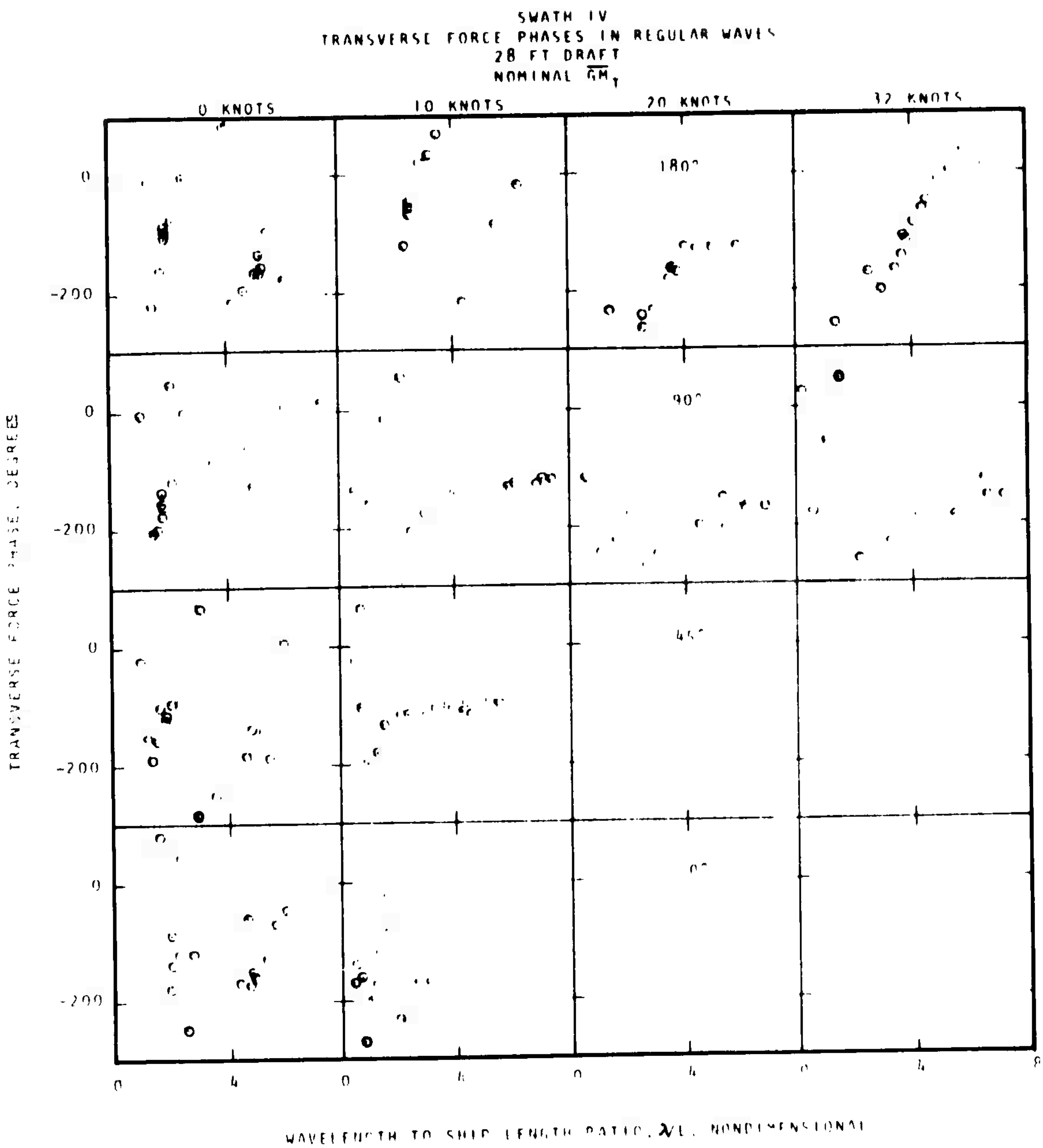

Figure 27 - Transverse Force Phase in Regular Waves, 28 ft Draft, Nominal $\overline{GM}_t$

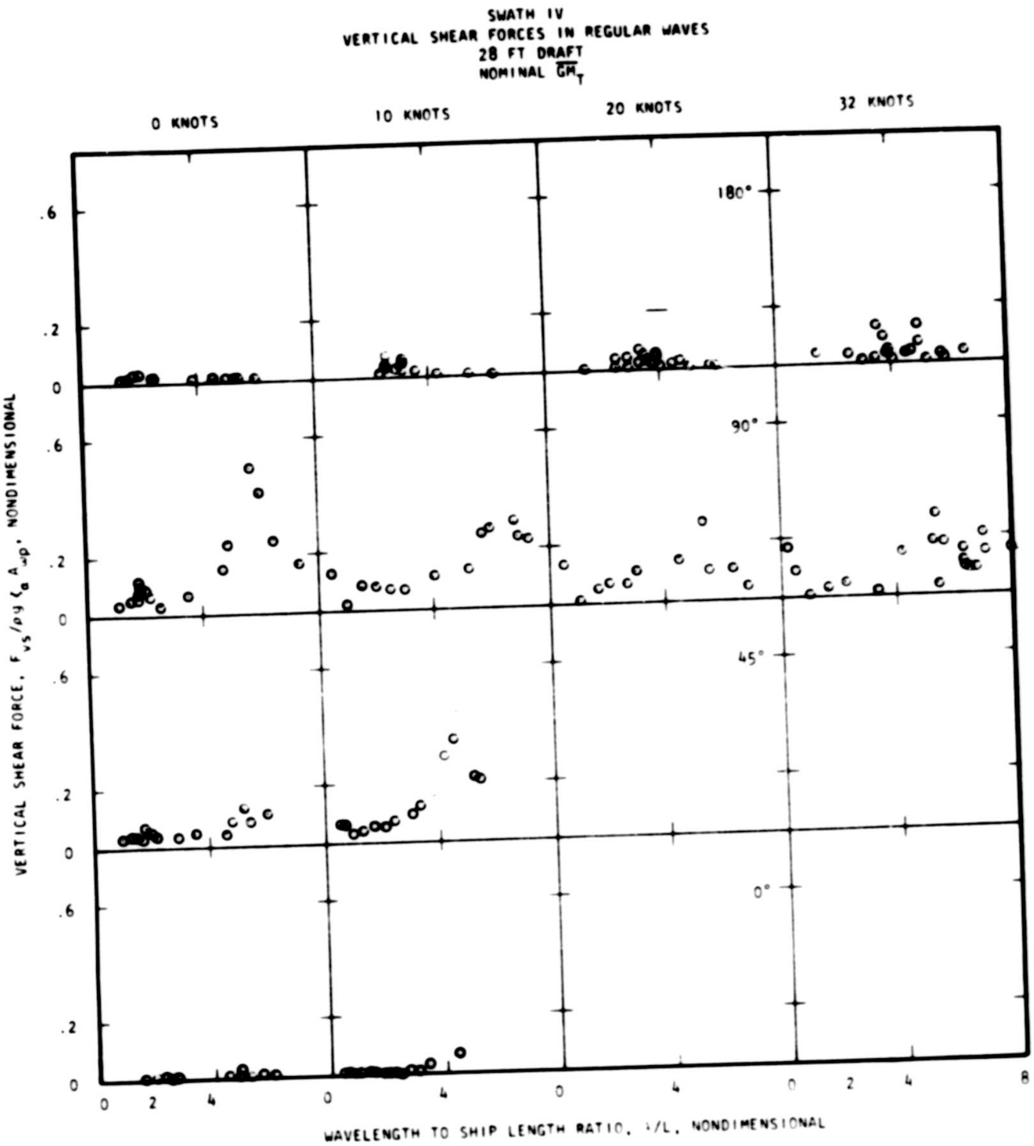

Figure 28 - Dimensionless Vertical Shear Force in Regular Waves, 28 ft Draft, Nominal $\overline{GM}t$

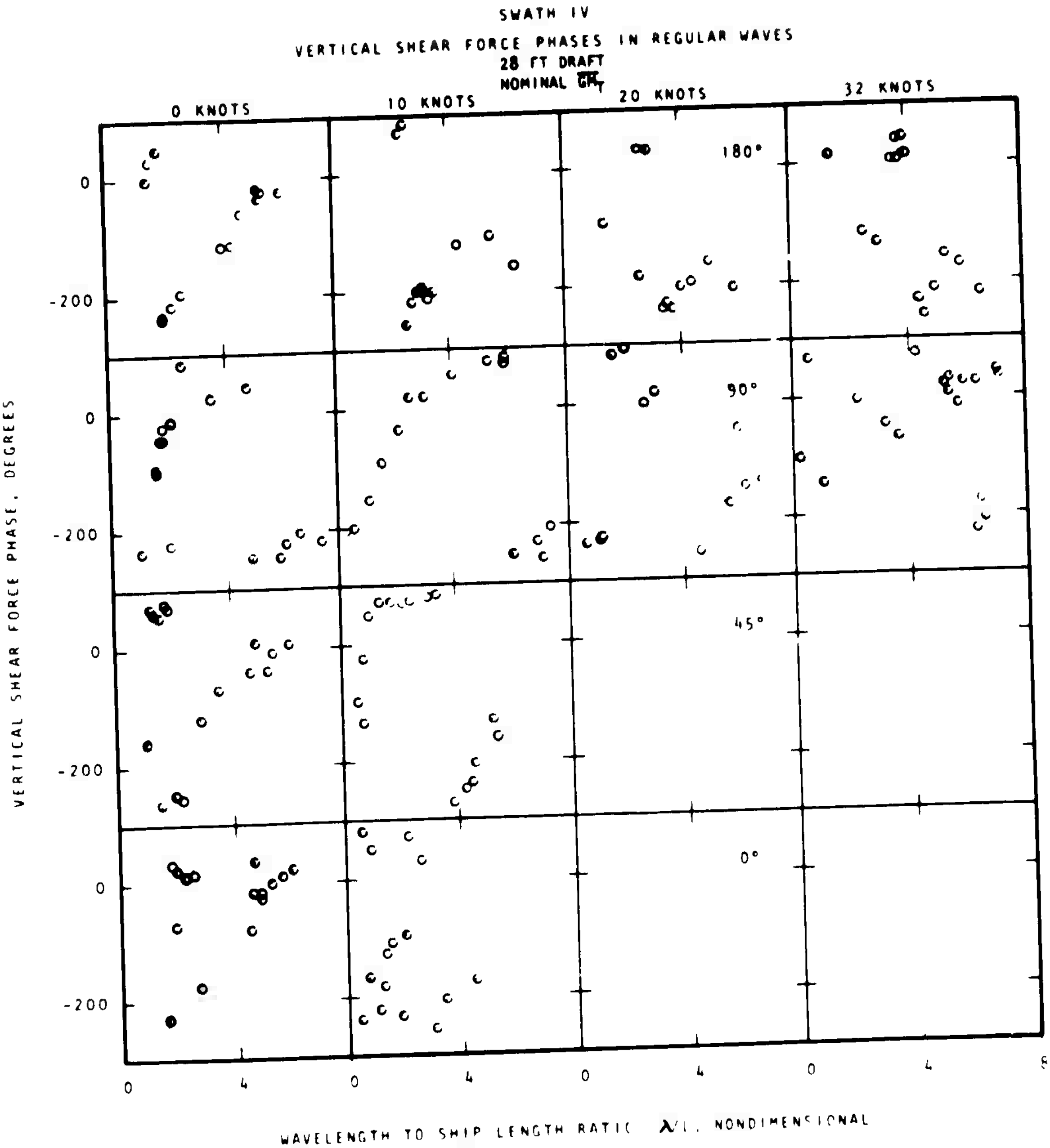

Figure 29 - Vertical Shear Force Phase in Regular Waves,
28 ft Draft, Nominal $\overline{GM}_t$

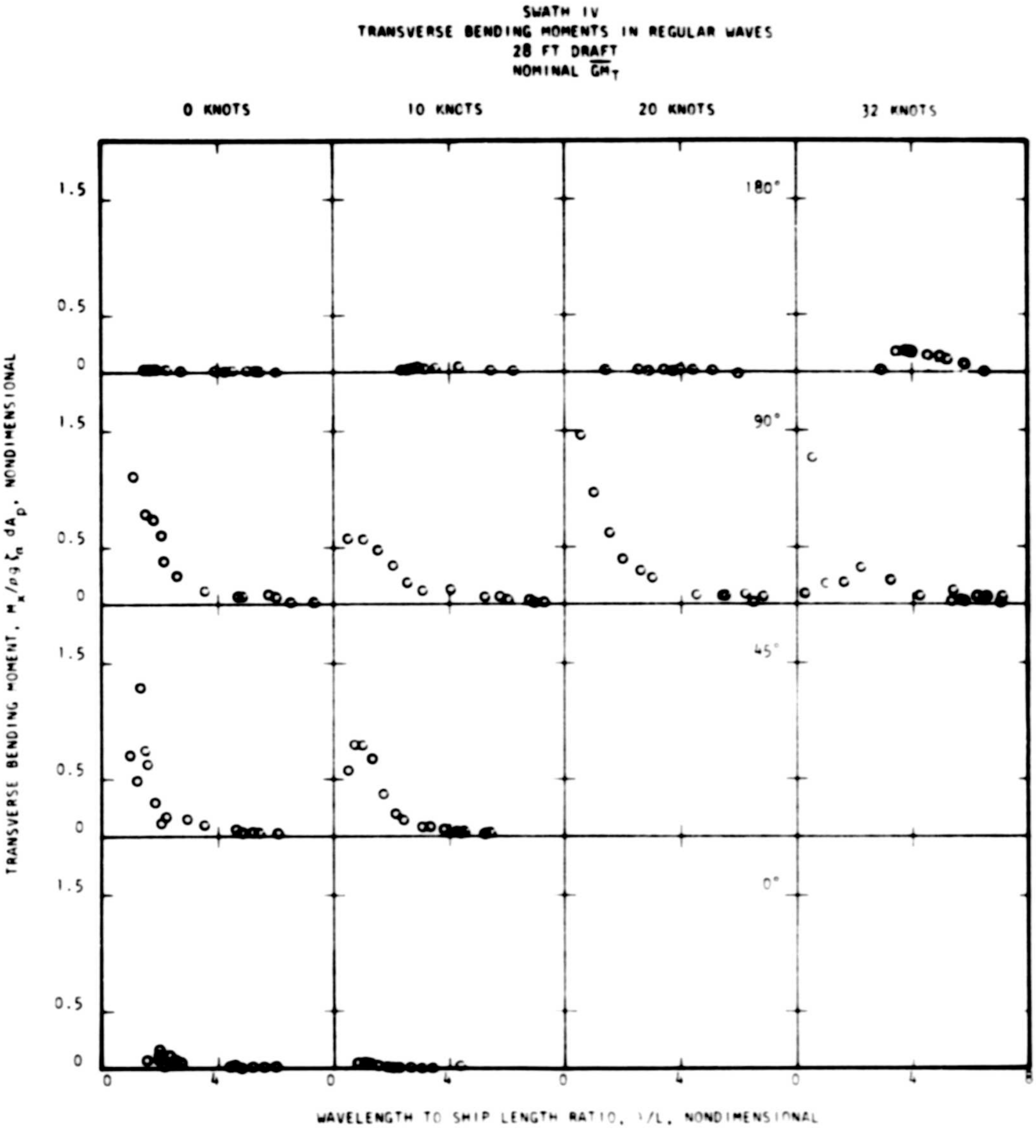

Figure 30 - Dimensionless Transverse Vertical Bending Moment in Regular Waves, 28 ft Draft, Nominal $\overline{GM}_t$

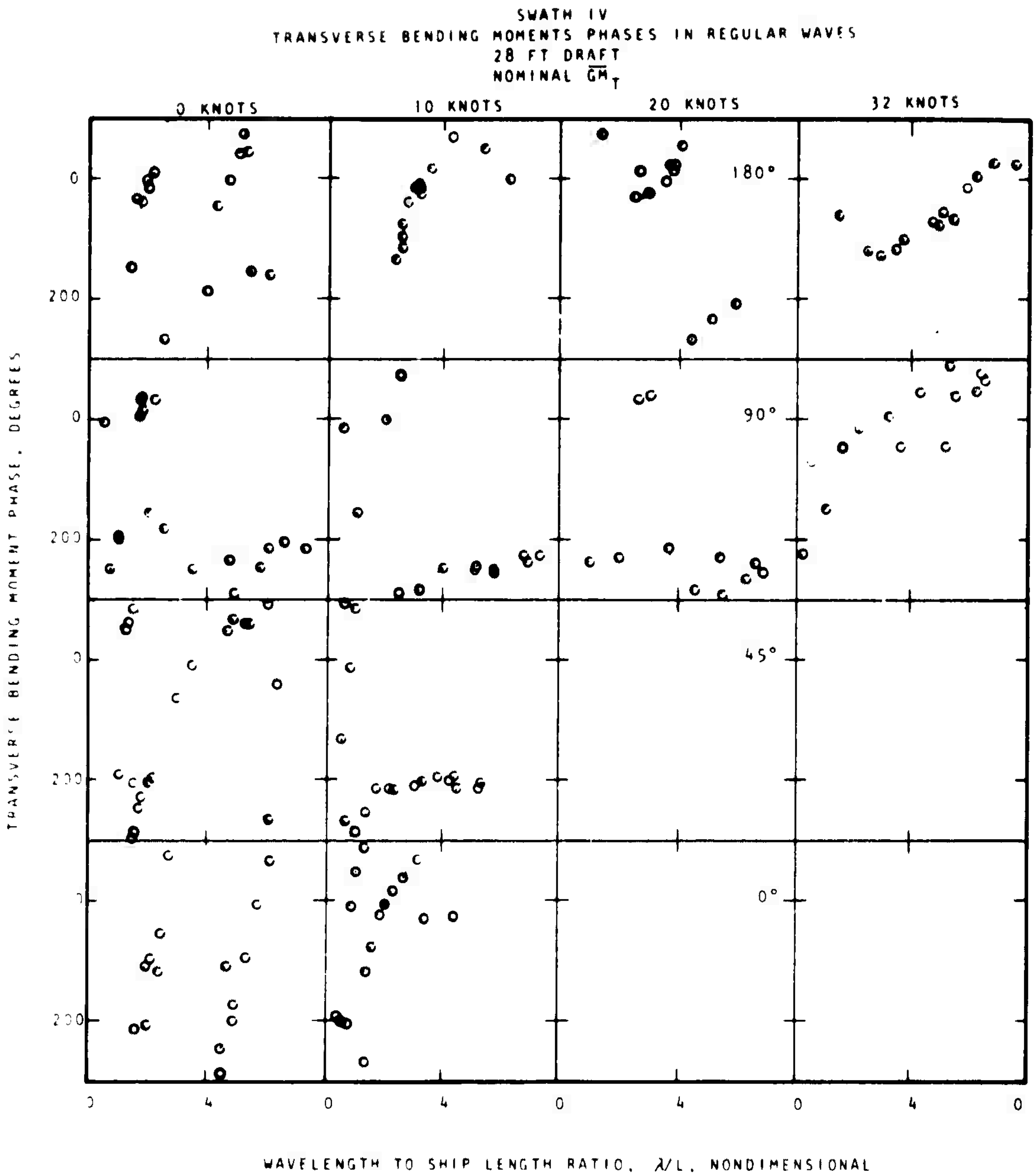

Figure 31 - Transverse Vertical Bending Moment Phase in Regular Waves, 28 ft Draft, Nominal $\overline{GM}_t$

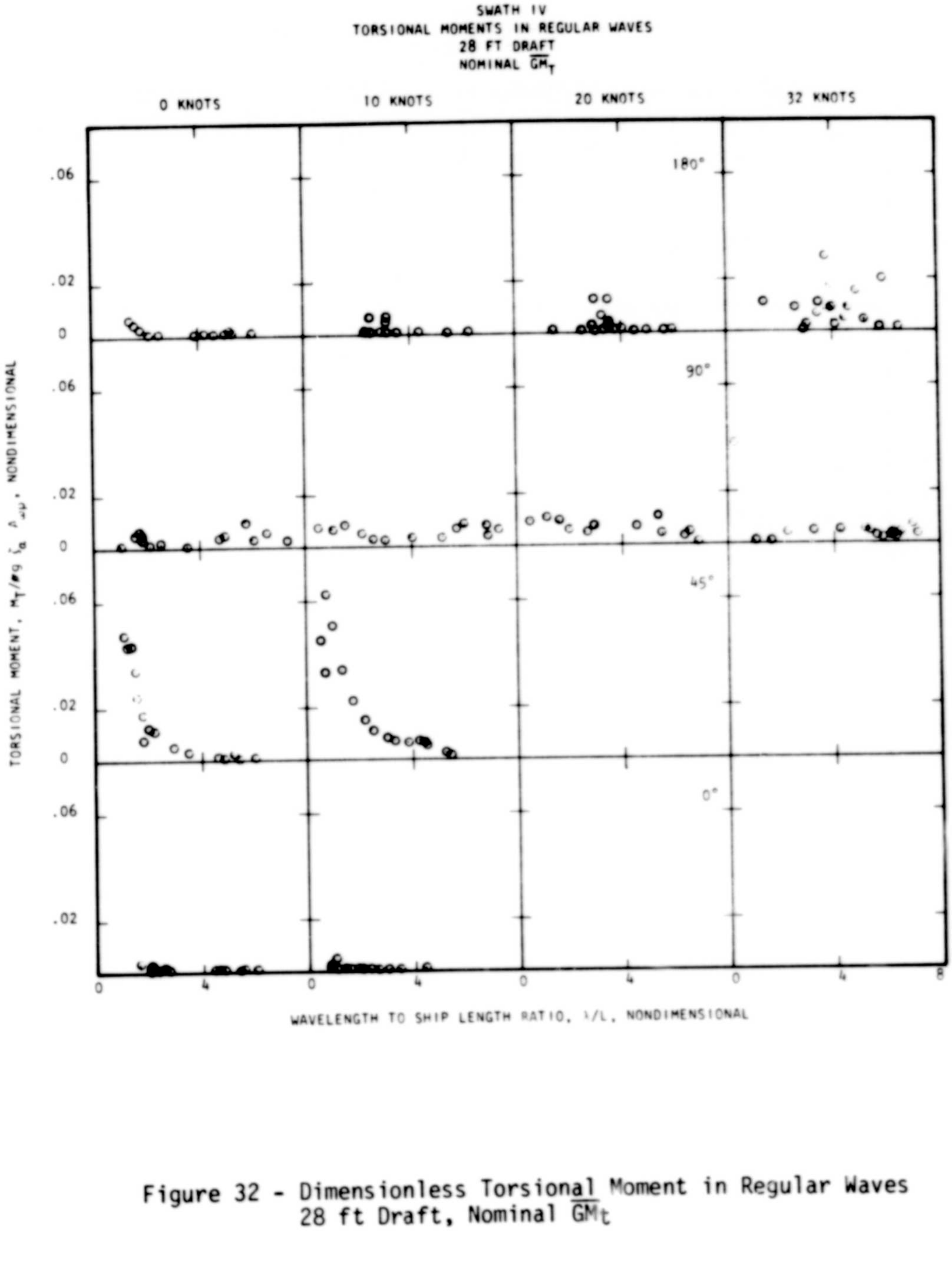

Figure 32 - Dimensionless Torsional Moment in Regular Waves
28 ft Draft, Nominal $\overline{GM}_t$

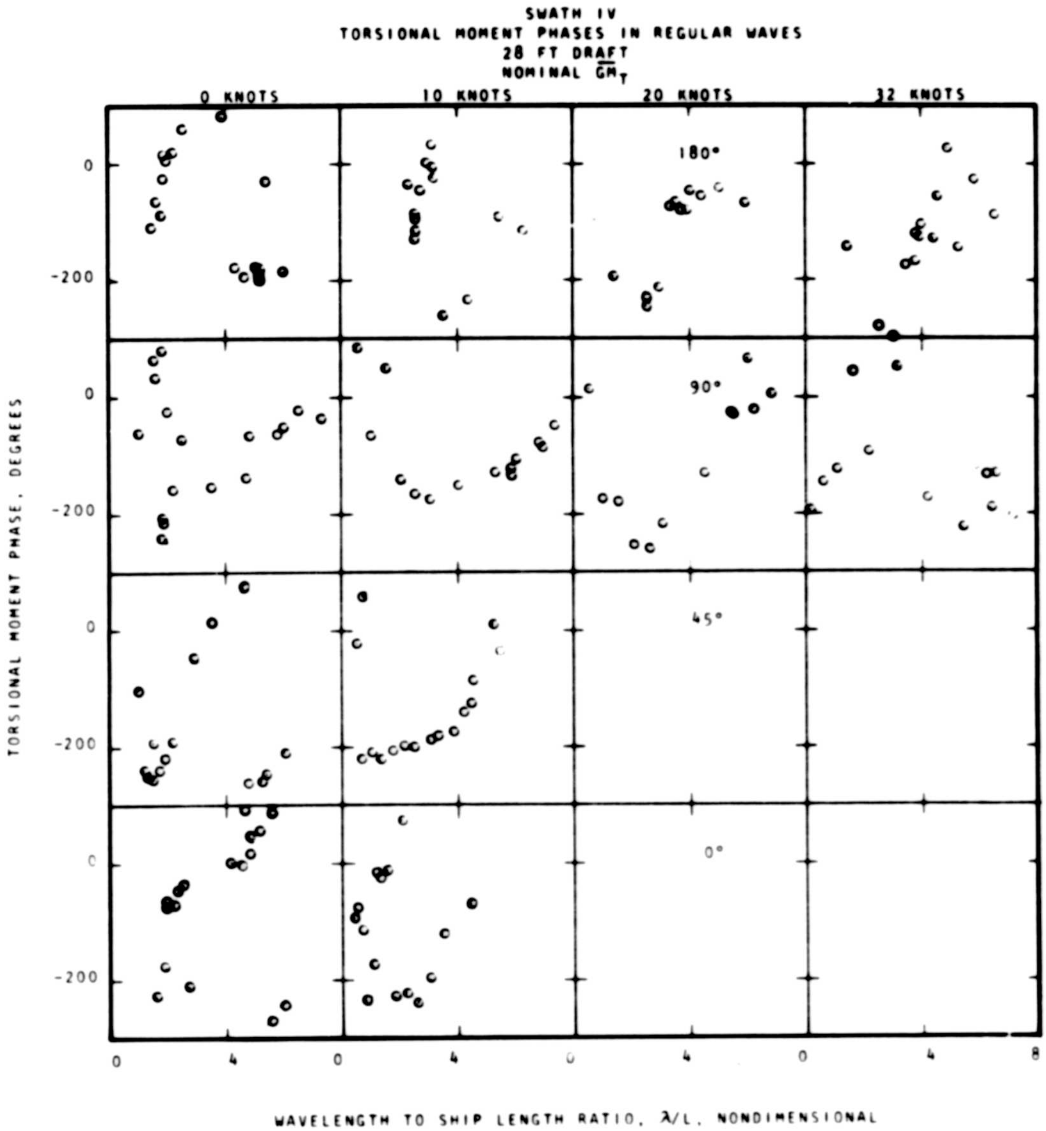

Figure 33- Torsional Moment Phase in Regular Waves, 28 ft Draft, Nominal $\overline{GM}_t$

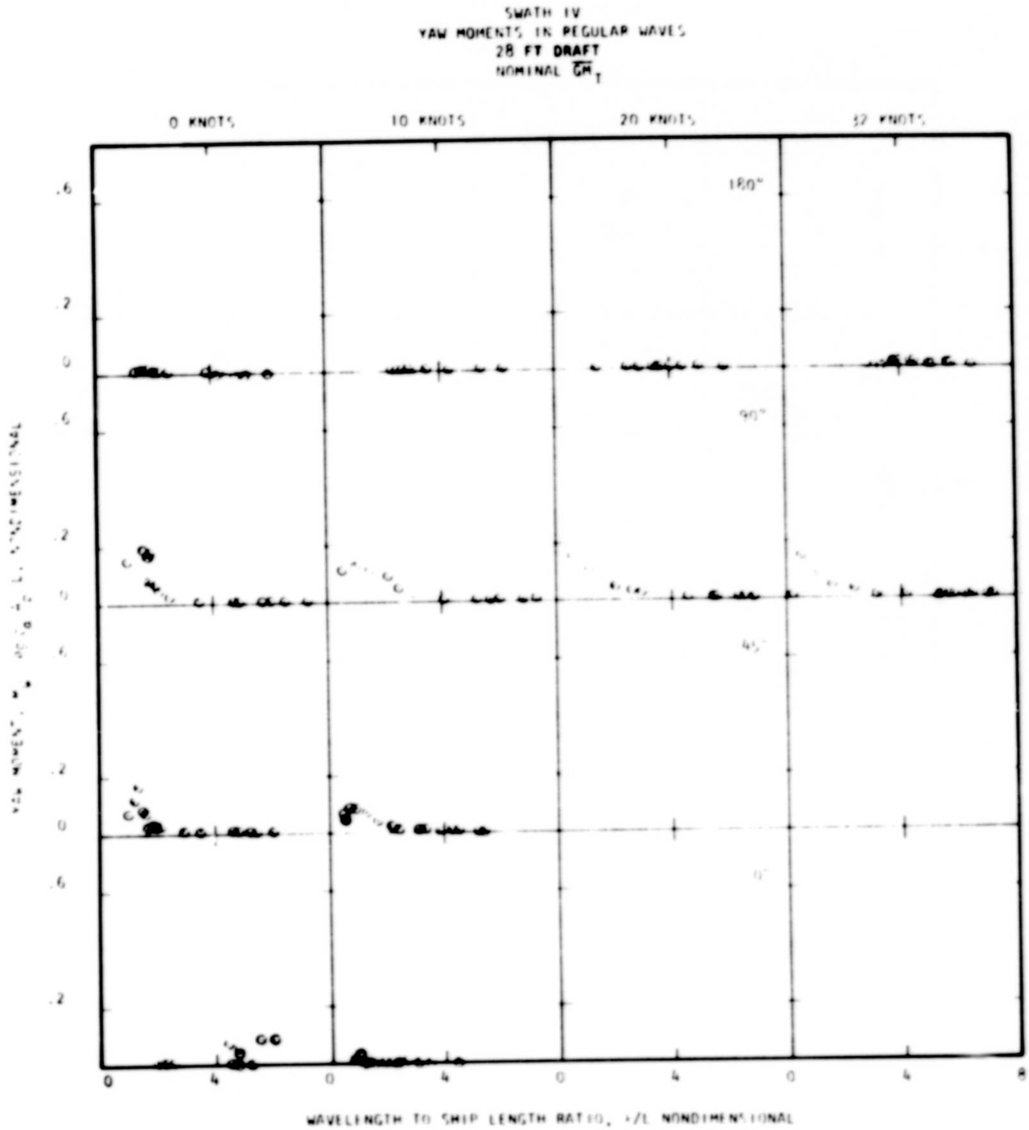

Figure 34 - Dimensionless Yaw Moment in Regular Waves, 28 ft Draft, Nominal $\overline{GM}_t$

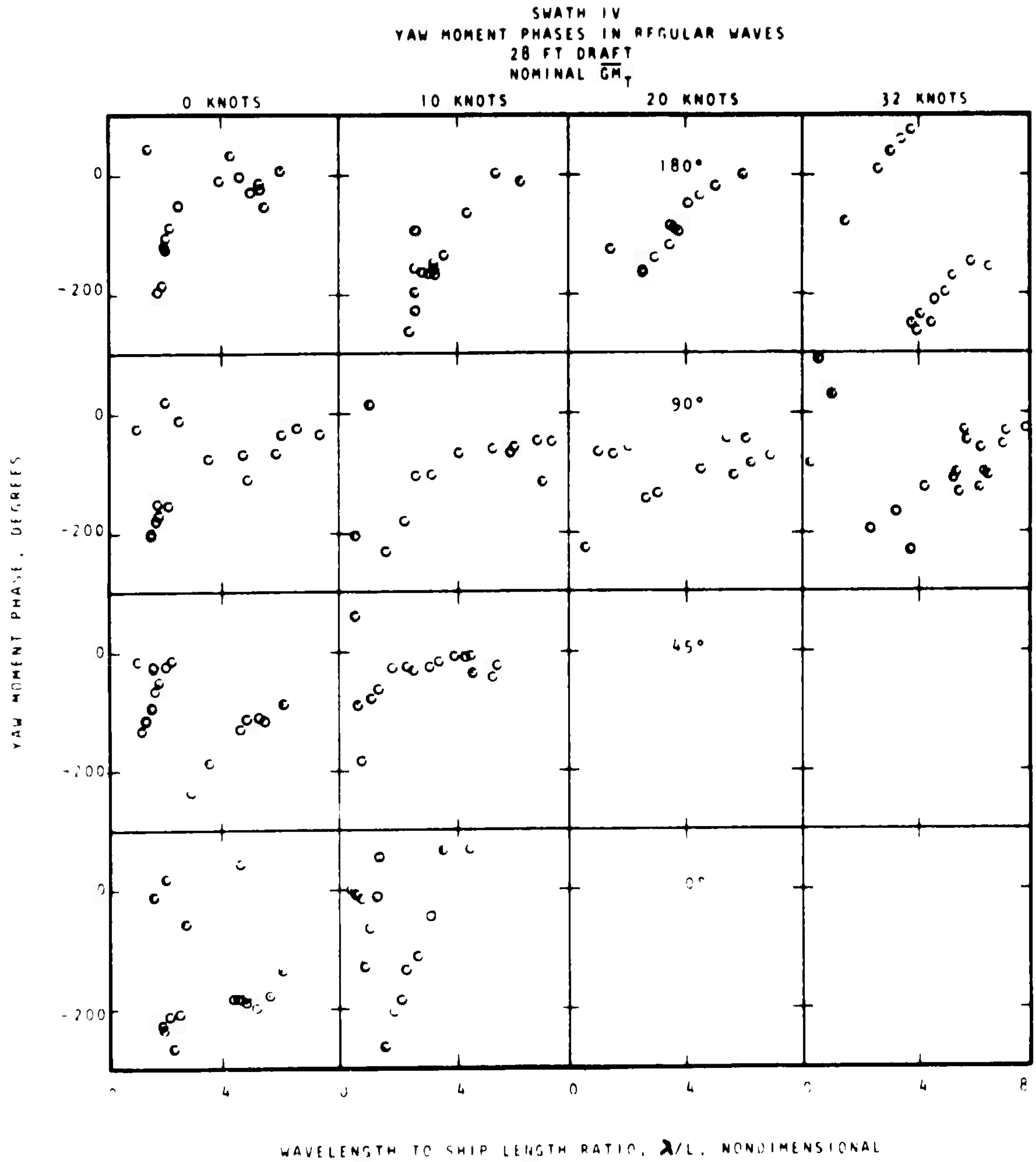

Figure 35 - Yaw Moment Phase in Regular Waves, 28 ft Draft, Nominal $\overline{GM}_t$

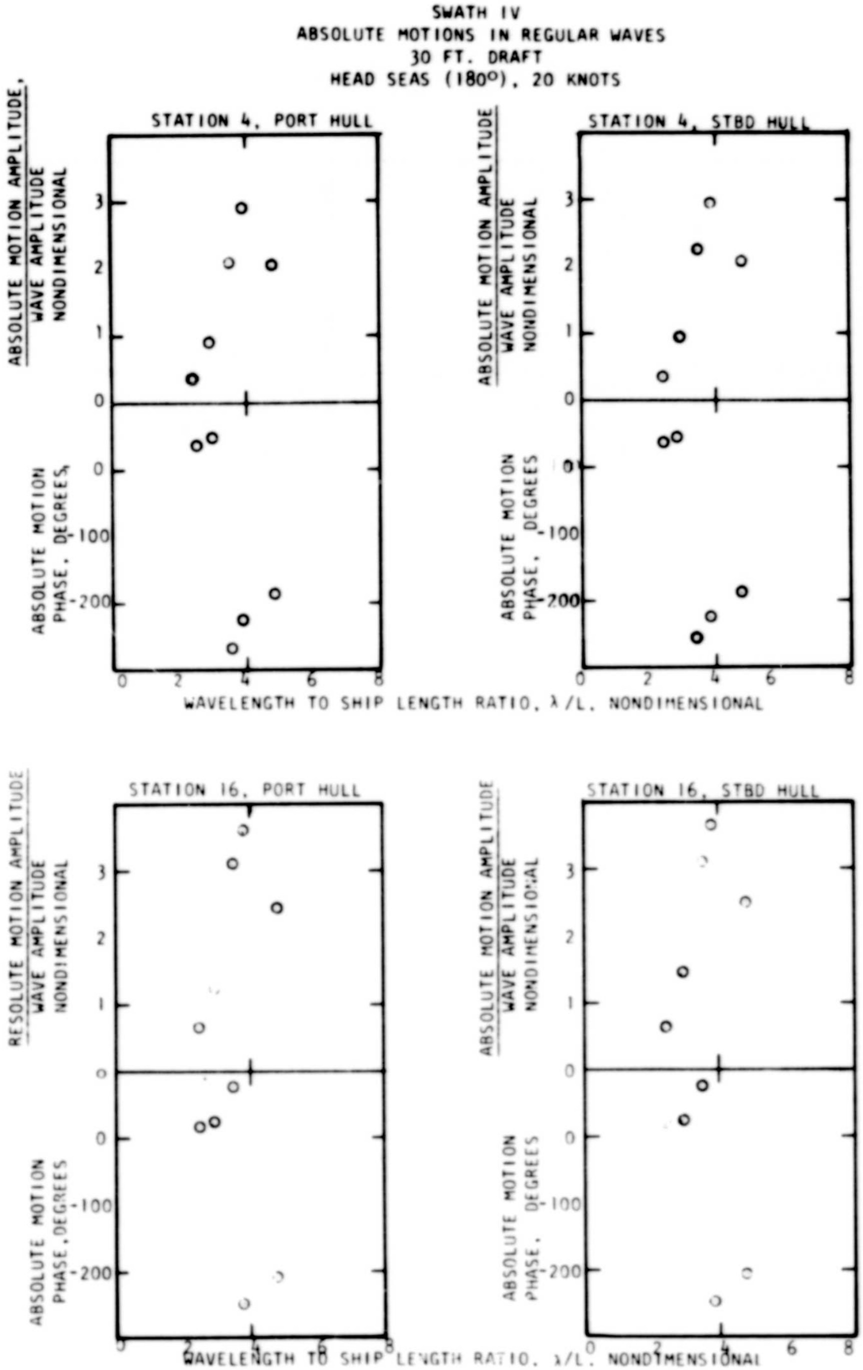

Figure 36 - Absolute Motions and Phases in Regular Head Seas, 30 ft Draft, 20 Knots

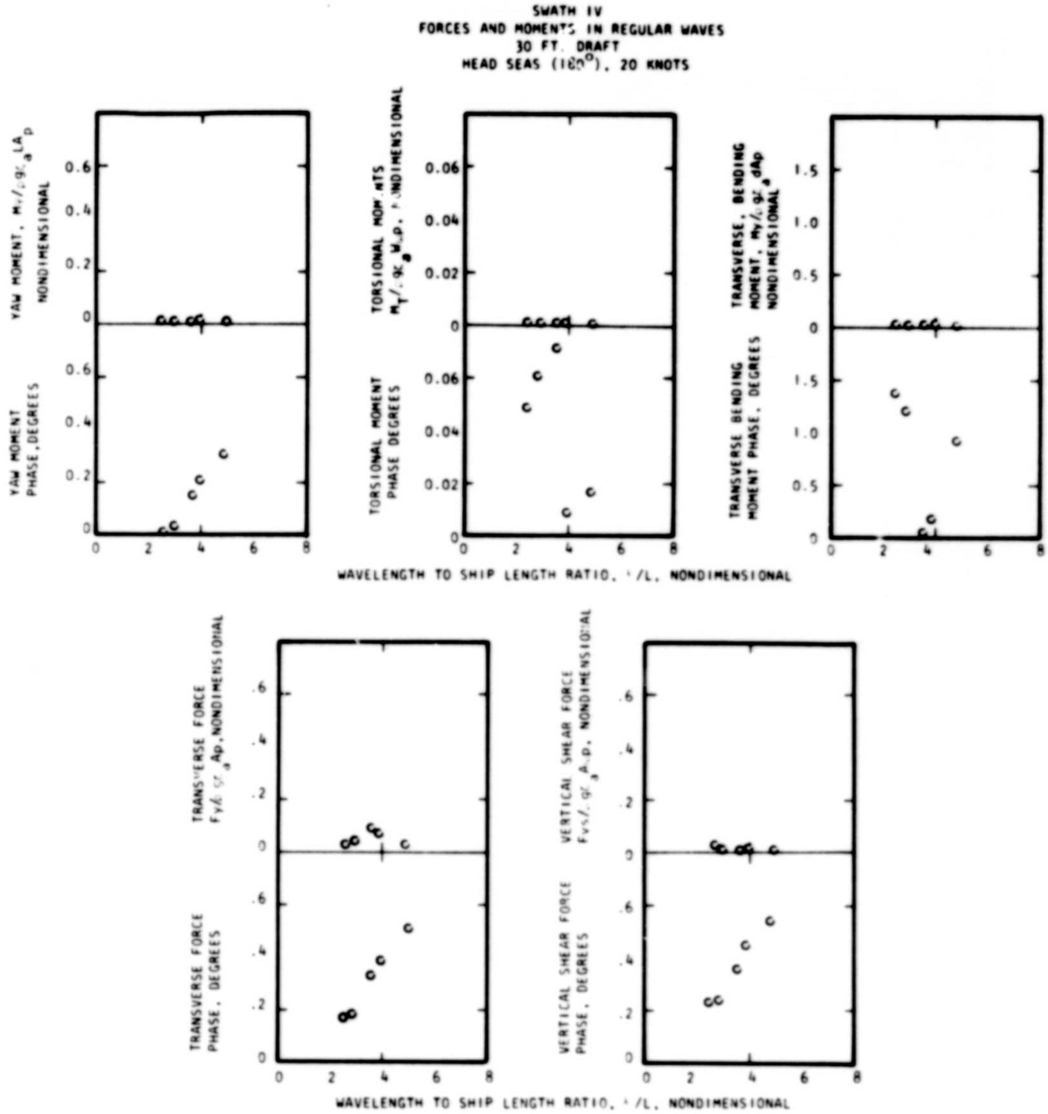

Figure 37 - Forces, Moments and their Phases in Regular Head Seas, 30 ft Draft, 20 Knots

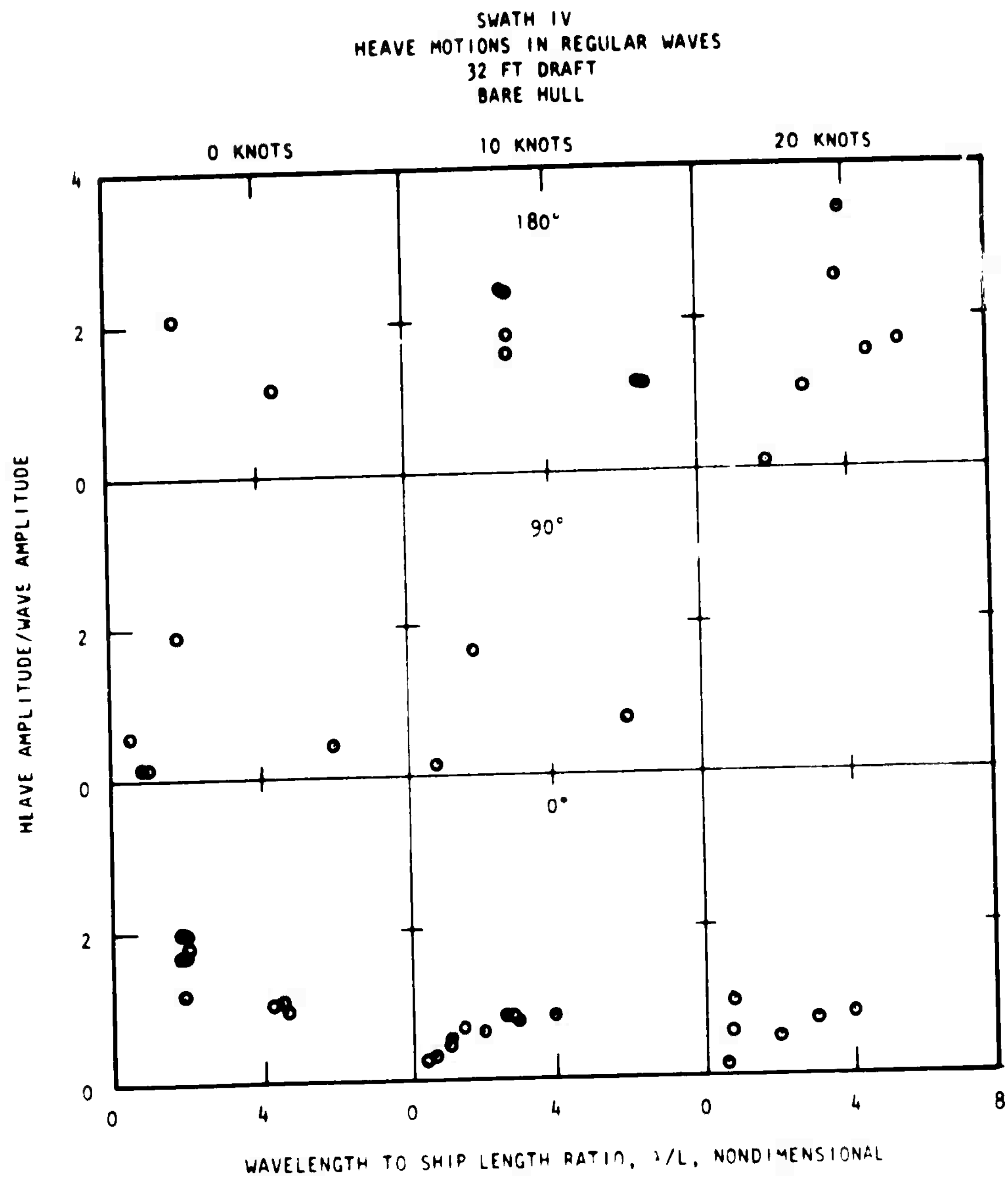

Figure 38 - Dimensionless Heave in Regular Waves, 32 ft Draft, Nominal $\overline{GM}_t$

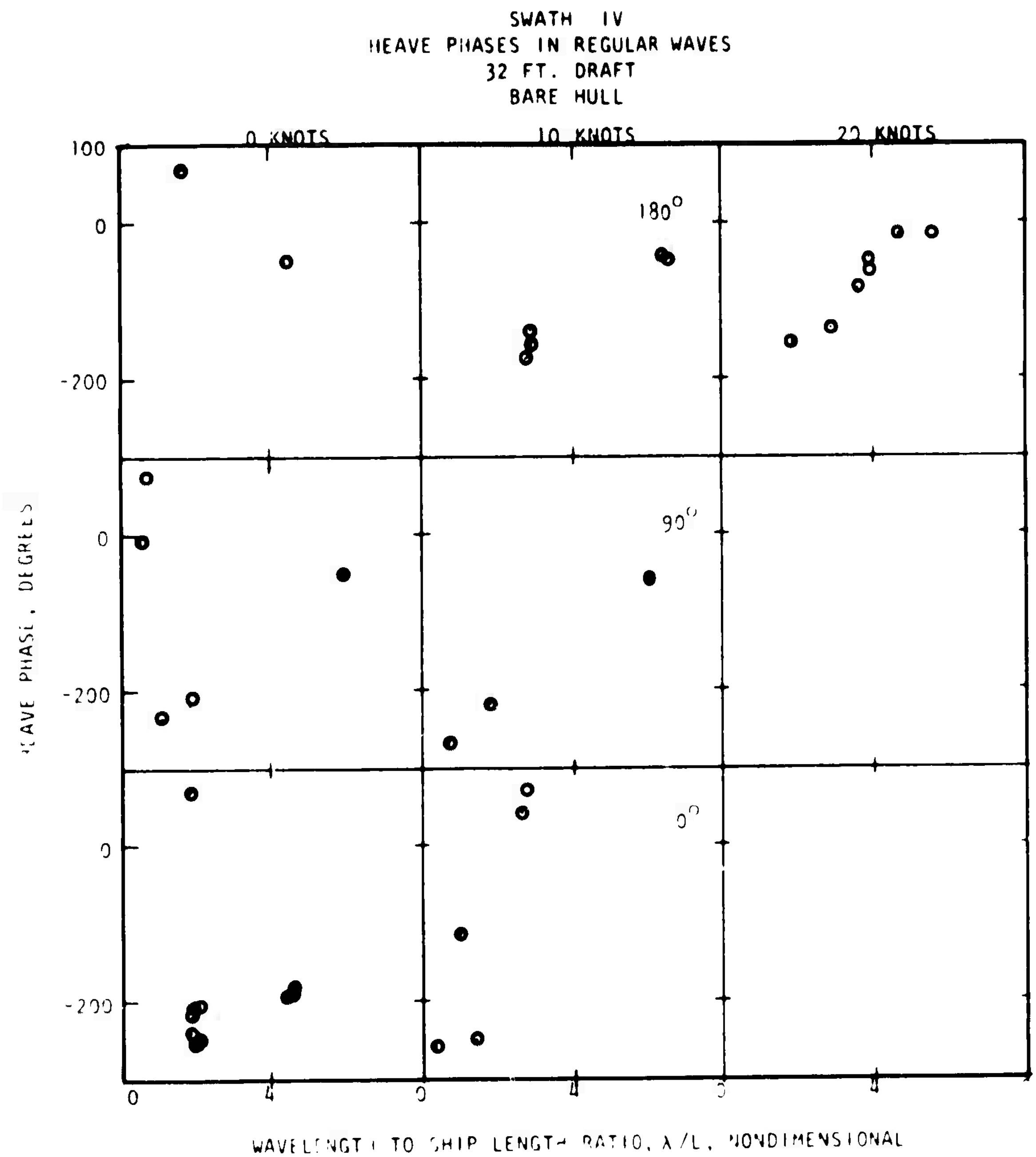

Figure 39 - Heave Phase in Regular Waves, 32 ft Draft, Nominal $\overline{GM}_t$

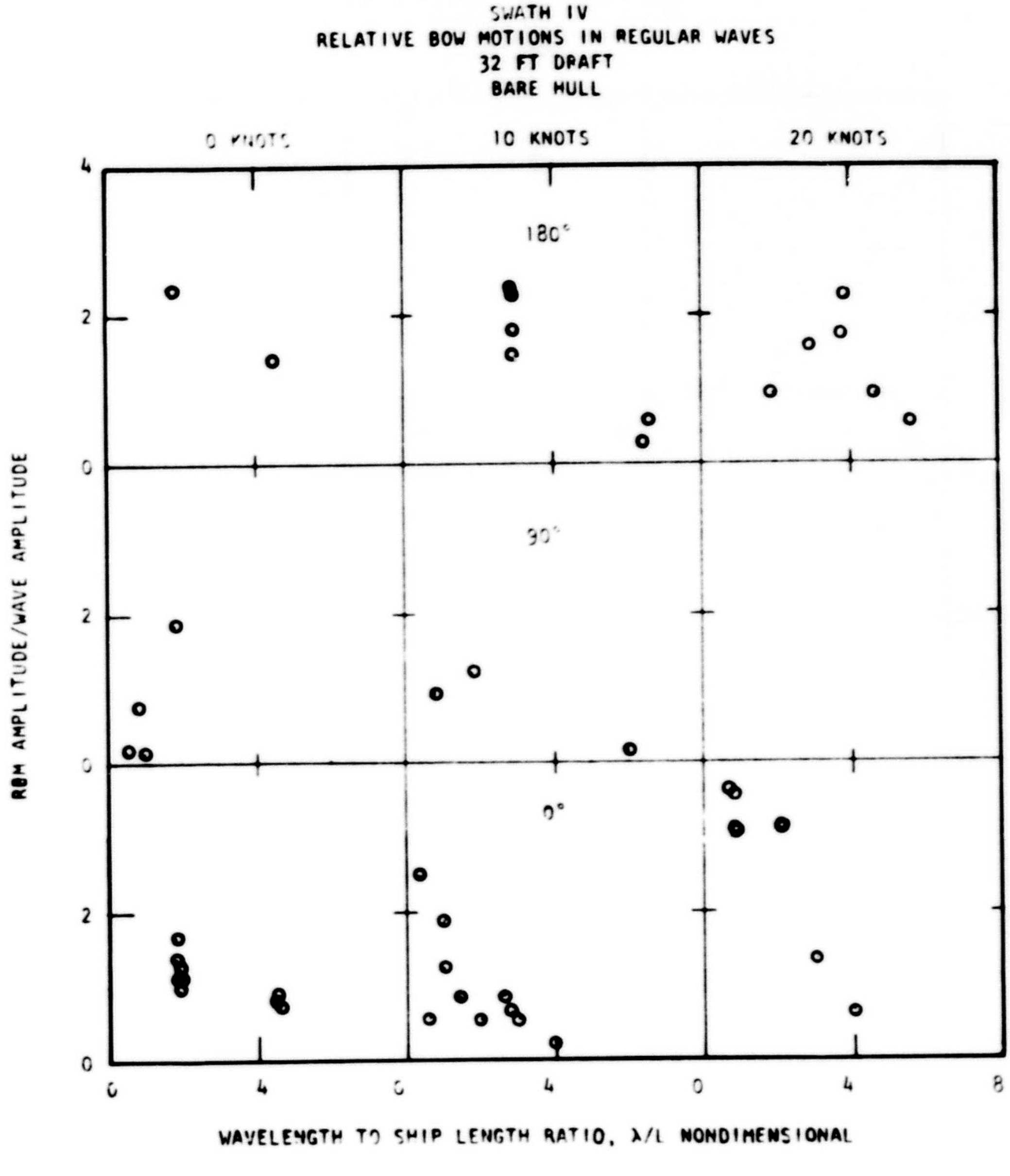

Figure 40 - Dimensionless Relative Bow Motion in Regular Waves, 32 ft Draft, Nominal $\overline{GM}_t$

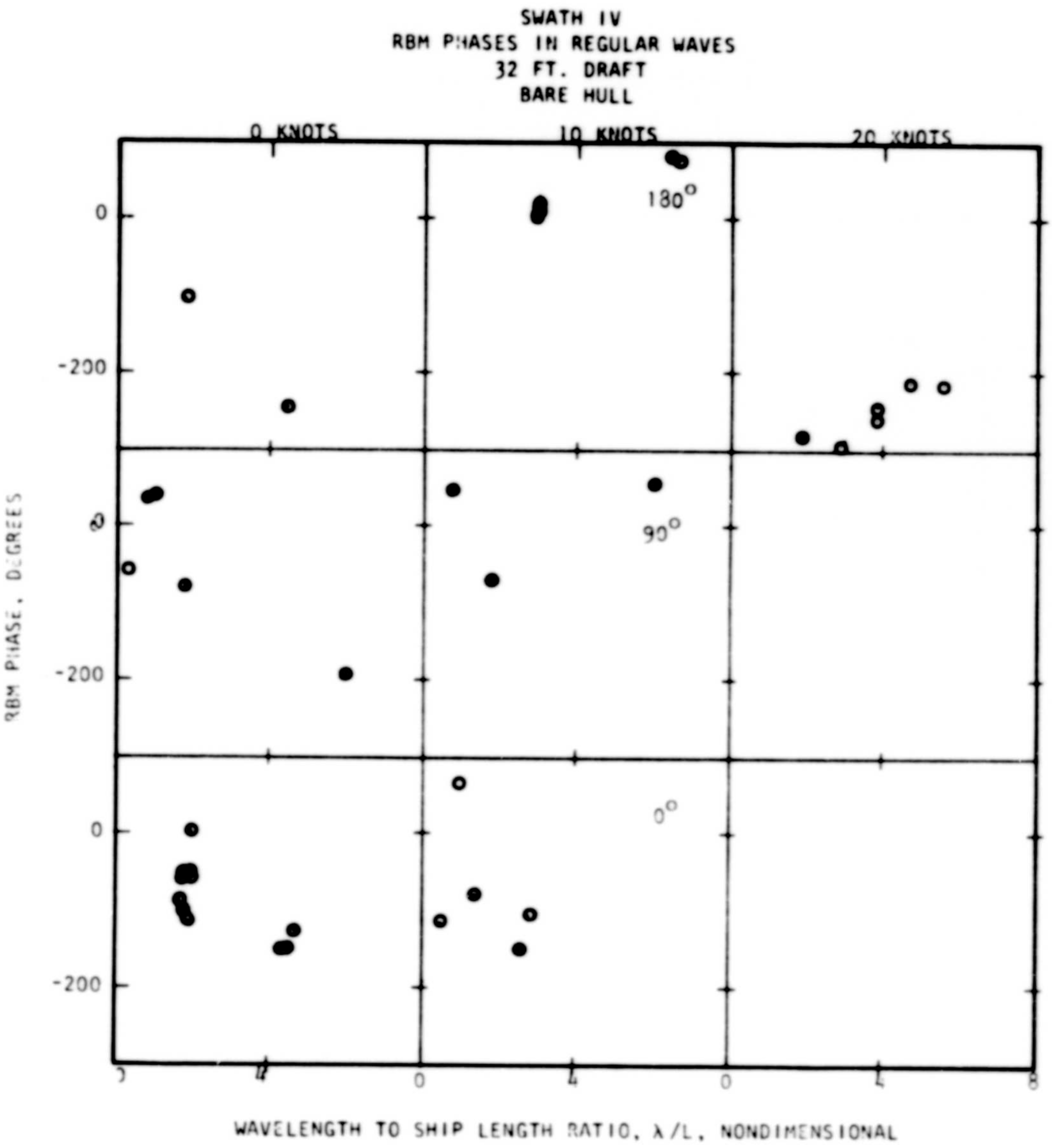

Figure 41 - Relative Bow Motion Phase in Regular Waves, 32 ft Draft, Nominal $\overline{GM}_t$

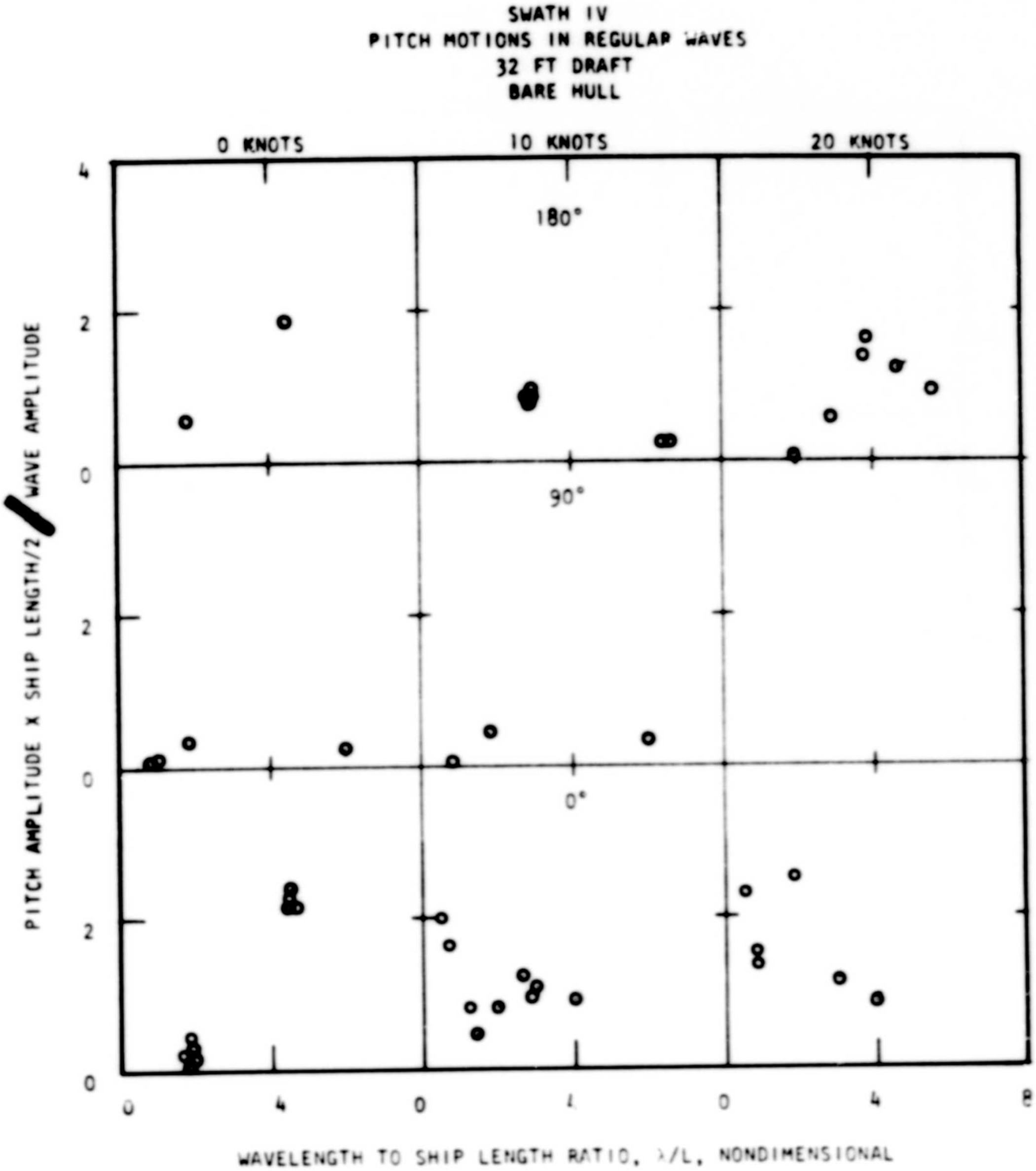

Figure 42 - Dimensionless Pitch in Regular Waves, 32 ft Draft, Nominal $\overline{GM}_t$

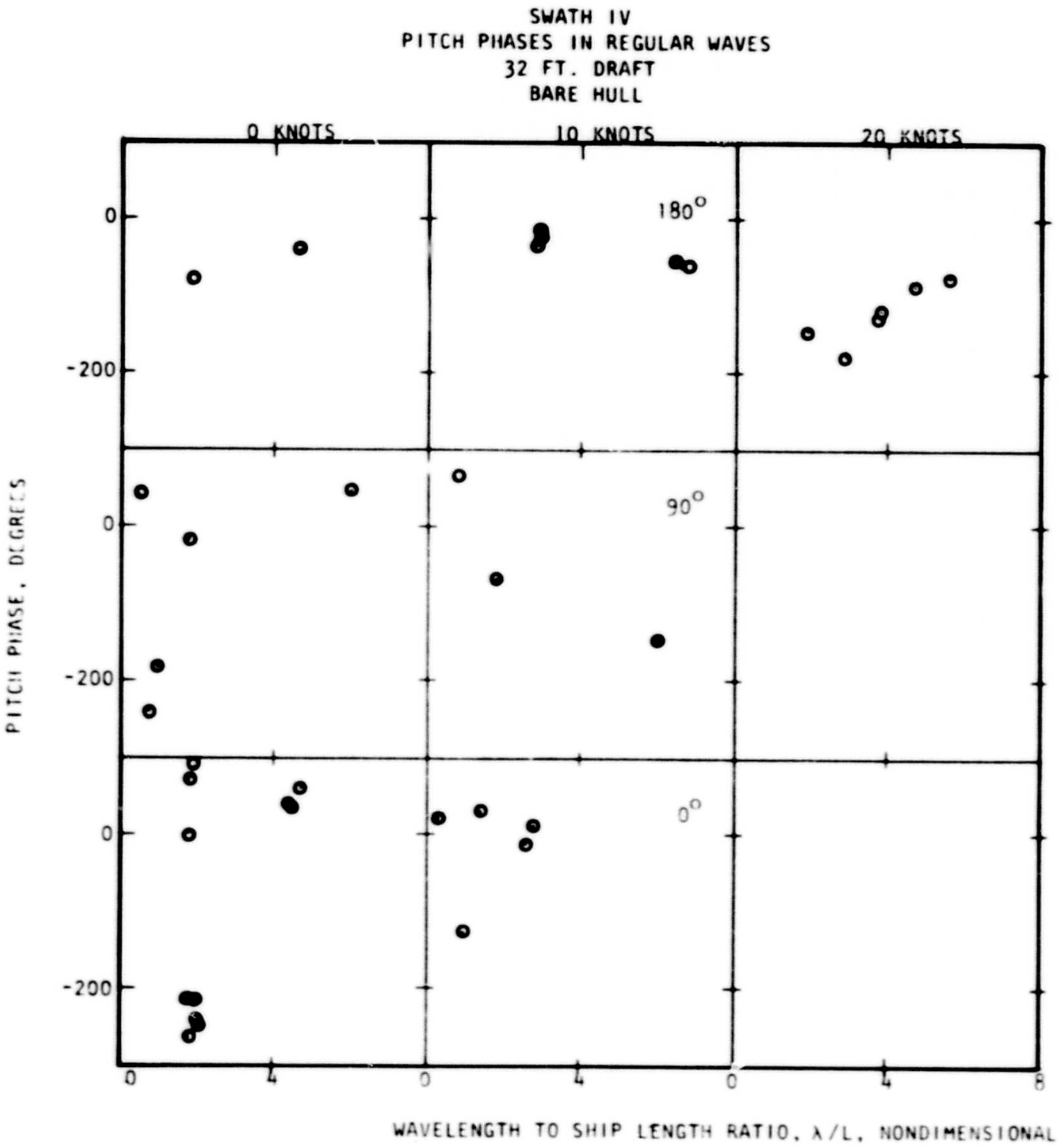

Figure 43 - Pitch Phase in Regular Waves, 32 ft Draft, Nominal $\overline{GM}_t$

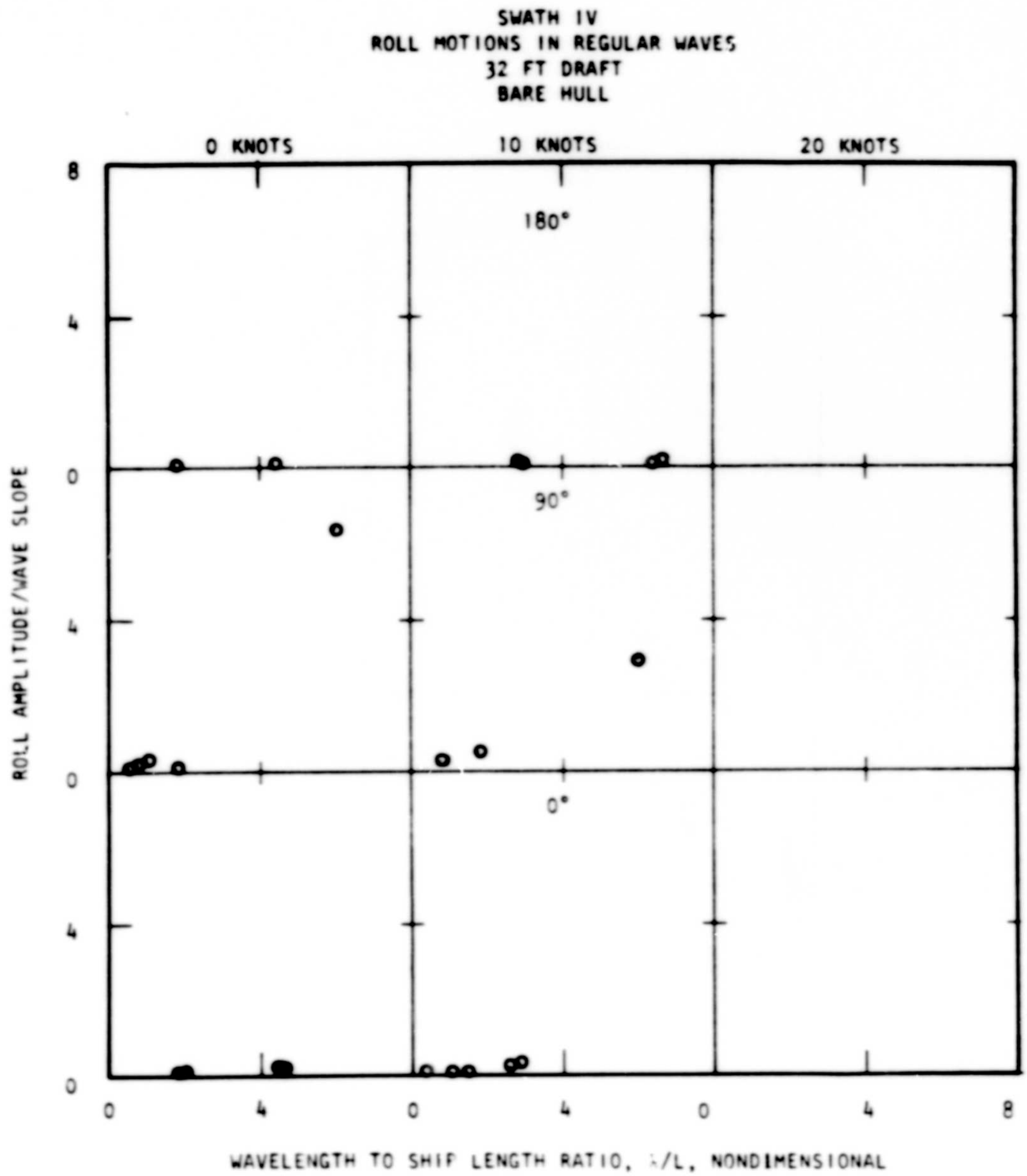

Figure 44 - Dimensionless Roll in Regular Waves, 32 ft Draft, Nominal $\overline{GM}_t$

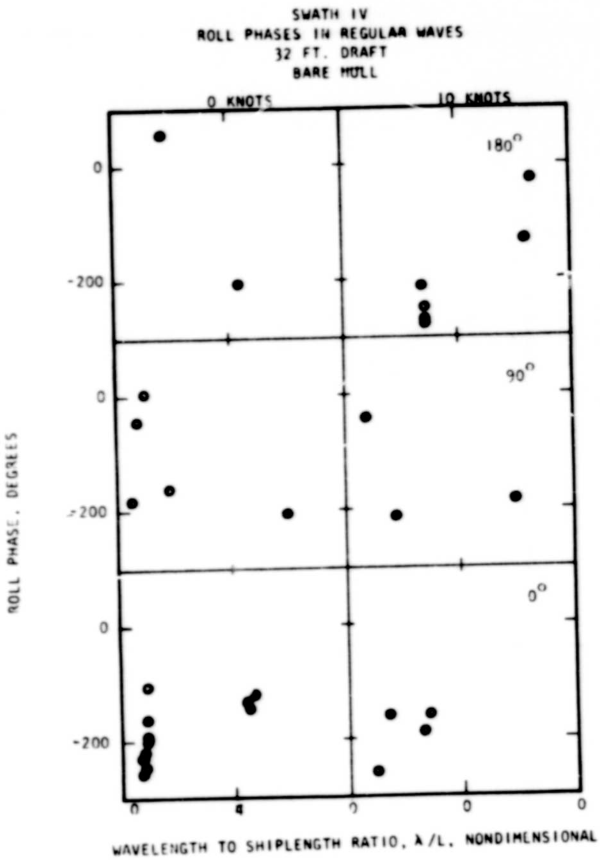

Figure 45 - Roll Phase in Regular Waves, 32 ft Draft
Nominal $\overline{GM}_t$

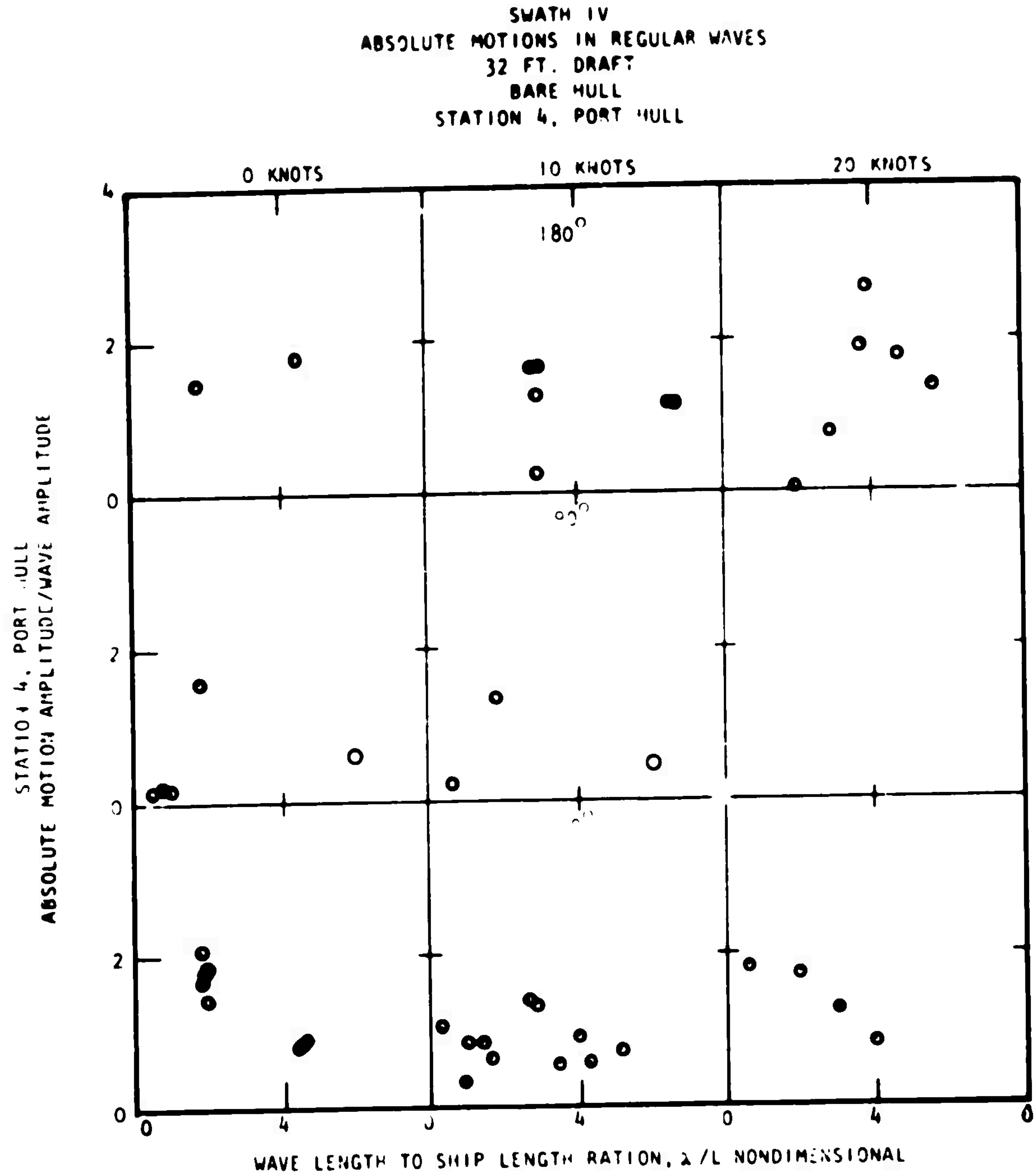

Figure 46 - Dimensionless Absolute Motion in Regular Waves, Forward Port, 32 ft Draft, Nominal $\overline{GM}_t$

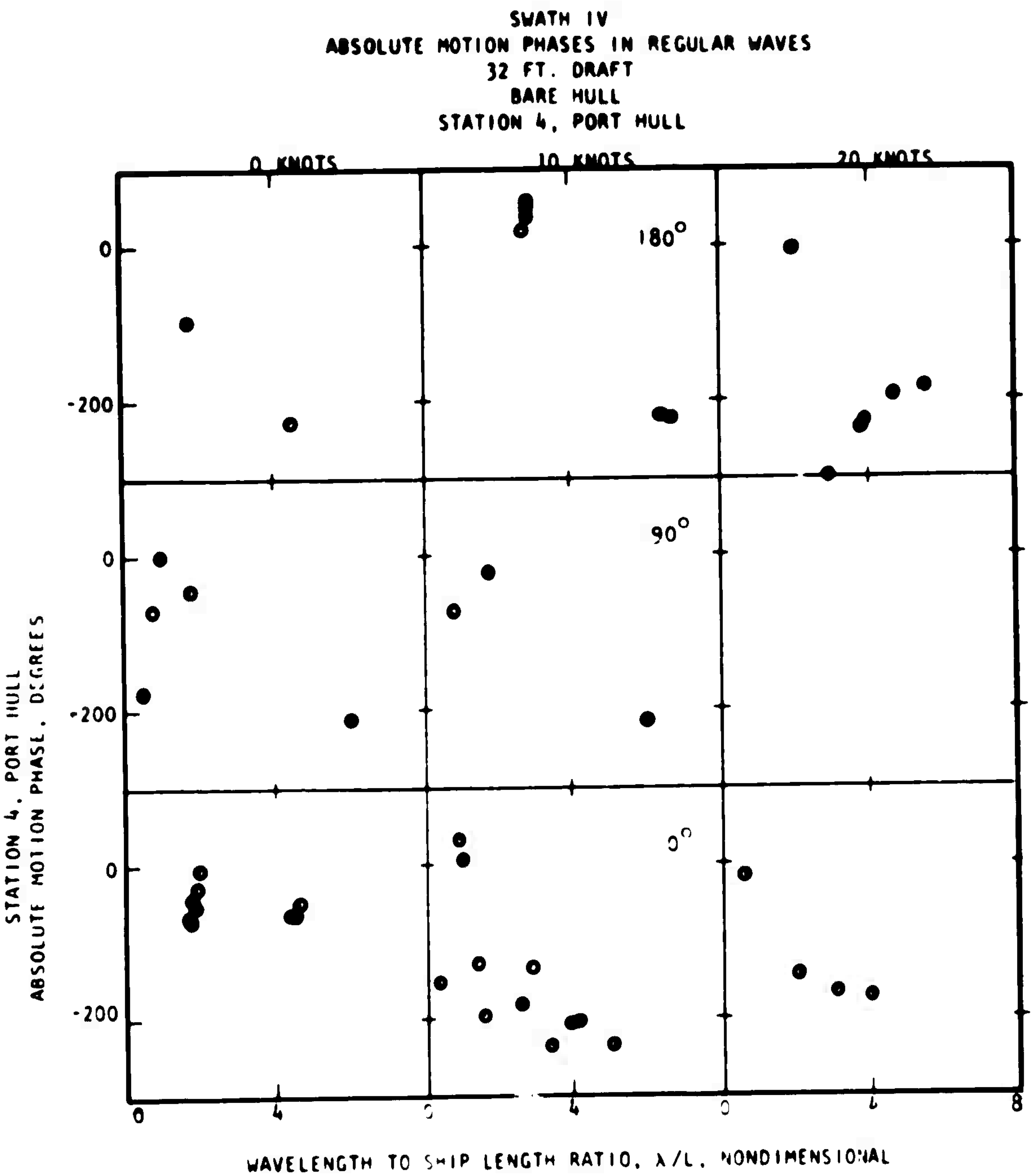

Figure 47 - Absolute Motion Phase in Regular Waves, Forward Port, 32 ft Draft, Nominal $\overline{GM}_t$

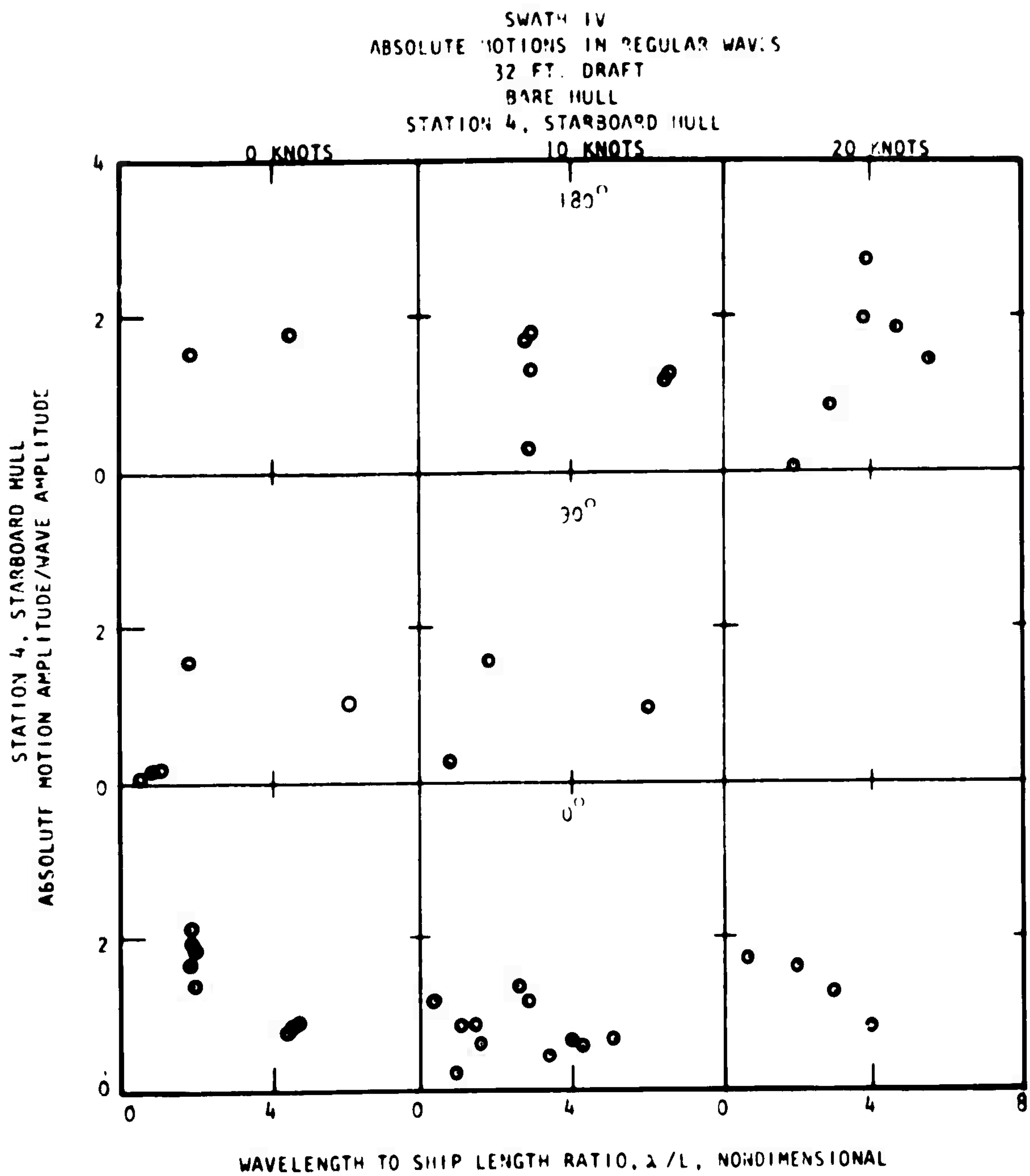

Figure 48 - Dimensionless Absolute Motion in Regular Waves, Forward Starboard, 32 ft Draft, Nominal $\overline{GM}_t$

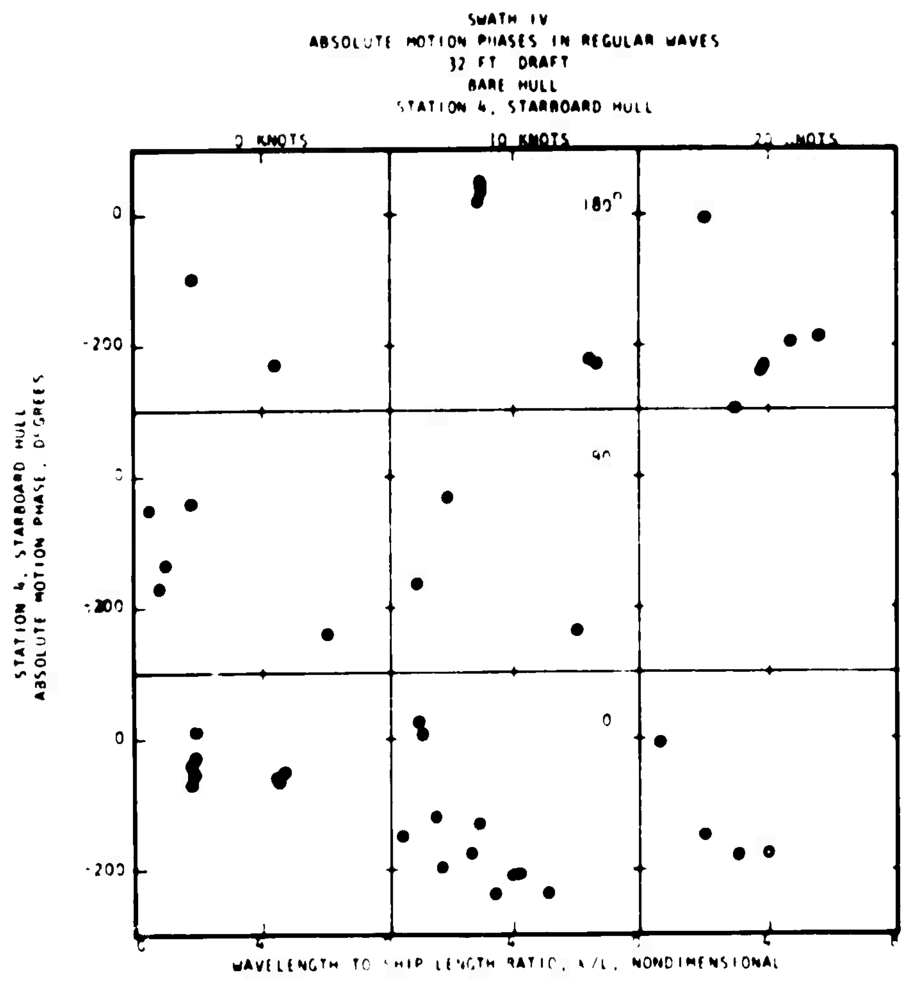

Figure 49 - Absolute Motion Phase in Regular Waves, Forward Starboard, 32 ft Draft, Nominal $\overline{GM}_t$

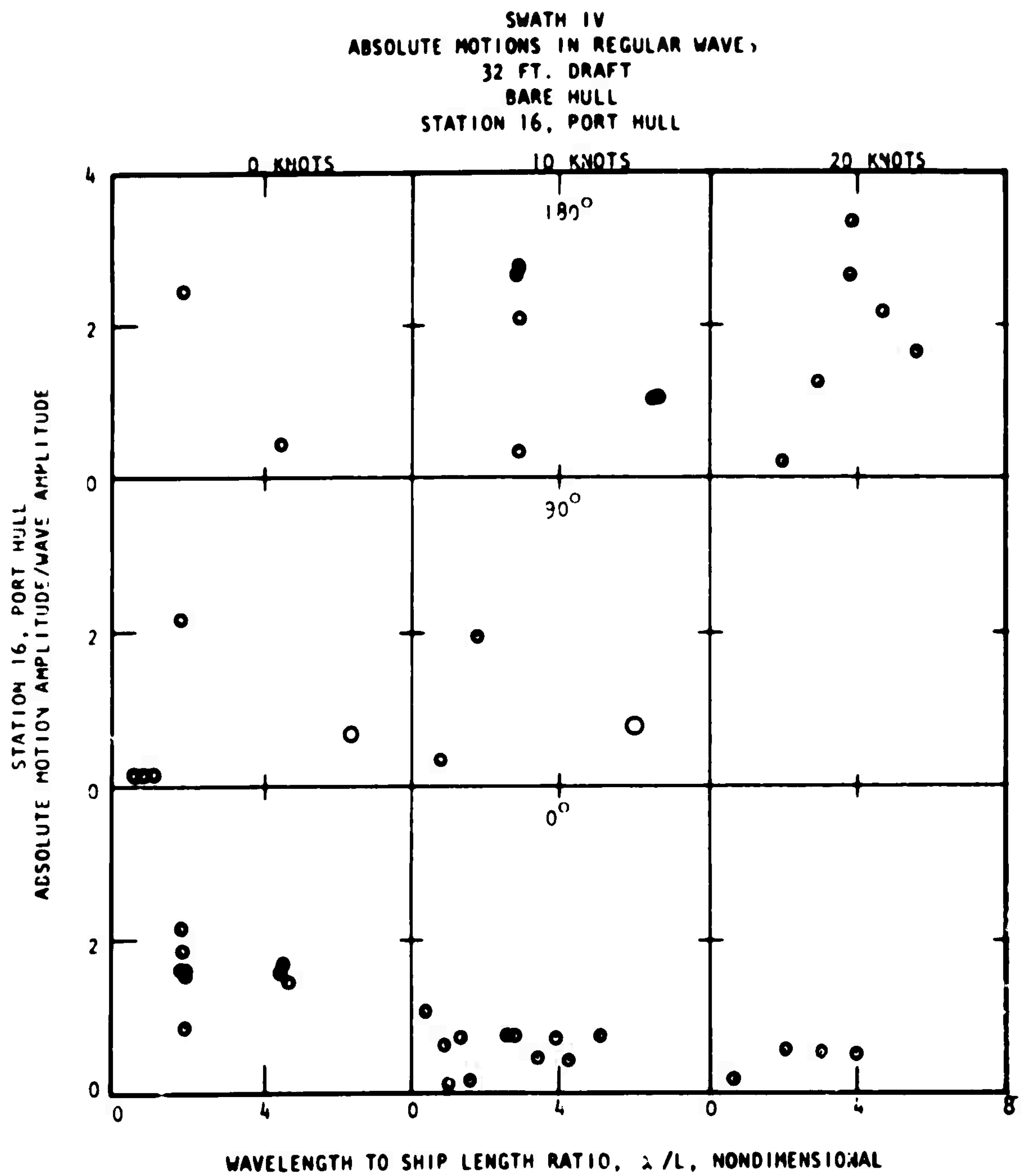

Figure 50 - Dimensionless Absolute Motion in Regular Waves, Aft Port, 32 ft Draft, Nominal $\overline{GM}_t$

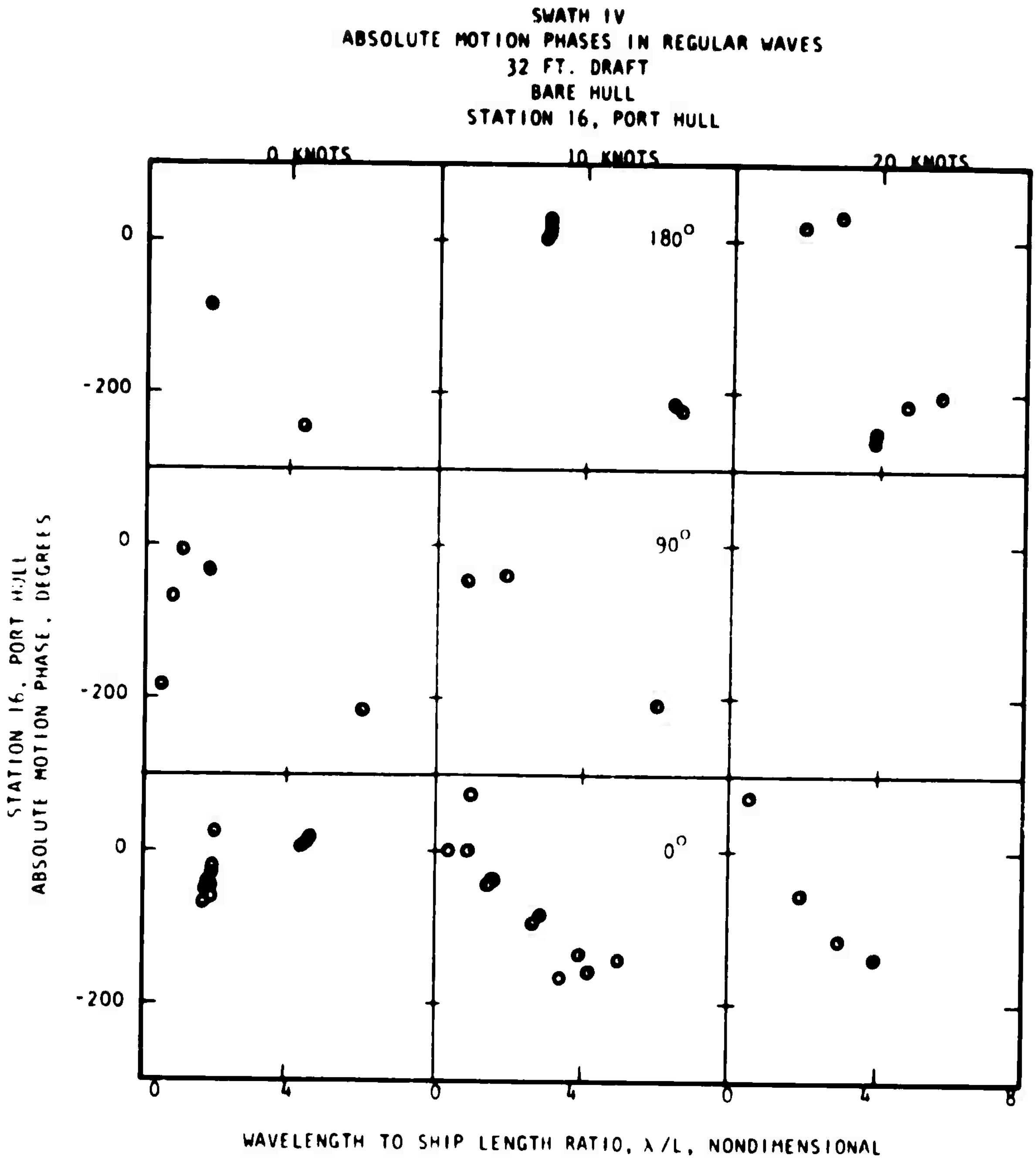

Figure 51 - Absolute Motion Phase in Regular Waves, Aft Port, 32 ft Draft, Nominal $\overline{GM}_t$

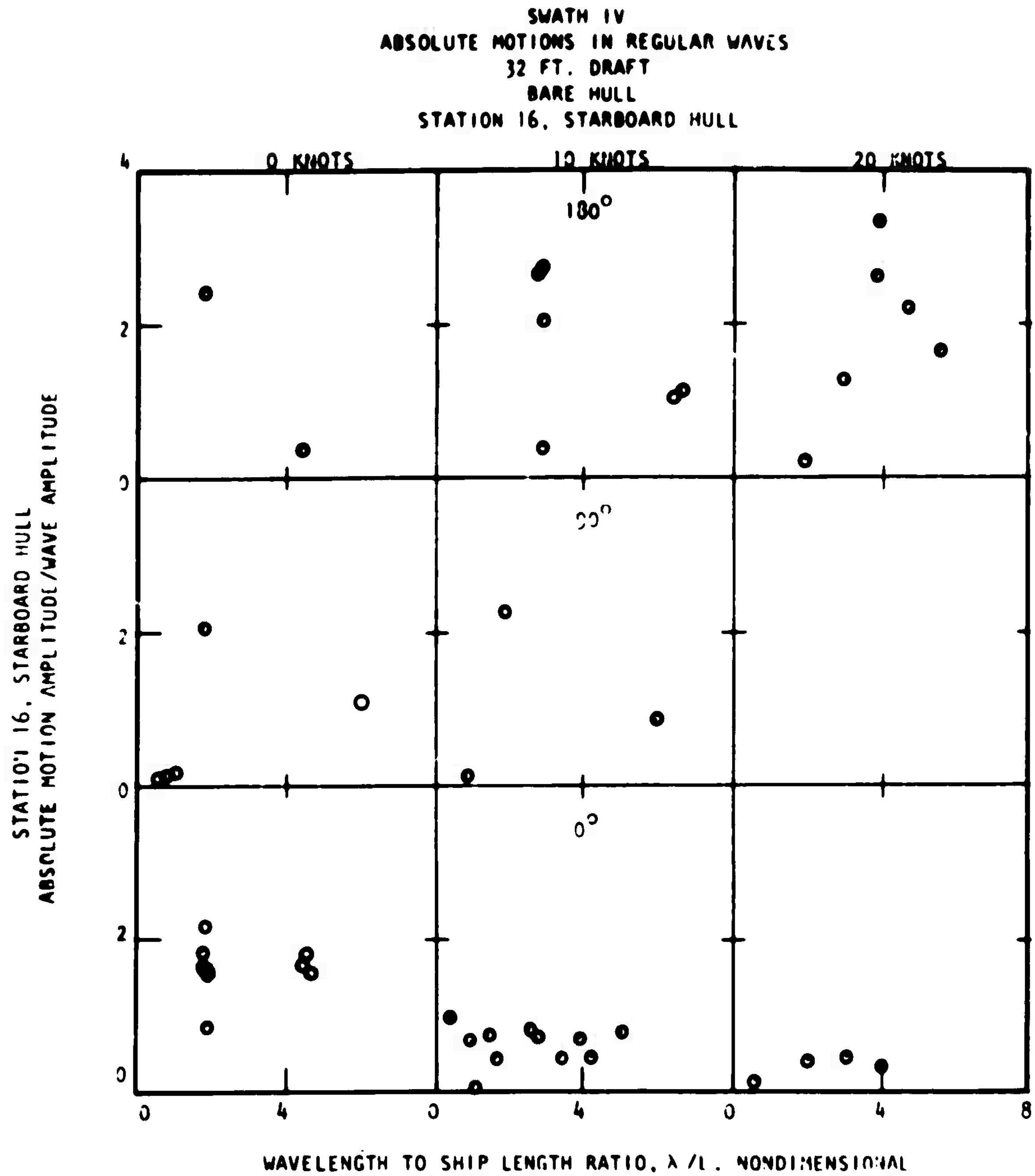

Figure 52 - Dimensionless Absolute Motion in Regular Waves, Aft Starboard, 32 ft Draft, Nominal $\overline{GM}_t$

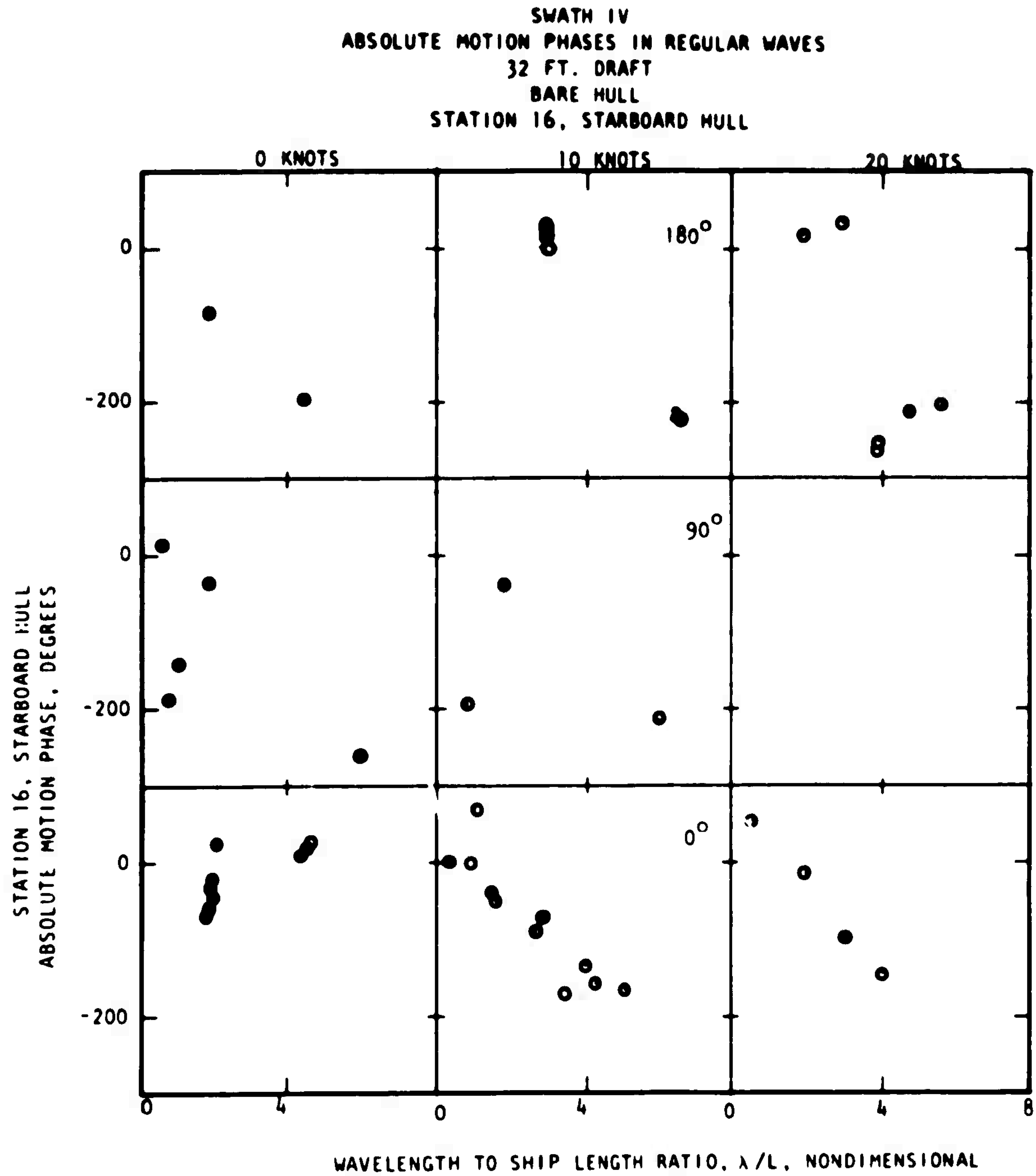

Figure 53 - Absolute Motion Phase in Regular Waves, Aft Starboard, 32 ft Draft, Nominal $\overline{GM}_t$

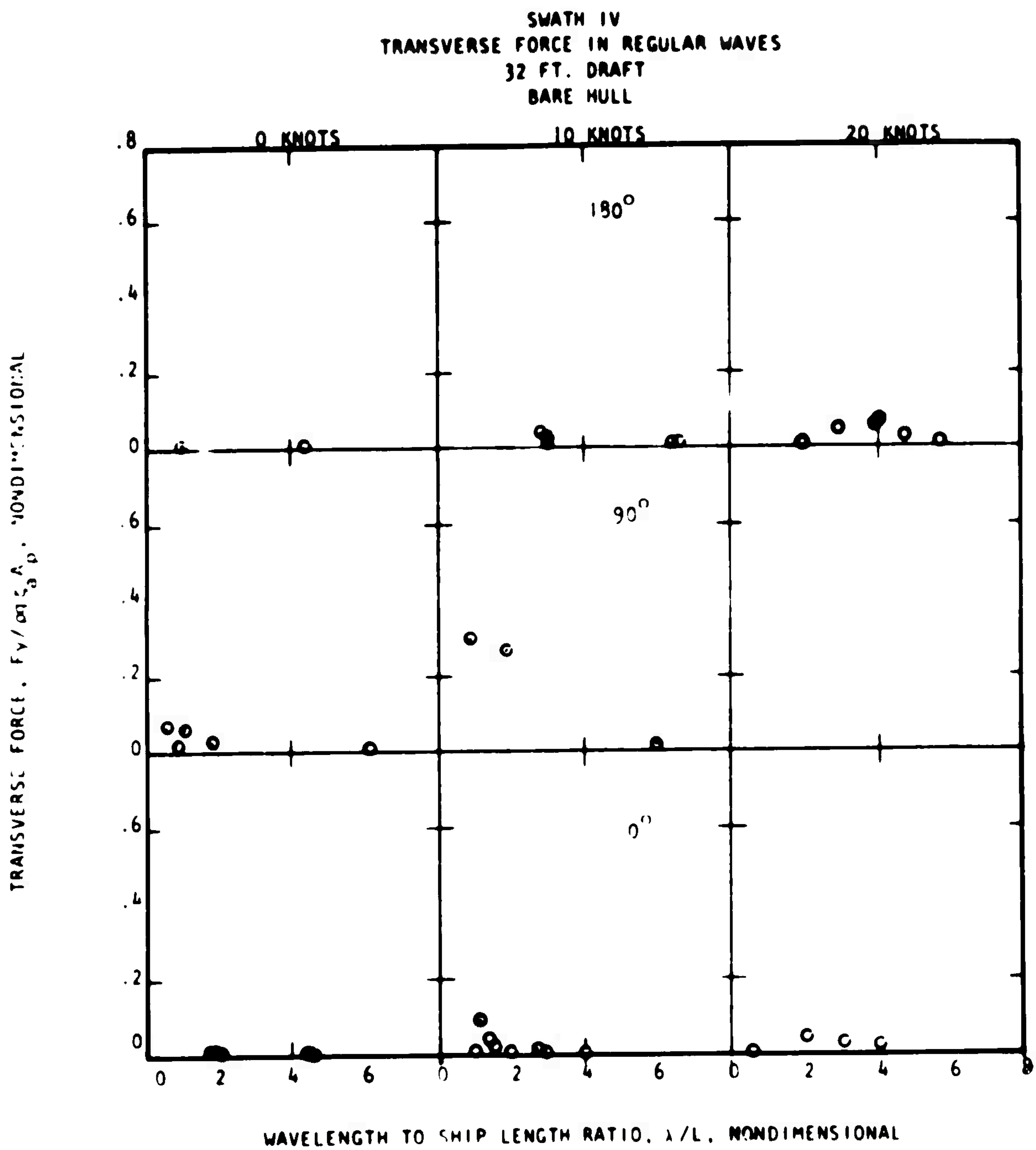

Figure 54 - Dimensionless Transverse Force in Regular Waves, 32 ft Draft, Nominal $\overline{GM}_t$

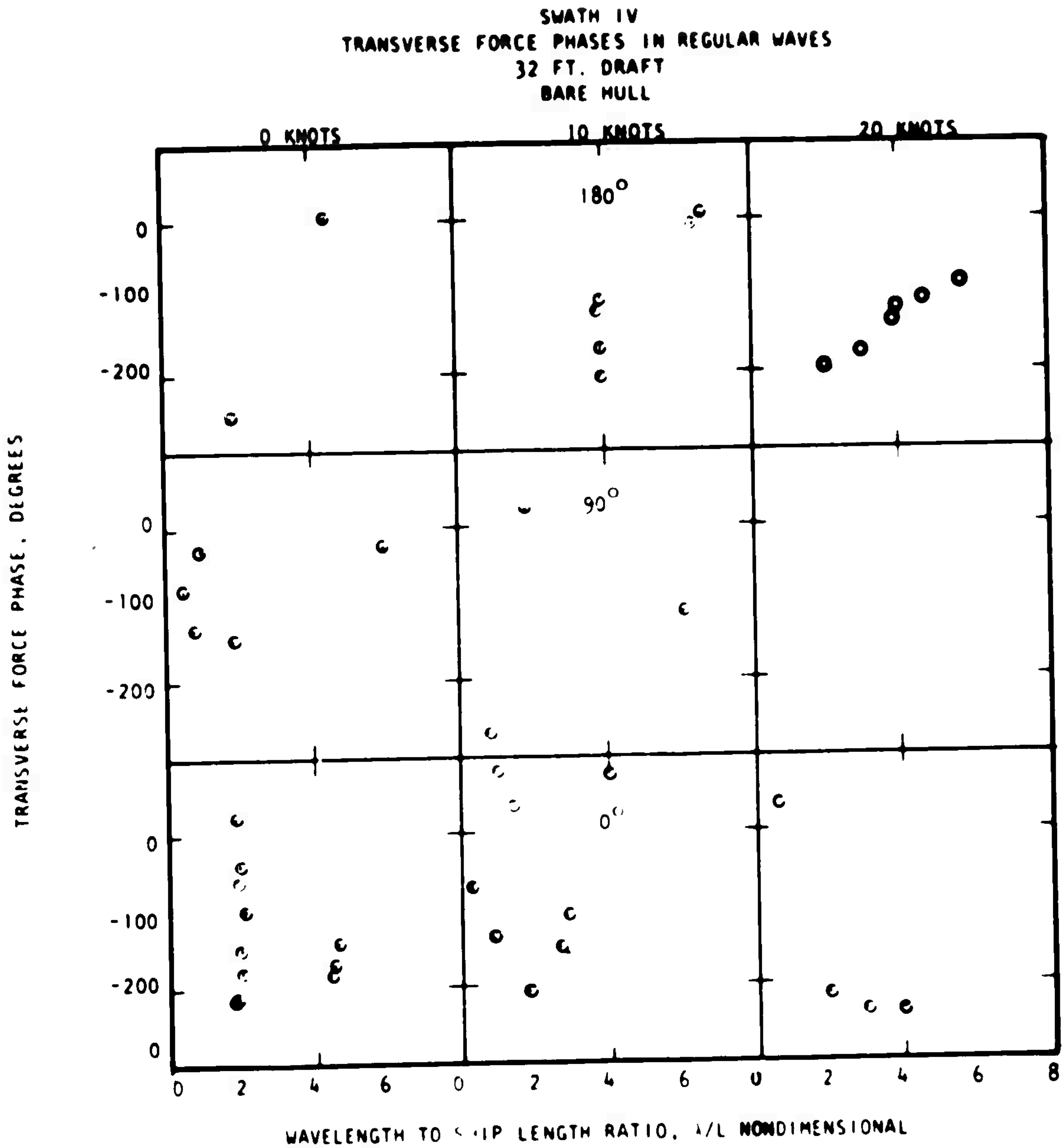

Figure 55 - Transverse Force Phase in Regular Waves, 32 ft Draft, Nominal $\overline{GM}_t$

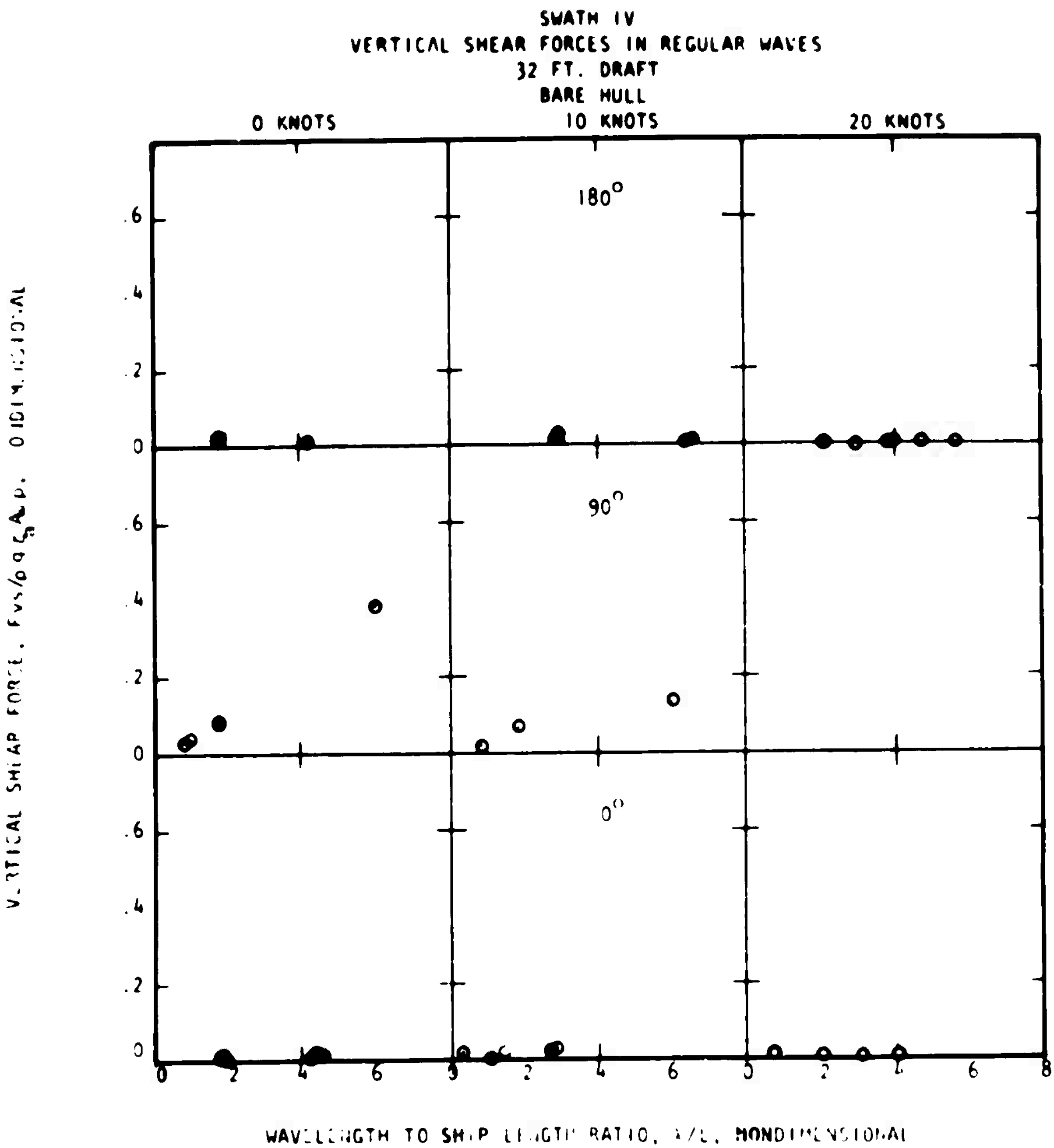

Figure 56 - Dimensionless Vertical Shear Force in Regular Waves, 32 ft Draft, Nominal $\overline{GM}_t$

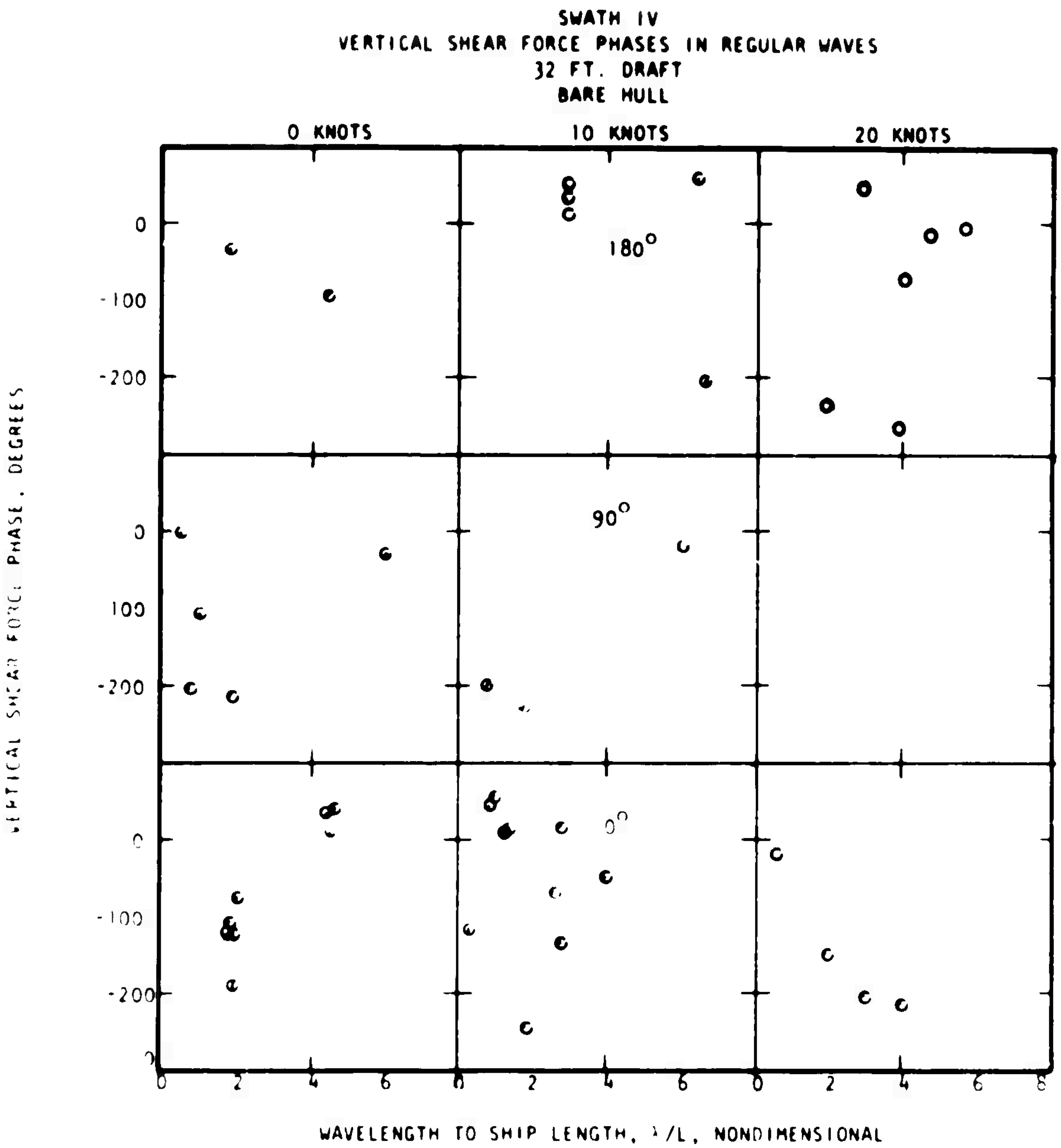

Figure 57 - Vertical Shear Force Phase in Regular Waves, 32 ft Draft, Nominal $\overline{GM}_t$

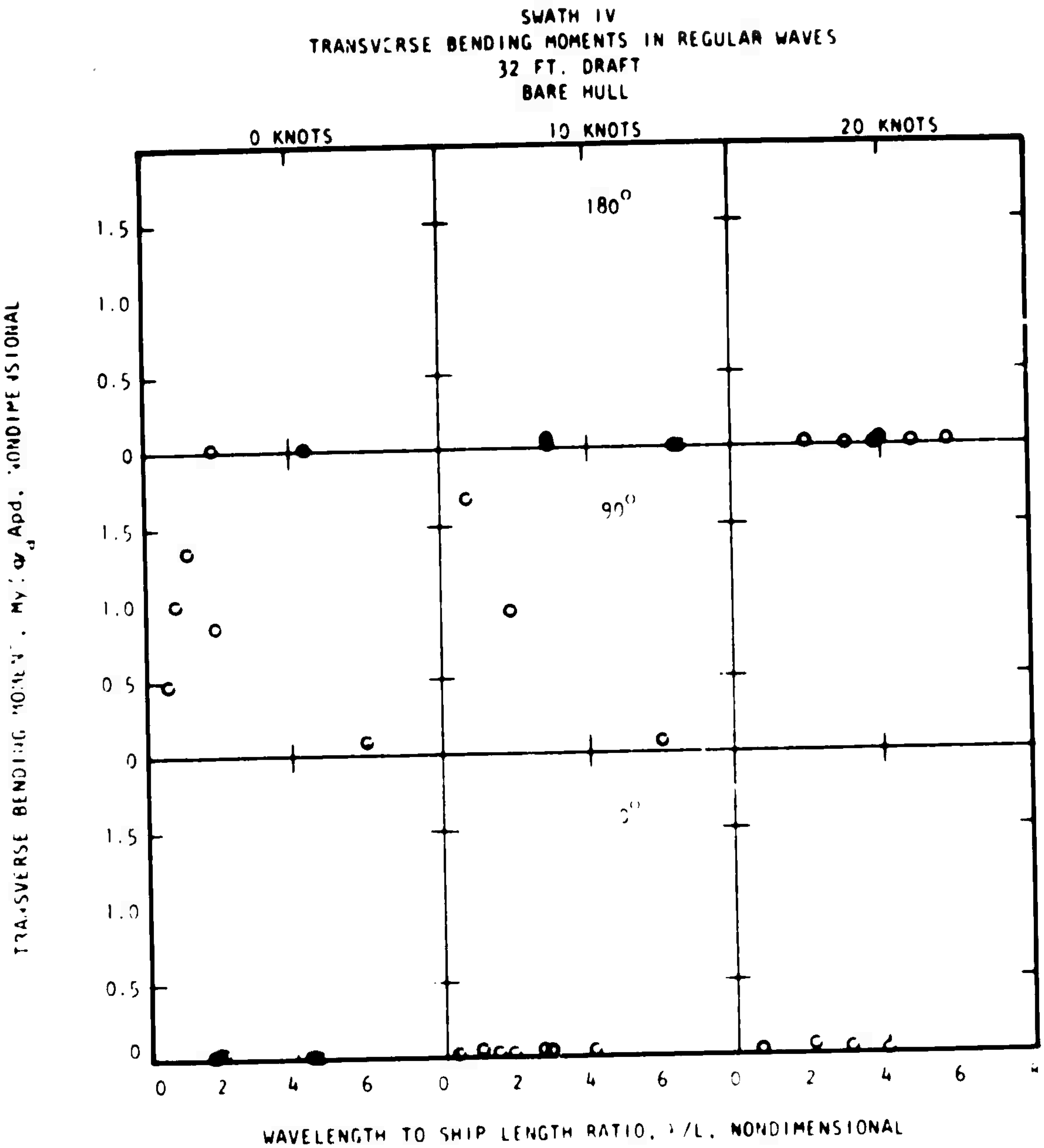

Figure 58 - Dimensionless Transverse Vertical Bending Moment in Regular Waves, 32 ft Draft, Nominal $\overline{GM}_t$

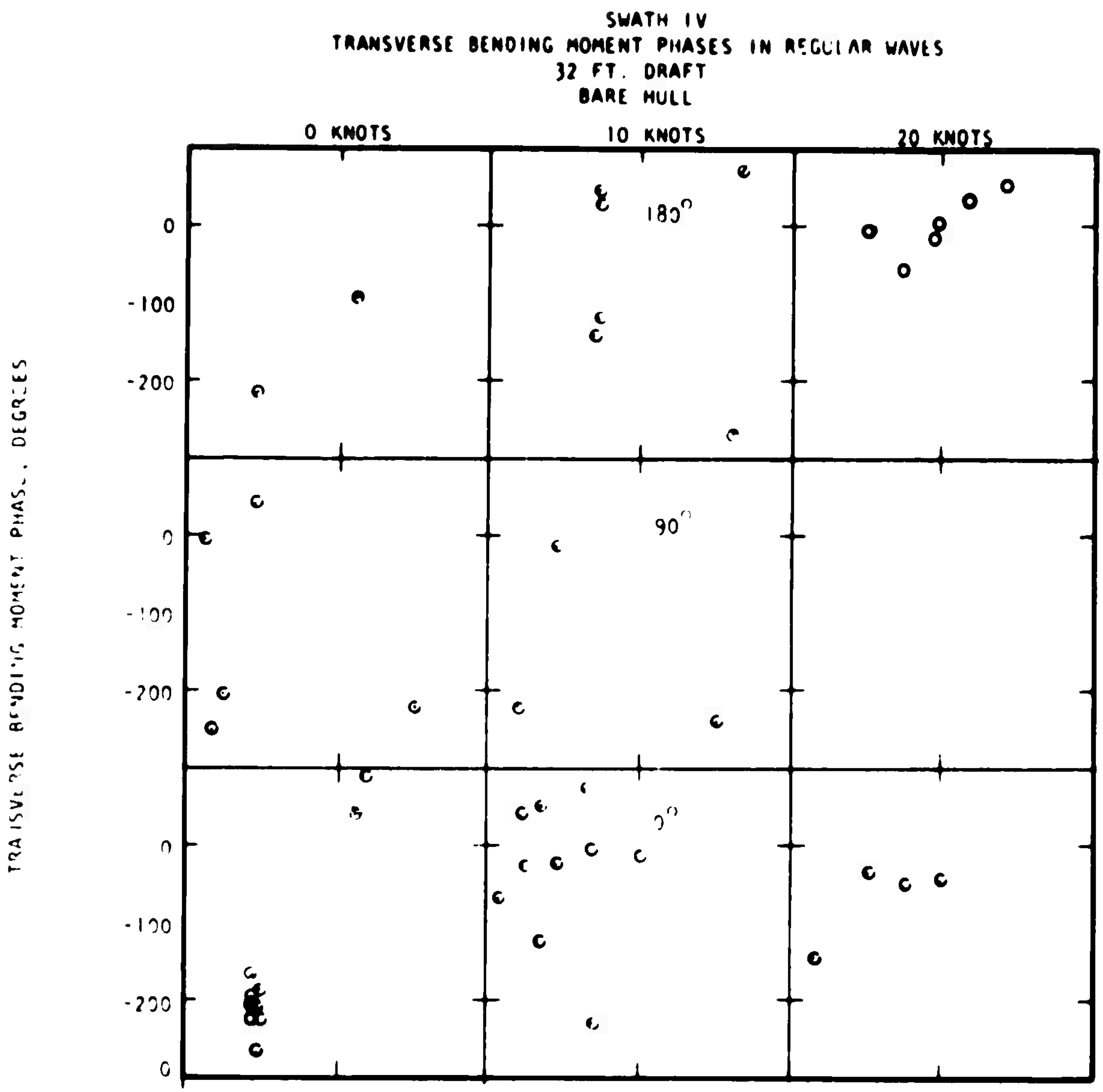

Figure 59 - Transverse Vertical Bending Moment Phase in Regular Waves, 32 ft Draft, Nominal $\overline{GM}_t$

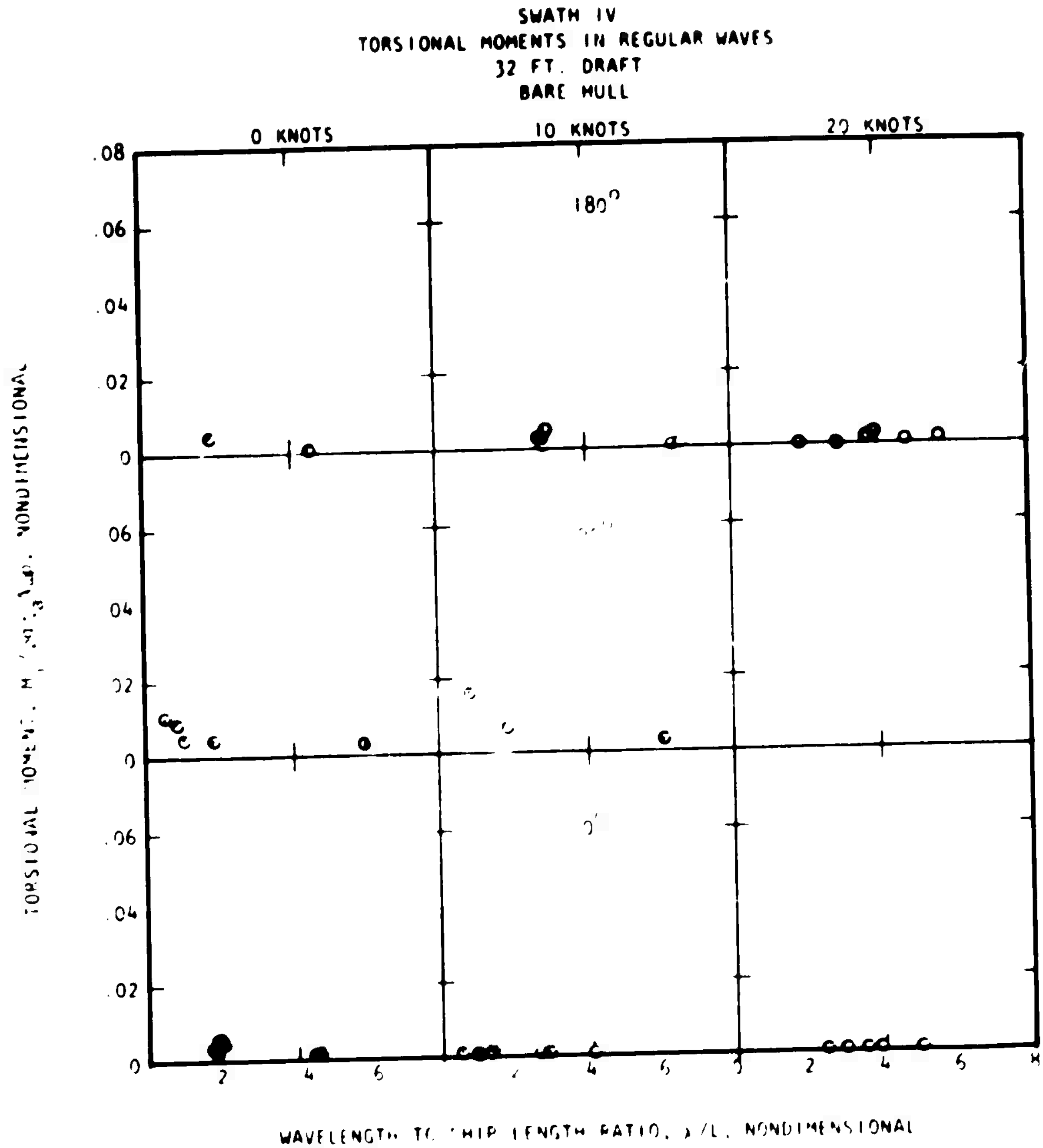

Figure 60 - Dimensionless Torsional Moment in Regular Waves, 32 ft Draft, Nominal $\overline{GM}_t$

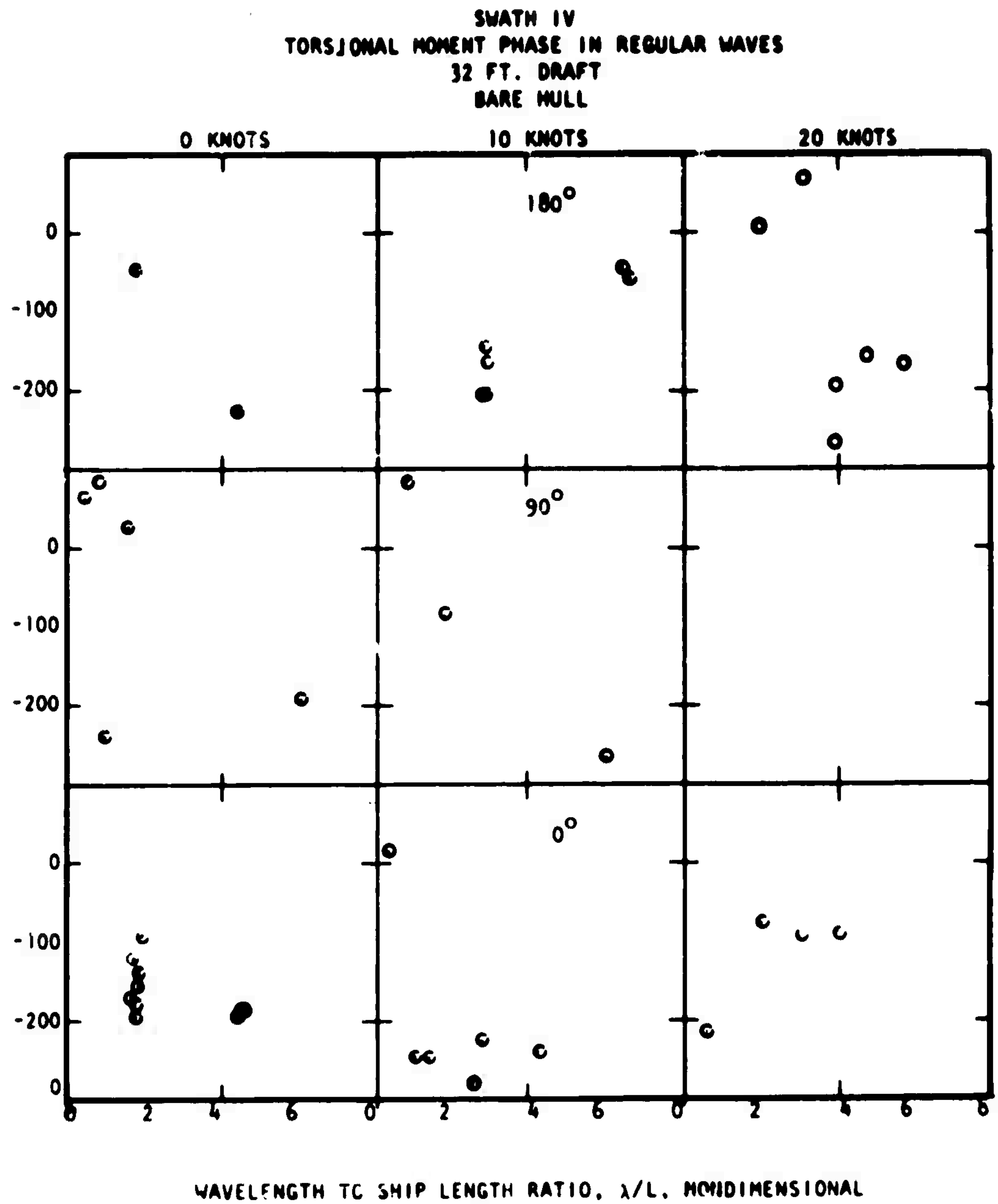

Figure 61 - Torsional Moment Phase in Regular Waves, 32 ft Draft, Nominal $\overline{GM}_t$

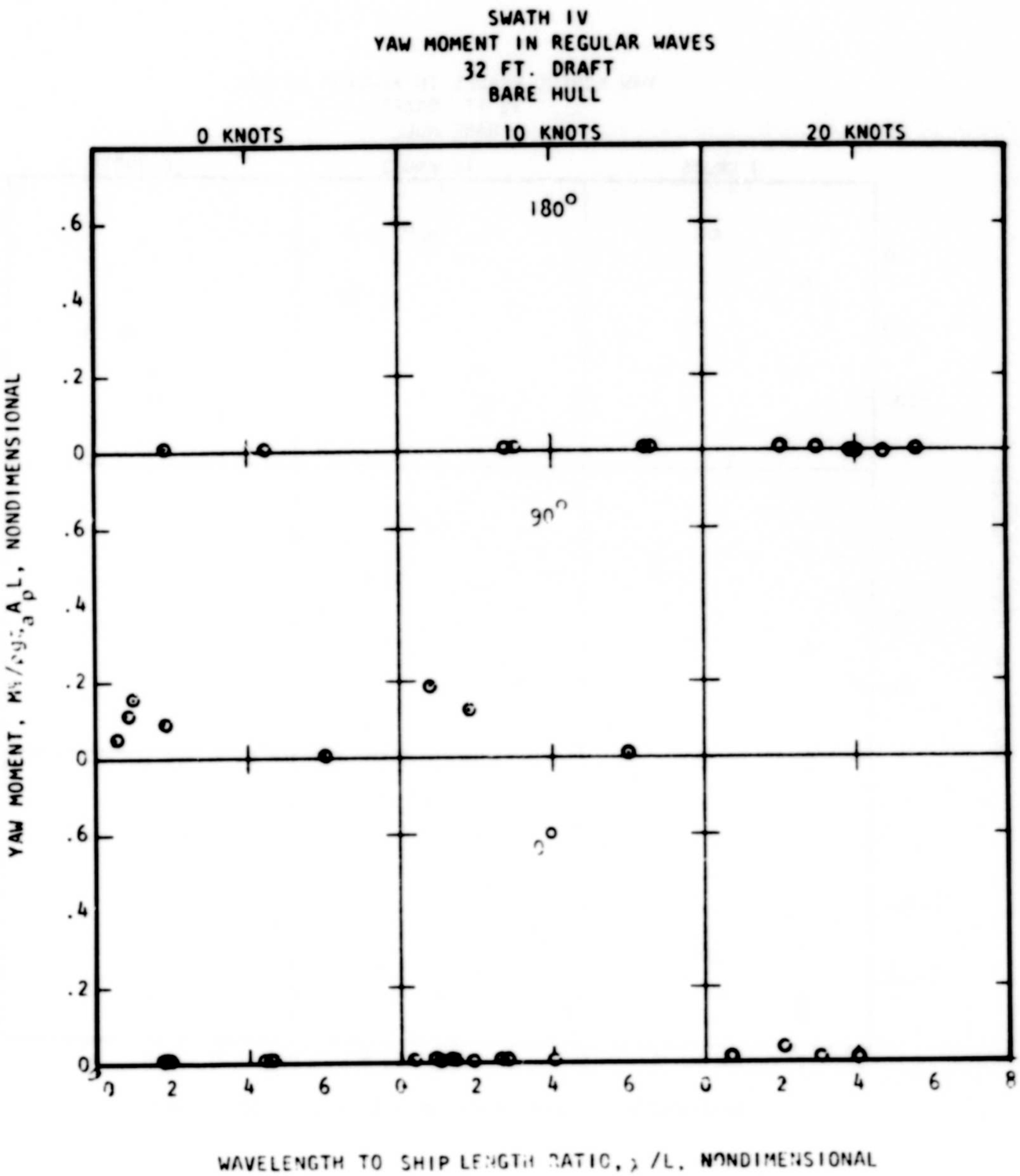

Figure 62 - Dimensionless Yaw Moment in Regular Waves, 32 ft Draft, Nominal $\overline{GM}_t$

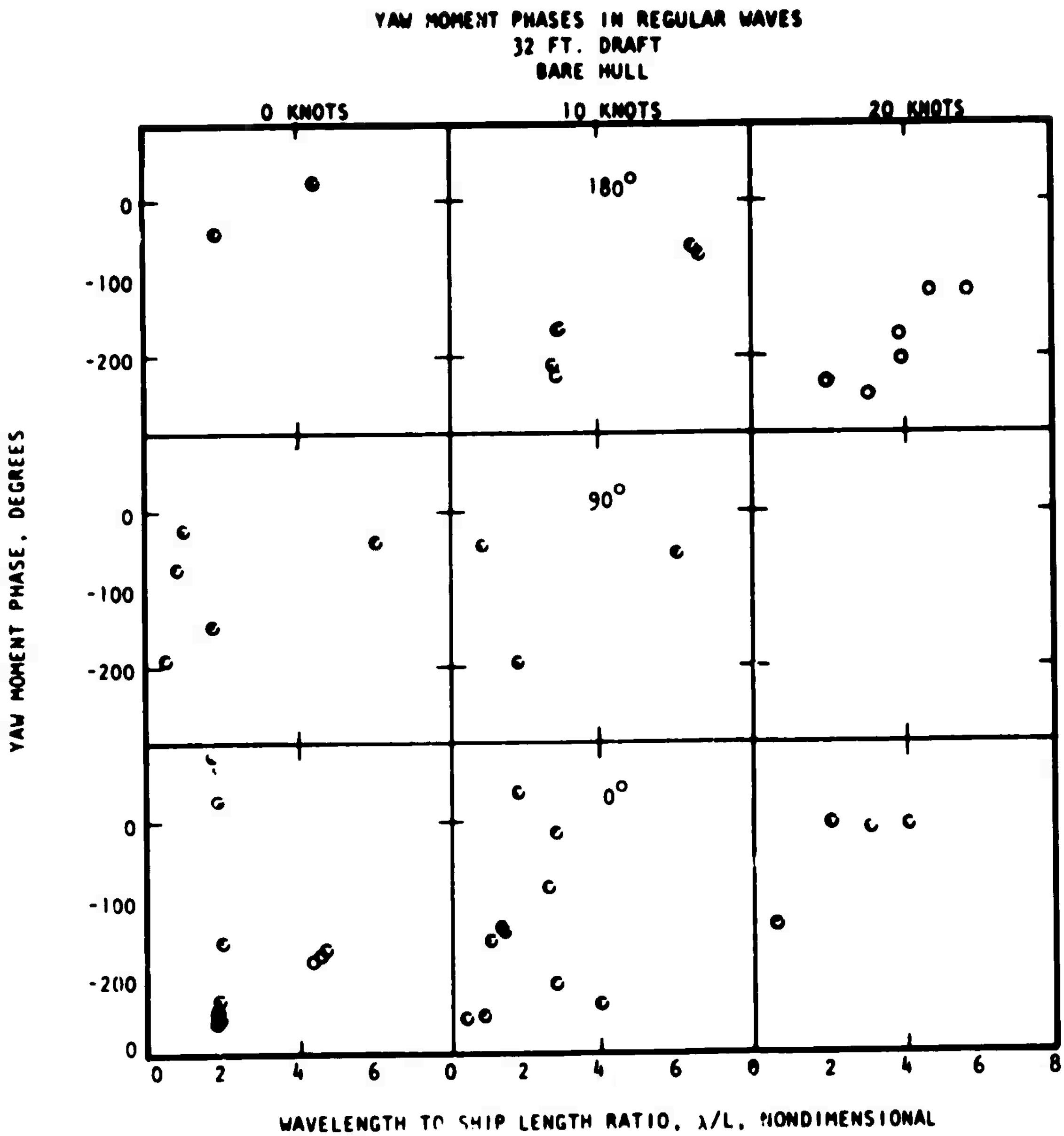

Figure 63 - Yaw Moment Phase in Regular Waves, 32 ft Draft, Nominal $\overline{GM}_t$

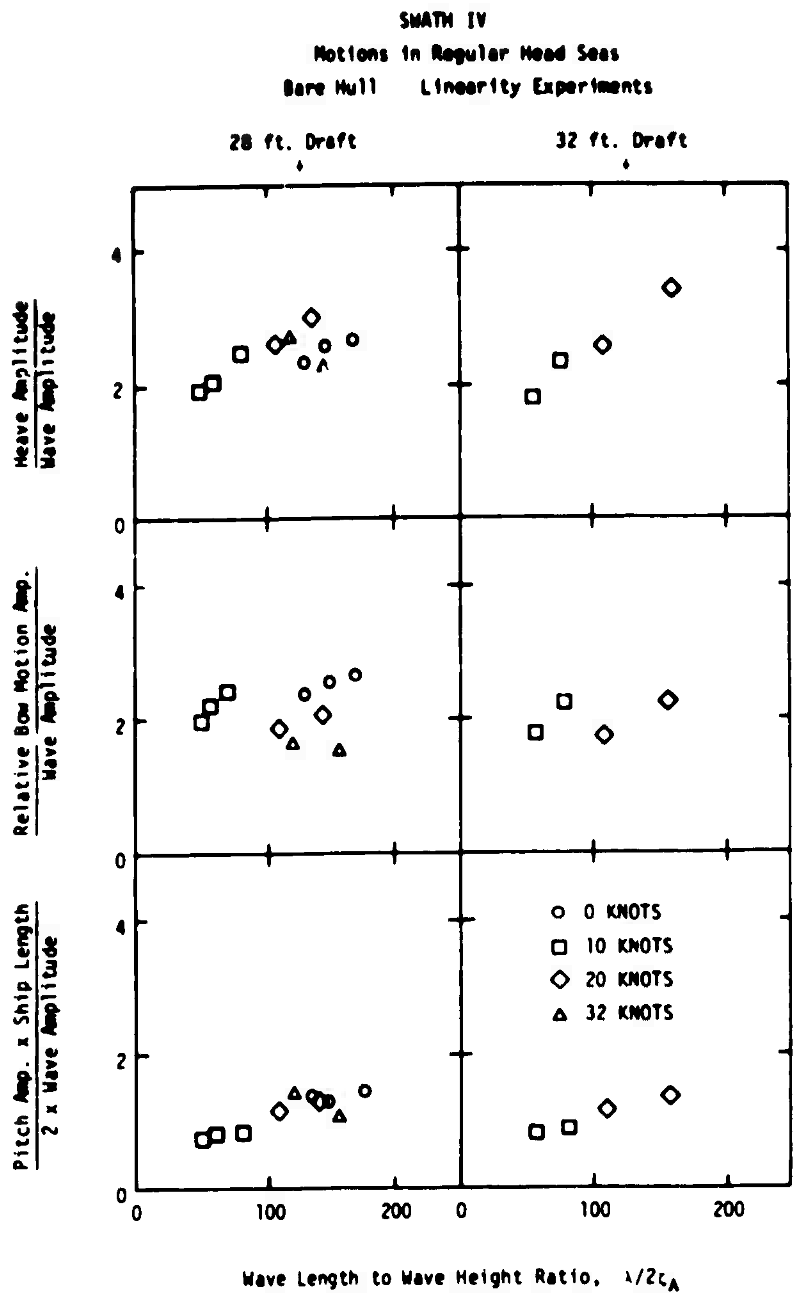

Figure 64a - Linearity Experiments in Regular Head Seas, Bare Hull, Nominal $\overline{GM}_t$

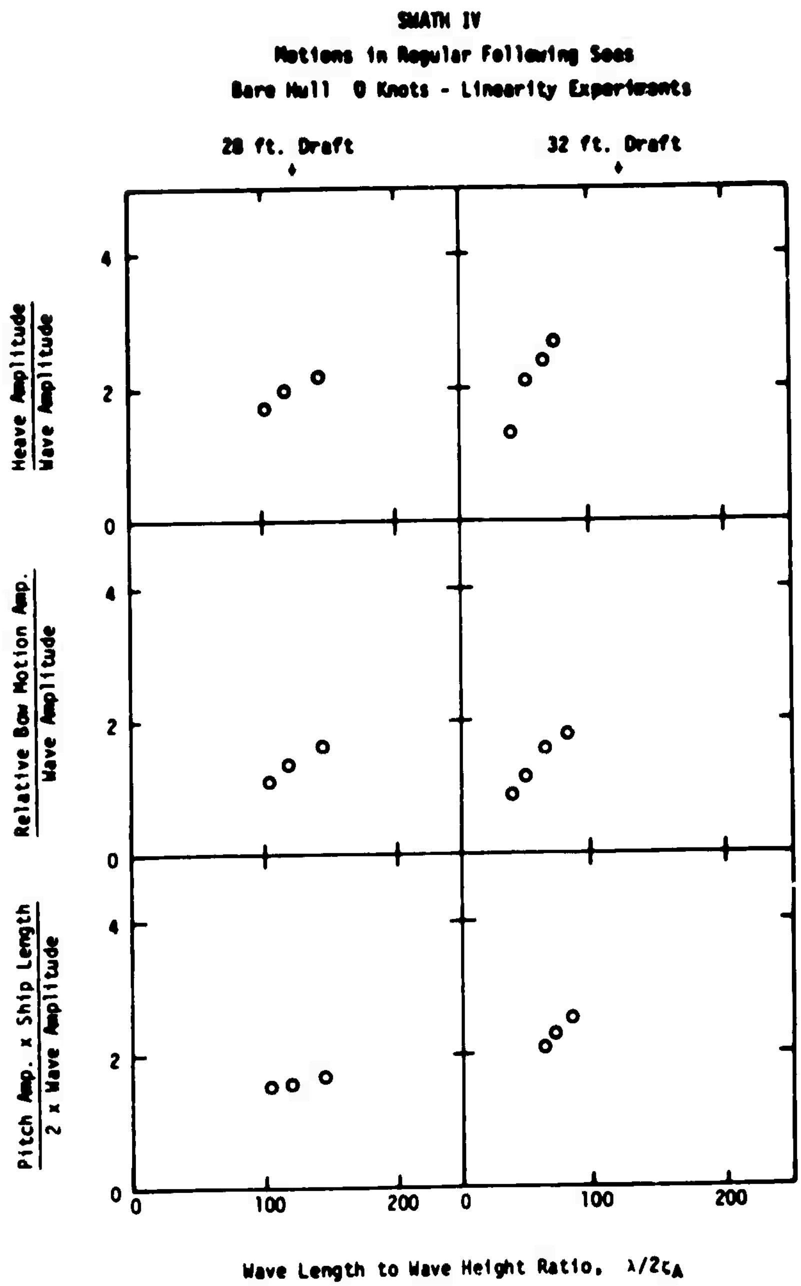

Figure 64b - Linearity Experiments in Regular Following Seas, Bare Hull, Nominal $\overline{GM}_t$

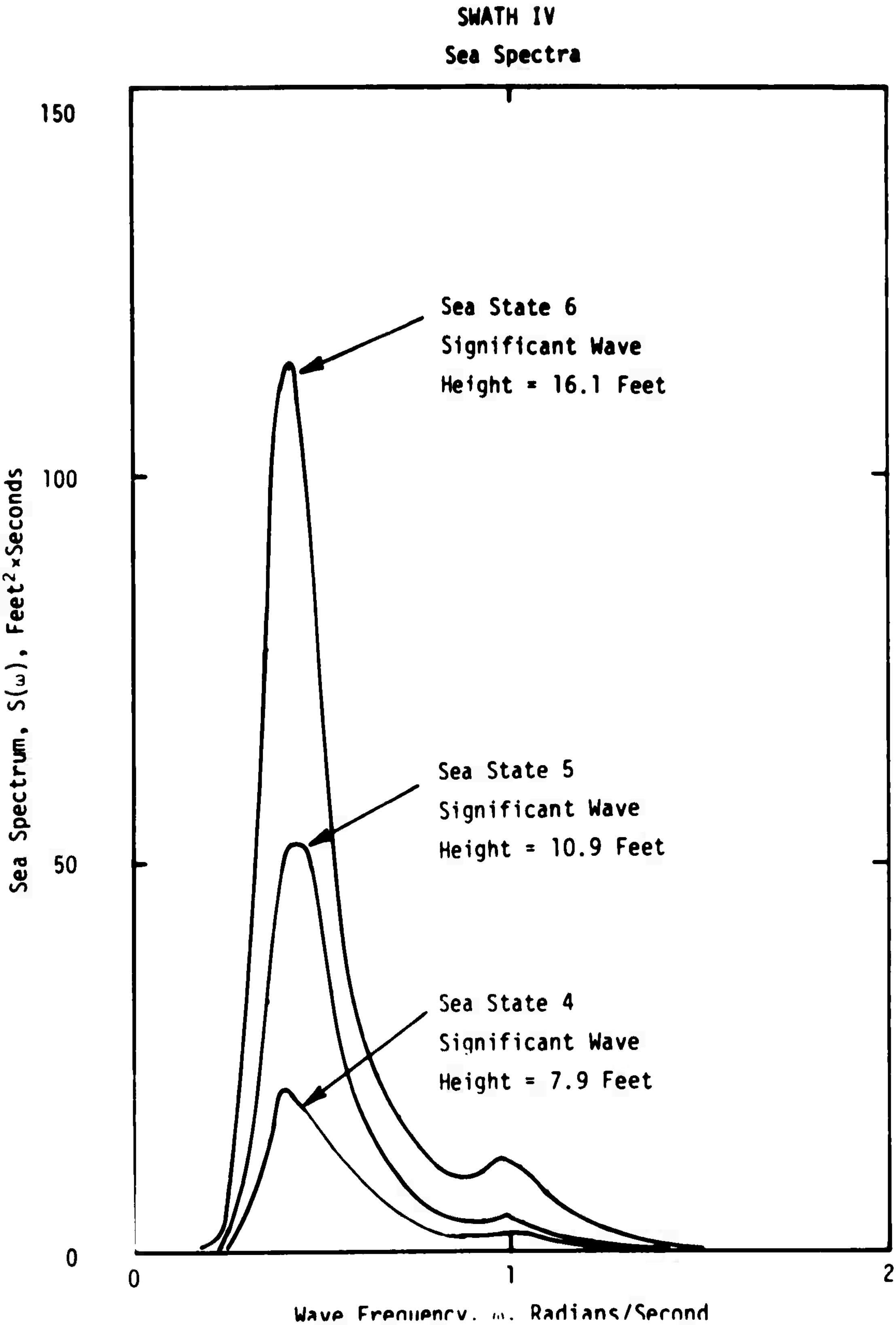

Figure 65 - Experimental Spectra for State 4, 5 and 6 Seas

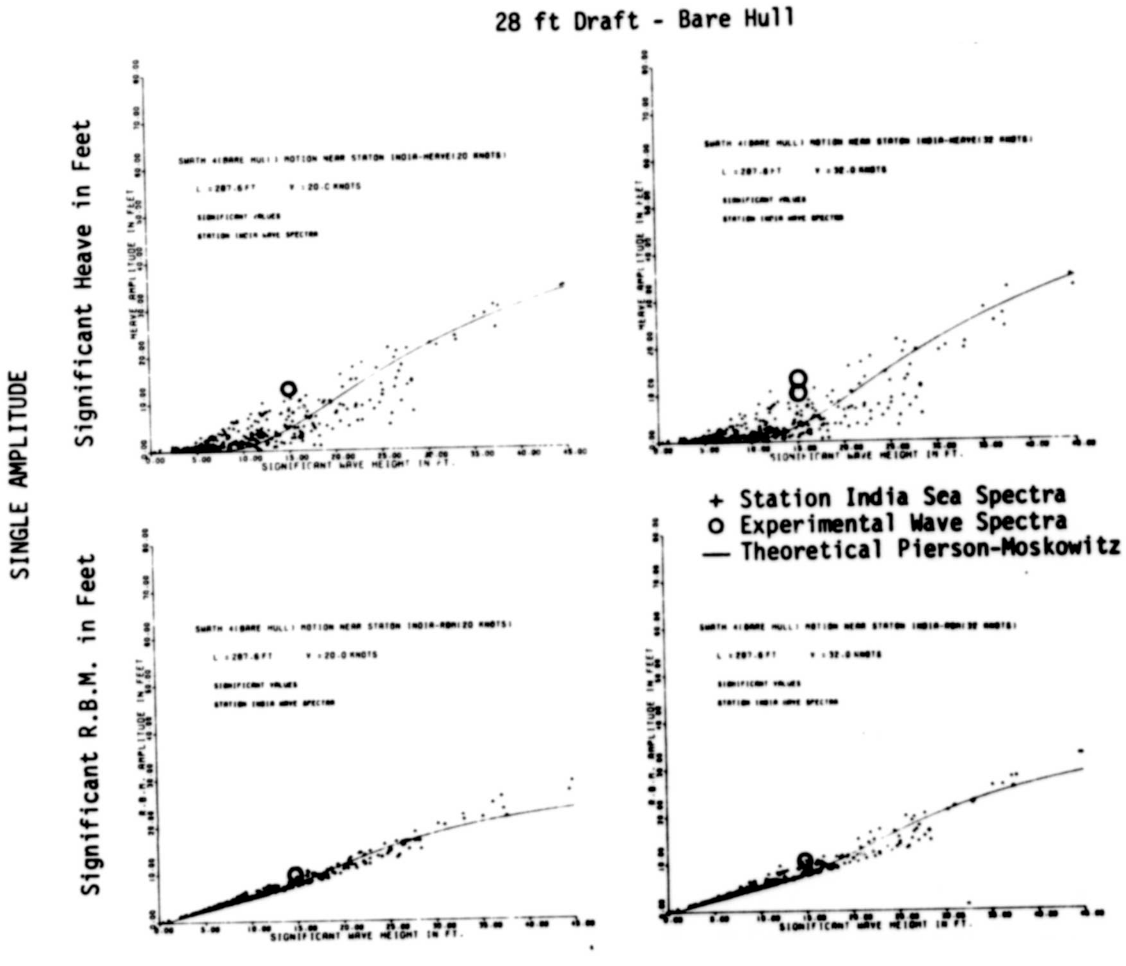

Figure 65A - Significanr Motions in Random Waves, 28 ft Draft, Bare Hull

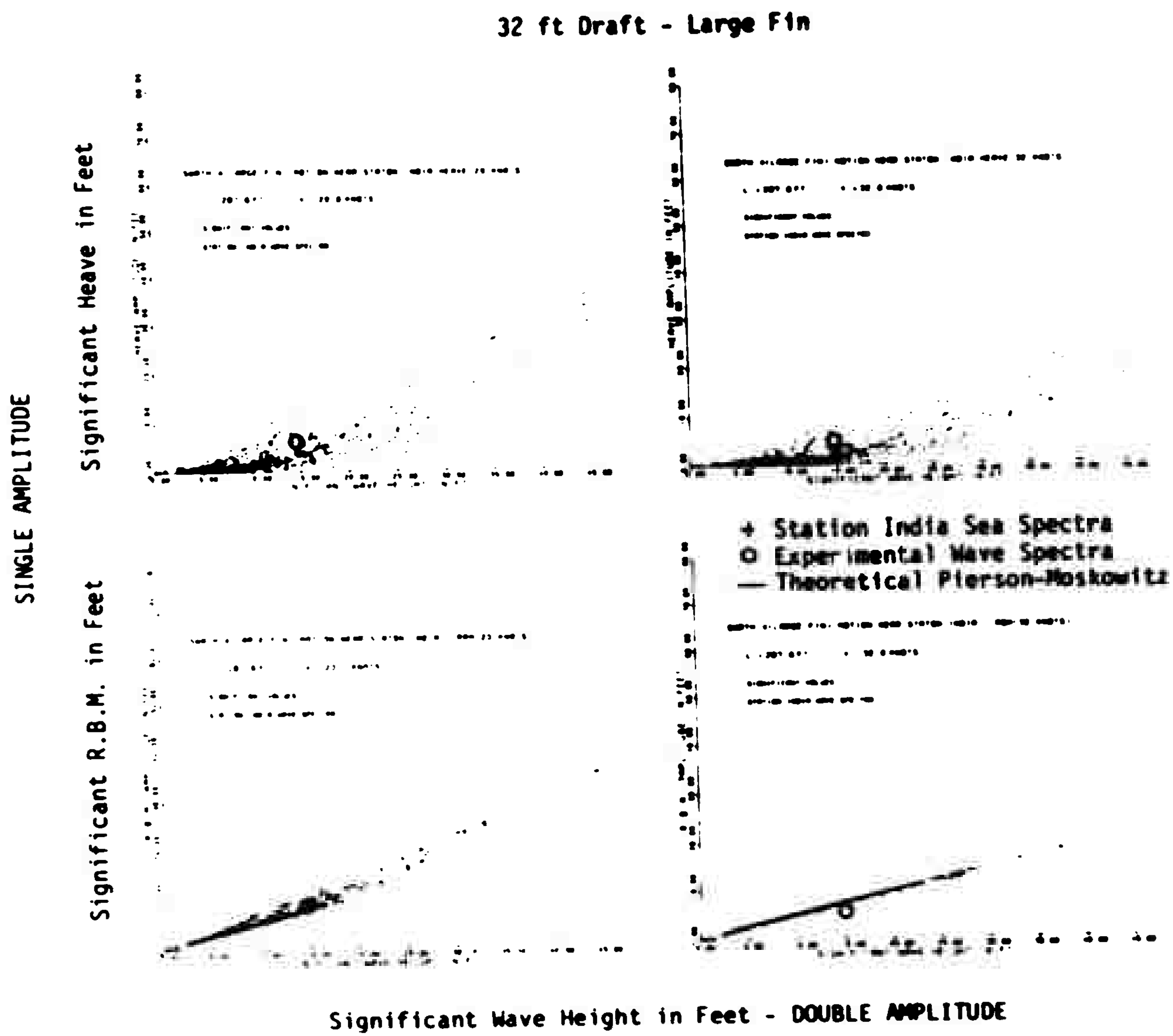

Figure 65B - Significant Motions in Random Waves, 32 ft Draft, Large Fins

SWATH IV

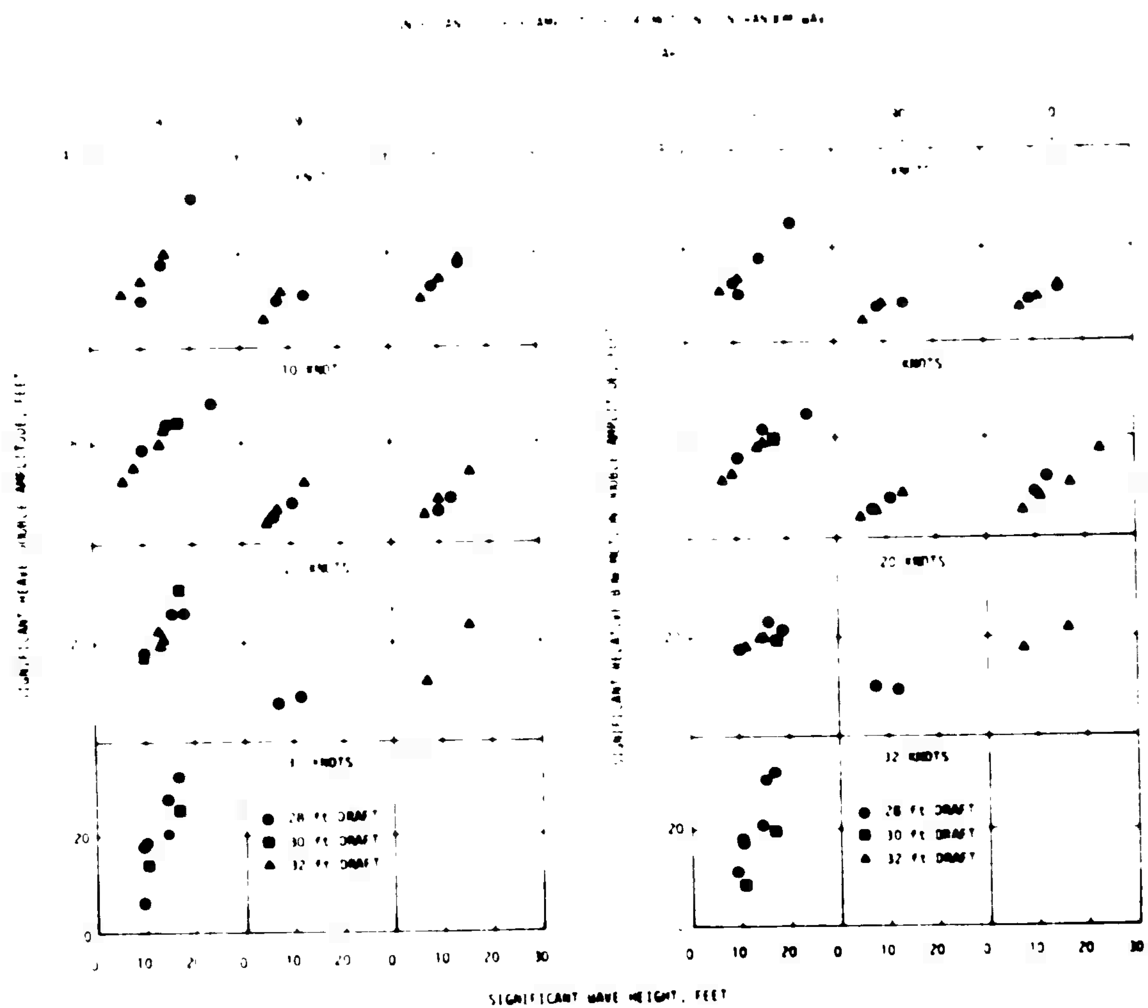

Figure 66 - Significant Double Amplitudes of Heave and Relative Bow Motion in Random Waves, Bare Hull, Nominal $\overline{GM}_t$

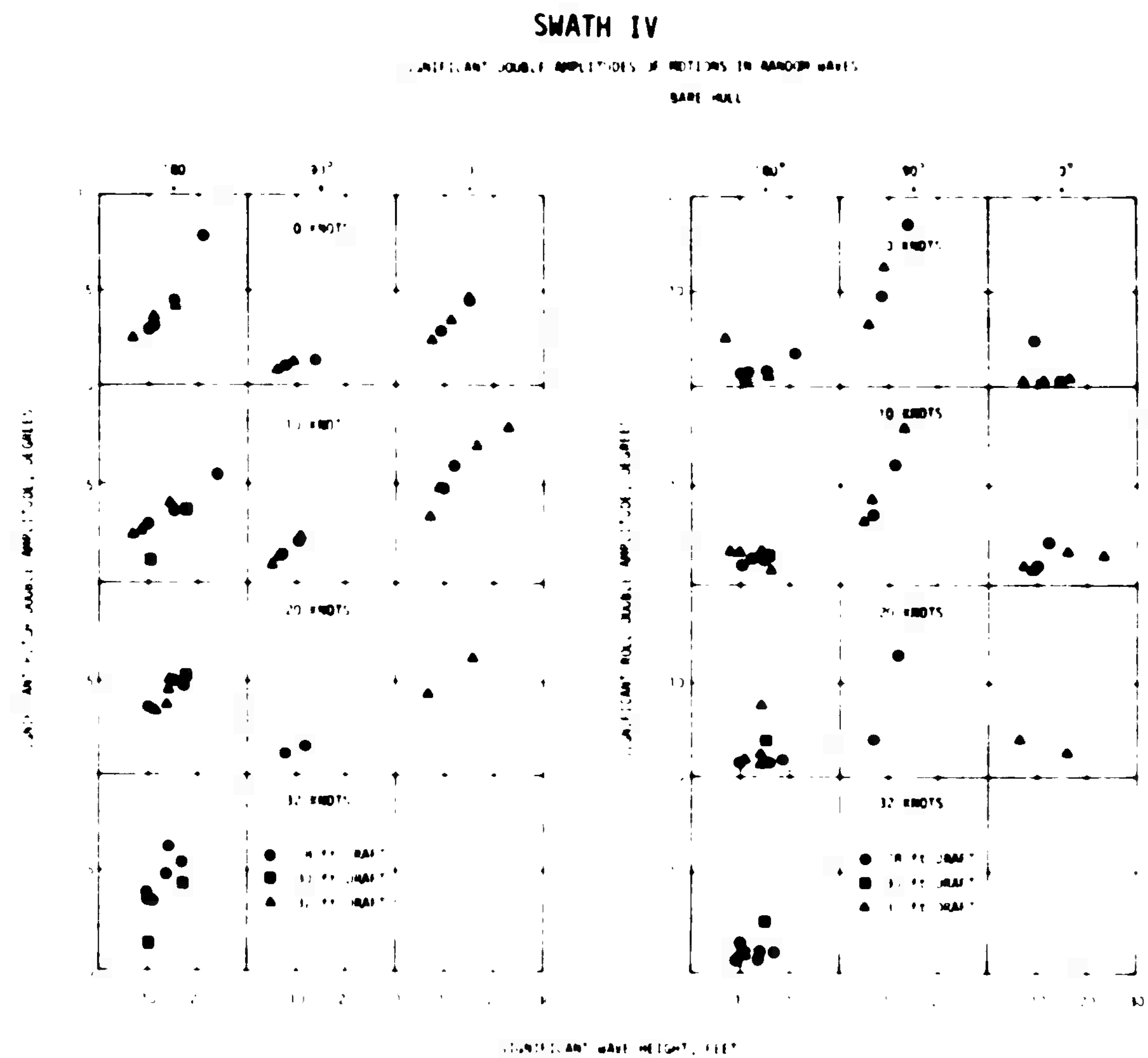

Figure 67 - Significant Double Amplitudes of Pitch and Roll in Random Waves, Bare Hull, Nominal $\overline{CM}_t$

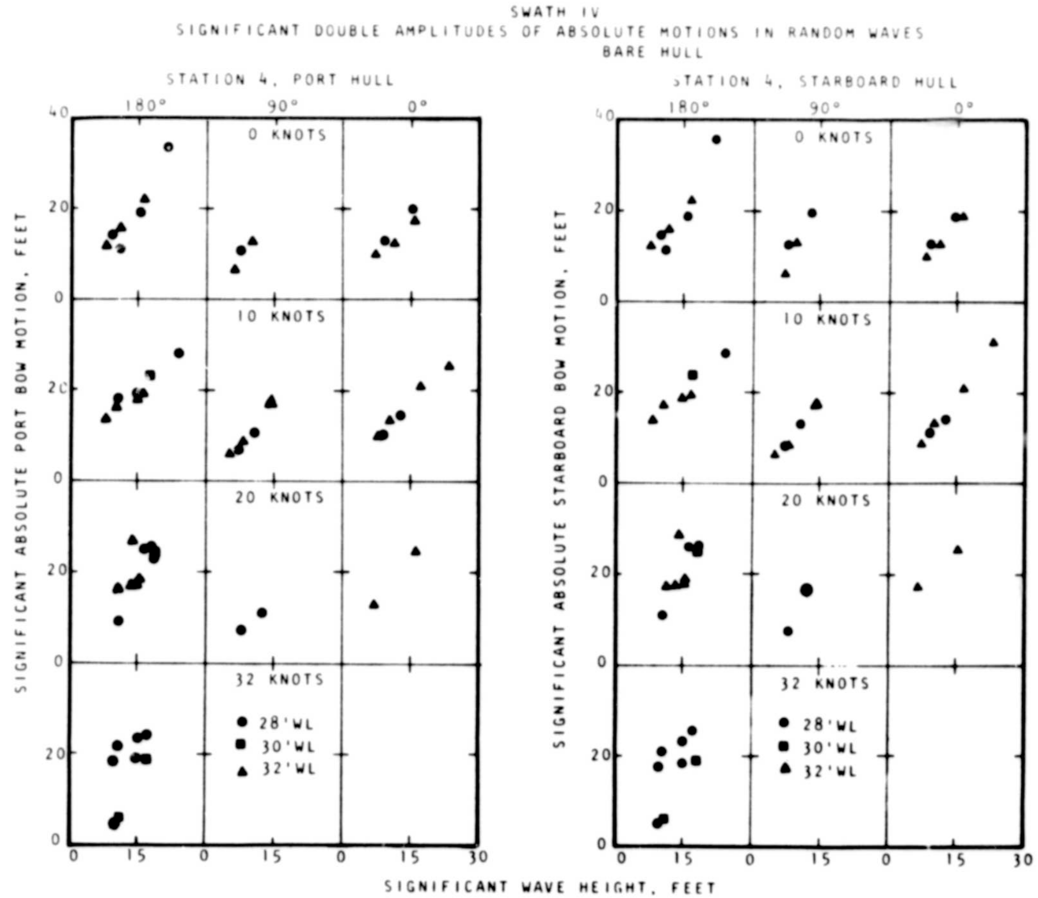

Figure 68 - Significant Double Amplitudes of Absolute Bow Motion in Random Waves, Port and Starboard, Bare Hull, Nominal $\overline{GM}_t$

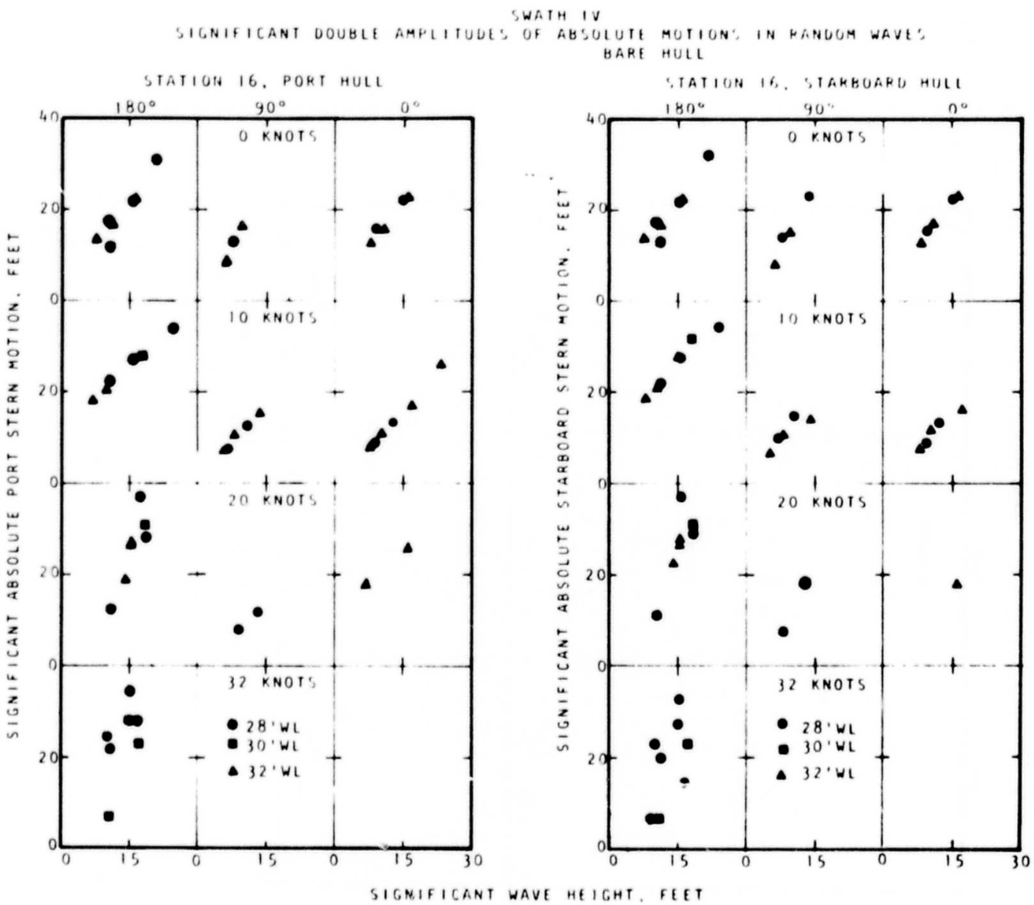

Figure 69 - Significant Double Amplitudes of Absolute Stern Motion in Random Waves, Port and Starboard, Bare Hull, Nominal $\overline{GM}_t$

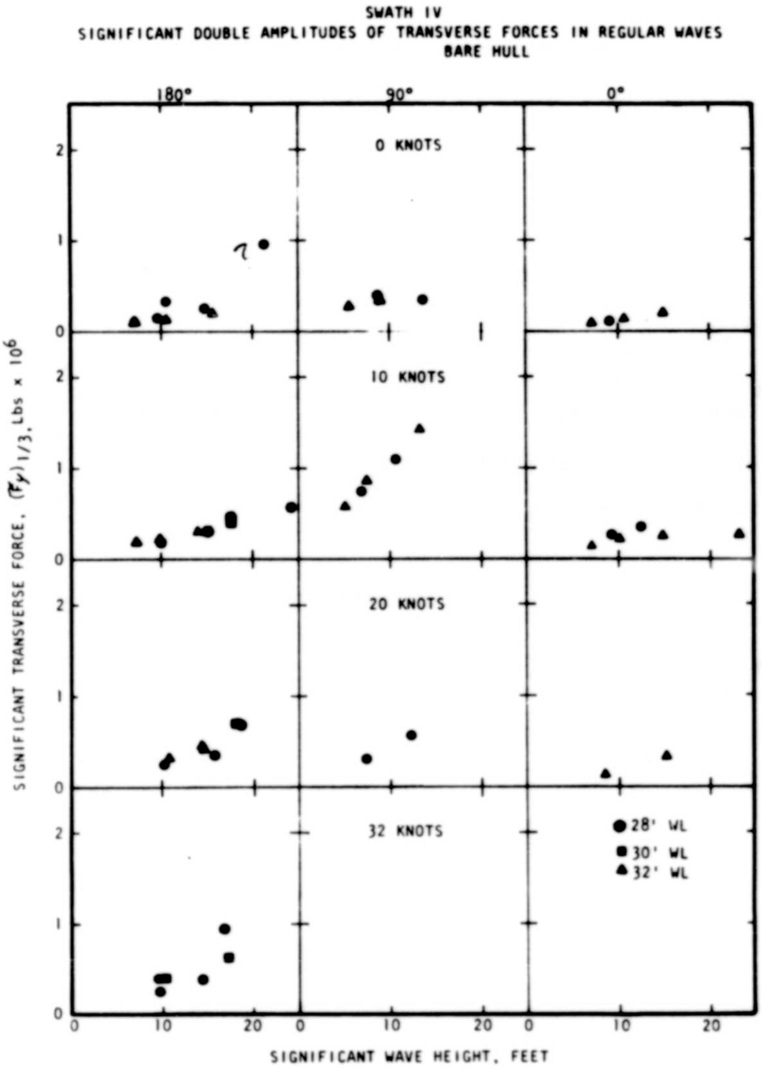

Figure 70 - Significant Double Amplitudes of Transverse Force in Random Waves, Bare Hull, Nominal $\overline{GM}_t$

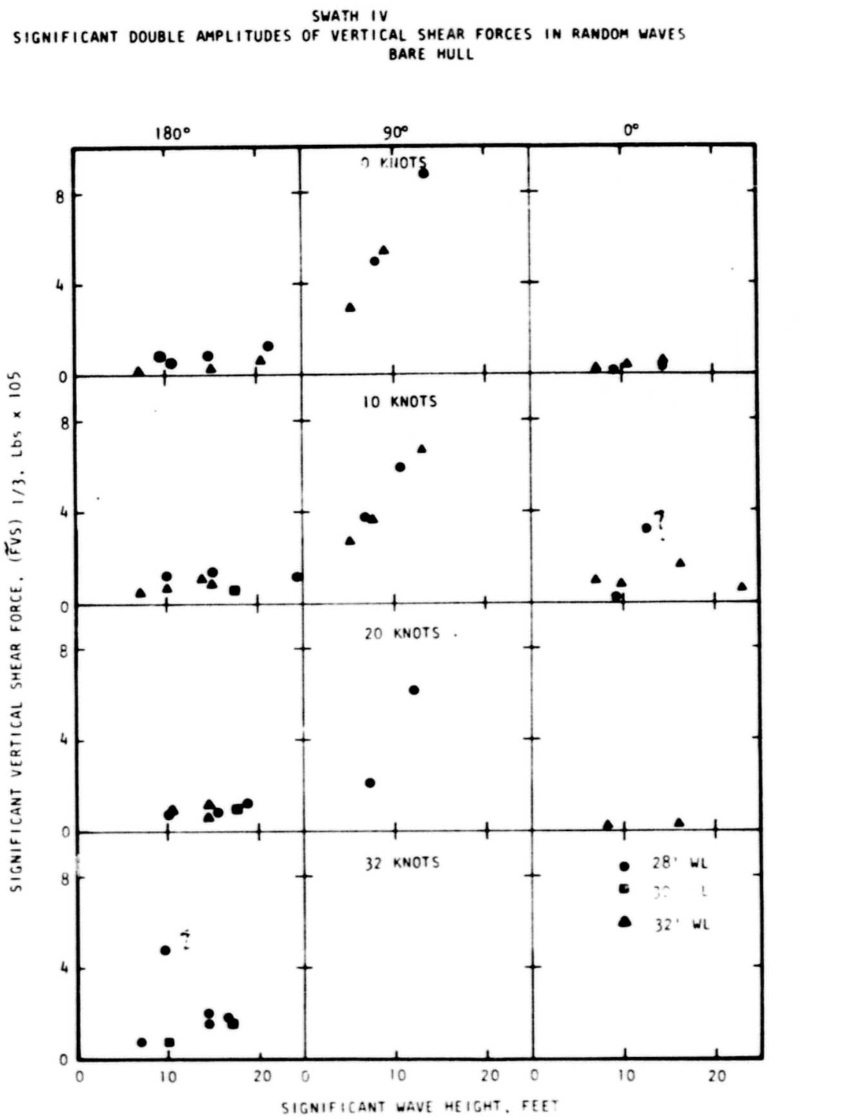

Figure 71 - Significant Double Amplitudes of Vertical Shear Force in Random Waves, Bare Hull, Nominal $\overline{GM}_t$

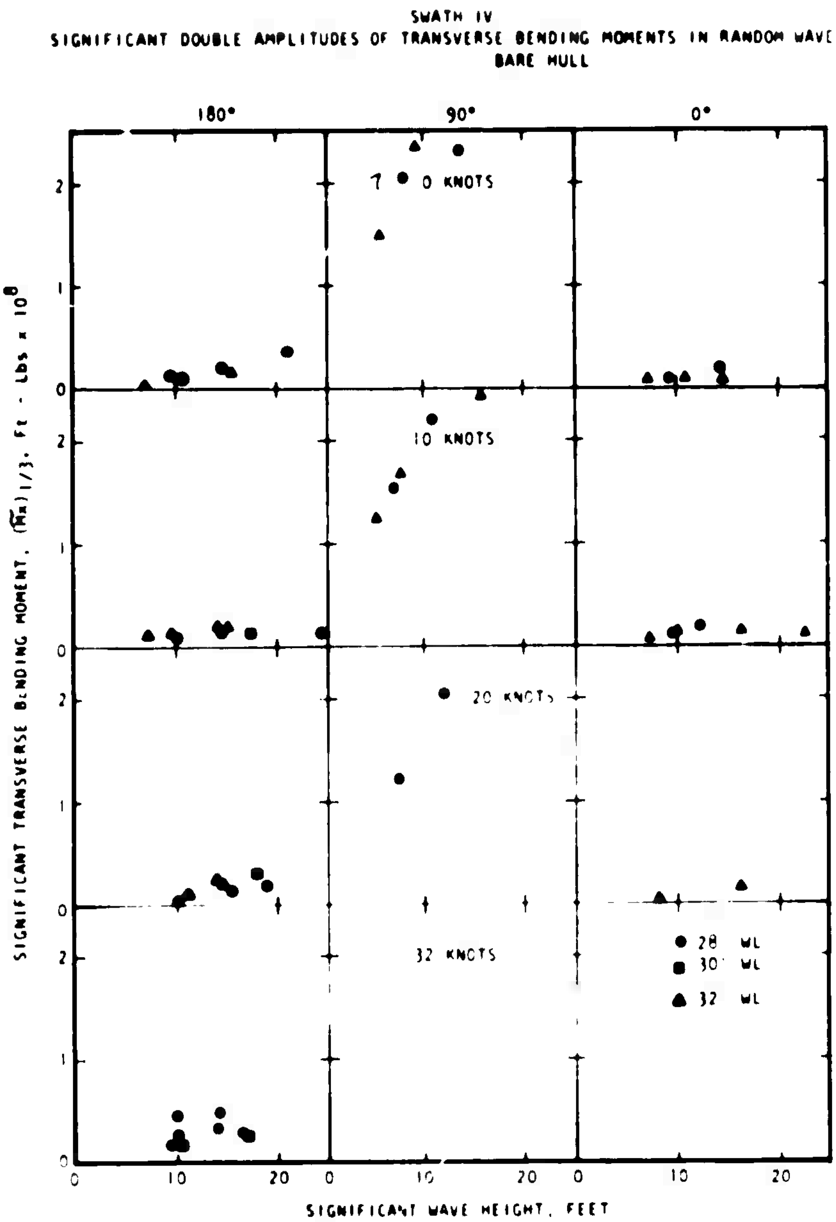

Figure 72 - Significant Double Amplitudes of Transverse Vertical Bending Moment in Random Waves, Bare Hull, Nominal $\overline{GM}_t$

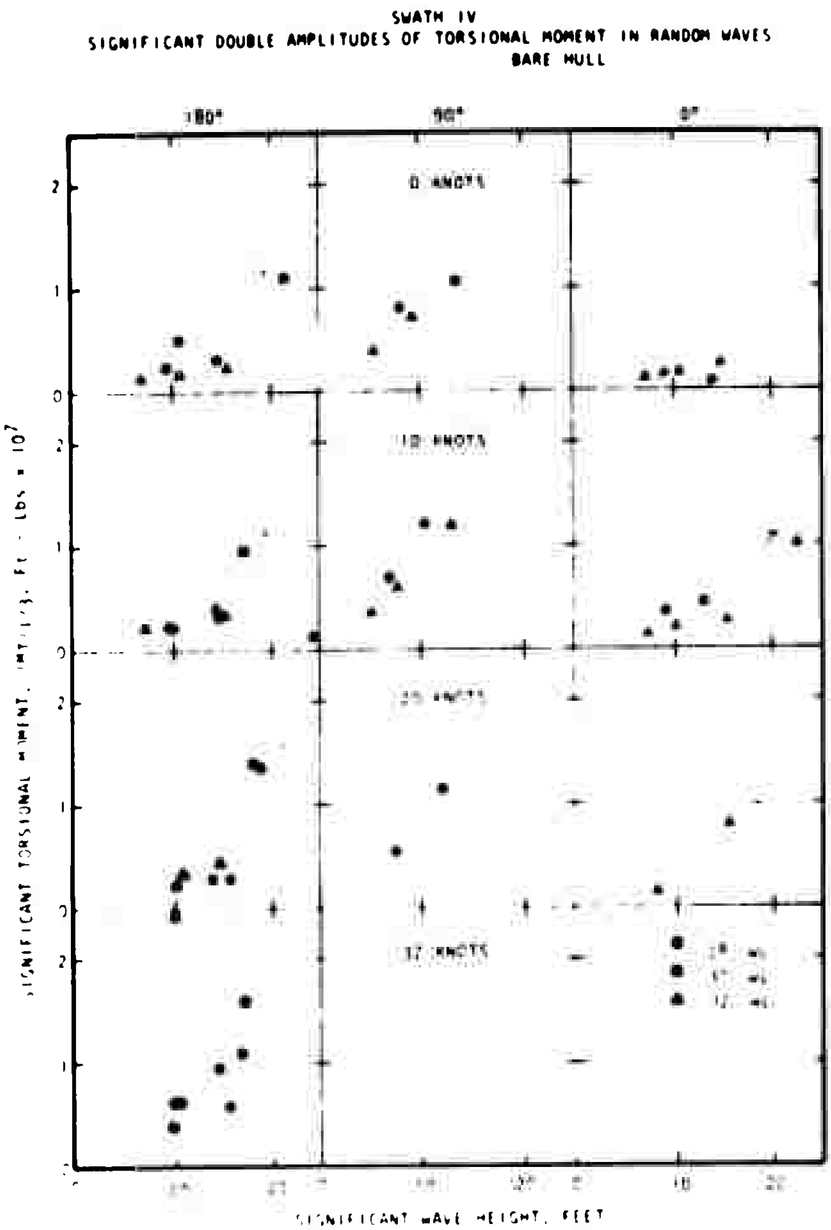

Figure 73 - Significant Double Amplitudes of Torsional Moment in Random Waves, Bare Hull, Nominal $\overline{GM}_t$

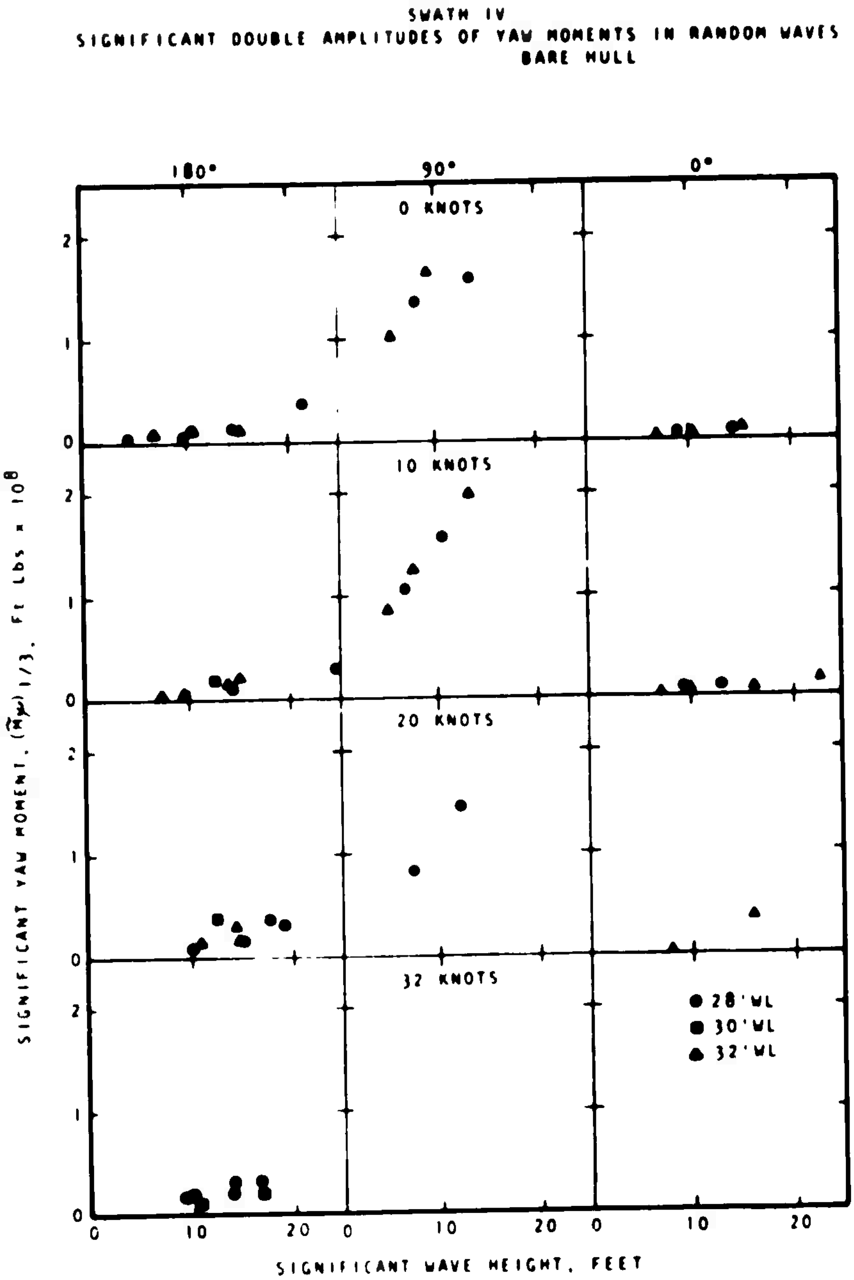

Figure 74 - Significant Double Amplitudes of Yaw Moment in Random Waves, Bare Hull, Nominal $\overline{GM}_t$

SWATH IV
Impact Pressure Cumulative Relative Frequency Distribution
Bare Hull - 32 ft Draft
Following Sea State 6 10 Knots

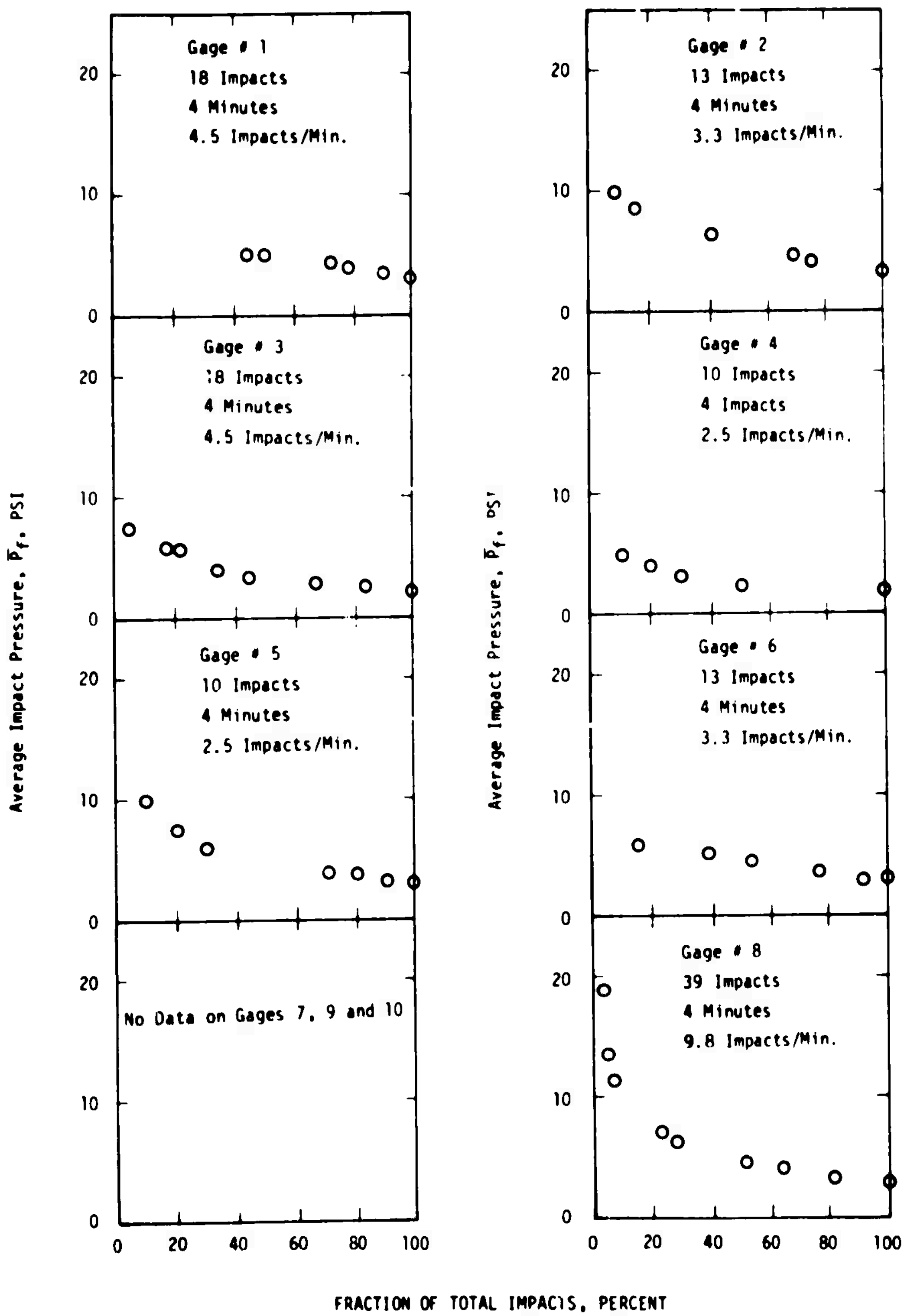

Figure 75 - Impact Pressure Cumulative Relative Frequency Distribution, Following Sea State 6, Bare Hull, 32 ft Draft, 10 Knots

SWATH IV

Impact Pressure Distribution

Bare Hull - 32 ft Draft

Following Sea State 6   10 Knots

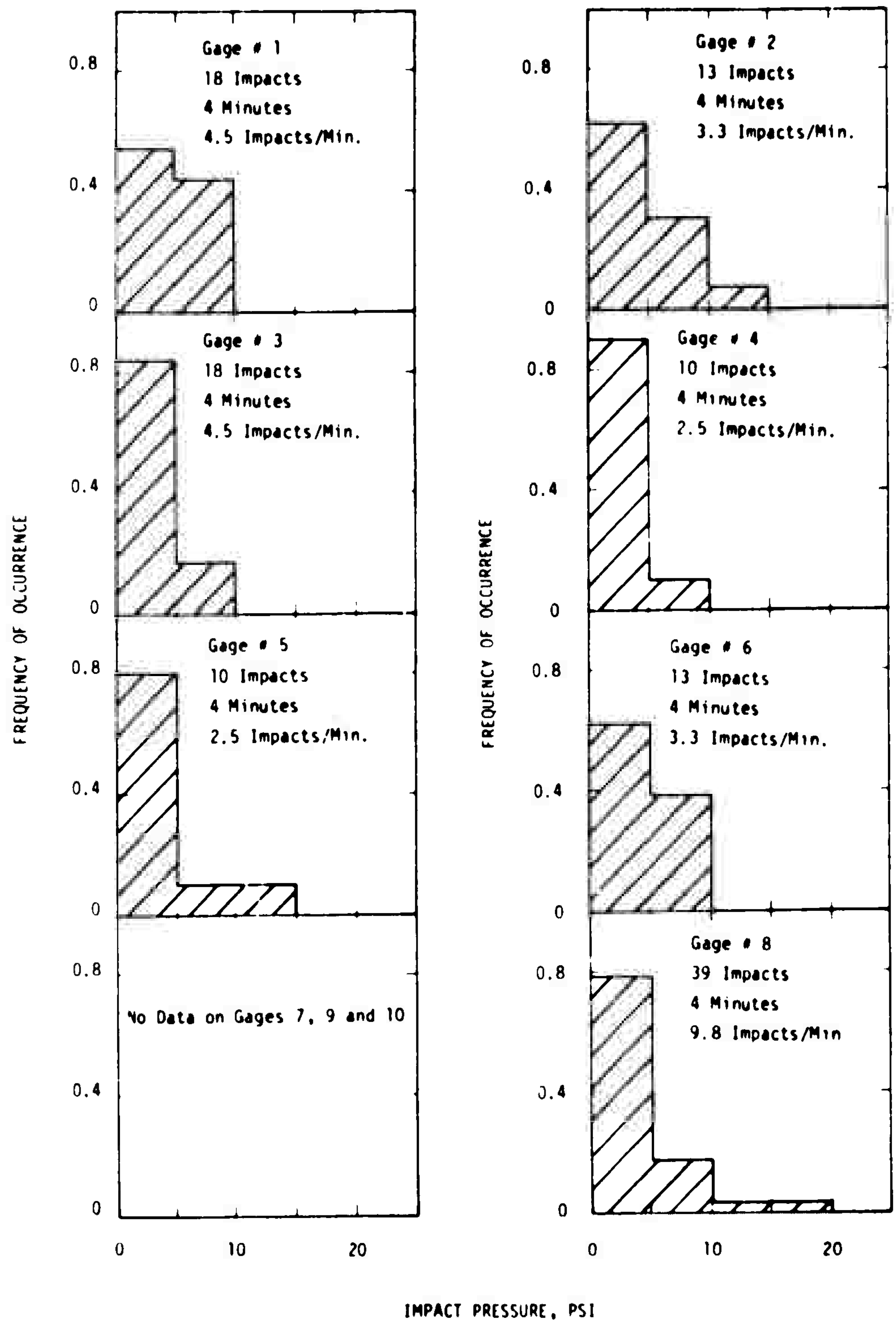

Figure 76 - Impact Pressure Histogram, Following Sea State 6, Bare Hull, 32 ft Draft, 10 Knots

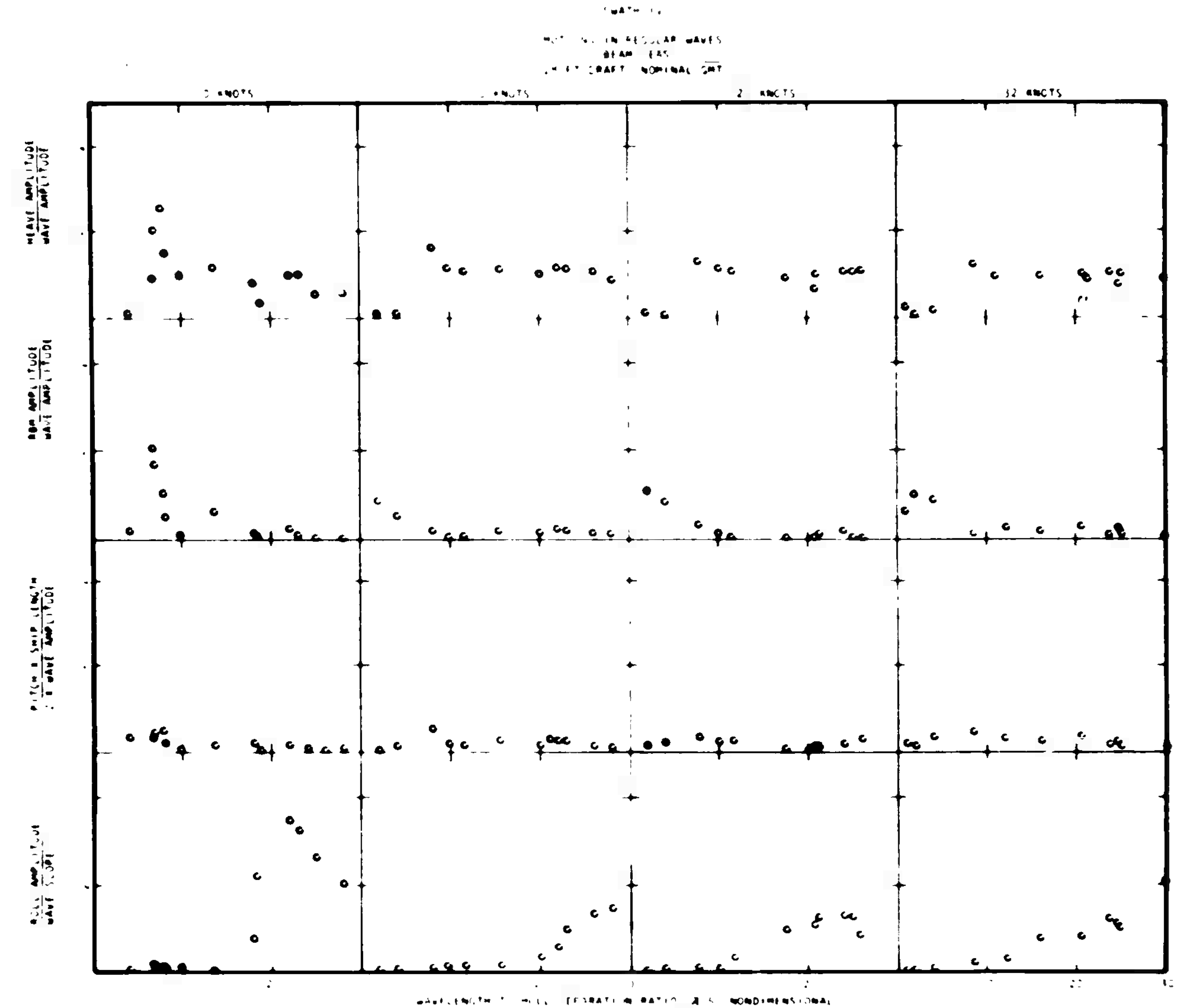

Figure 77 - Dimensionless Motions in Regular Beam Seas, 28 ft Draft, Nominal $\overline{GM}_t$

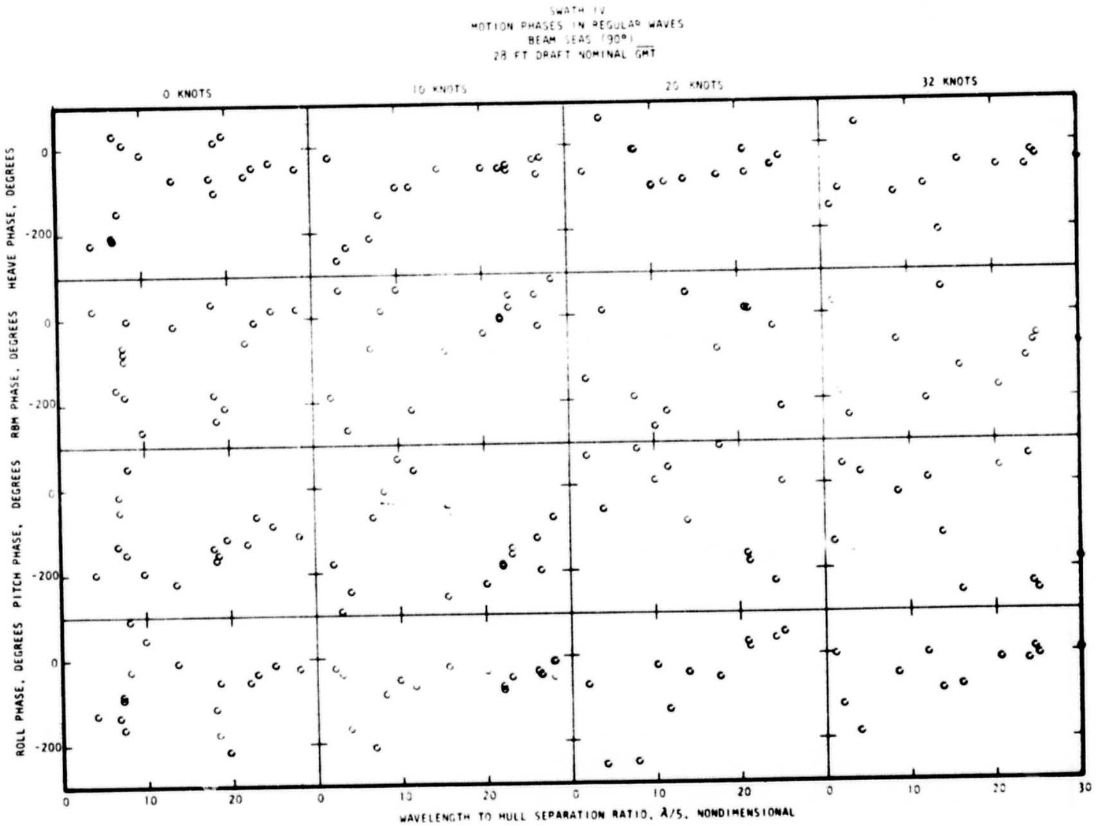

Figure 78 - Motion Phases in Regular Beam Seas, 28 ft Draft, Nominal $\overline{GM}_t$

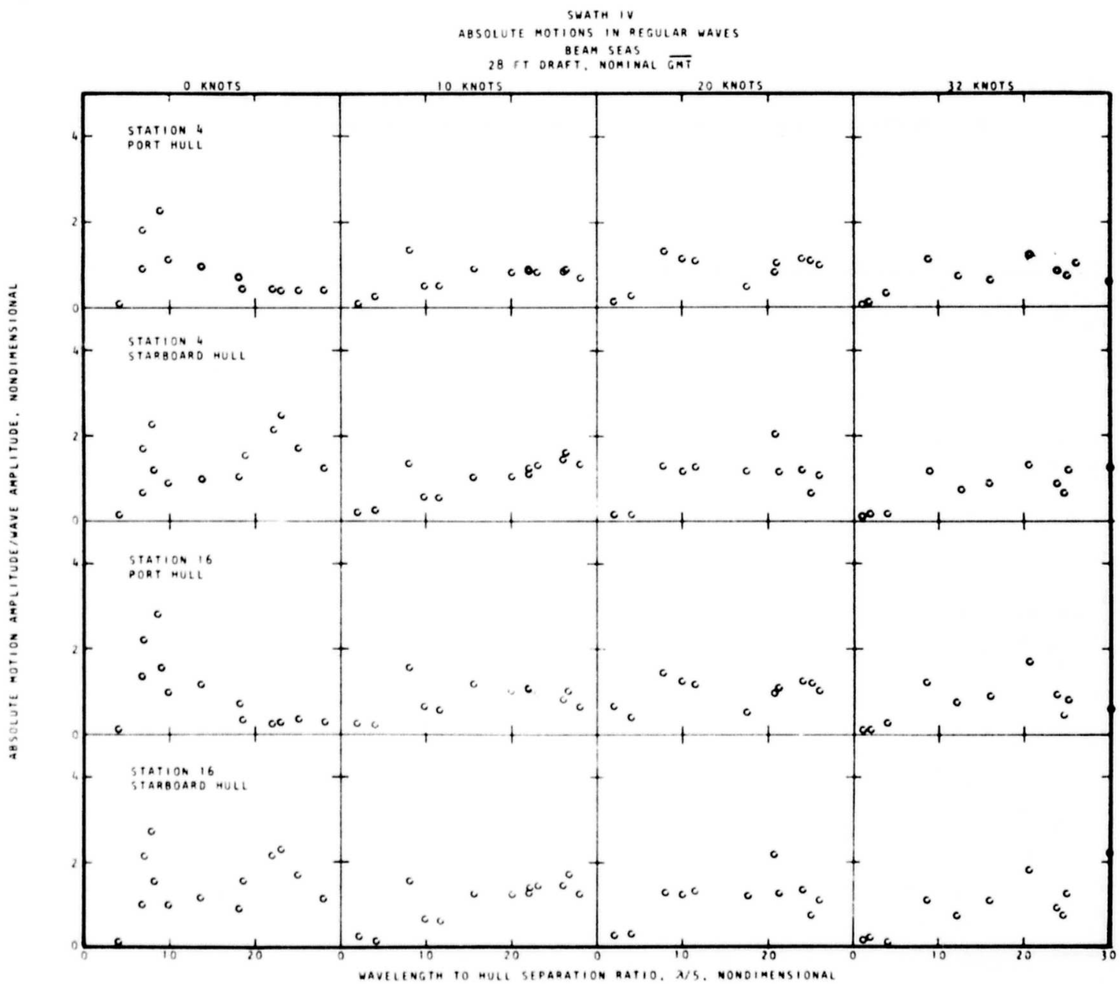

Figure 79 - Dimensionless Absolute Bow And Stern Motions in Regular Beam Seas, 28 ft Draft, Nominal $\overline{GM}_t$

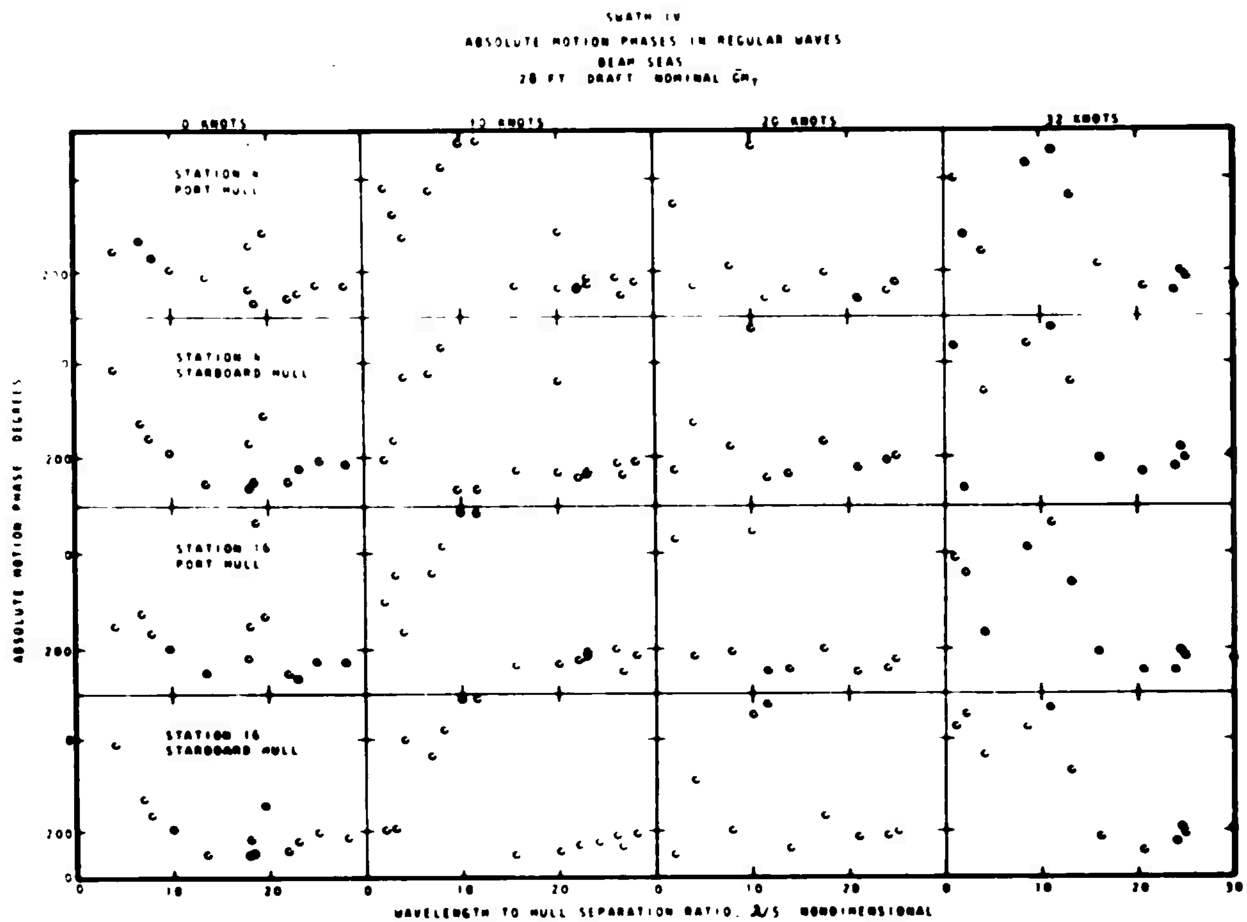

Figure 80 - Absolute Bow and Stern Motion Phases in Regular Beam Seas, 28 ft Draft, Nominal $\overline{GM}_t$

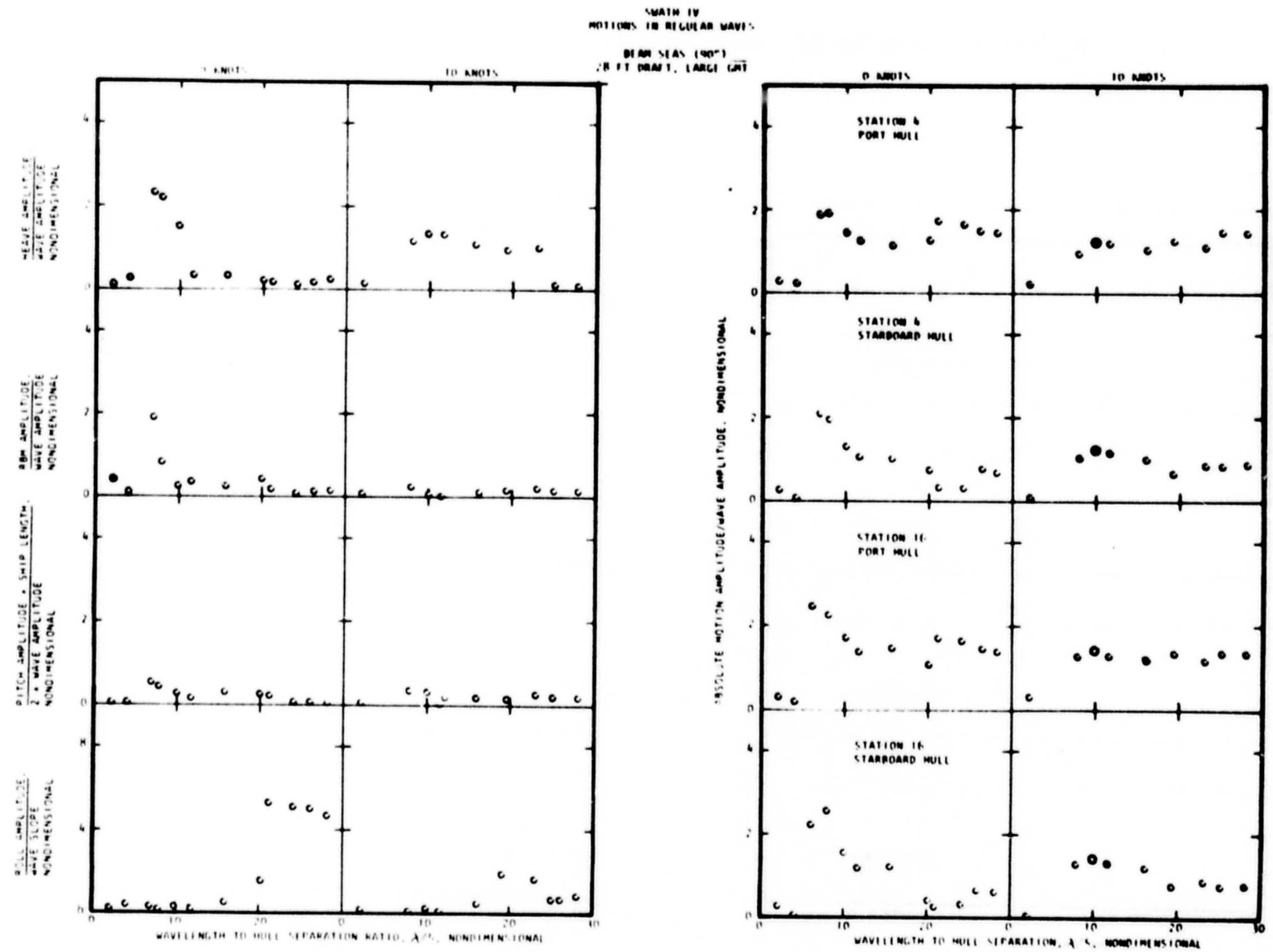

Figure 81 - Dimensionless Motions in Regular Beam Seas, 28 ft Draft, Large $\overline{GM}_t$

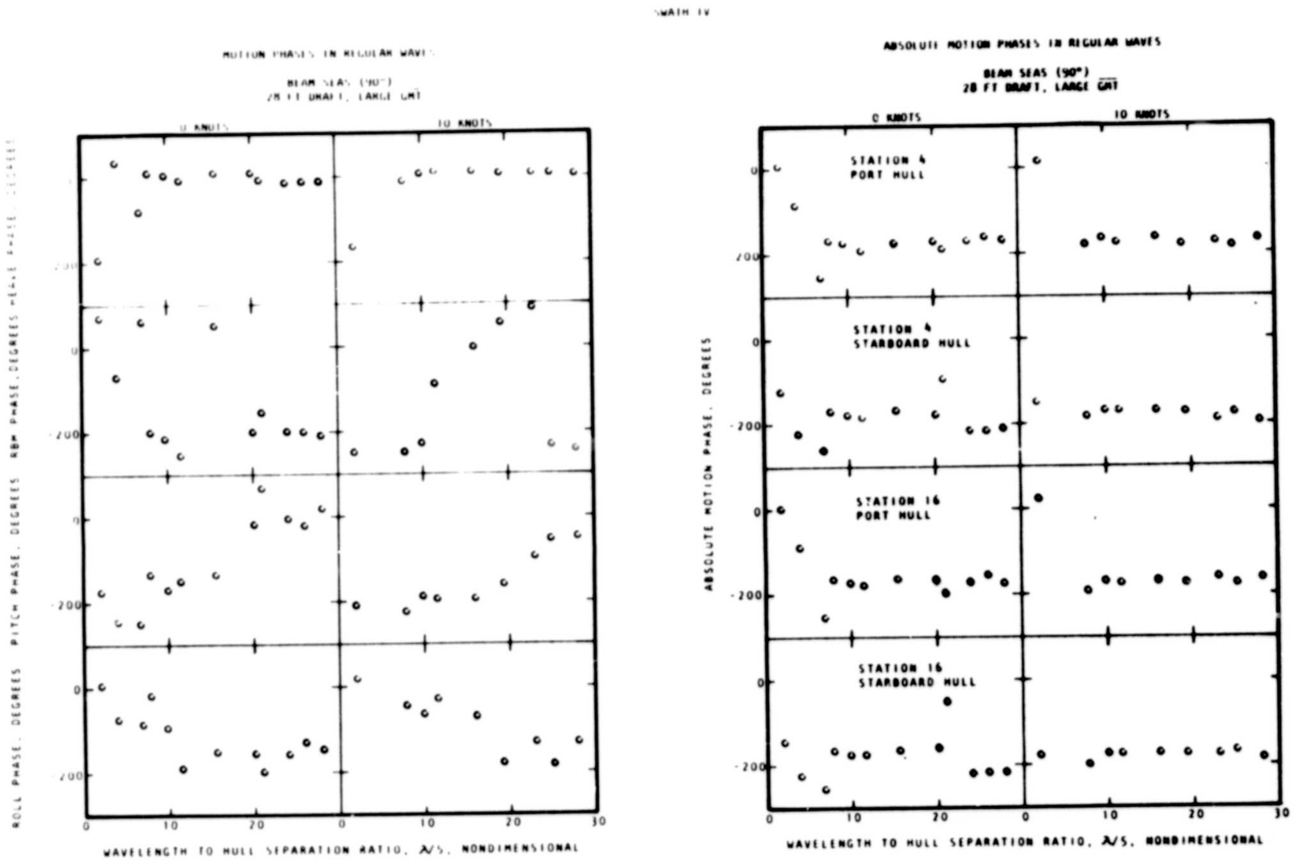

Figure 82 - Motion Phases in Regular Beam Seas, 28 ft Draft, Large $\overline{GM}_t$

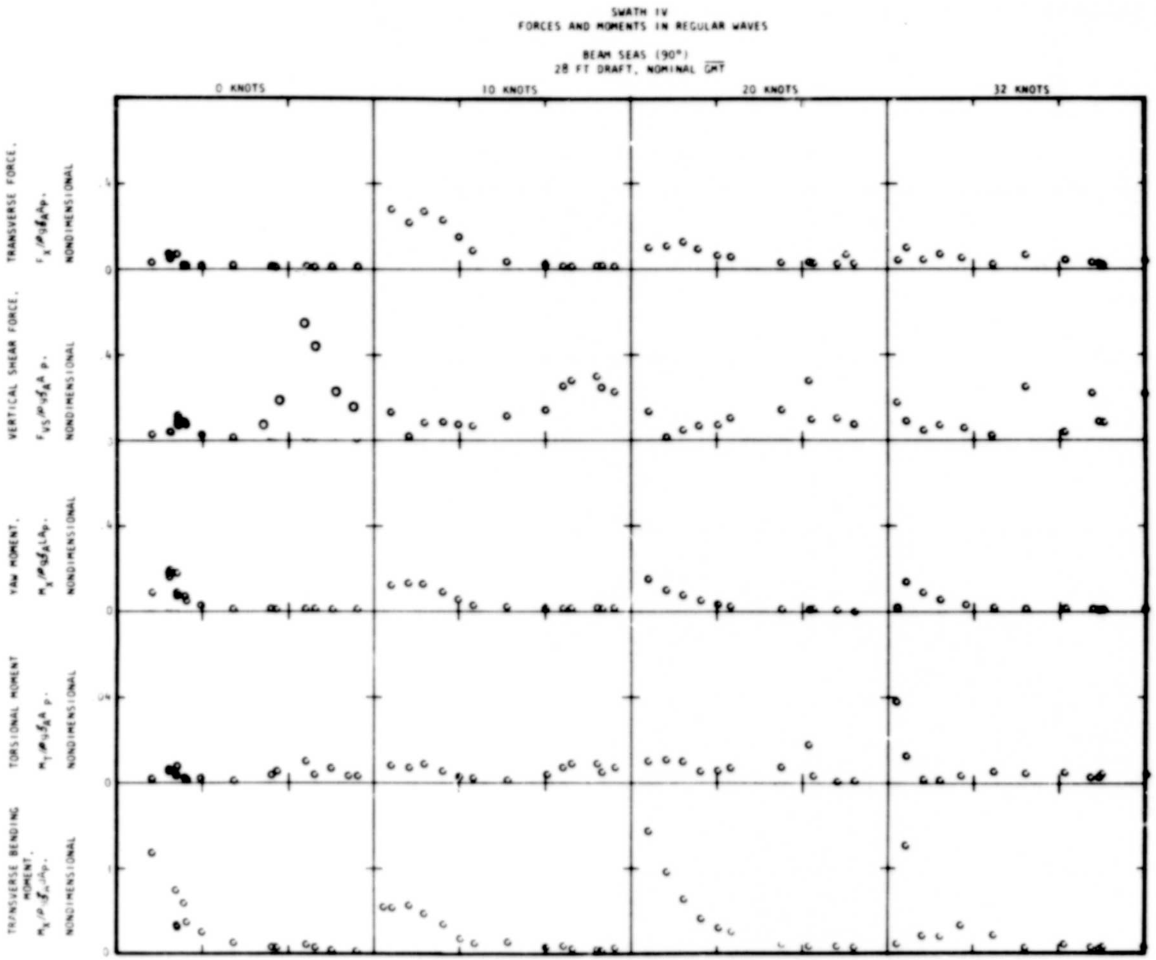

Figure 83 - Dimensionless Forces and Moments in Regular Beam Seas, 28 ft Draft, Nominal $\overline{GM}_t$

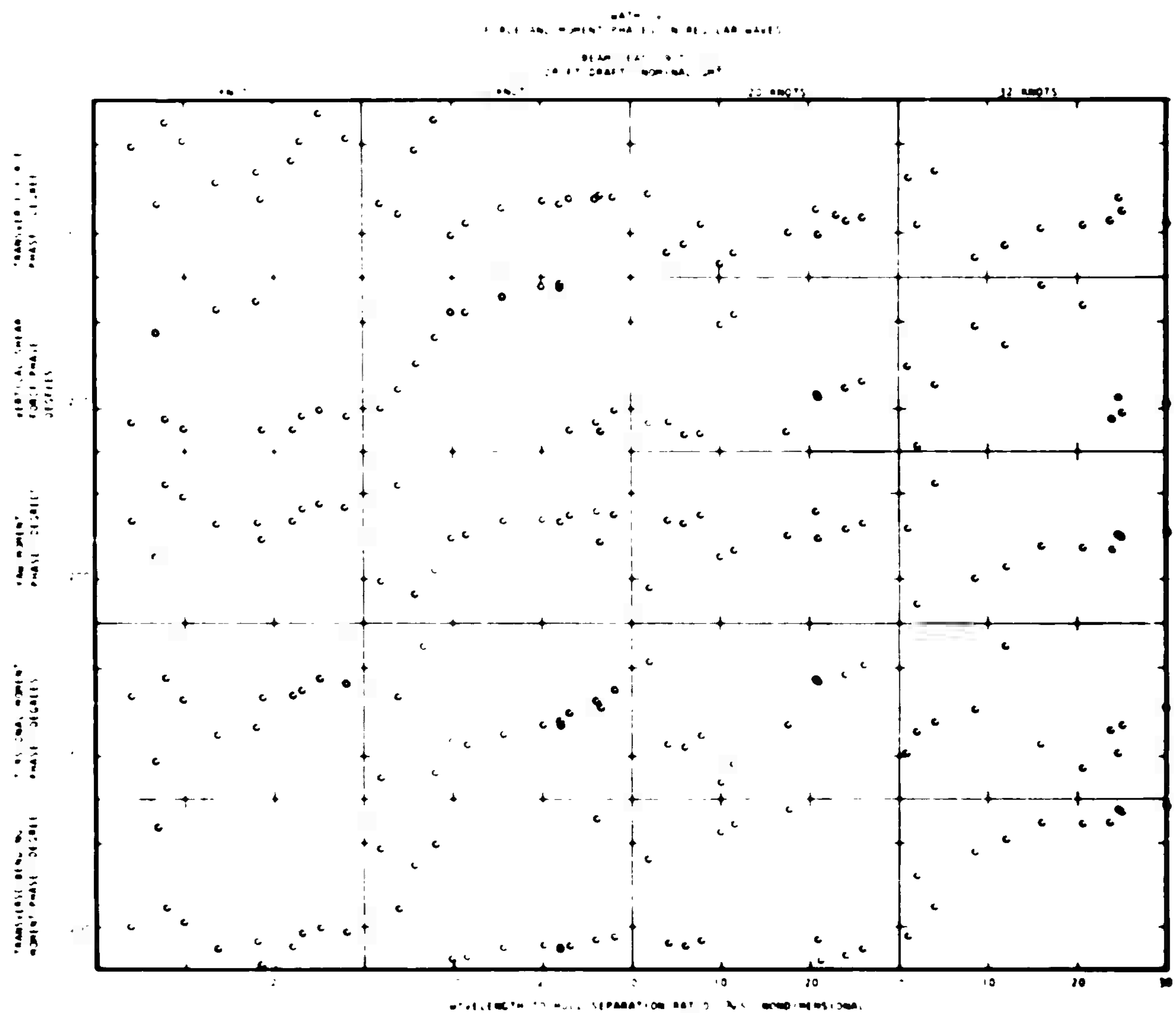

Figure 84 - Force and Moment Phases in Regular Beam Seas, 28 ft Draft, Nominal $\overline{GM}_t$

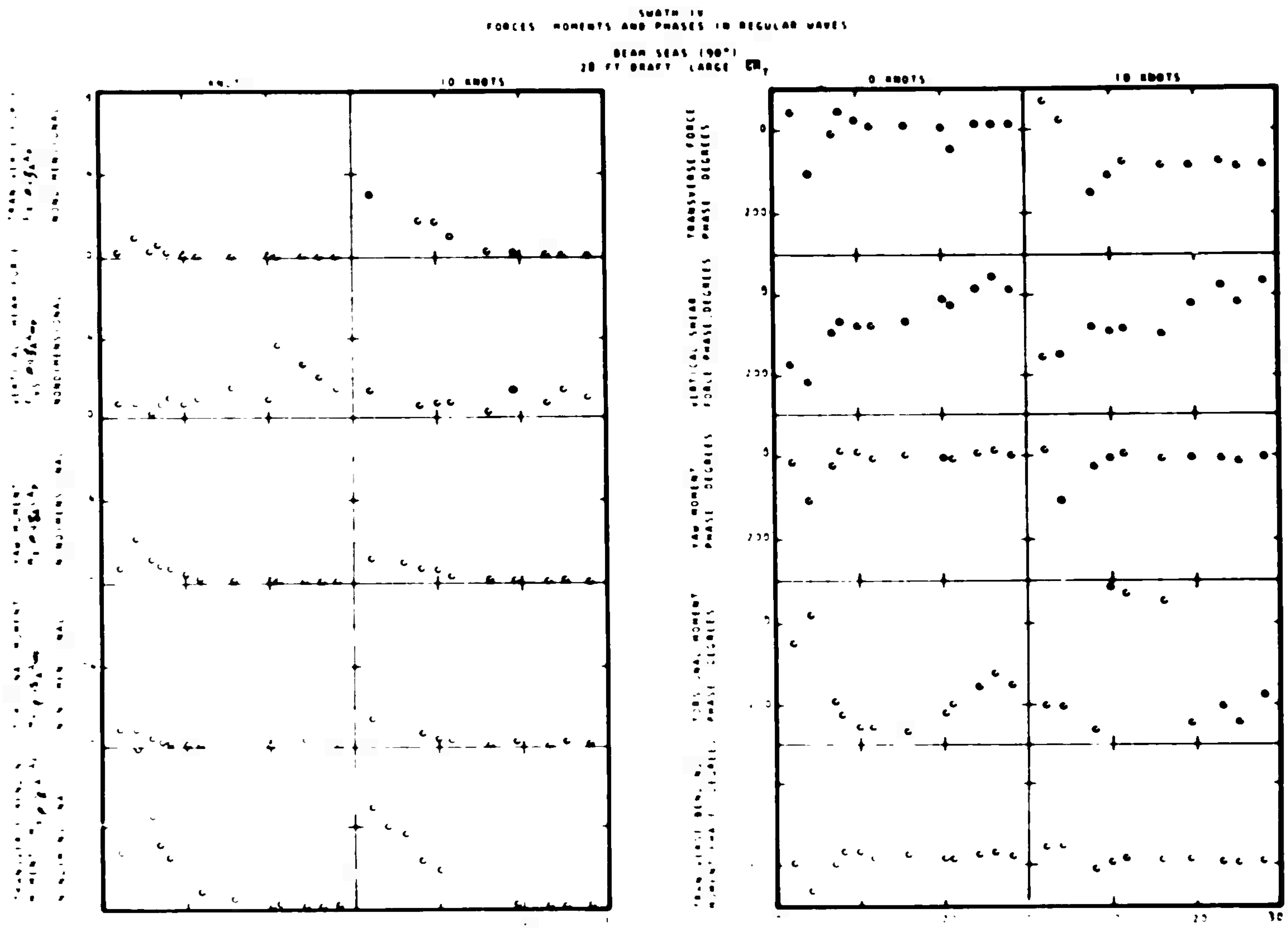

Figure 85 - Dimensionless Forces and Moments and their Phases in Regular Beam Seas, 28 ft Draft, Large $\overline{GM}_t$

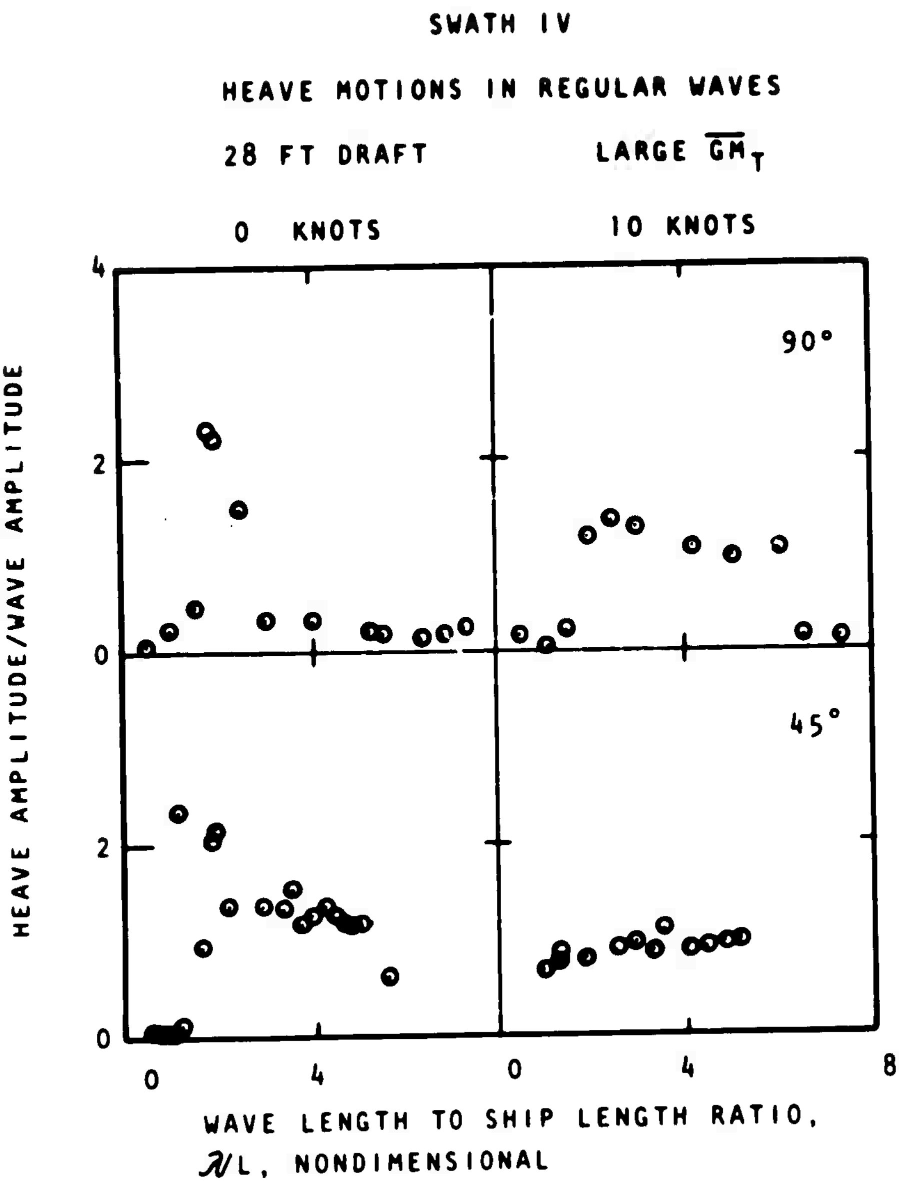

Figure 86 - Dimensionless Heave in Regular Beam and Quartering Seas, 28 ft Draft, Large $\overline{GM}_t$

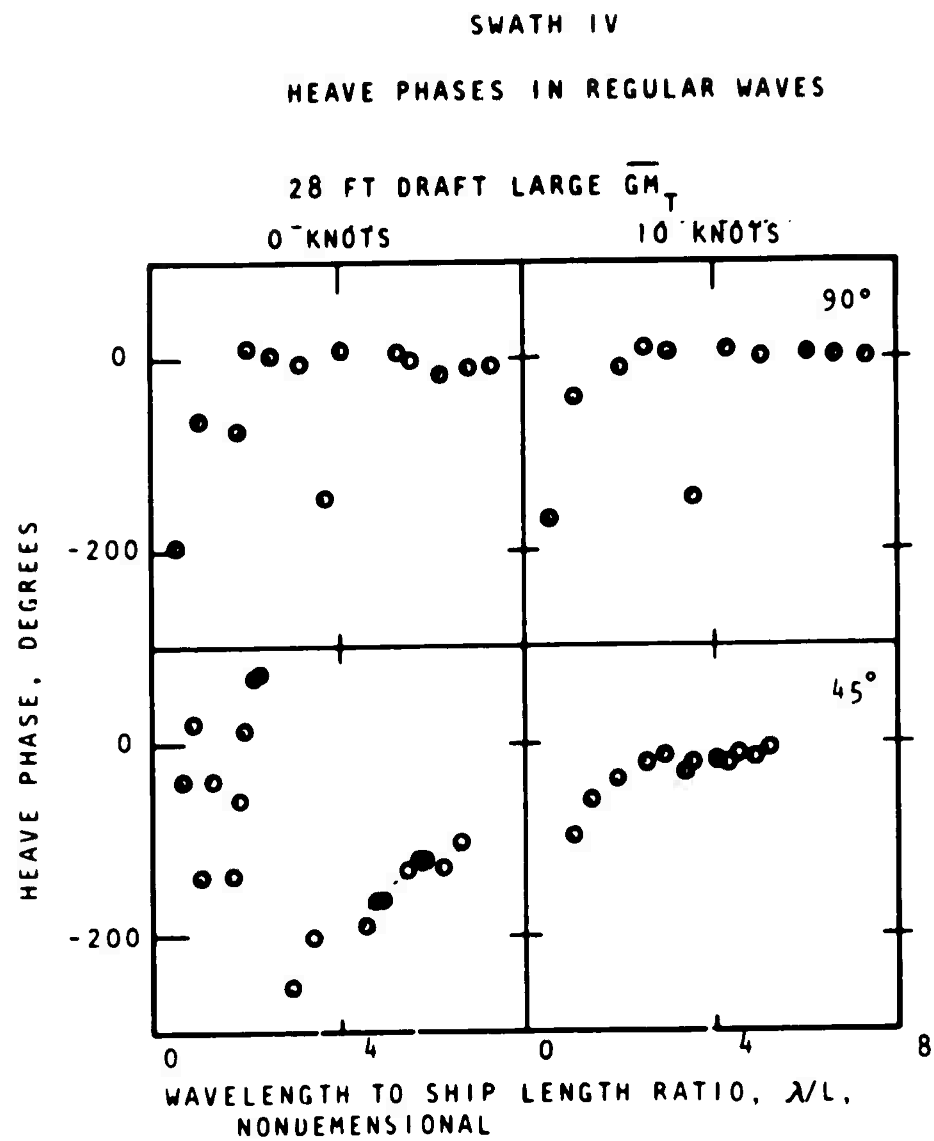

Figure 87 - Heave Phase in Regular Beam and Quartering Seas, 28 ft Draft, Large $\overline{GM}_t$

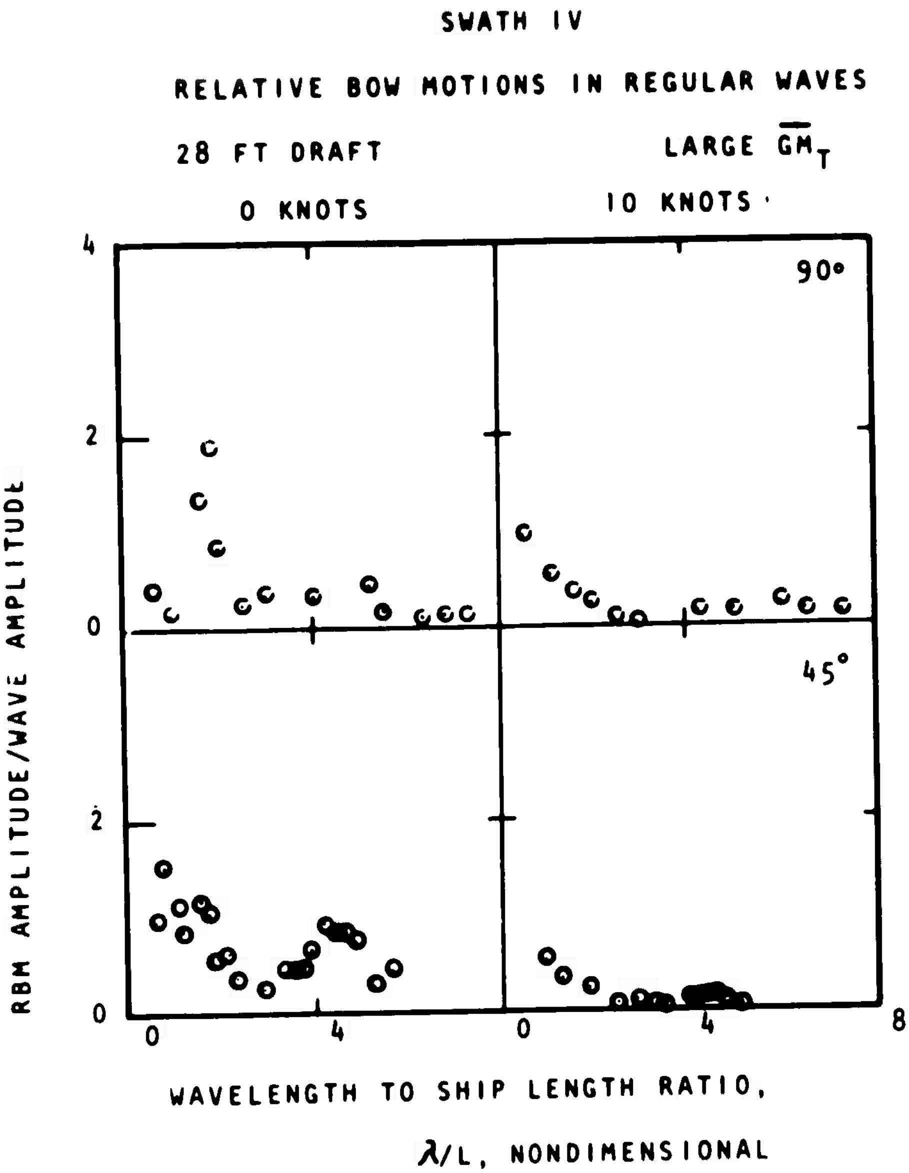

Figure 88 - Dimensionless Relative Bow Motion in Regular Beam and Quartering Seas, 28 ft Draft, Large $\overline{GM}_t$

SWATH IV

RBM PHASES IN REGULAR WAVES

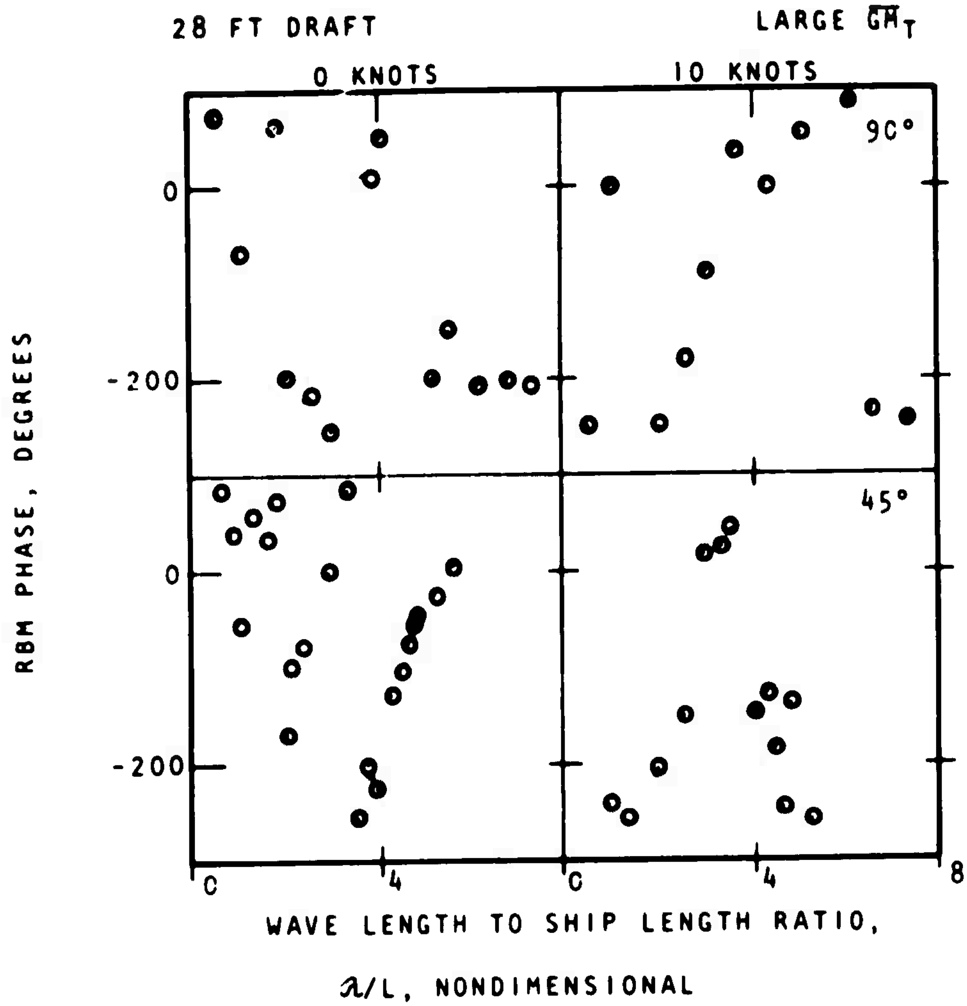

Figure 89 - Relative Bow Motion Phase in Regular Beam and Quartering Seas, 28 ft Draft, Large $\overline{GM}_t$

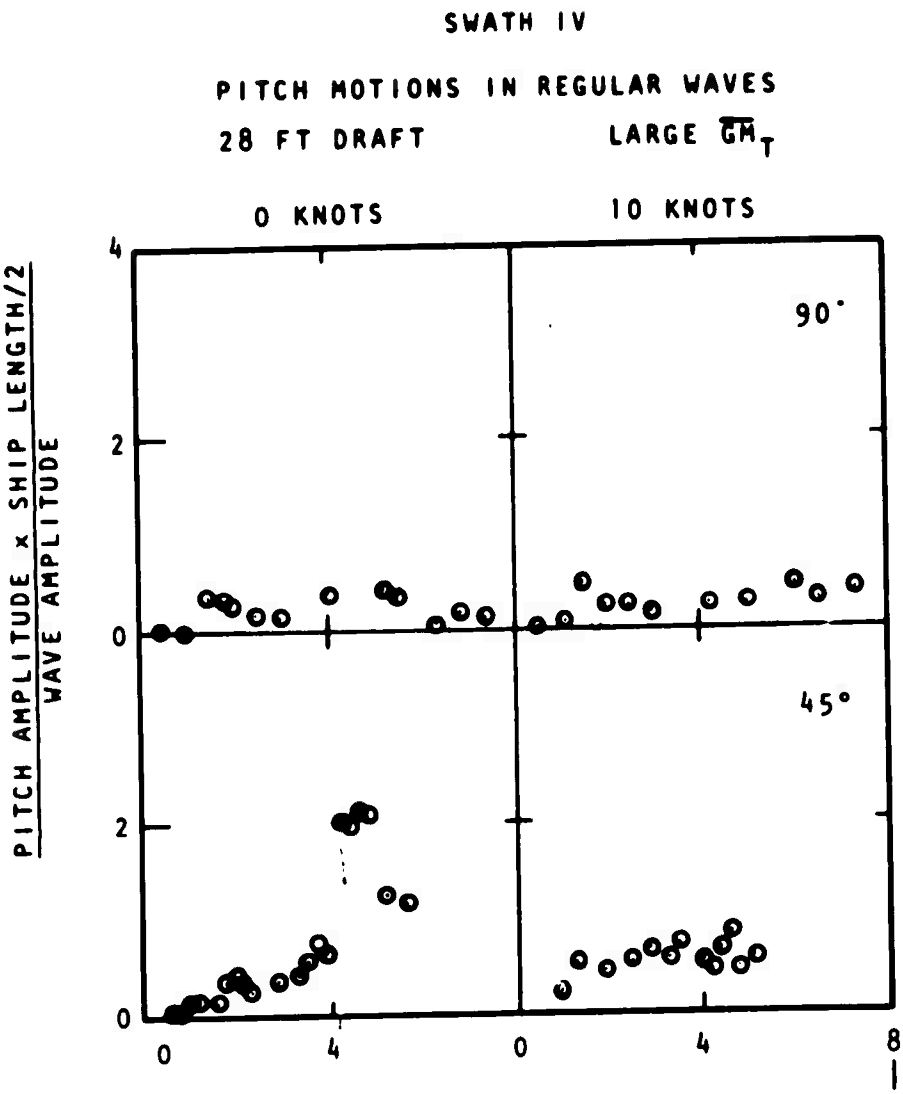

Figure 90 - Dimensionless Pitch in Regular Beam and Quartering Seas, 28 ft Draft, Large $\overline{GM}_t$

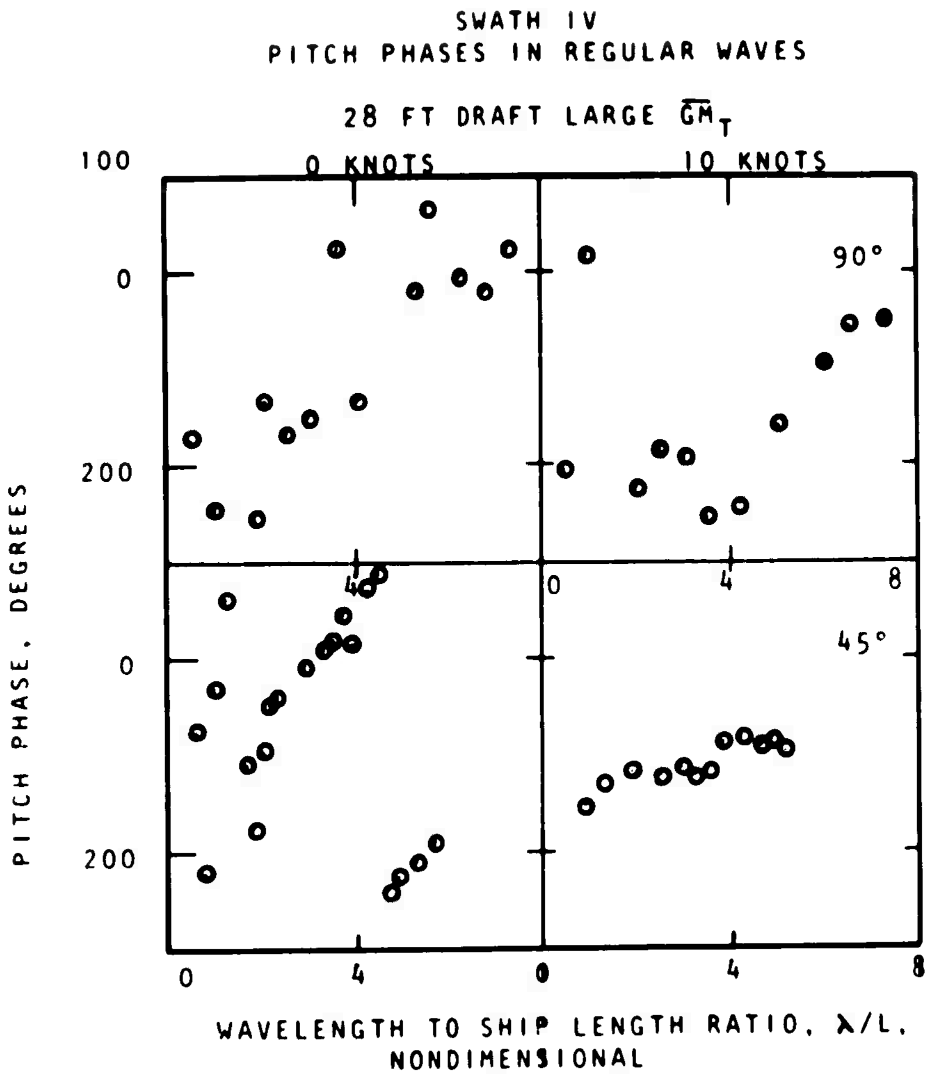

Figure 91 - Pitch Phase in Regular Beam and Quartering Seas, 28 ft Draft, Large $\overline{GM}_t$

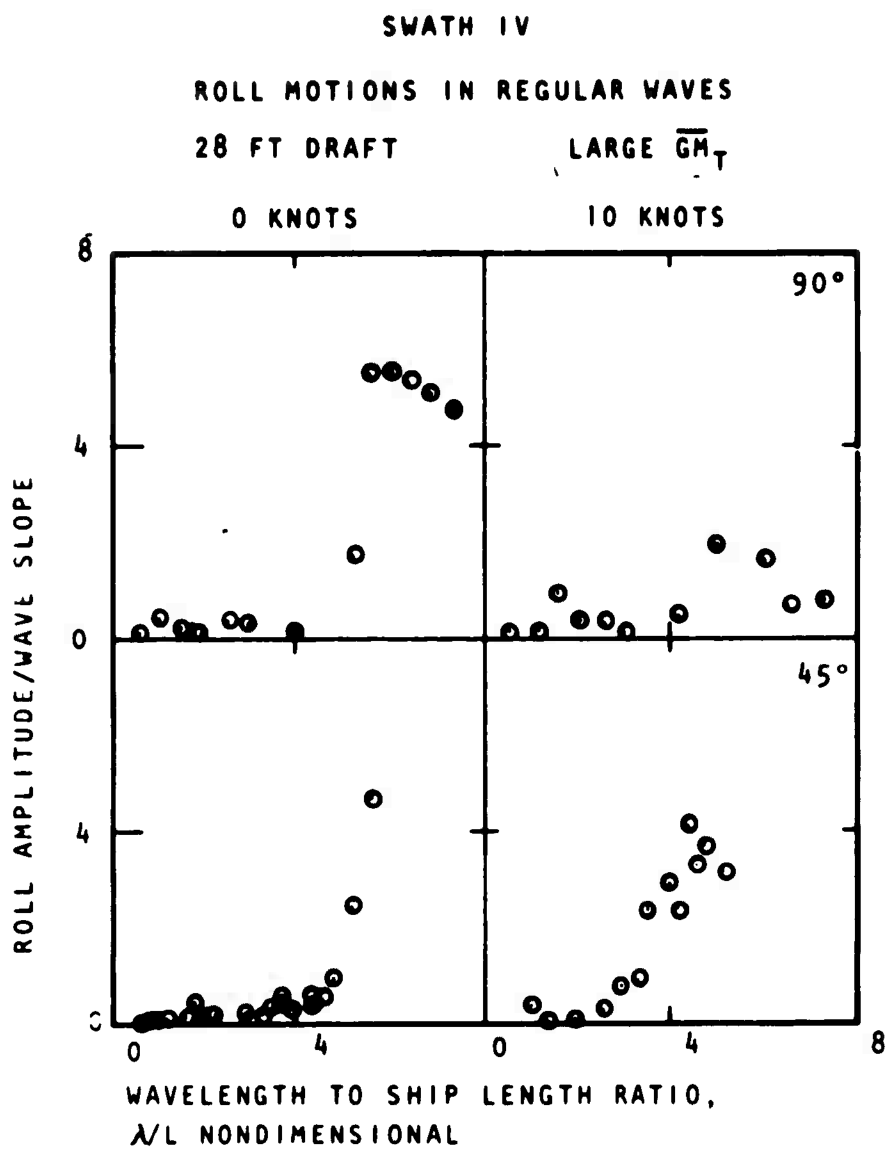

Figure 92 - Dimensionless Roll in Regular Beam and Quartering Seas, 28 ft Draft, Large $\overline{GM}_t$

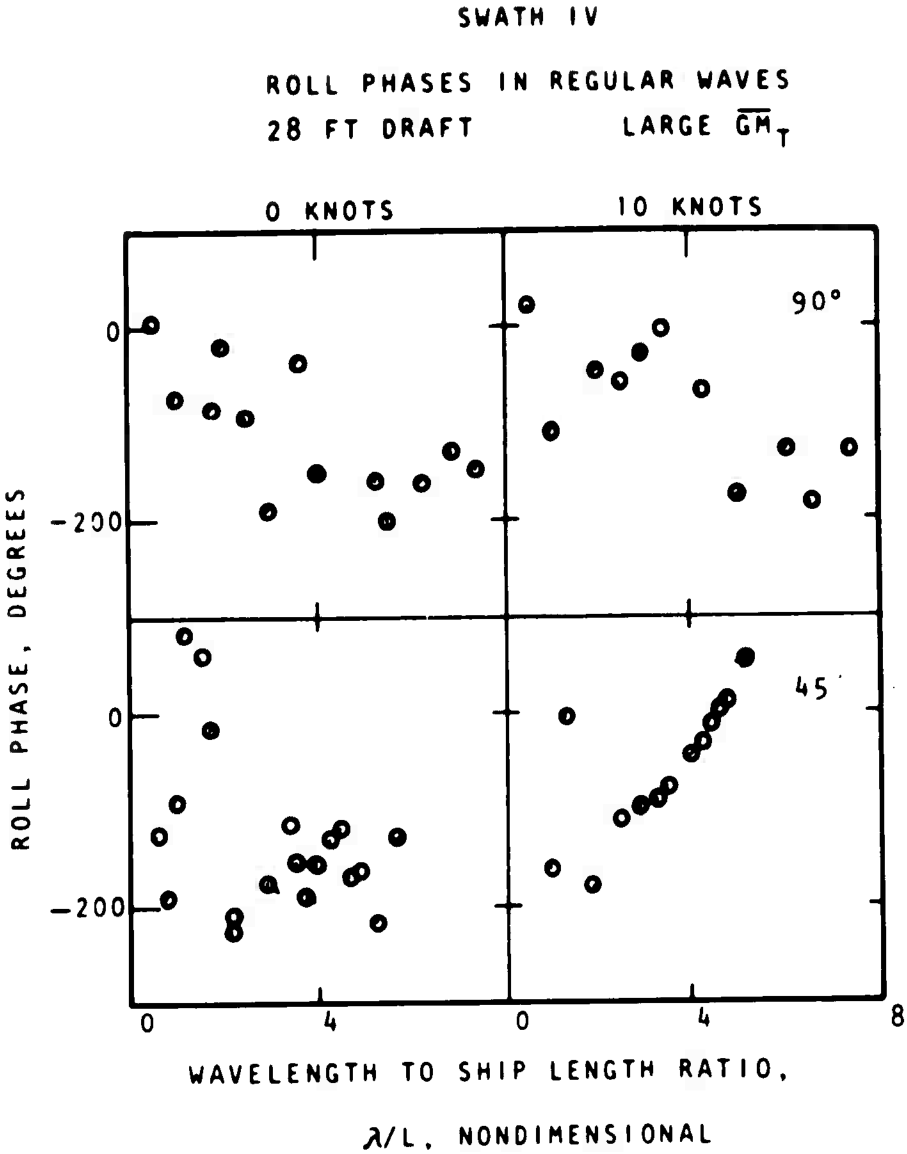

Figure 93 - Roll Phase in Regular Beam and Quartering Seas, 28 ft Draft, Large $\overline{GM}_t$

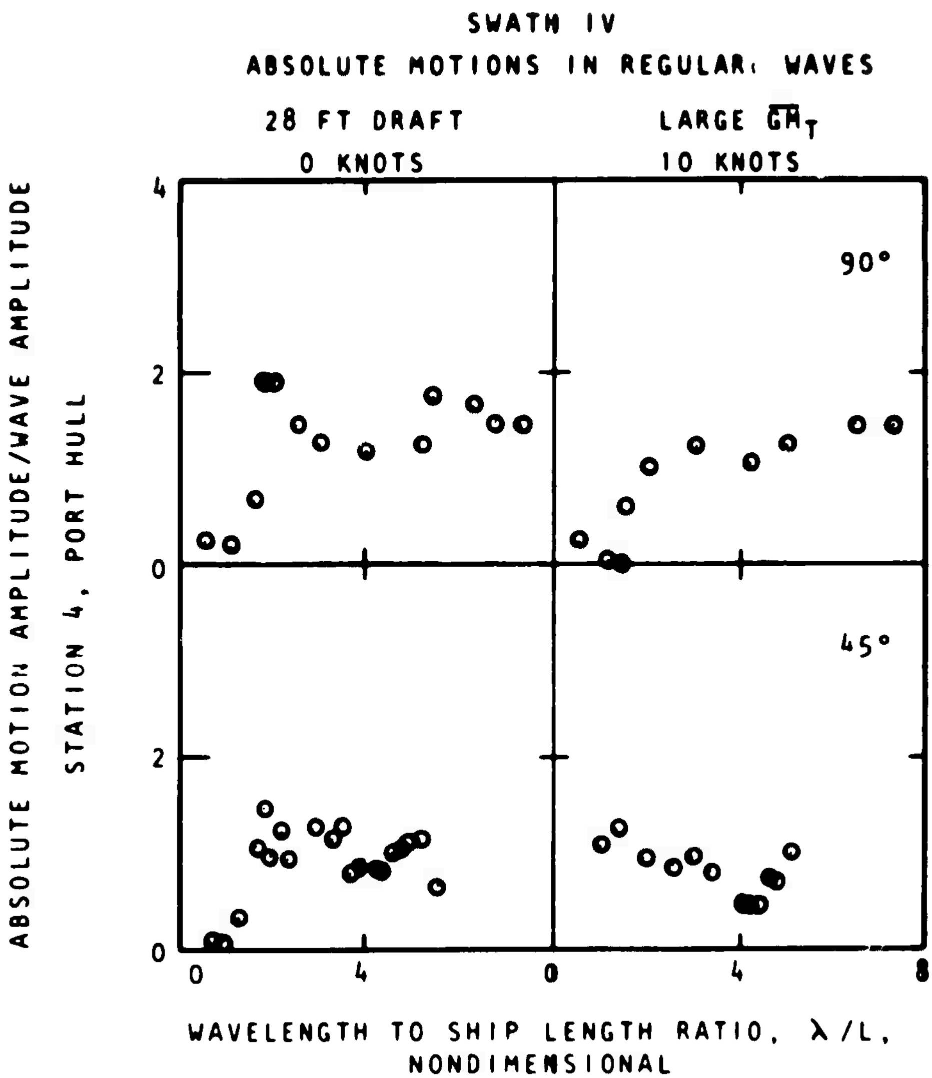

Figure 94 - Dimensionless Absolute Bow Motion in Regular Beam and Quartering Seas, Port Hull, 28 ft Draft, Large $\overline{GM}_t$

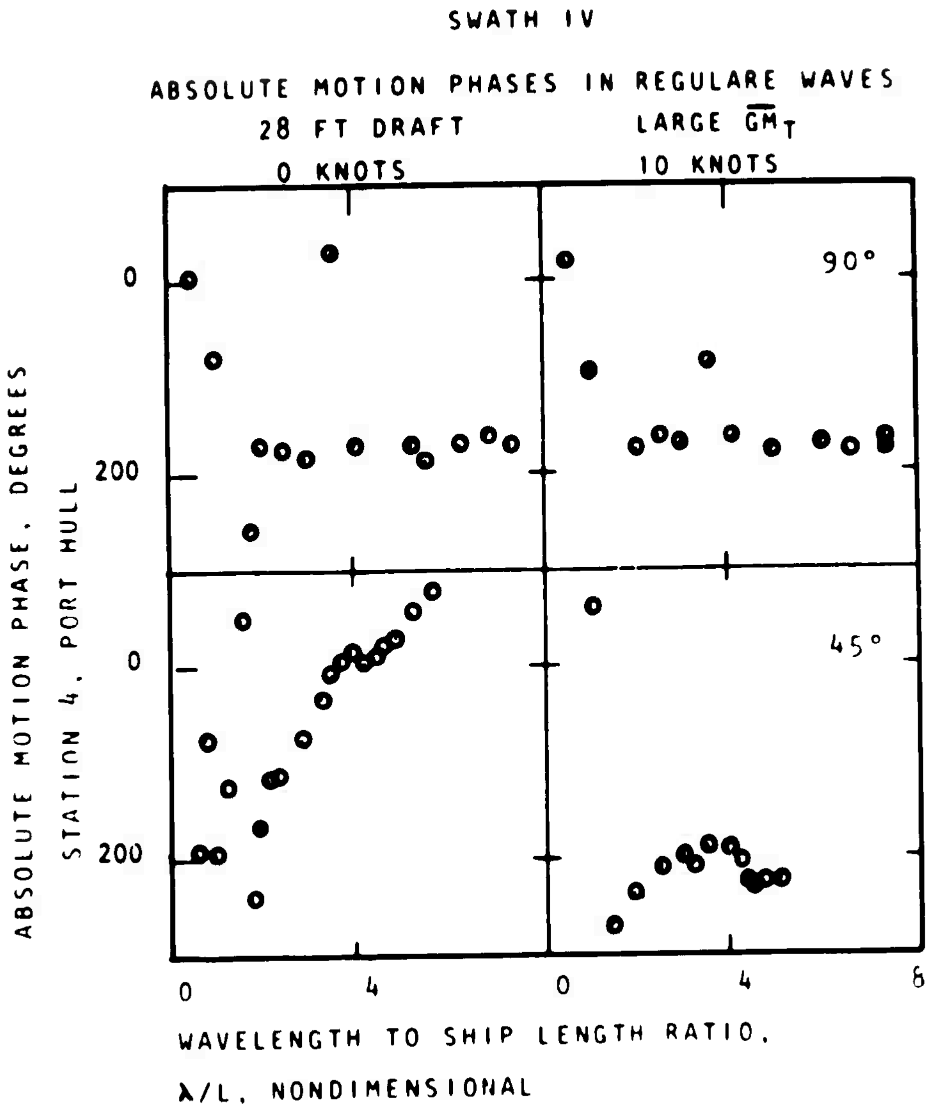

Figure 95 - Absolute Bow Motion Phase in Regular Beam and Quartering Seas, Port Hull, 28 Ft Draft, Large $\overline{GM}_t$

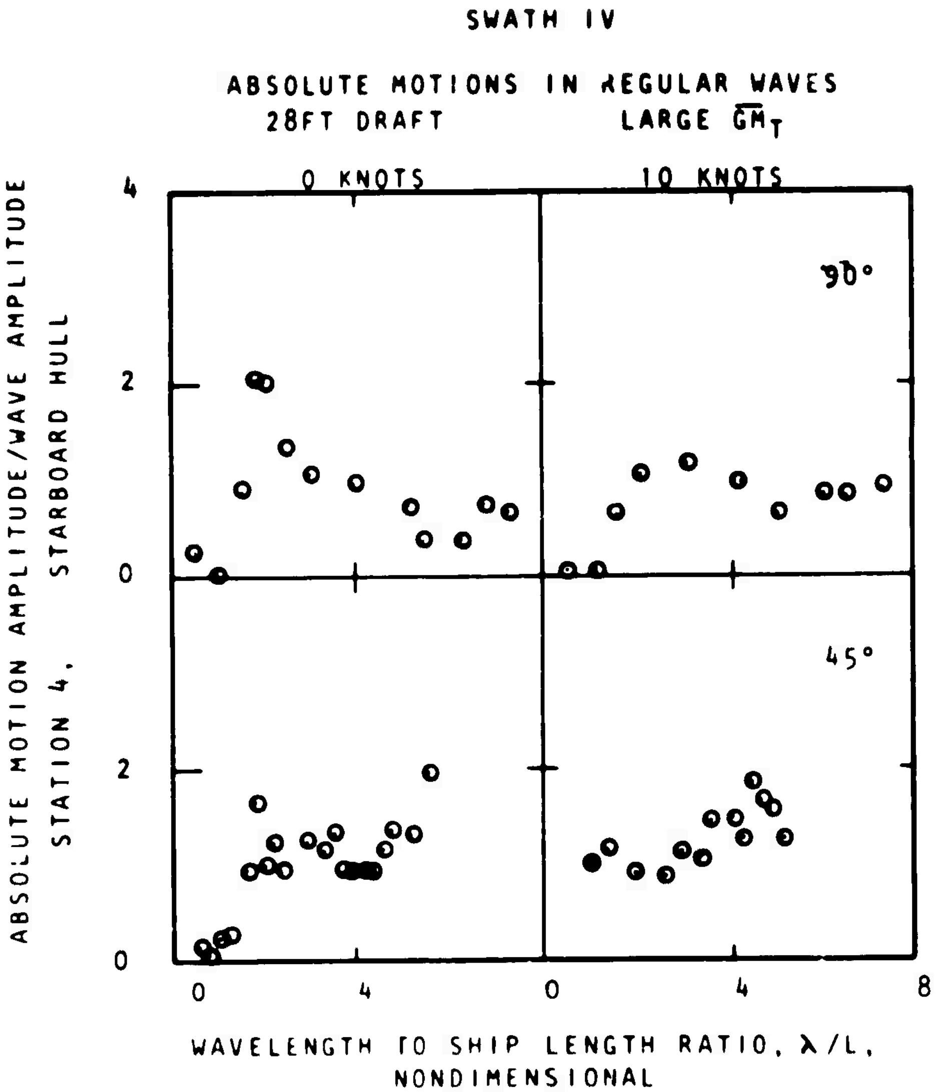

Figure 96 - Dimensionless Absolute Bow Motion In Regular Beam and Quartering Seas, Starboard Hull, 28 ft Draft, Large $\overline{GM}_t$

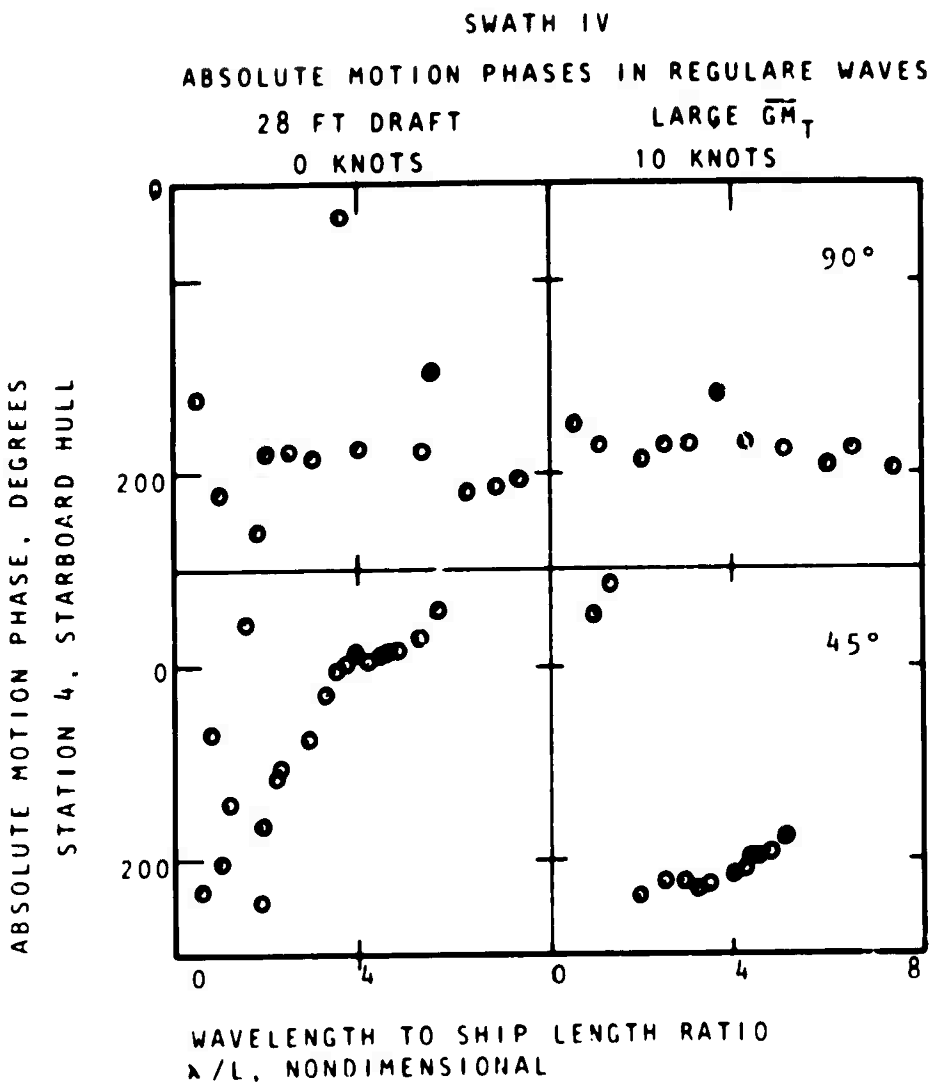

Figure 97 - Absolute Bow Motion Phase in Regular Beam and Quartering Seas, Starboard Hull, 28 ft Draft, Large $\overline{GM}_t$

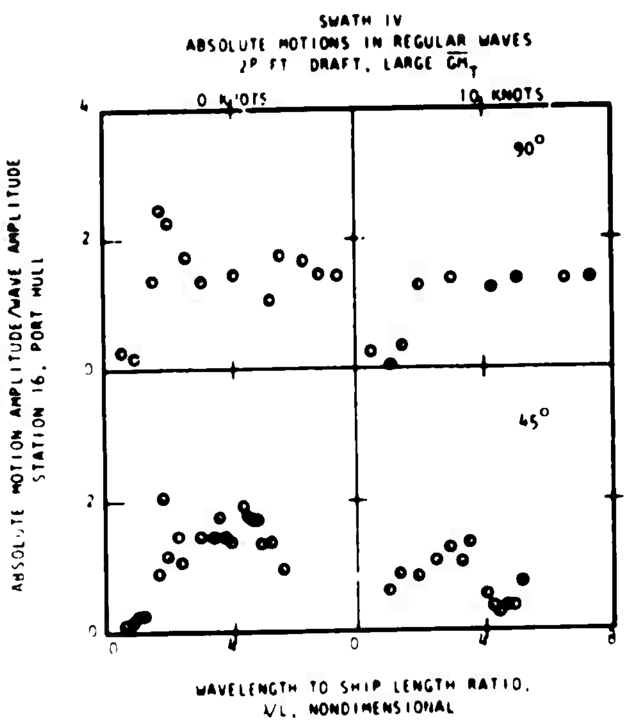

Figure 98 - Dimensionless Absolute Stern Motion in Regular Beam And Quartering Seas, Port Hull, 28 ft Draft, Large $\overline{GM}_t$

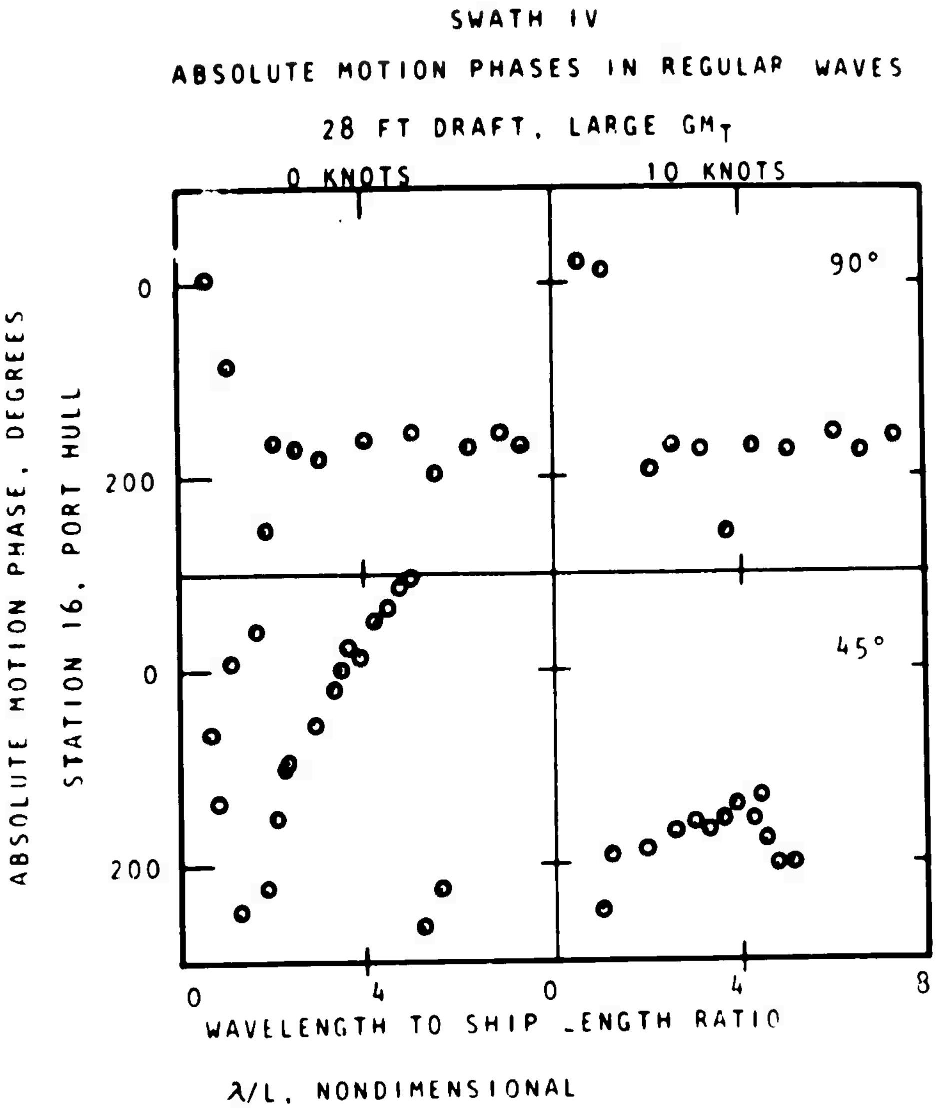

Figure 99 - Absolute Stern Motion Phase in Regular Beam and Quartering Seas, Port Hull, 28 ft Draft, Large $\overline{GM}_t$

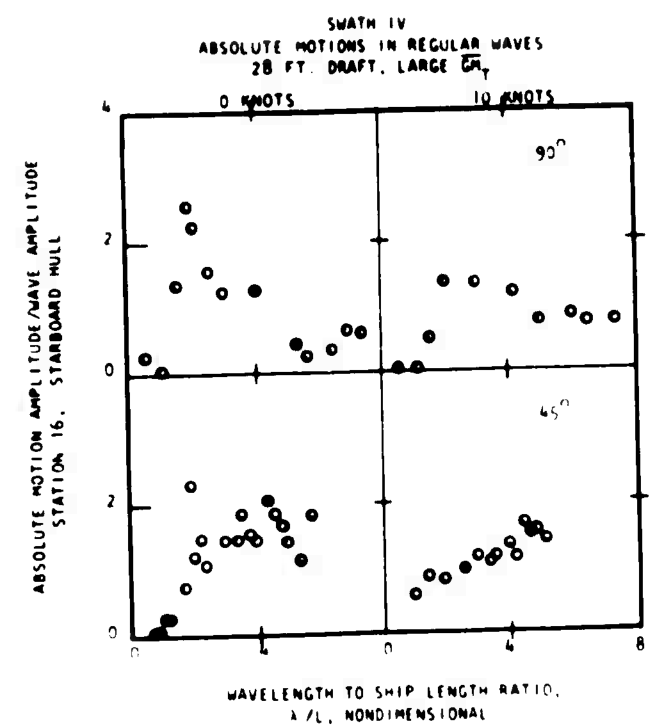

Figure 100 - Dimensionless Absolute Stern Motion in Regular Beam and Quartering Seas, Starboard Hull, 28 ft Draft, Large $\overline{GM}_t$

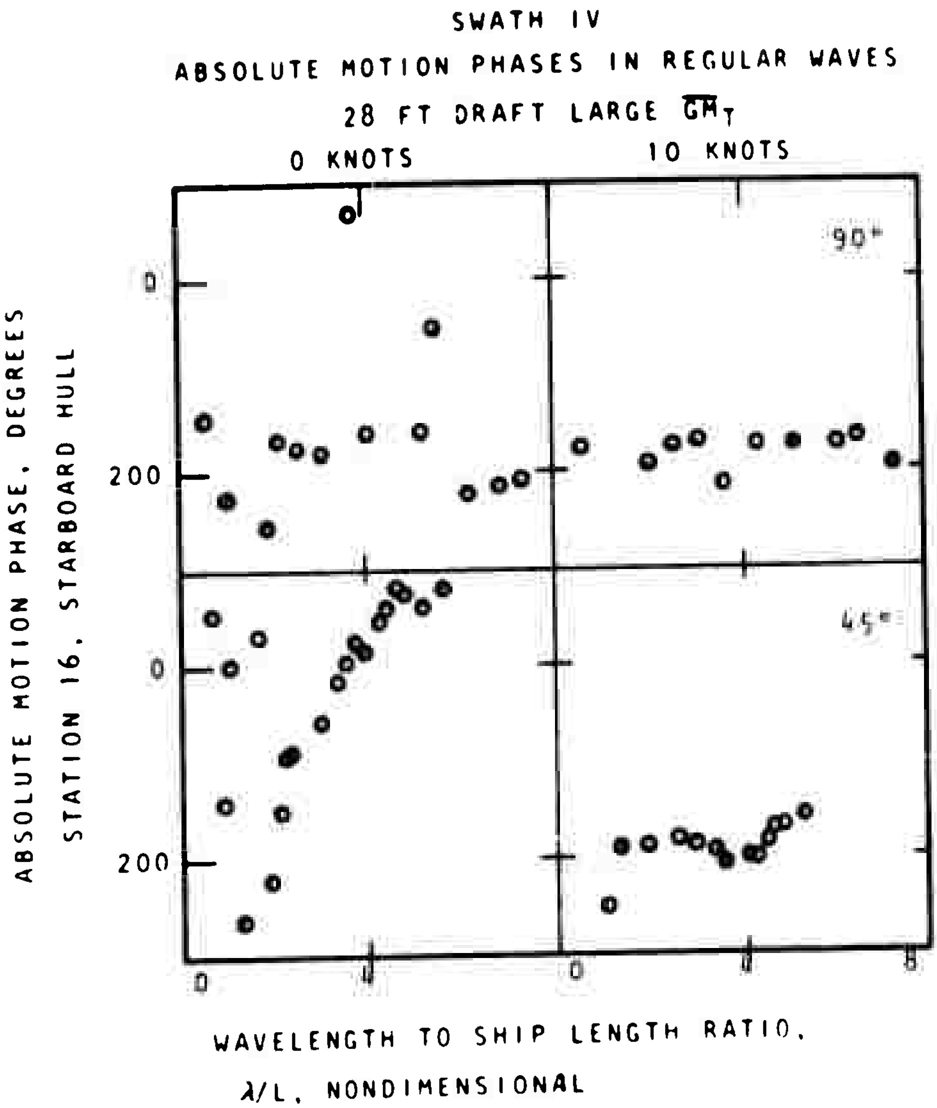

Figure 101 - Absolute Stern Motion Phase in Regular Beam and Quartering Seas, Starboard Hull, 28 ft Draft, Large $\overline{GM}_t$

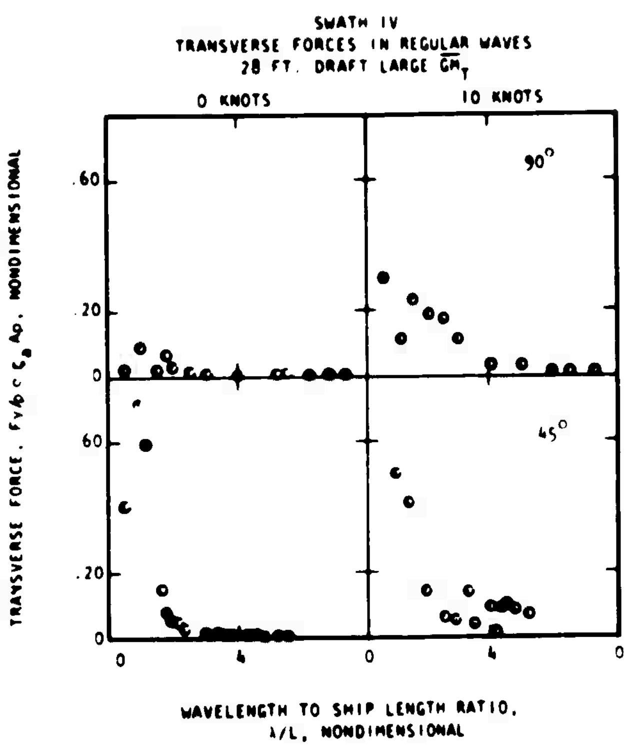

Figure 102 - Dimensionless Transverse Force in Regular Beam and Quartering Seas, 28 ft Draft, Large $\overline{GM}_t$

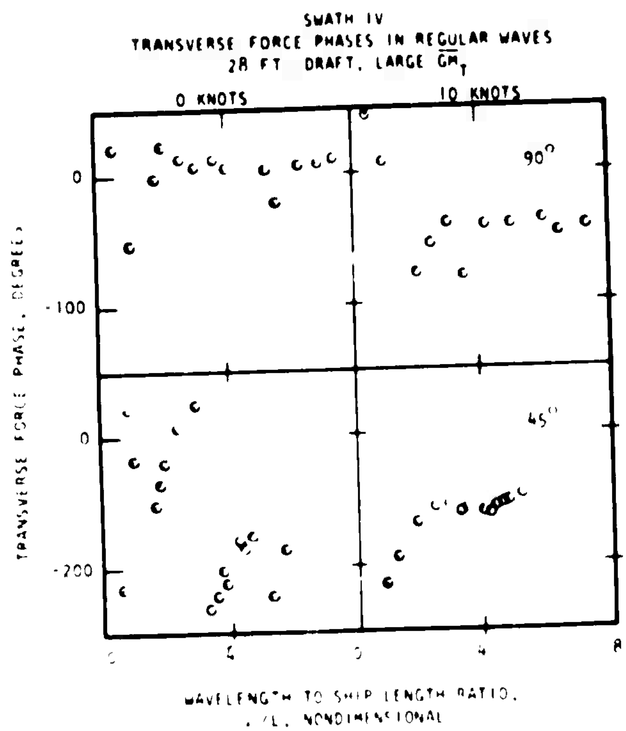

Figure 103 - Transverse Force Phase in Regular Beam and Quartering Seas, 28 ft Draft, Large $\overline{GM}_t$

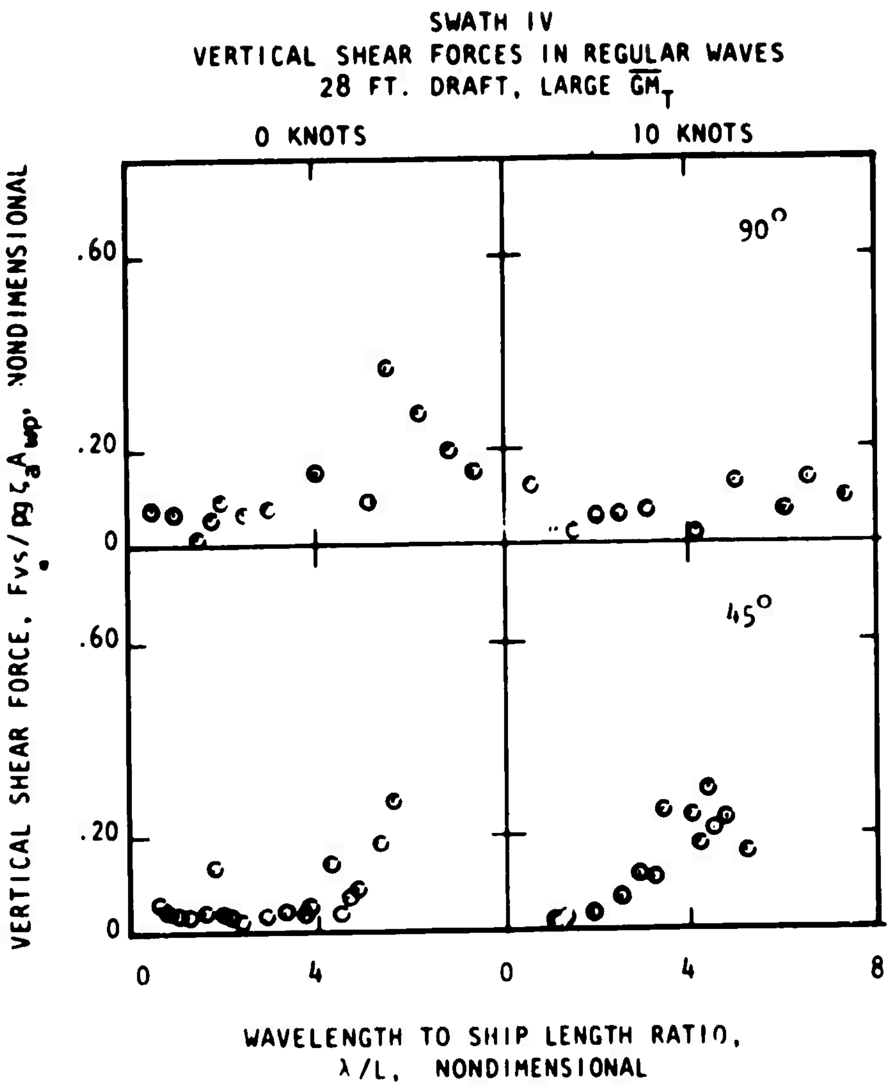

Figure 104 - Dimensionless Vertical Shear Force in Regular Beam and Quartering Seas, 28 ft Draft, Large $\overline{GM}_t$

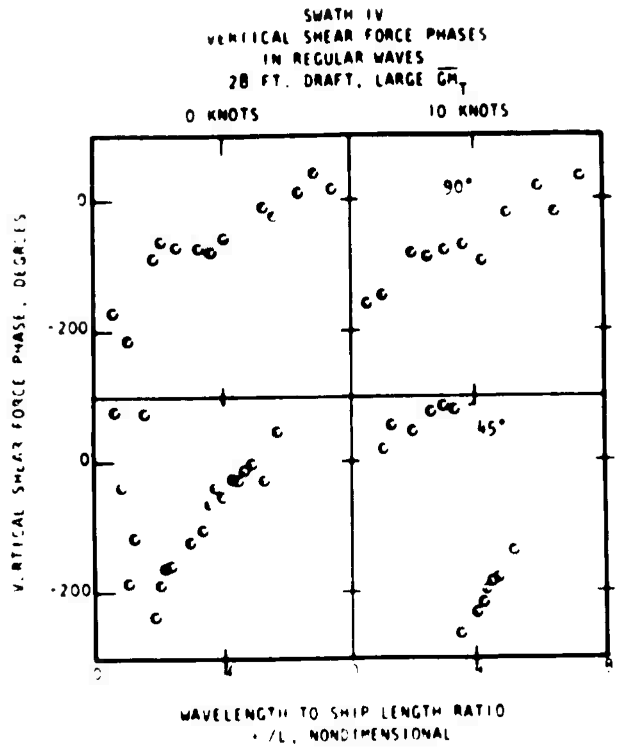

Figure 105 - Vertical Shear Force Phase in Regular Beam and Quartering Seas, 28 ft Draft, Large $\overline{GM}_t$

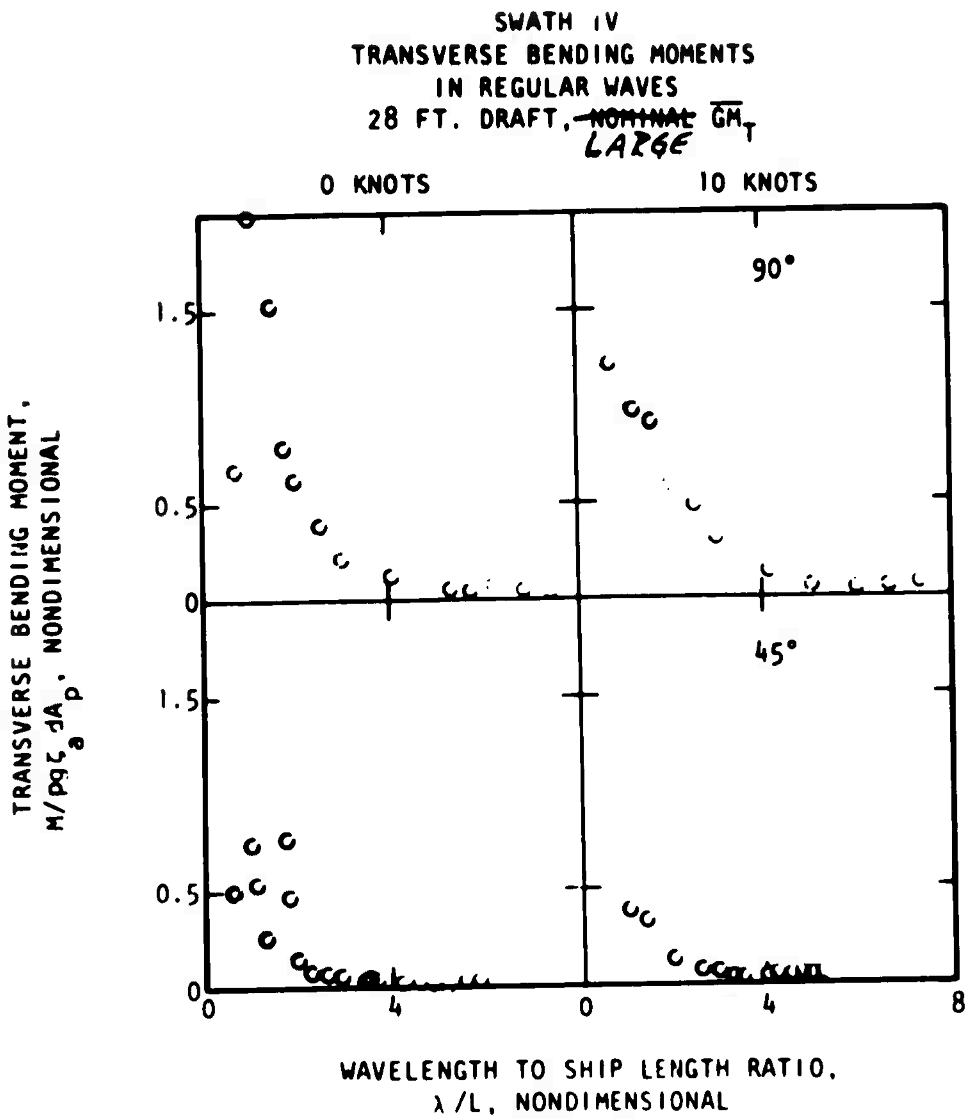

Figure 106 - Dimensionless Transverse Vertical Bending Moment in Regular Beam and Quartering Seas, 28 ft Draft, Large $\overline{GM}_t$

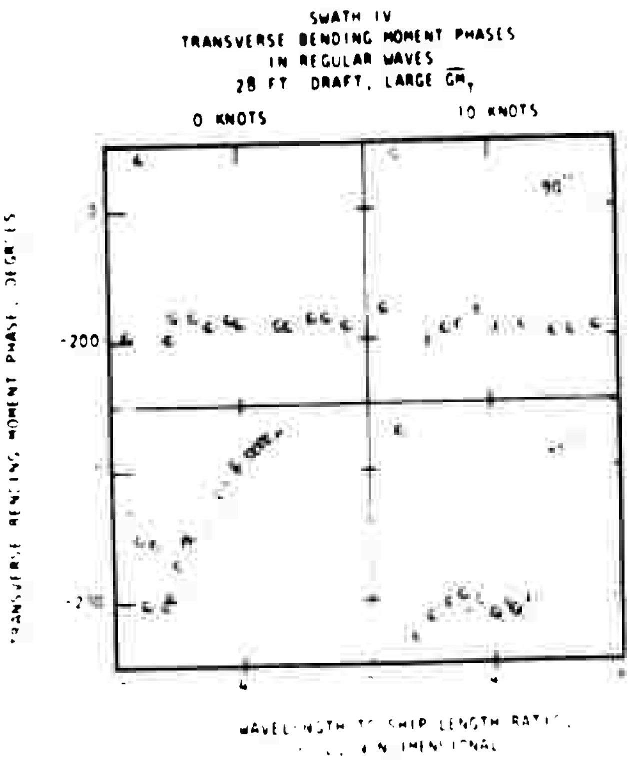

Figure 107 - Transverse Vertical Bending Moment Phase in Regular Beam and Quartering Seas, 28 ft Draft, Large $\overline{GM}_t$

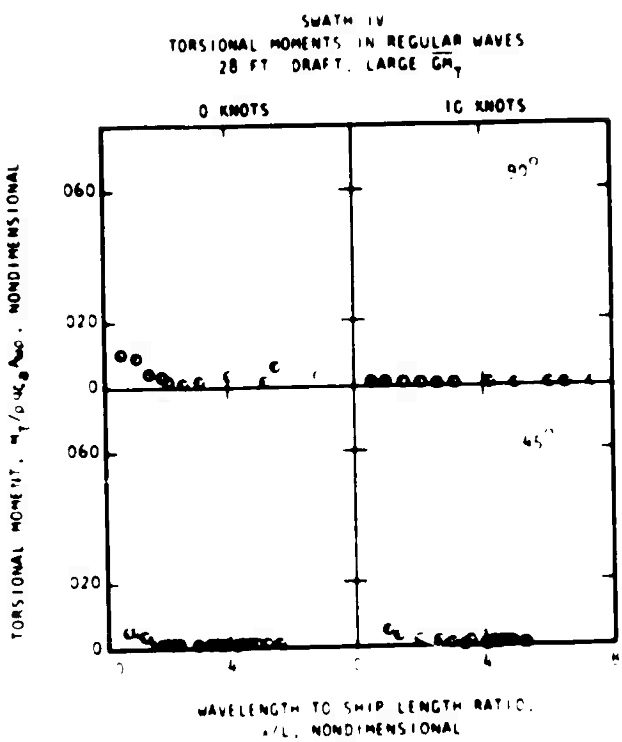

Figure 108 - Dimensionless Torsional Moment in Regular Beam and Quartering Seas, 28 ft Draft, Large $\overline{GM}_t$

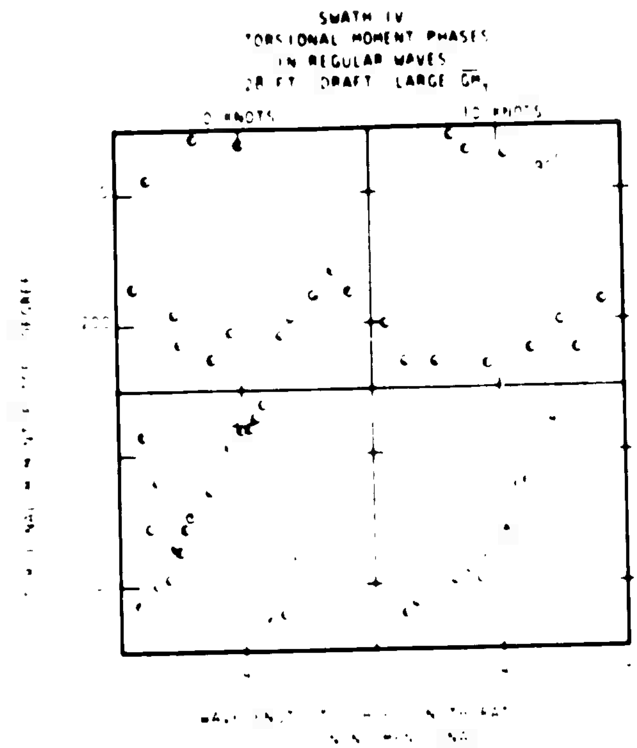

Figure 109 - Torsional Moment Phase in Regular Beam and Quartering Seas, 23 ft Draft, Large $\overline{GM}_t$

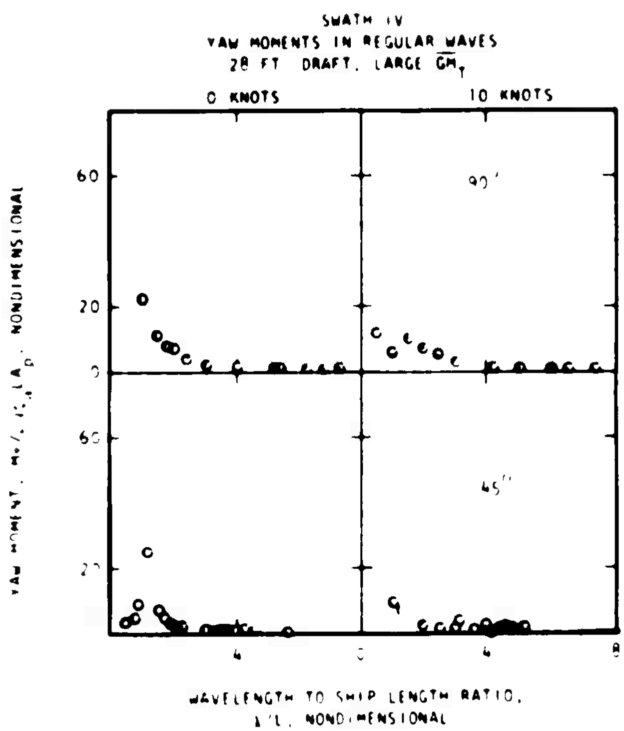

Figure 110 - Dimensionless Yaw Moment in Regular Beam and Quartering Seas, 28 ft Draft, Large $\overline{GM}_t$

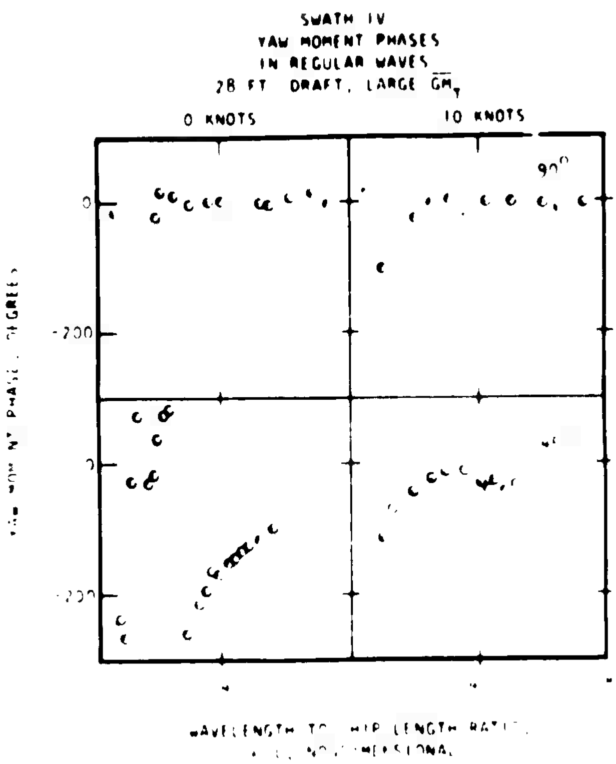

Figure 111 - Yaw Moment Phase in Regular Beam and Quartering Seas, 28 ft Draft, Large $\overline{GM}_t$

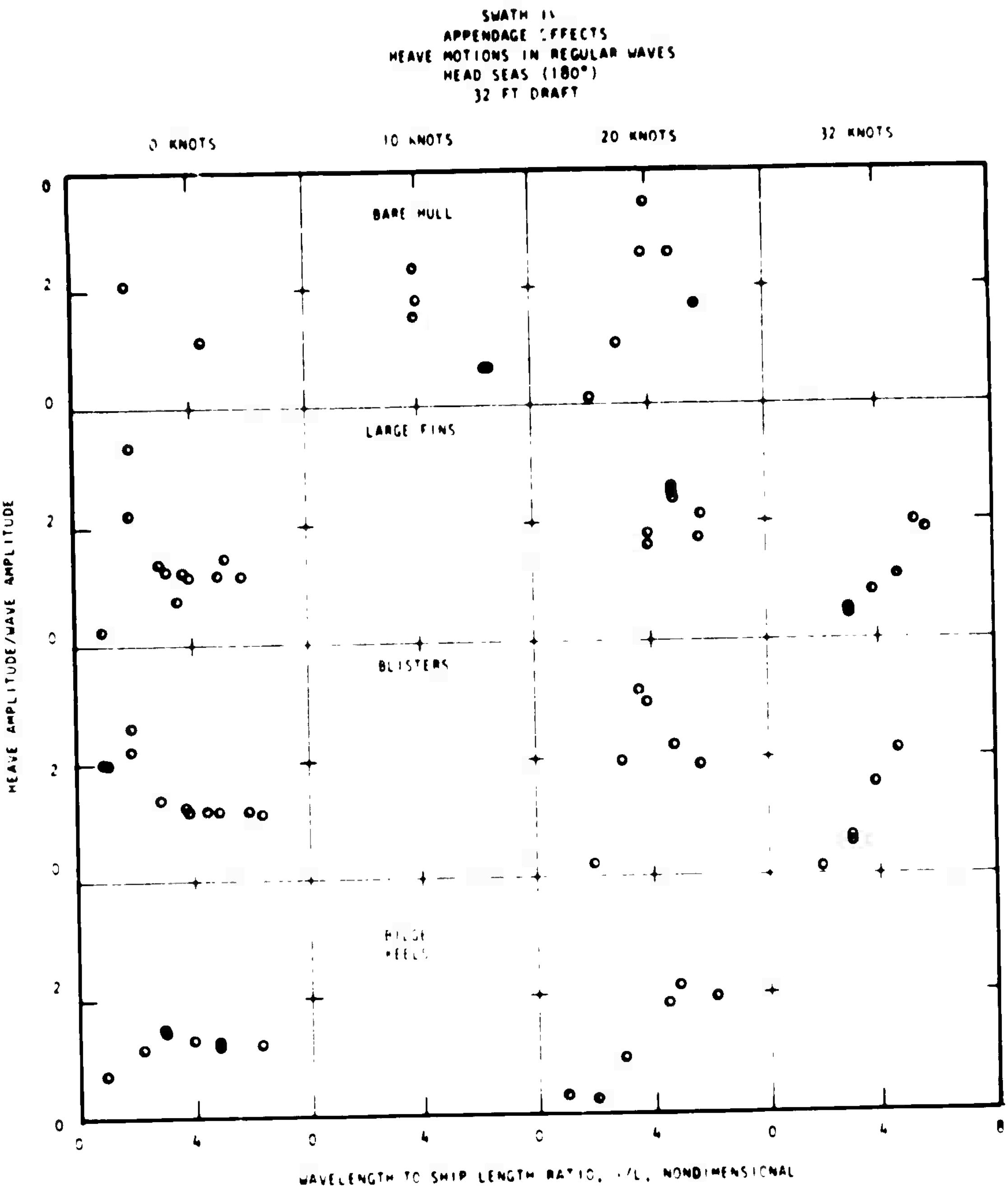

Figure 112 - Dimensionless Heave in Regular Head Seas, 32 ft Draft, APPENDAGE EFFECT

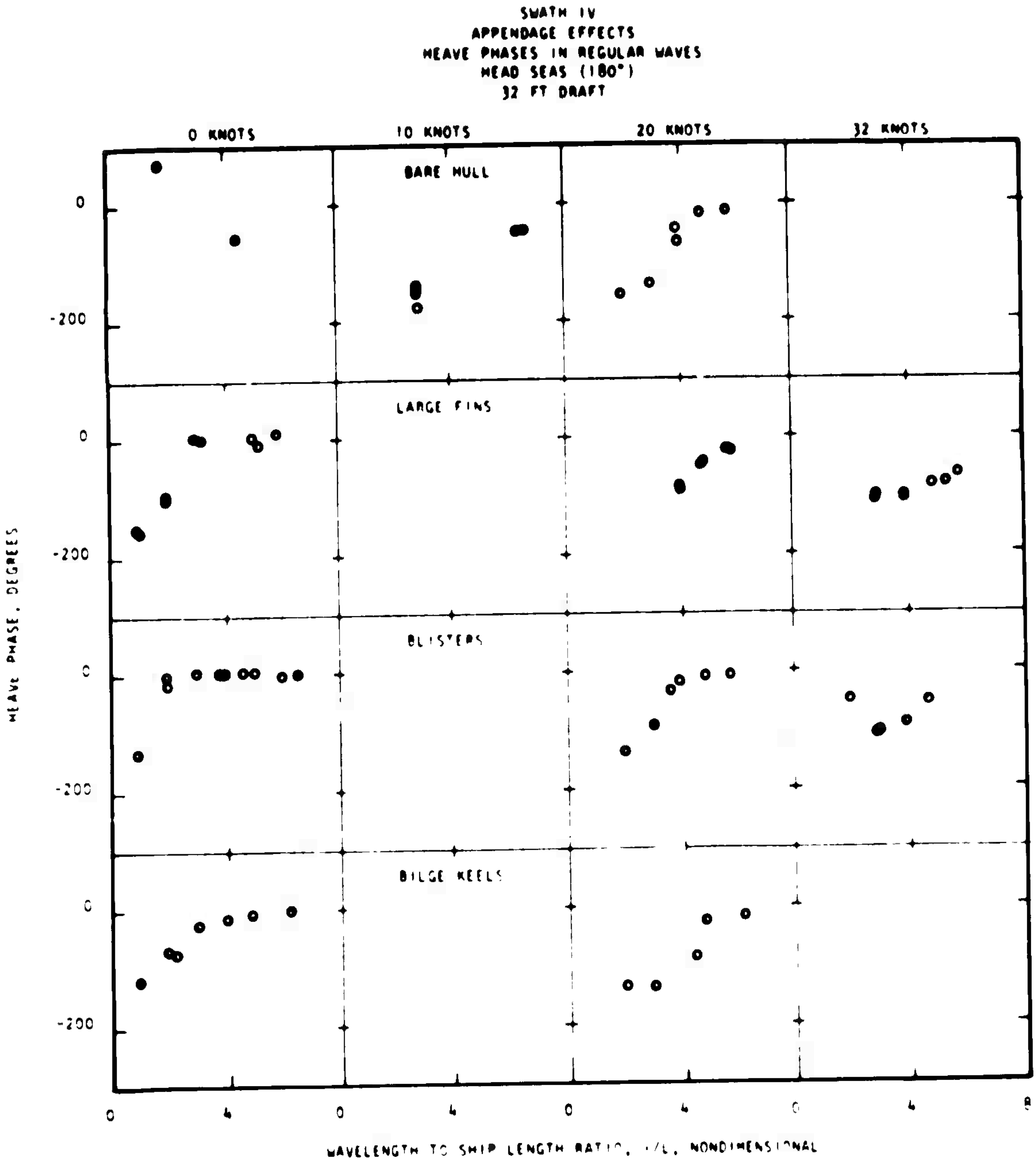

Figure 113 - Heave Phase in Regular Head Seas, 32 ft Draft, APPENDAGE EFFECT

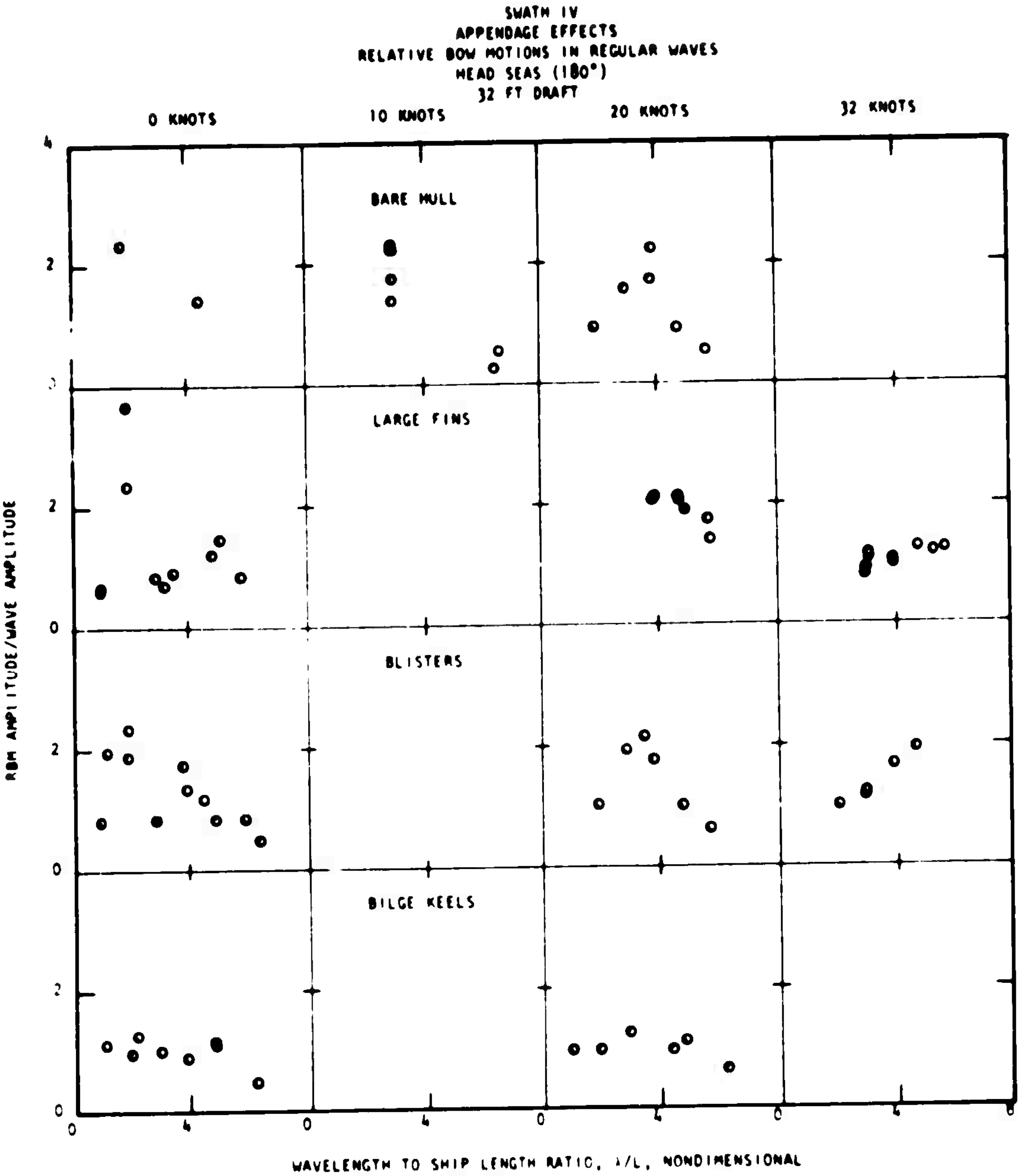

Figure 114 - Dimensionless Relative Bow Motion in Regular Head Seas, 32 ft Draft, APPENDAGE EFFECT

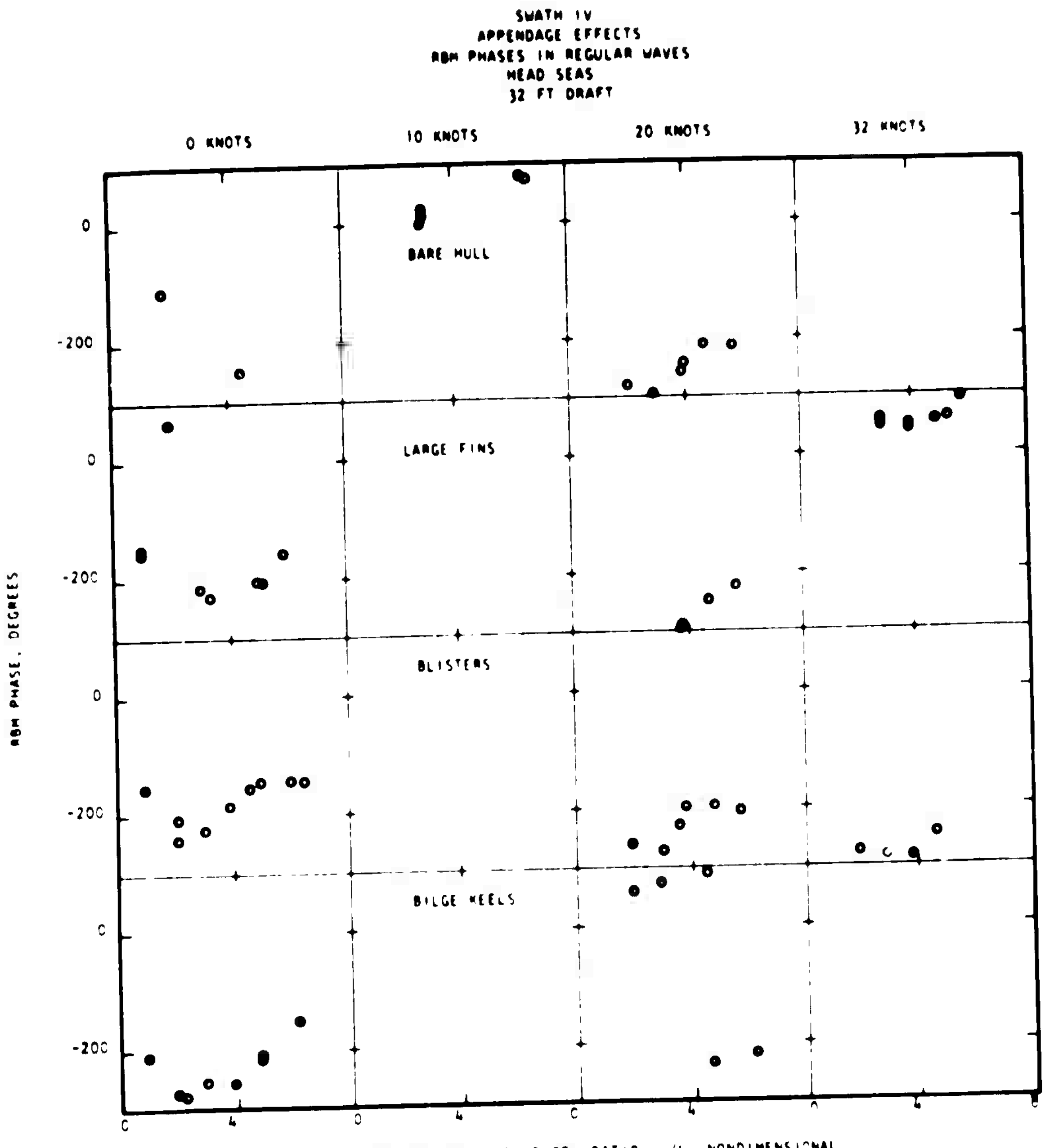

Figure 115 - Relative Bow Motion Phase in Regular Head Seas, 32 ft Draft, APPENDAGE EFFECT

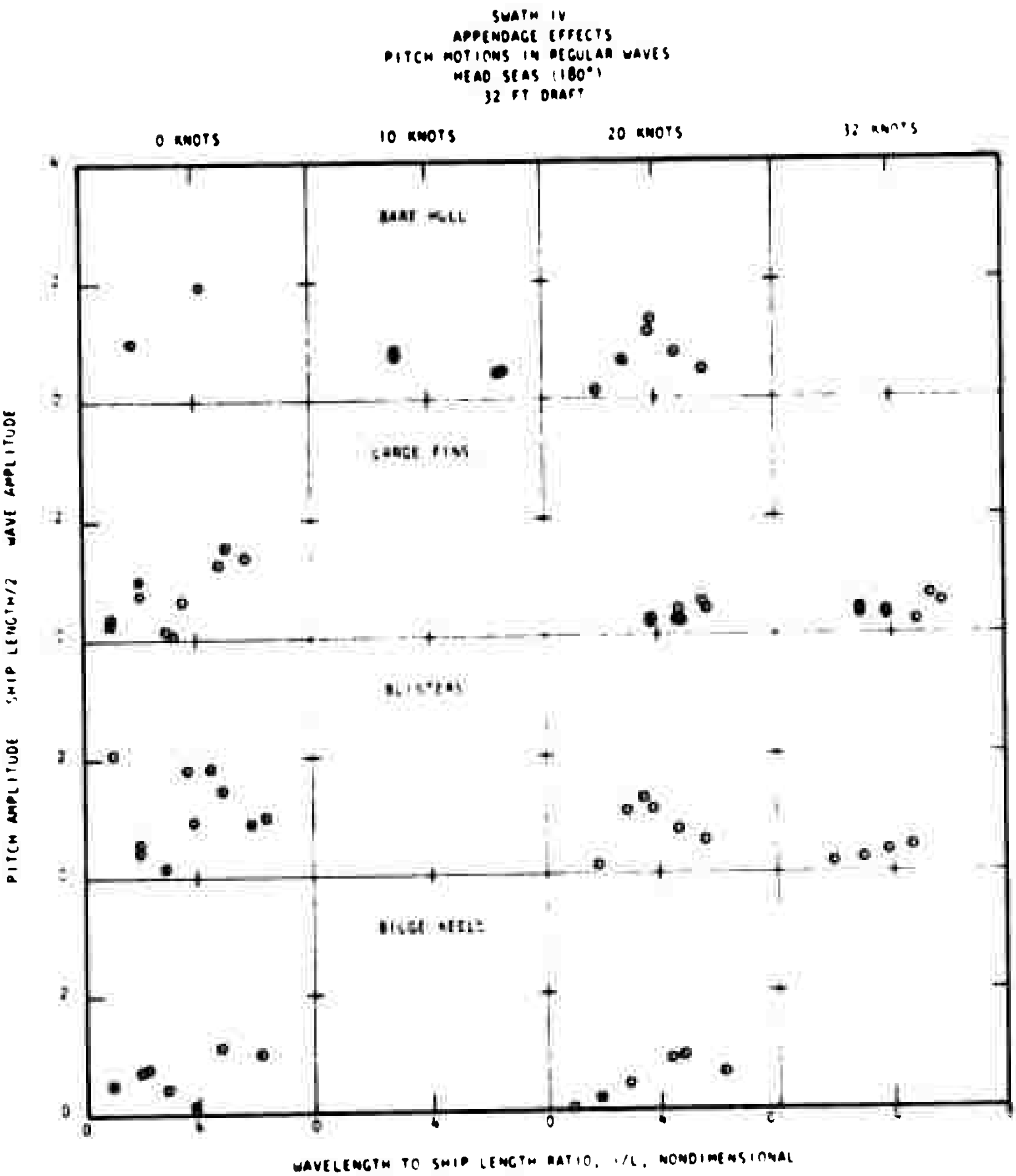

Figure 116 - Dimensionless Pitch In Regular Head Seas, 32 ft Draft, APPENDAGE EFFECT

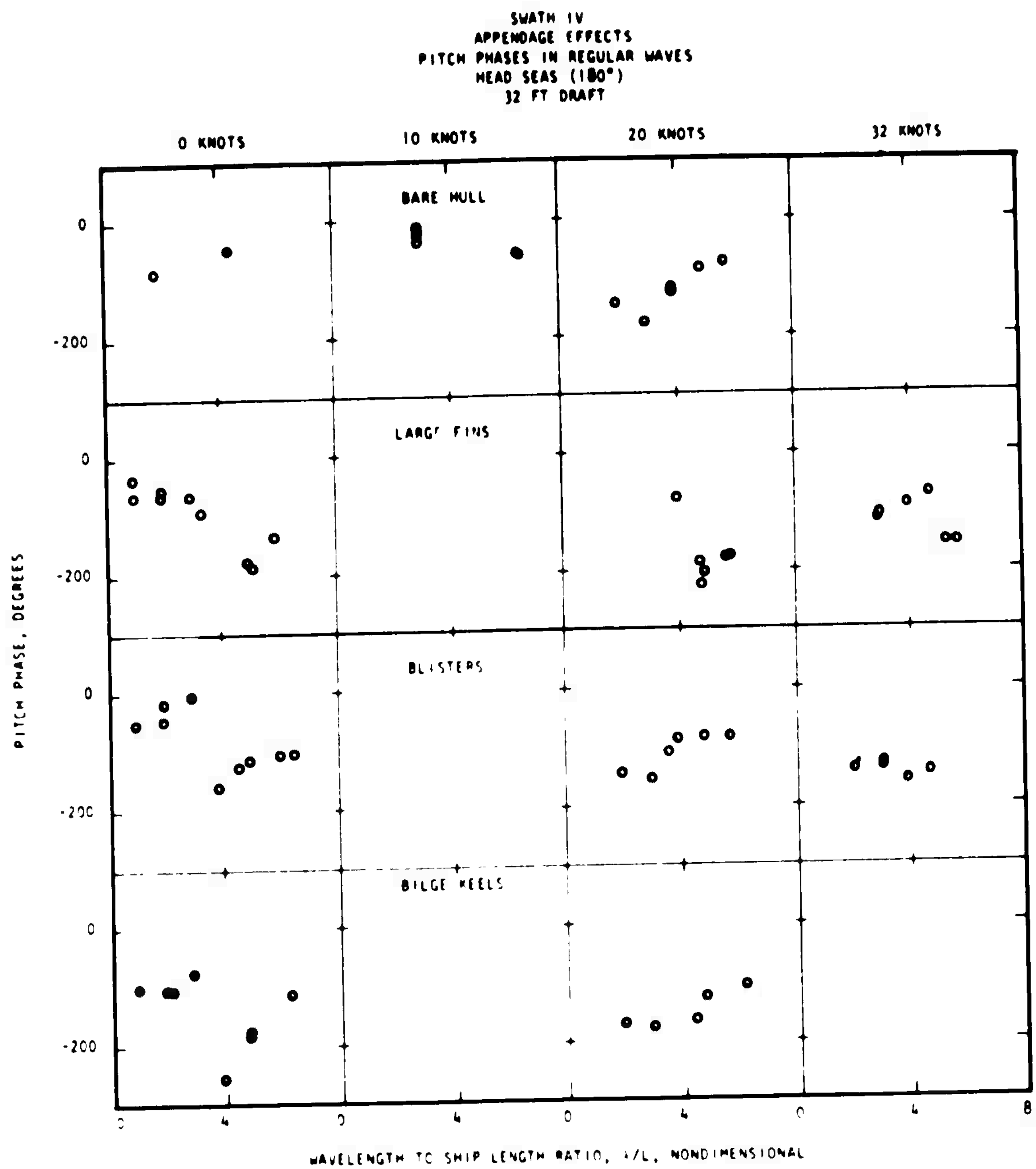

Figure 117 - Pitch Phase in Regular Head Seas, 32 ft Draft, APPENDAGE EFFECT

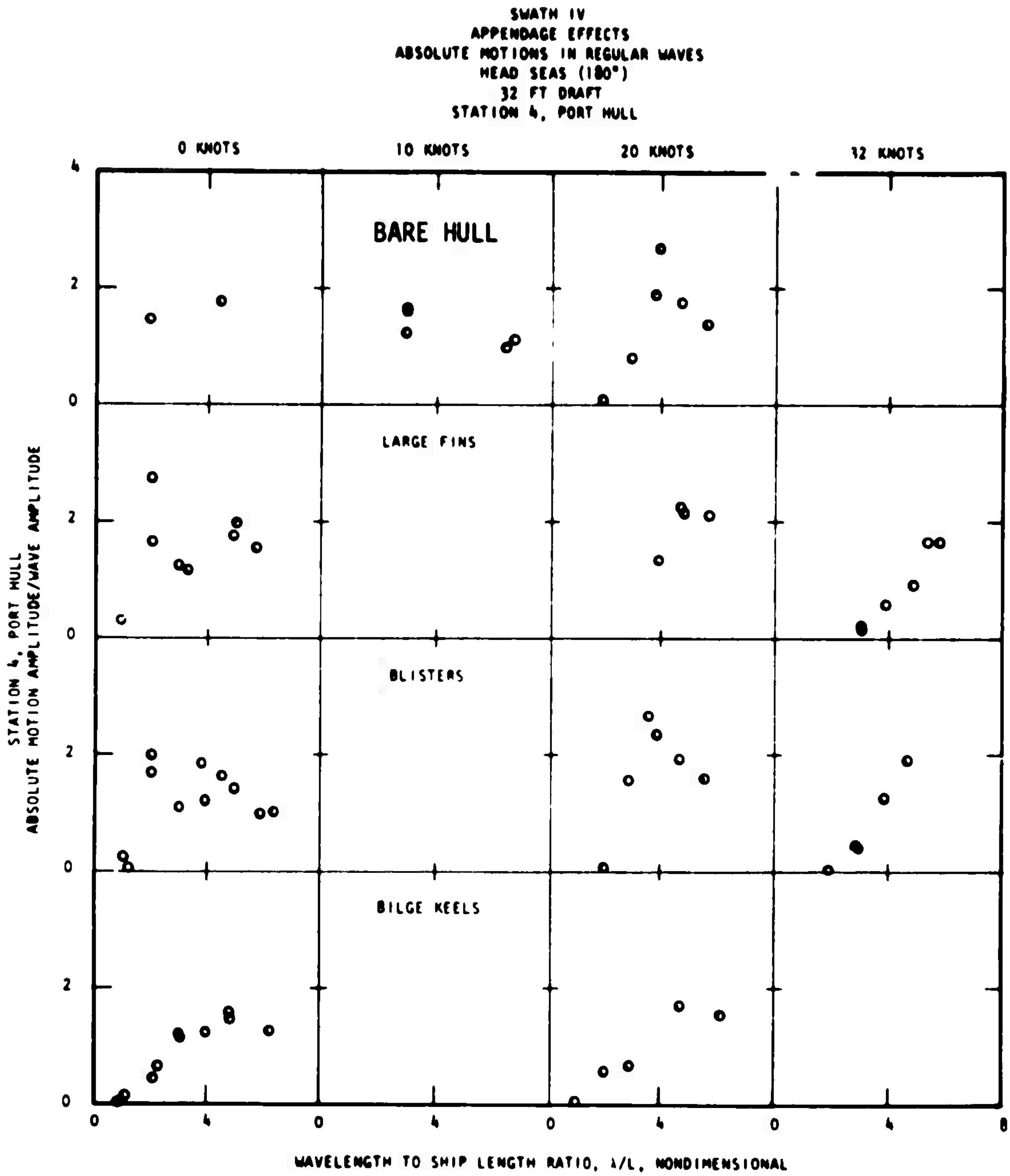

Figure 118 - Dimensionless Absolute Bow Motion in Regular Head Seas, Port Hull, 32 ft Draft, APPENDAGE EFFECT

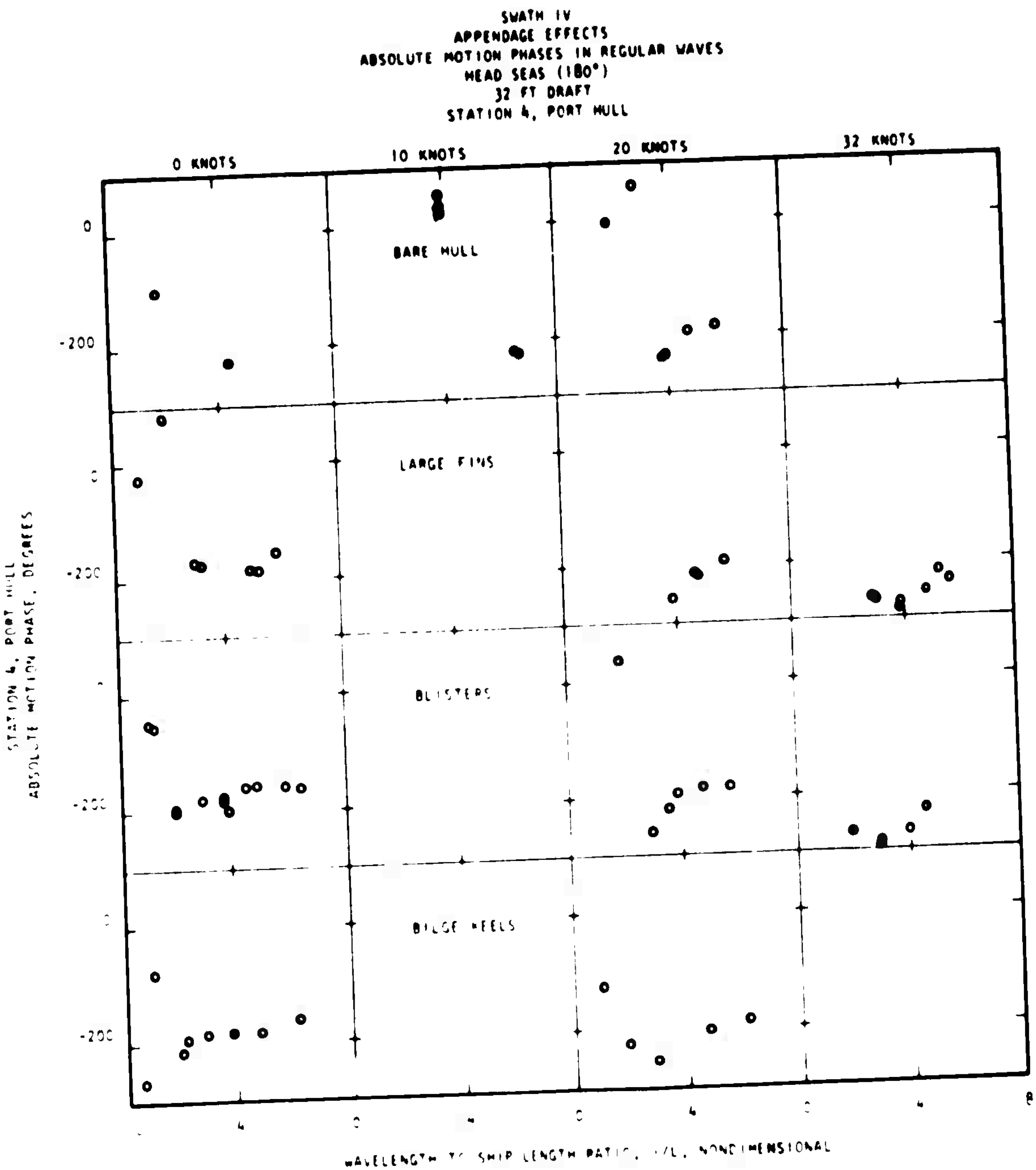

Figure 119 - Absolute Bow Motion Phase in Regular Head Seas, Port Hull, 32 ft Draft, APPENDAGE EFFECT

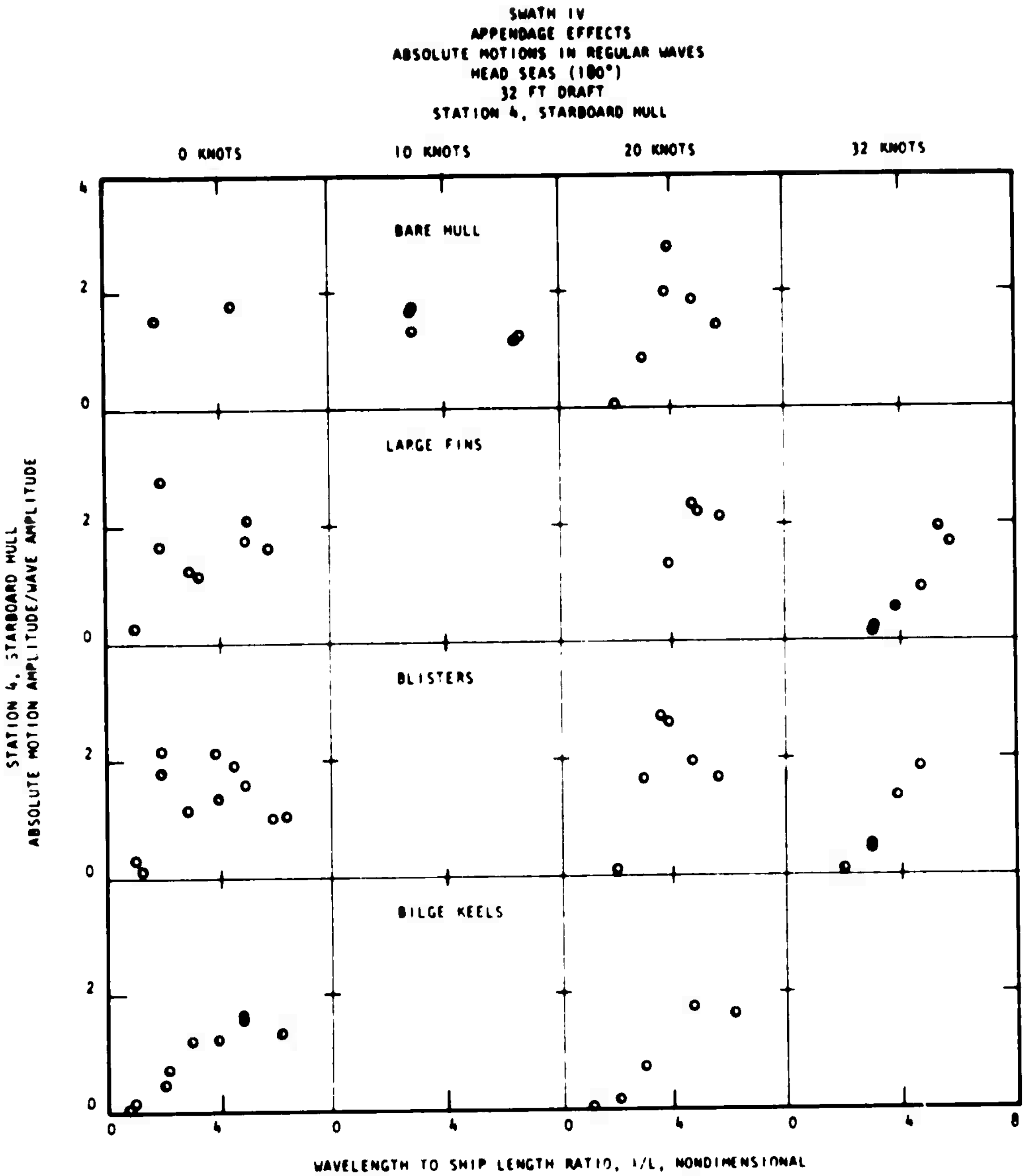

Figure 120 - Dimensionless Absolute Bow Motion in Regular Head Seas, Starboard Hull, 32 ft Draft, APPENDAGE EFFECT

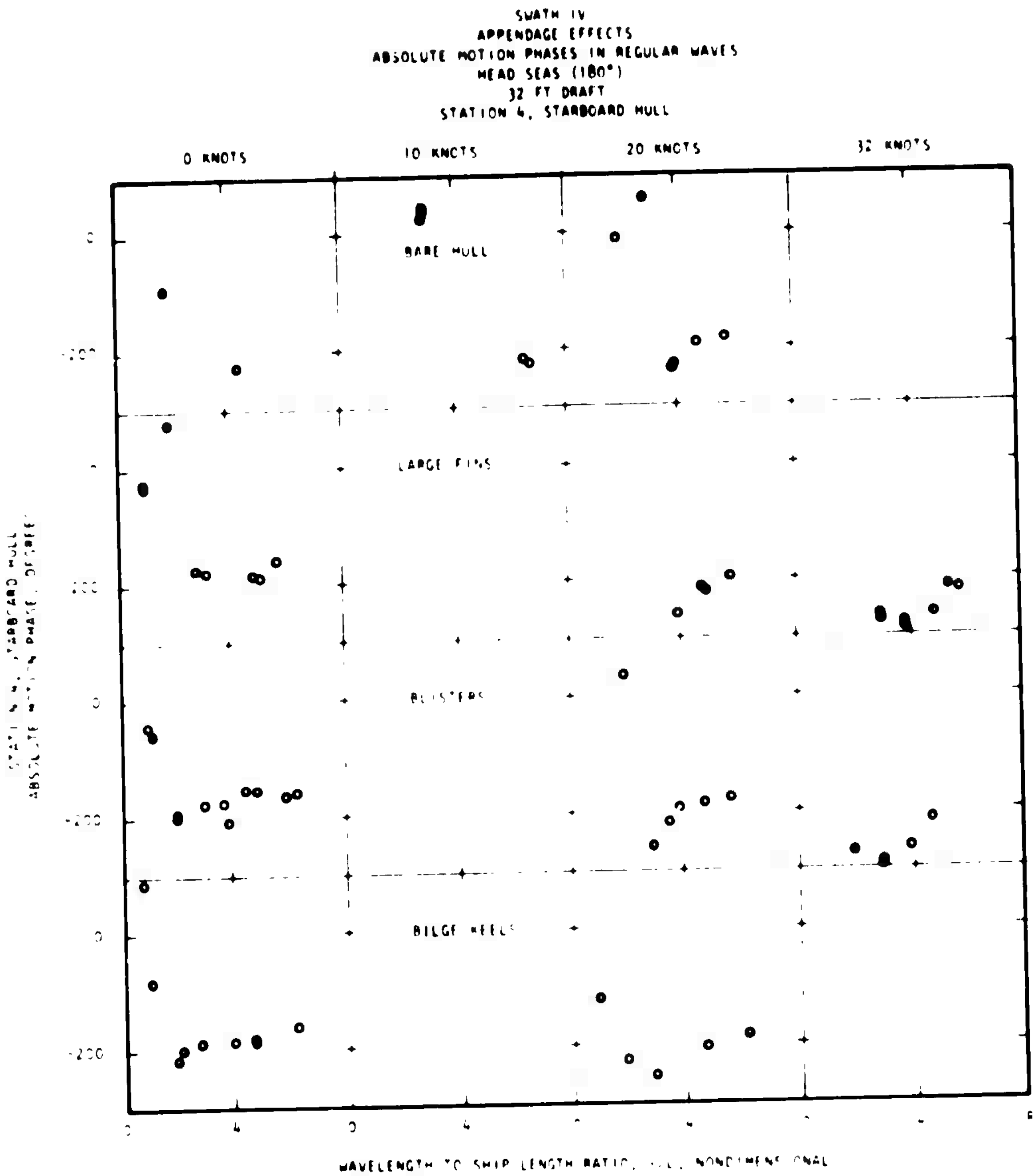

Figure 121 - Absolute Bow Motion Phase in Regular Head Seas, Starboard Hull, 32 ft Draft, APPENDAGE EFFECT

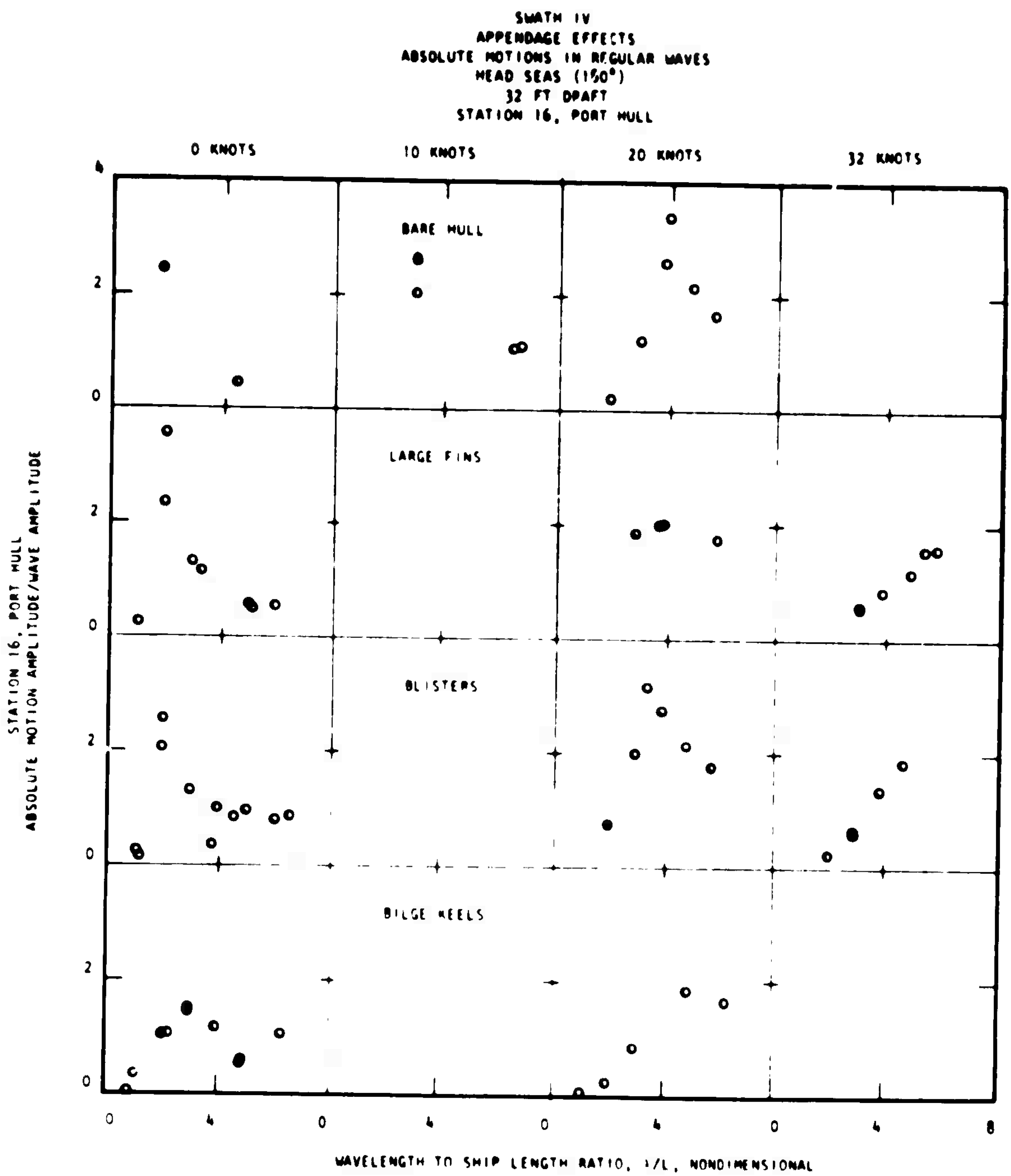

Figure 122 - Dimensionless Absolute Stern Motion in Regular Head Seas, Port Hull, 32 ft Draft, APPENDAGE EFFECT

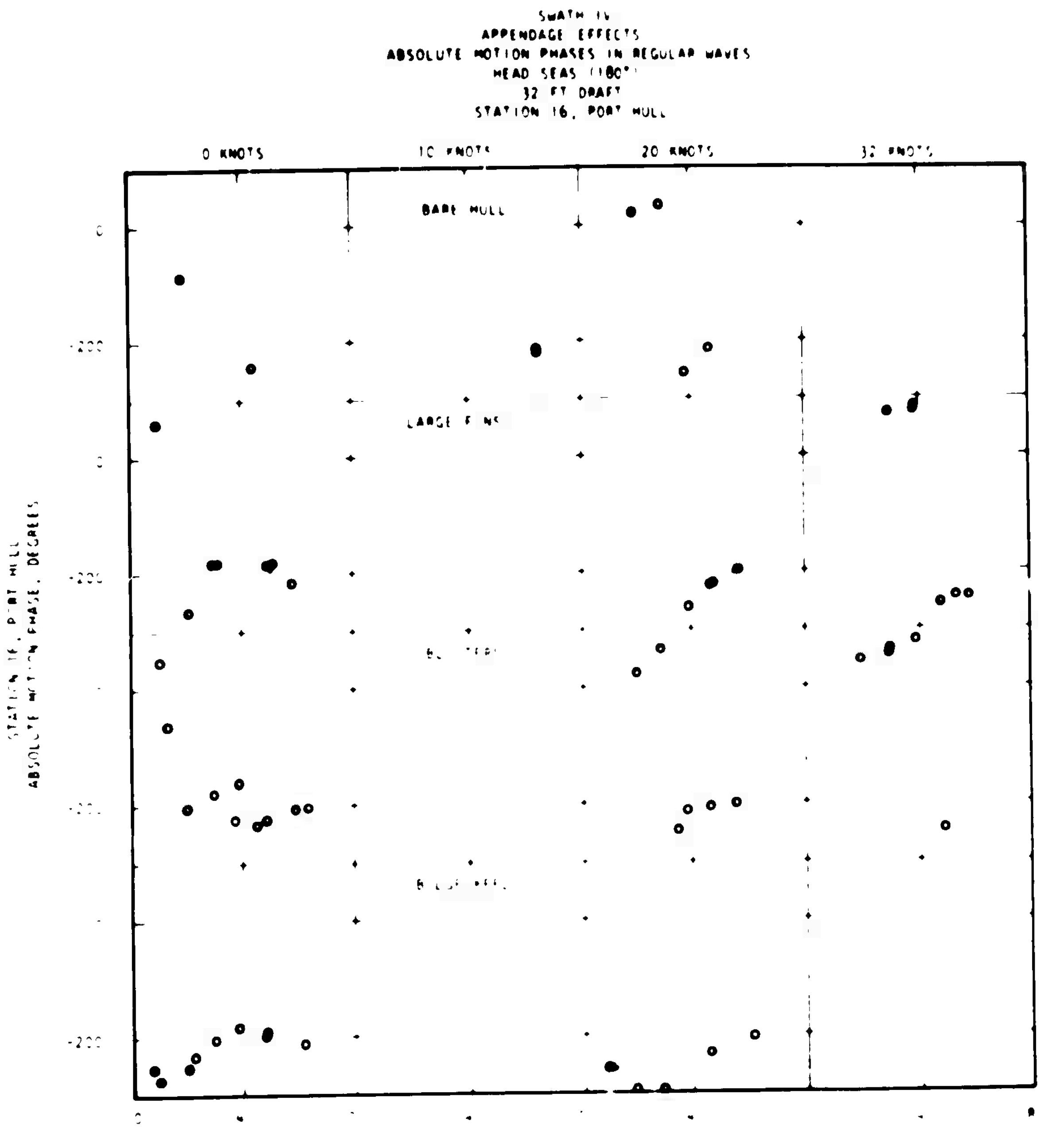

Figure 123 - Absolute Stern Motion Phase in Regular Head Seas, Port Hull, 32 ft Draft, APPENDAGE EFFECT

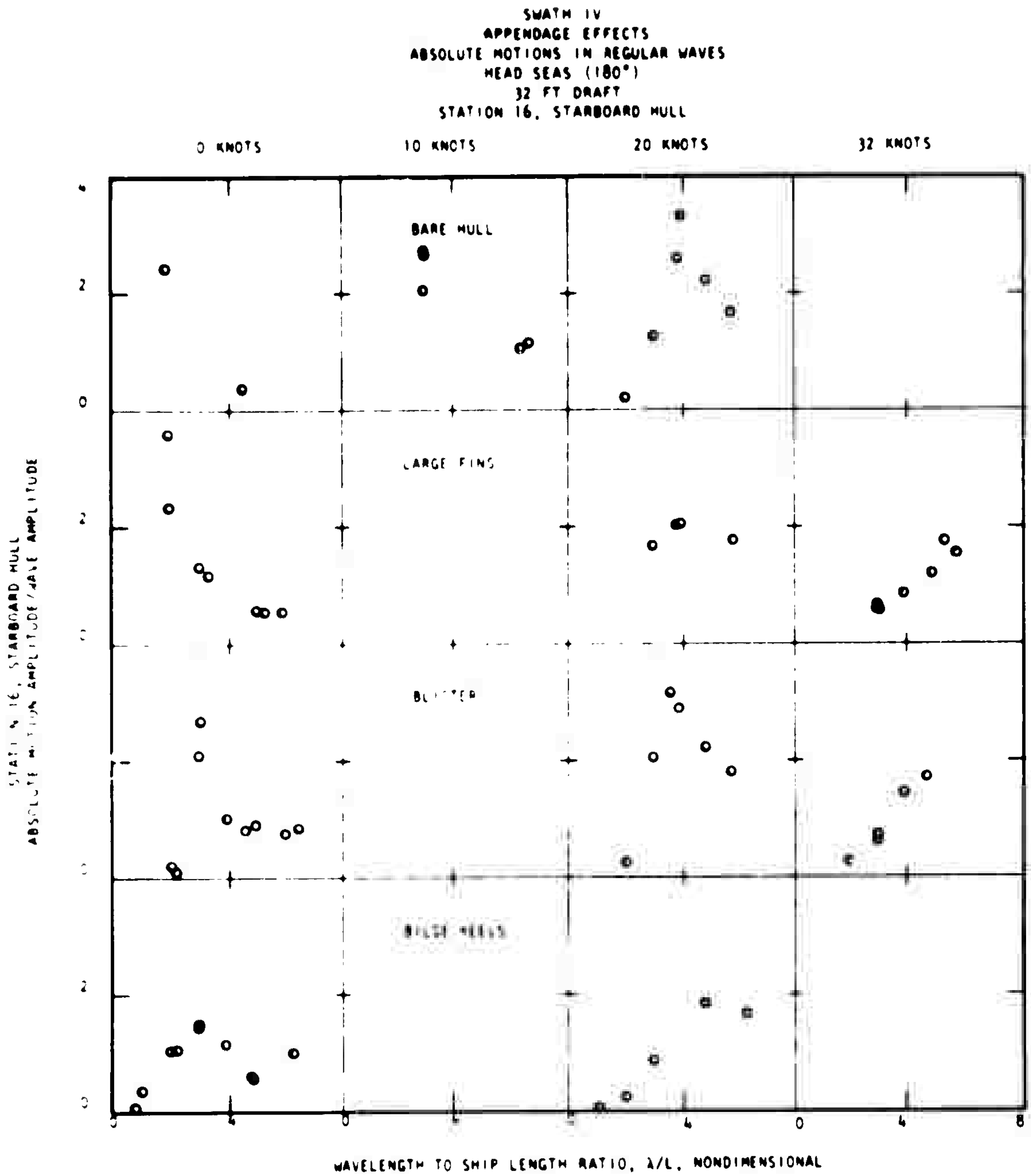

Figure 124 - Dimensionless Absolute Stern Motion in Regular Head Seas, Starboard Hull, 32 ft Draft, APPENDAGE EFFECT

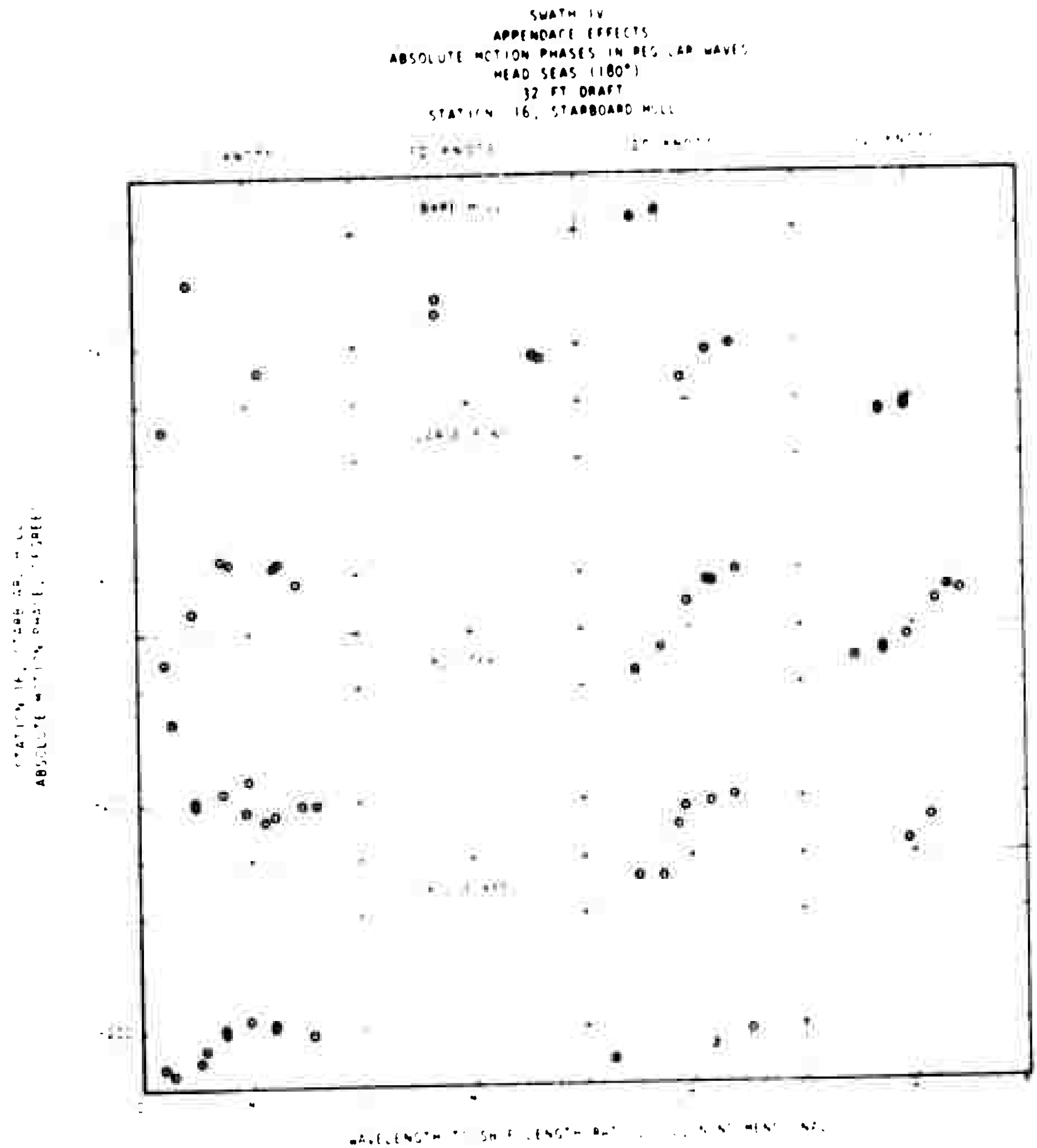

Figure 125 – Absolute Stern Motion Phase in Regular Head Seas, Starboard Hull, 32 ft Draft, APPENDAGE EFFECT

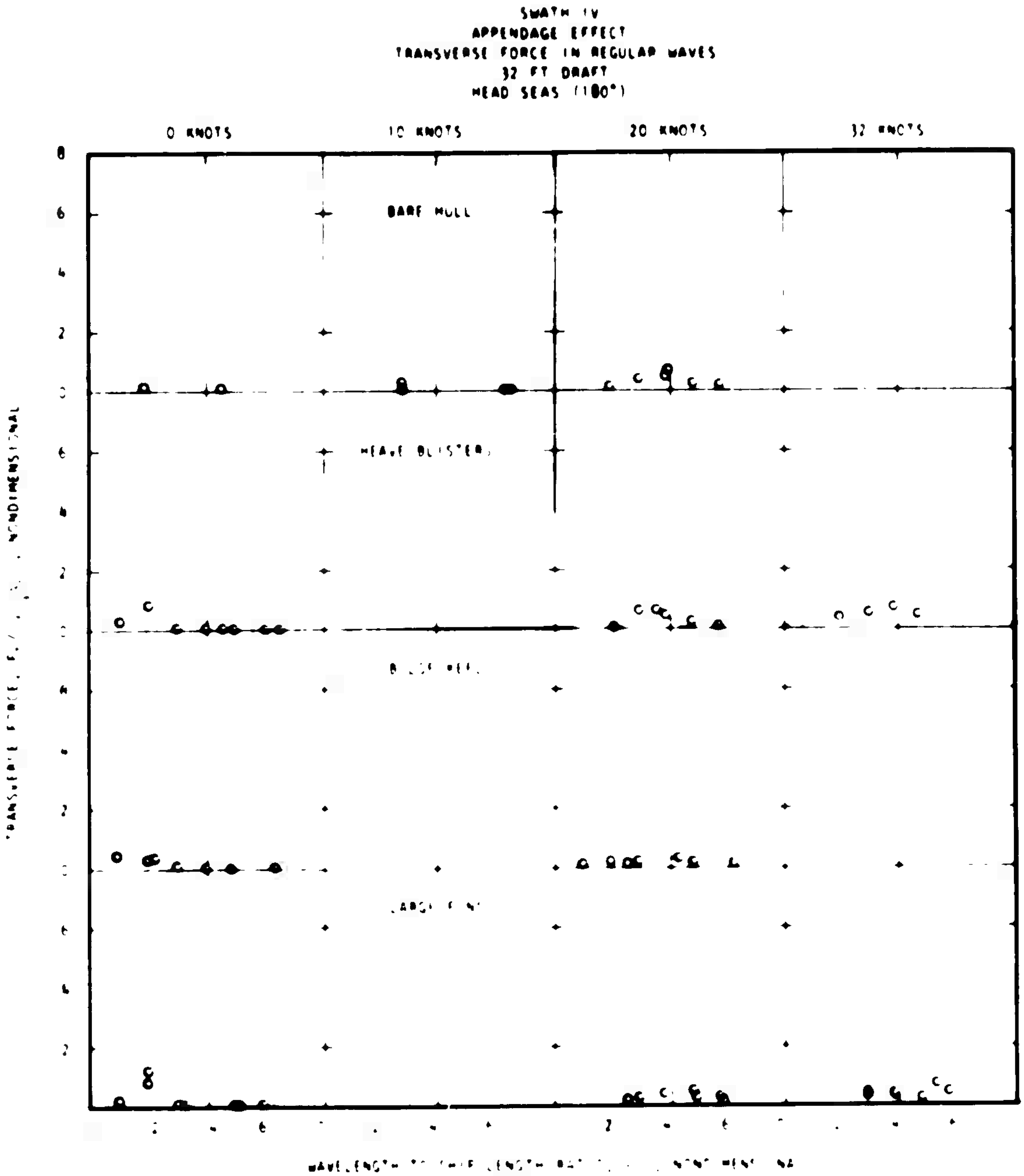

Figure 126 - Dimensionless Transverse Force in Regular Head Seas, 32 ft Draft, APPENDAGE EFFECT

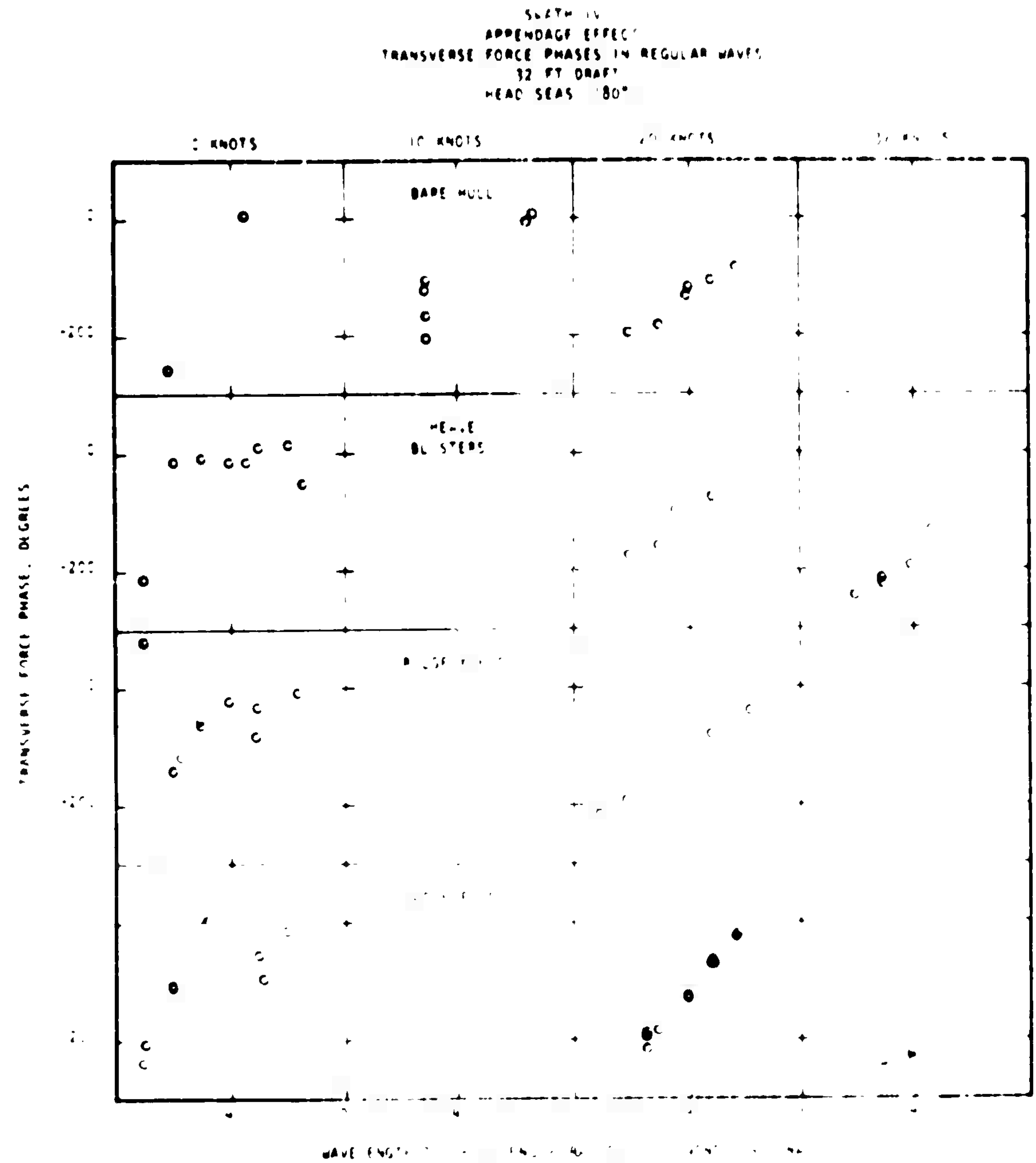

Figure 127 - Transverse Force Phase in Regular Head Seas, 32 ft Draft
APPENDAGE EFFECT

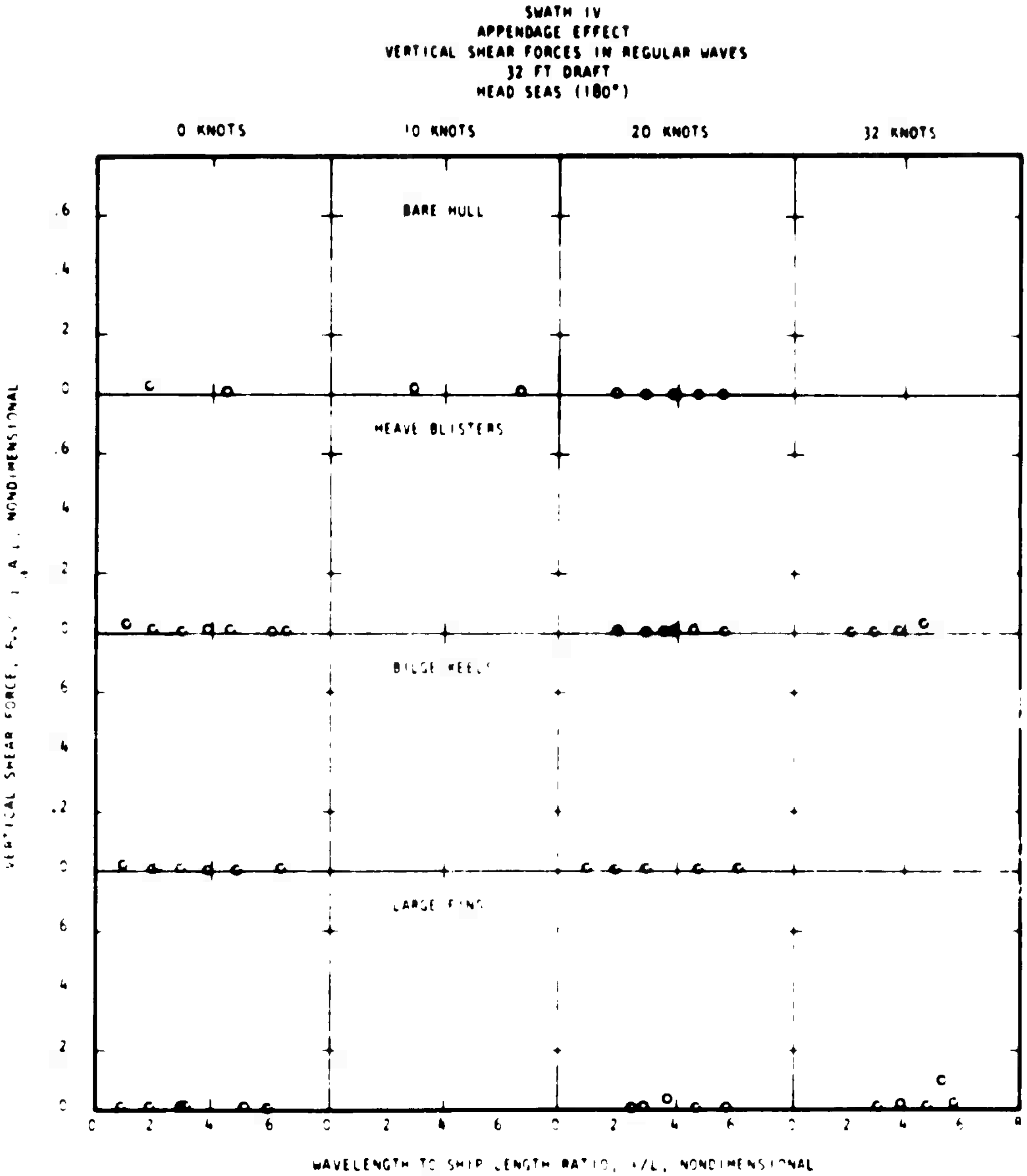

Figure 128 - Dimensionless Vertical Shear Force in Regular Head Seas, 32 ft Draft, APPENDAGE EFFECT

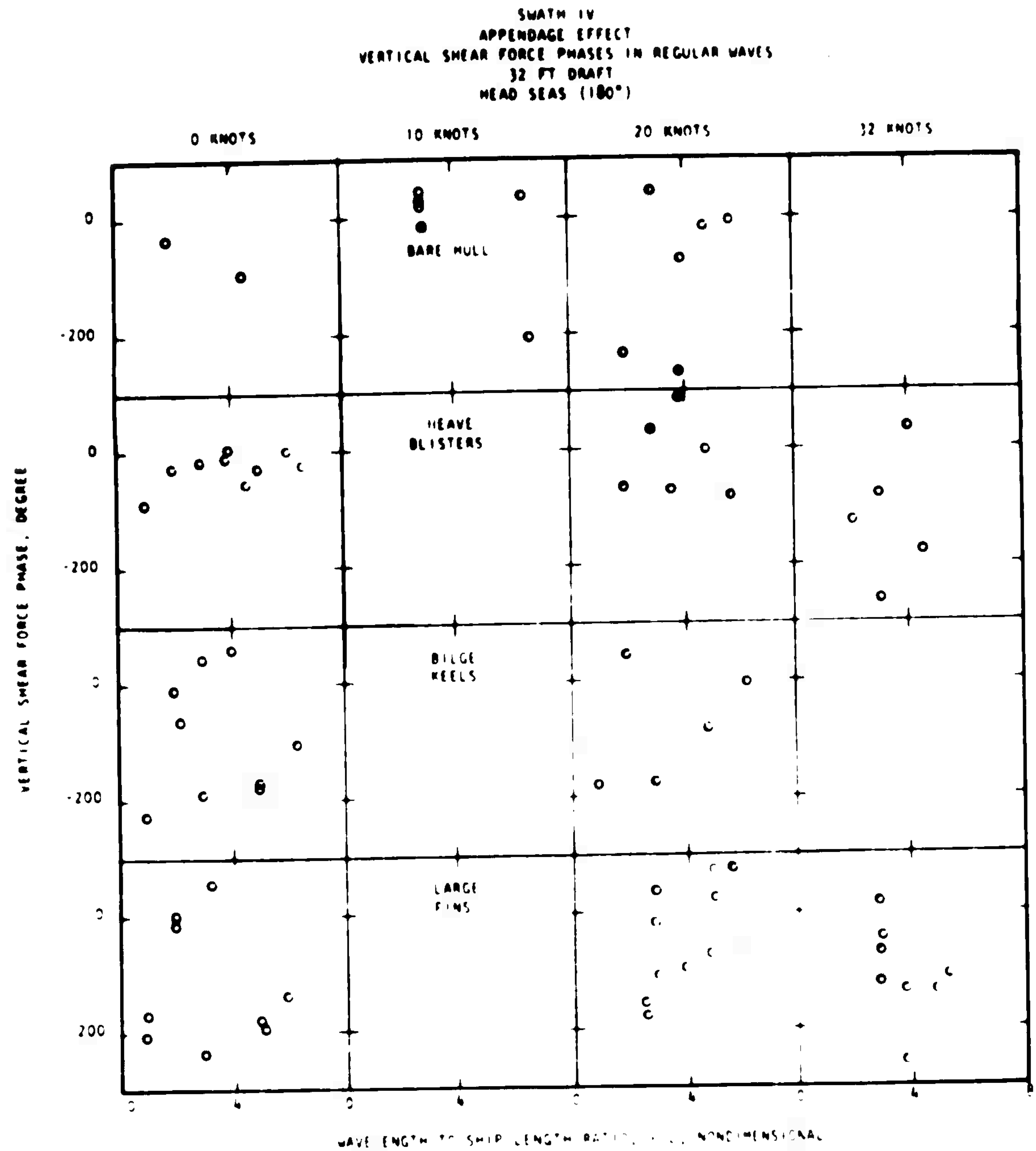

Figure 129 - Vertical Shear Force Phase in Regular Head Seas, 32 ft Draft, APPENDAGE EFFECT

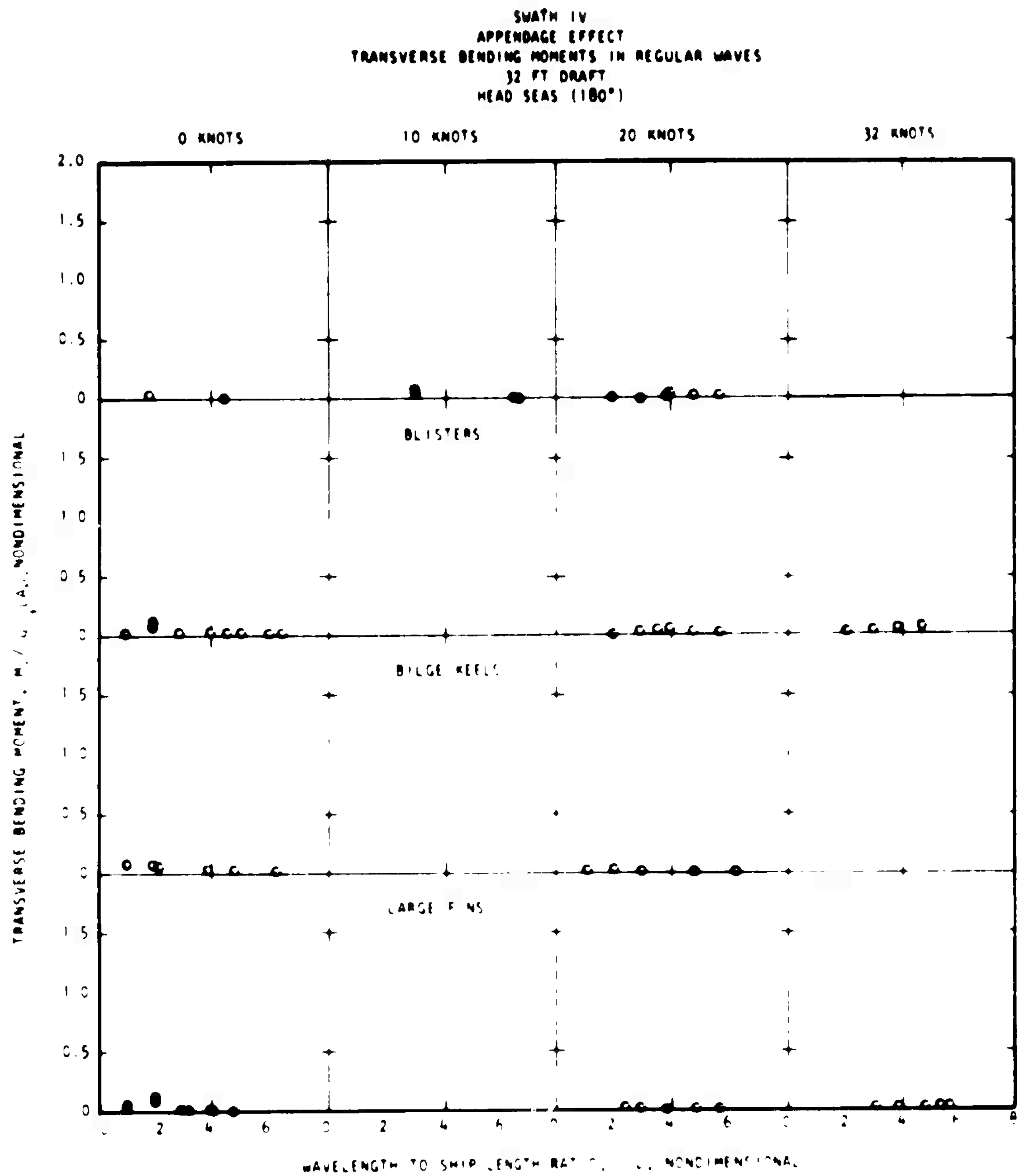

Figure 130 - Dimensionless Transverse Vertical Bending Moment in Regular Head Seas, 32 ft Draft, APPENDAGE EFFECT

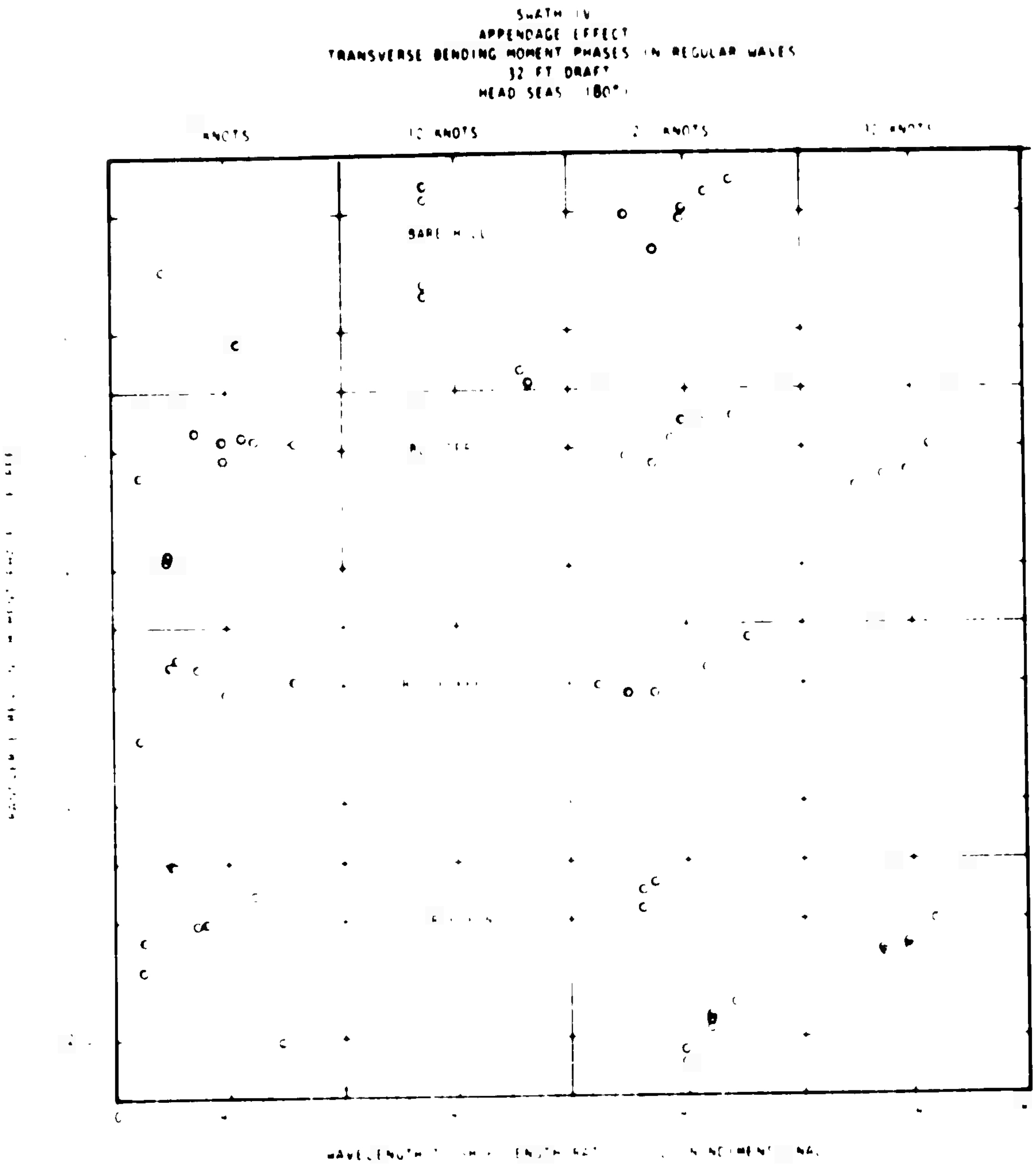

Figure 131 - Transverse Vertical Bending Moment Phase in Regular Head Seas, 32 ft Draft, APPENDAGE EFFECT

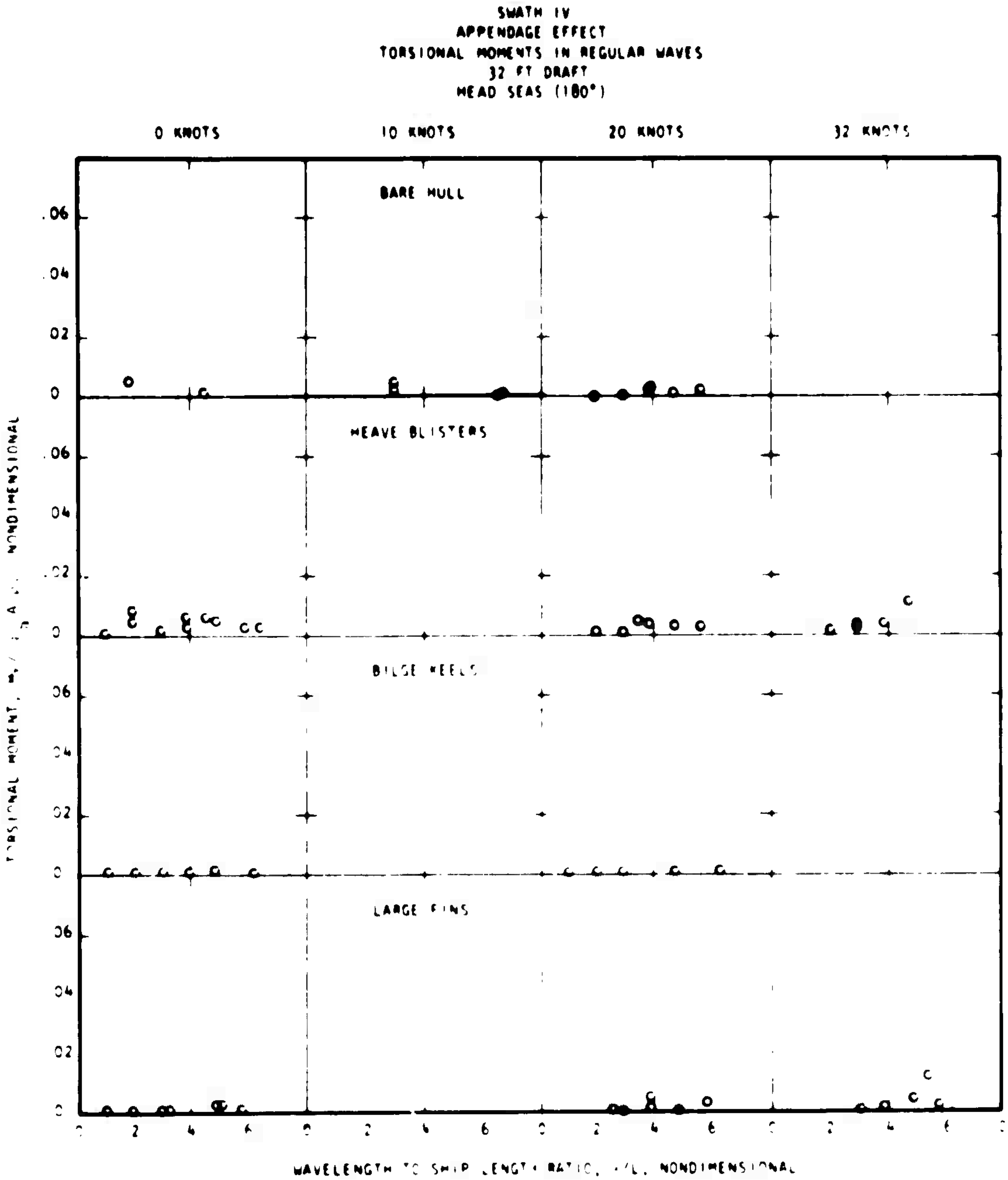

Figure 132 - Dimensionless Torsional Moment in Regular Head Seas, 32 ft Draft, APPENDAGE EFFECT

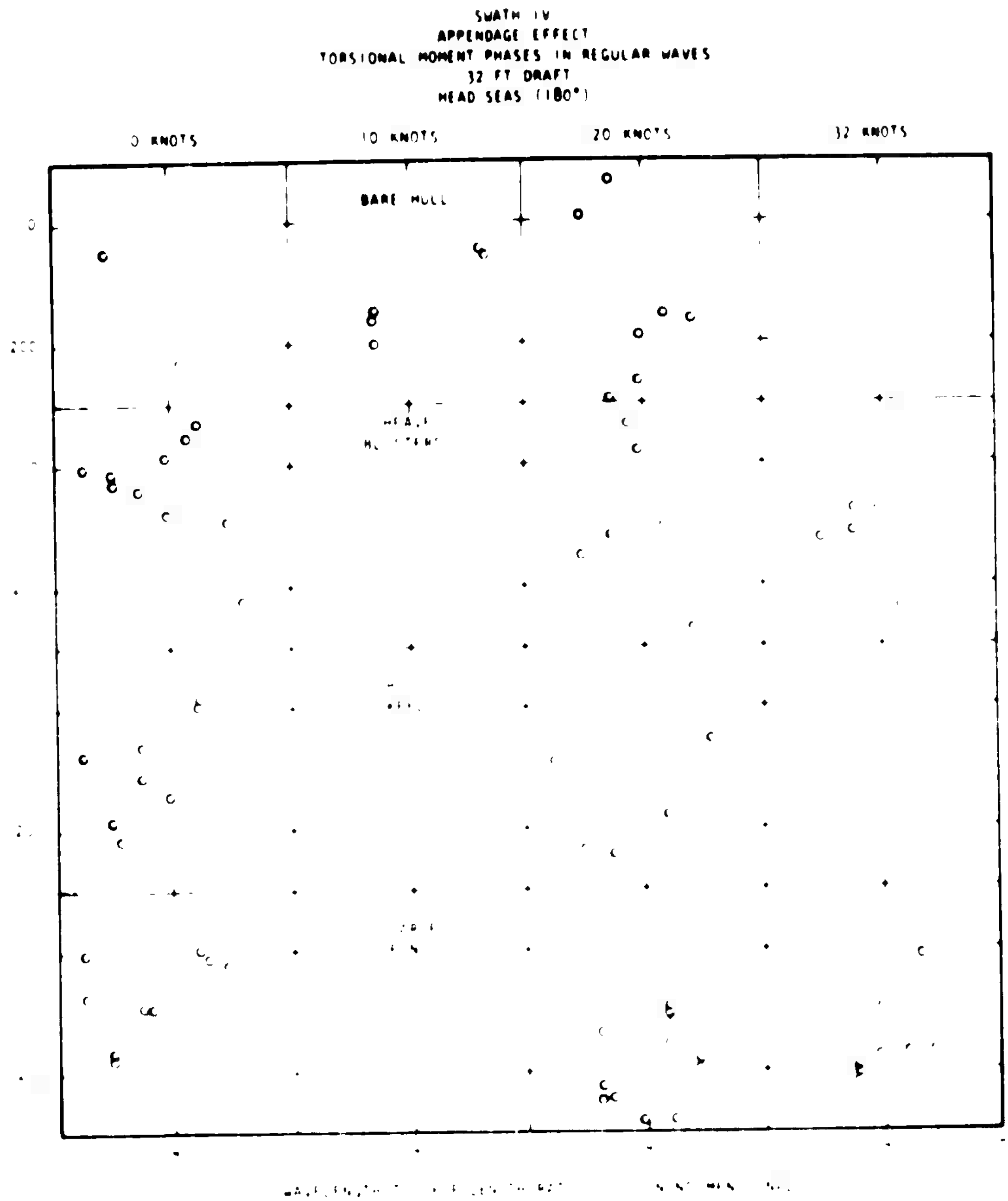

Figure 133 - Torsional Moment Phase in Regular Head Seas, 32 ft Draft, APPENDAGE EFFECT

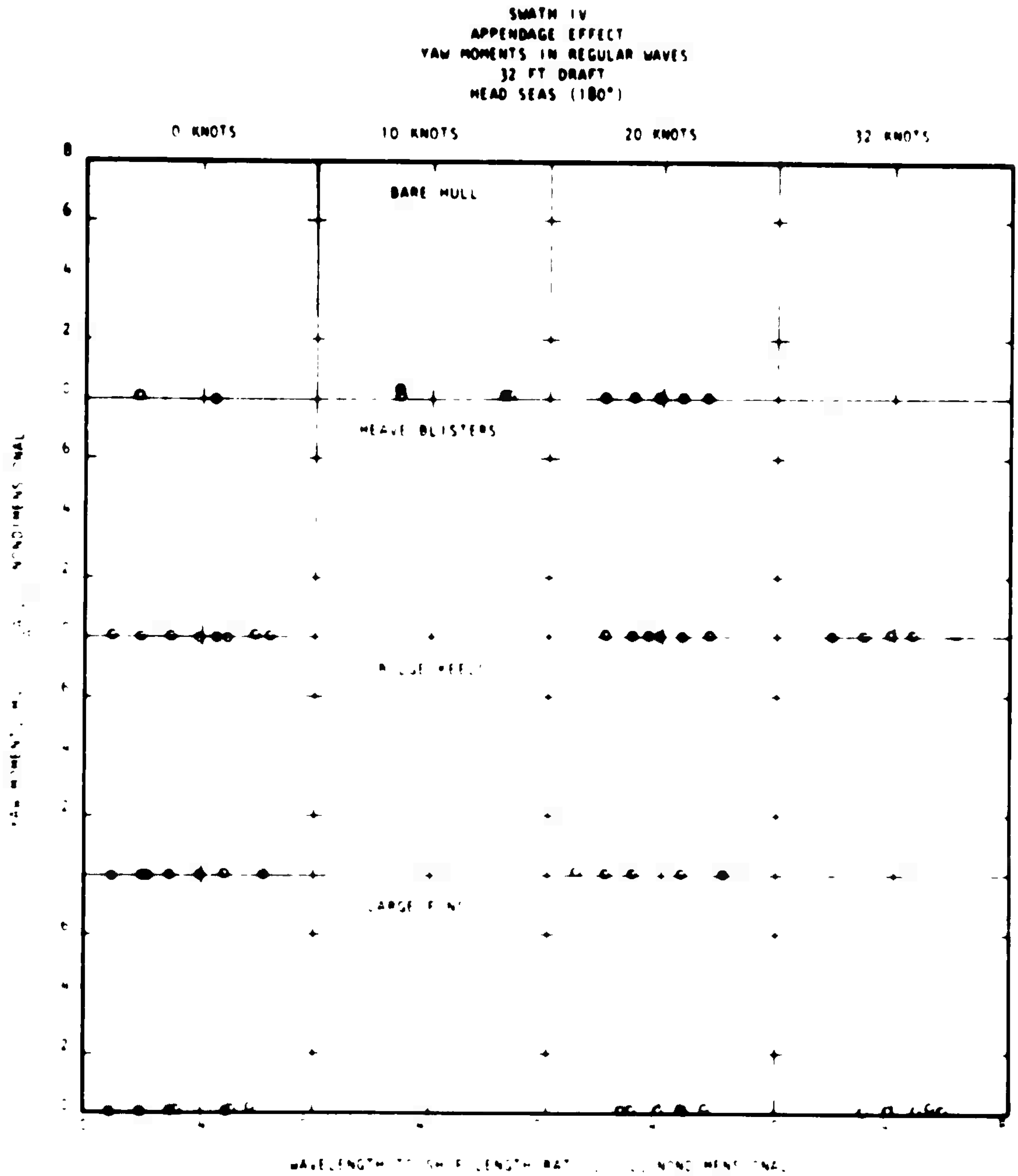

Figure 134 - Dimensionless Yaw Moment in Regular Head Seas, 32 ft Draft, APPENDAGE EFFECT

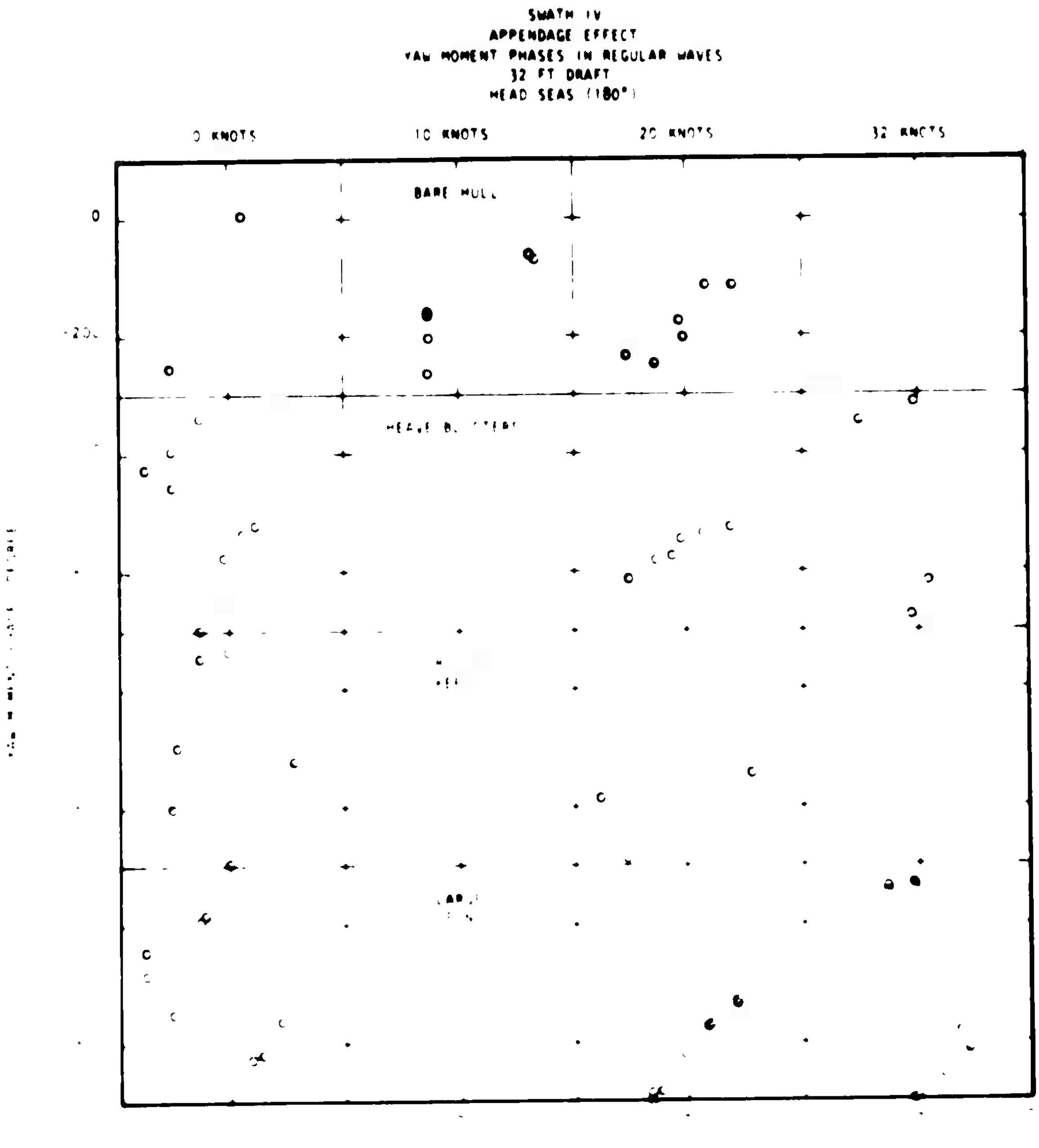

Figure 135 - Yaw Moment Phase in Regular Head Seas, 32 ft Draft, APPENDAGE EFFECT

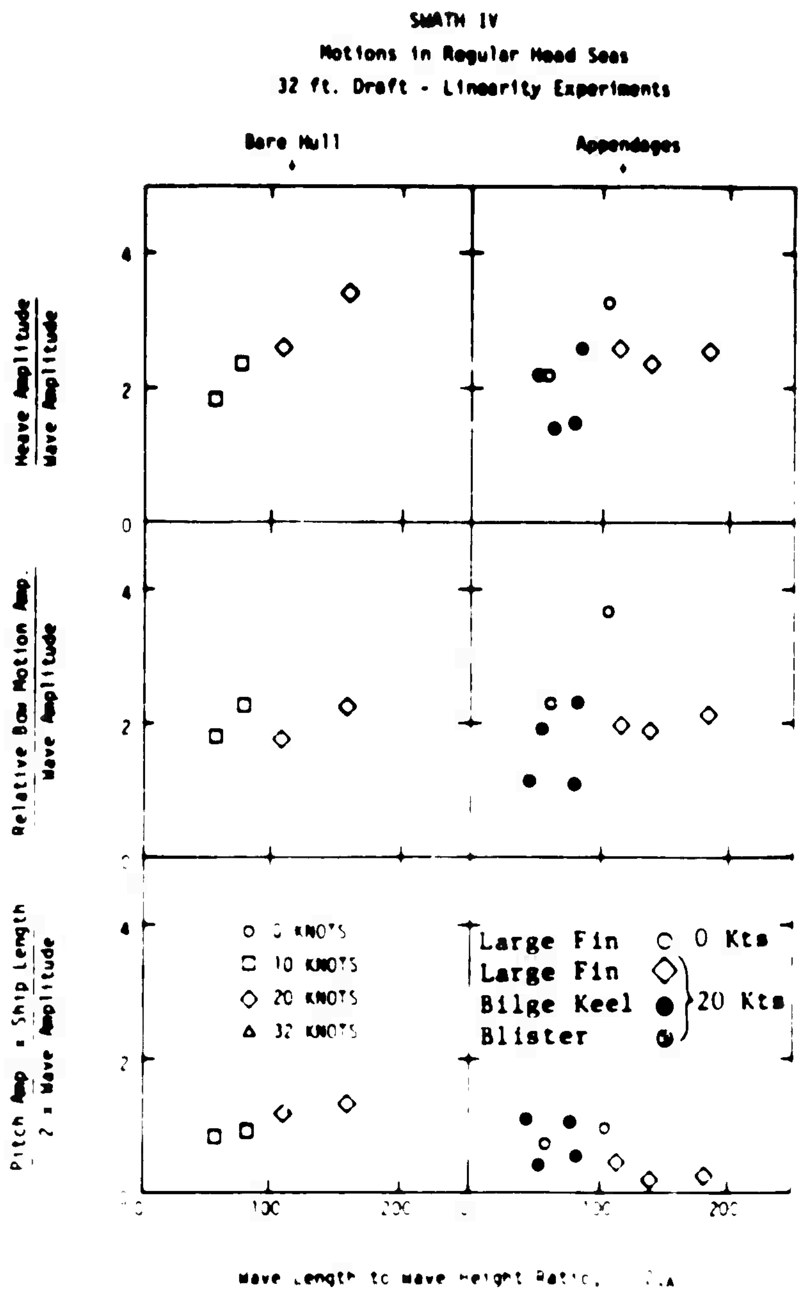

Figure 136 - Linearity Experiments in Regular Head Seas, 32 ft Draft, Bare Hull and Appendages

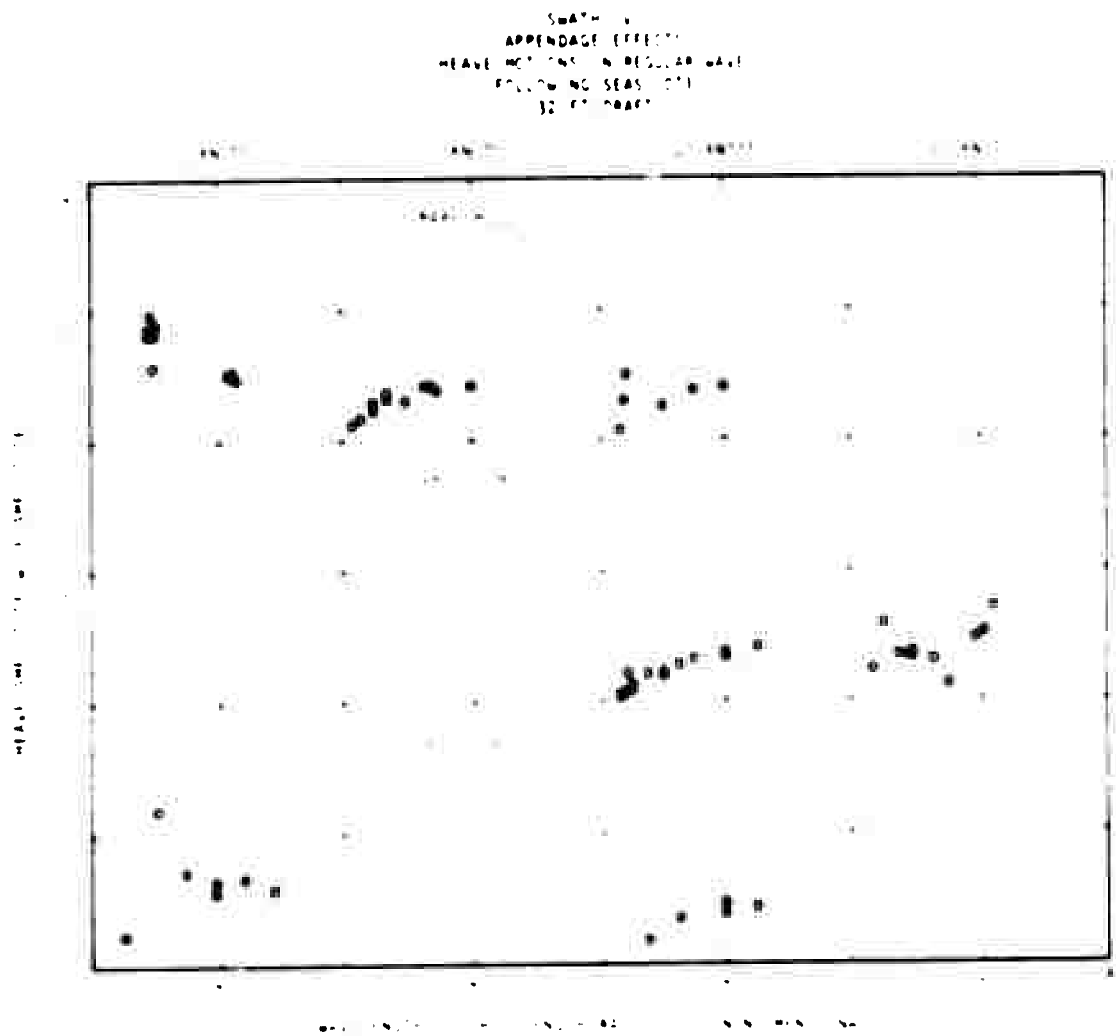

Figure 137 - Dimensionless Heave in Regular Following Seas, 32 ft Draft, APPENDAGE EFFECT

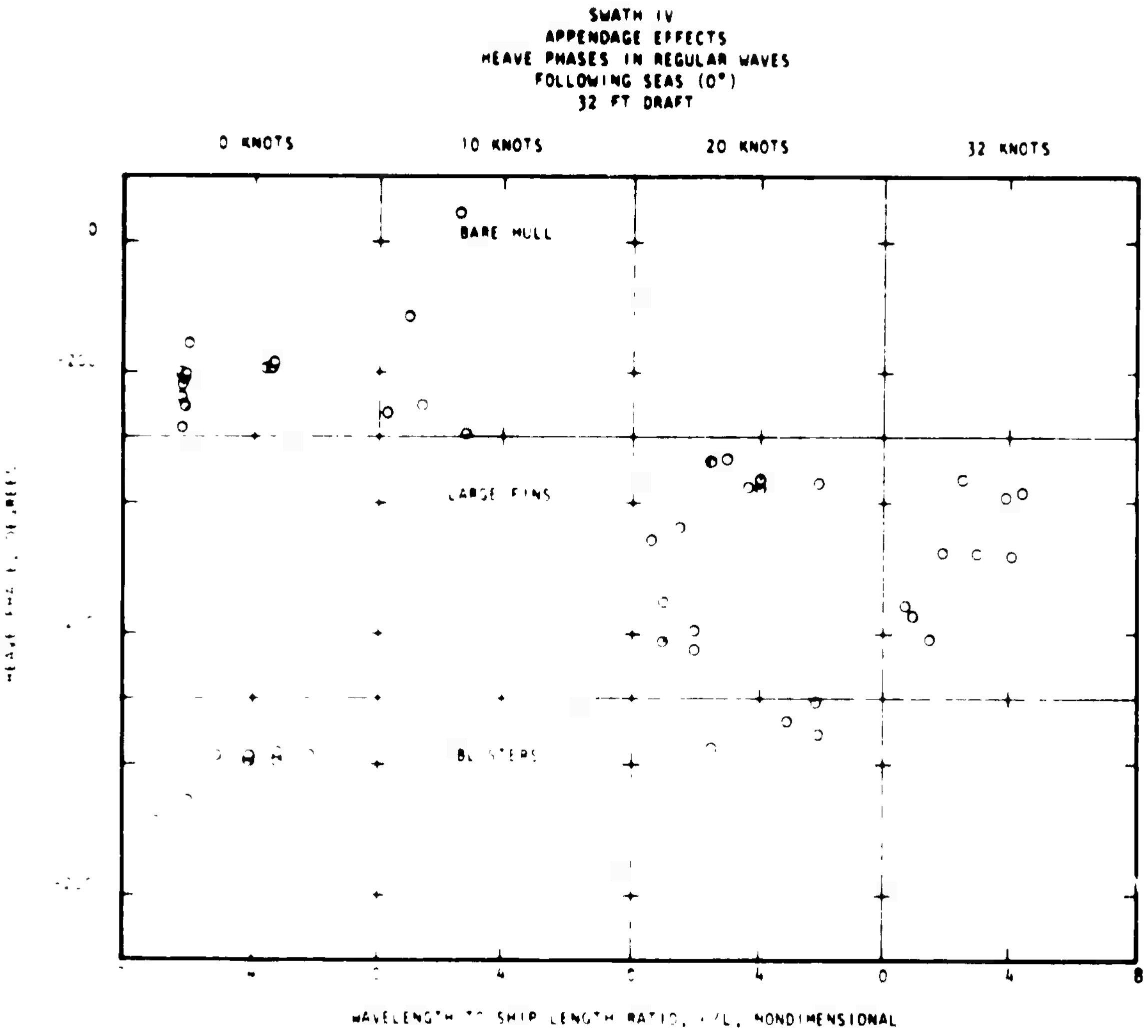

Figure 138 - Heave Phase in Regular Following Seas, 32 ft Draft, APPENDAGE EFFECT

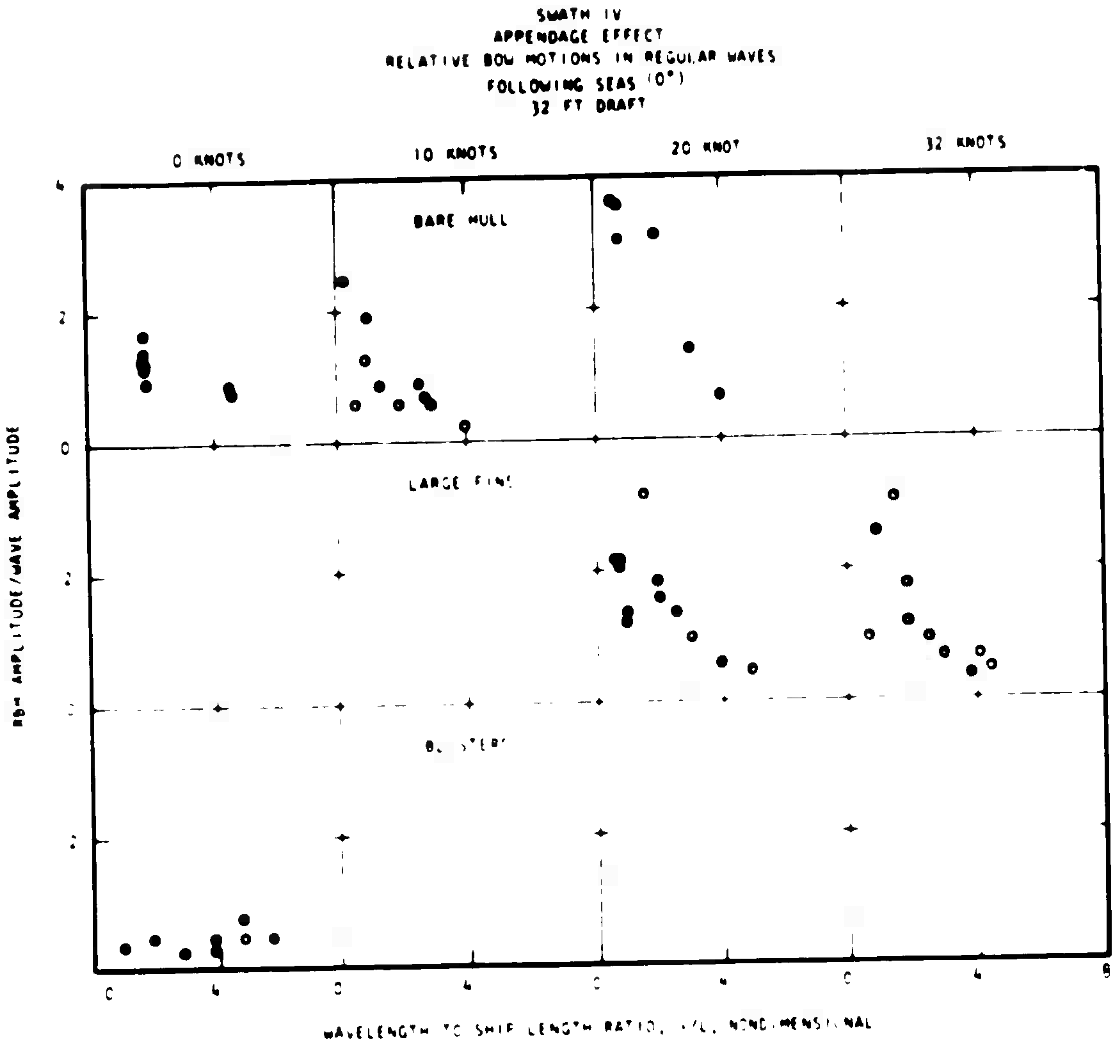

Figure 139 - Dimensionless Relative Bow Motion in Regular Following Seas, 32 ft Draft, APPENDAGE EFFECT

SWATH IV
APPENDAGE EFFECTS
RELATIVE BOW MOTION PHASES IN REGULAR WAVES
FOLLOWING SEAS (0°)
32 FT DRAFT

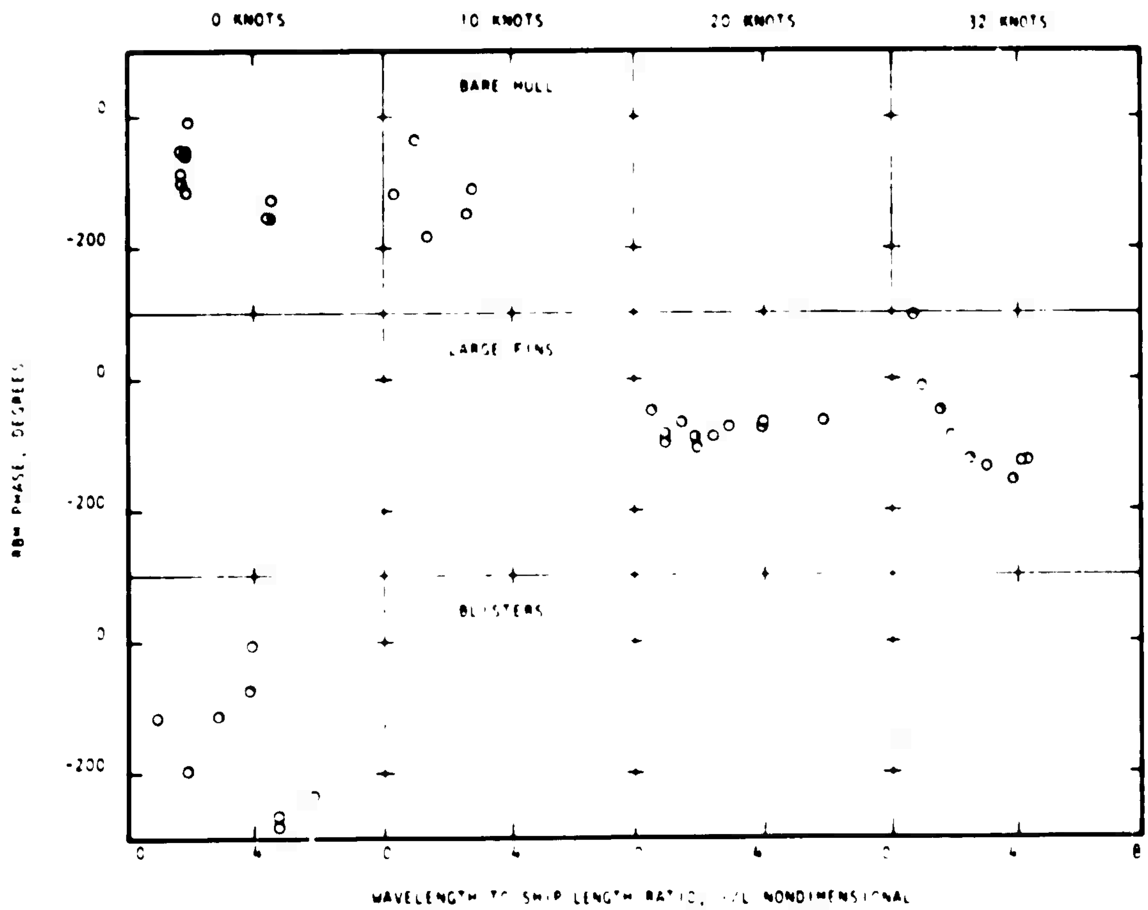

Figure 140 - Relative Bow Motion Phase in Regular Following Seas, 32 ft Draft, APPENDAGE EFFECT

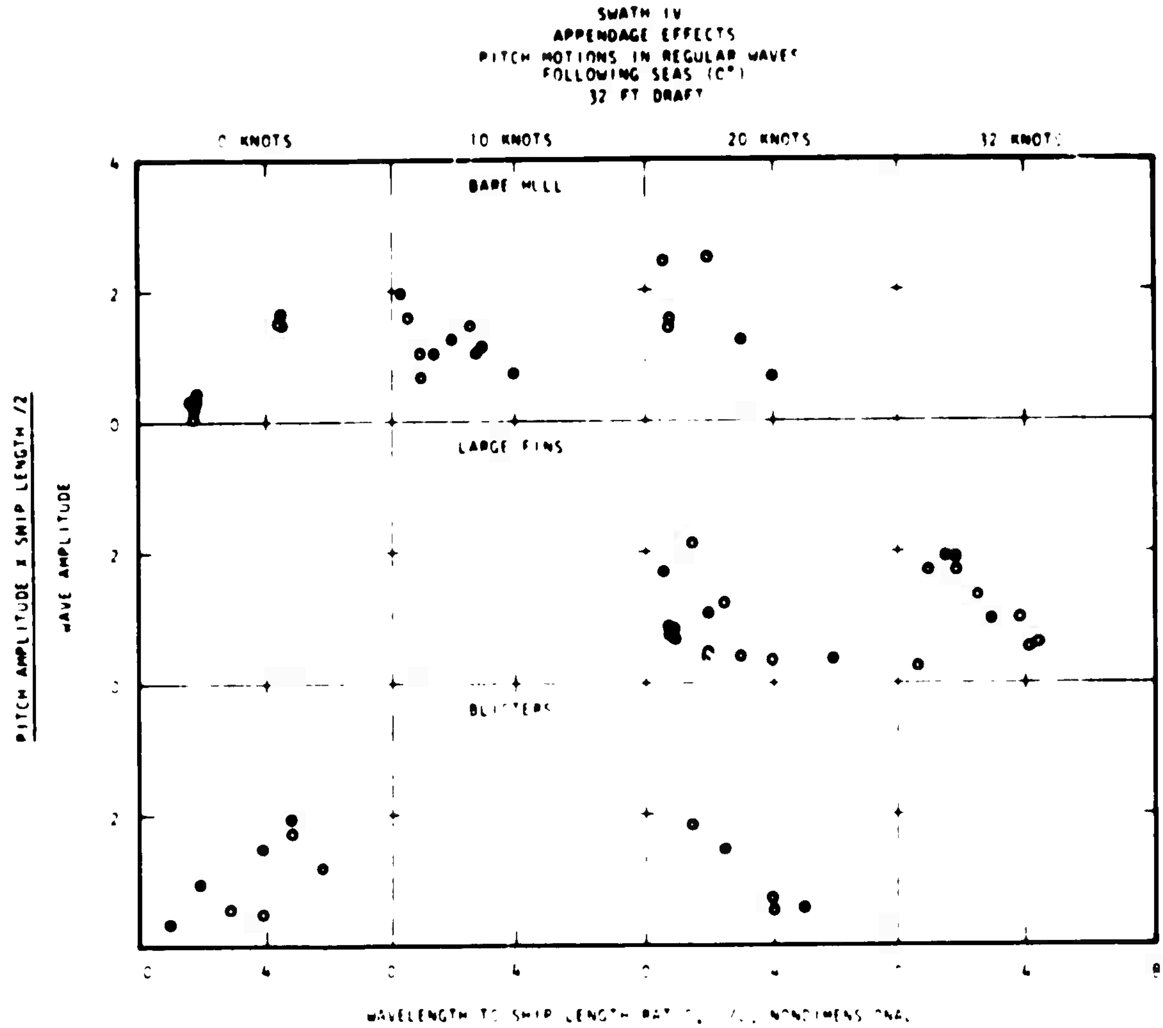

Figure 141 - Dimensionless Pitch in Regular Following Seas, 32 ft Draft, APPENDAGE EFFECT

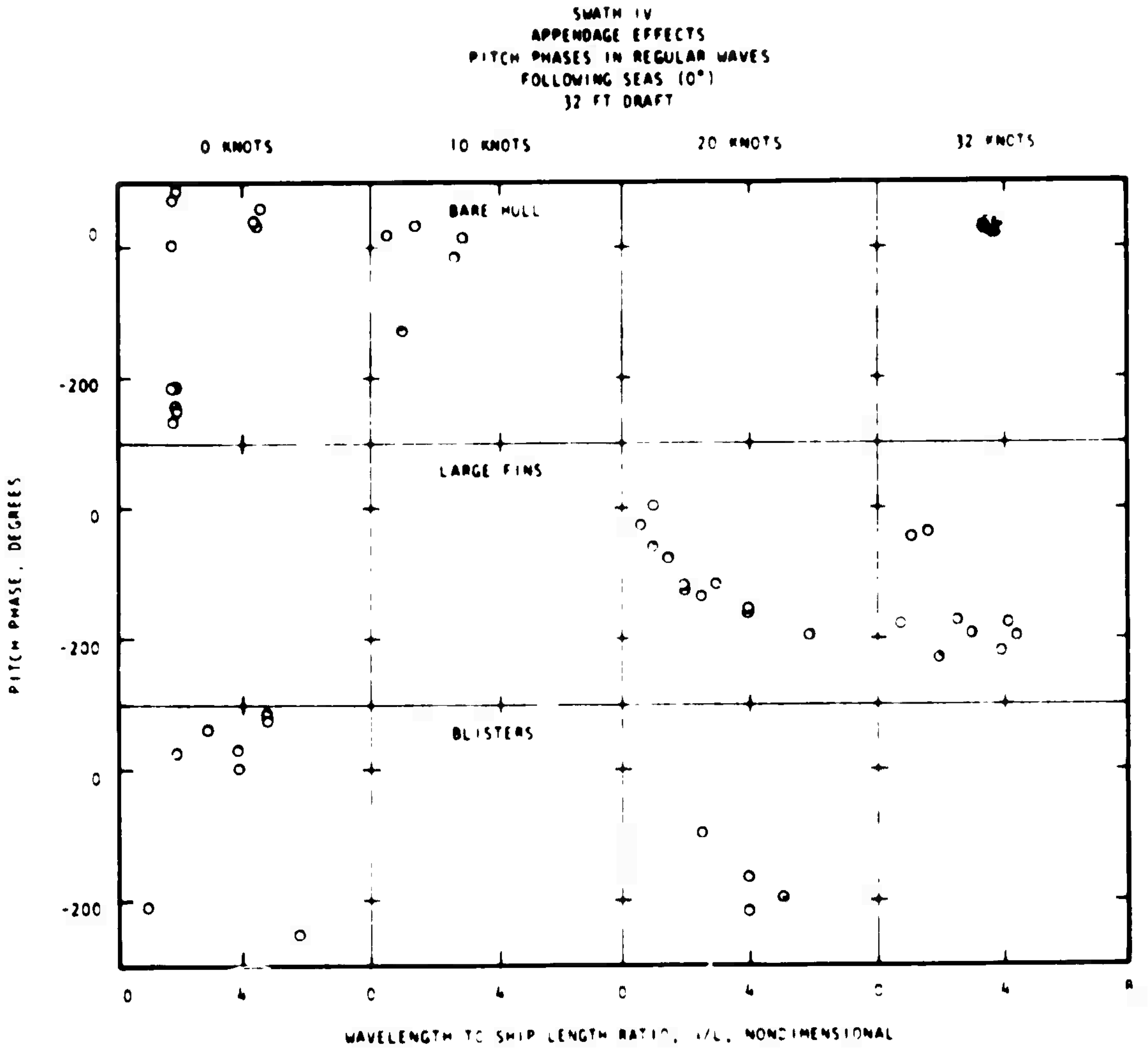

Figure 142 - Pitch Phase in Regular Following Seas, 32 ft Draft, APPENDAGE EFFECT

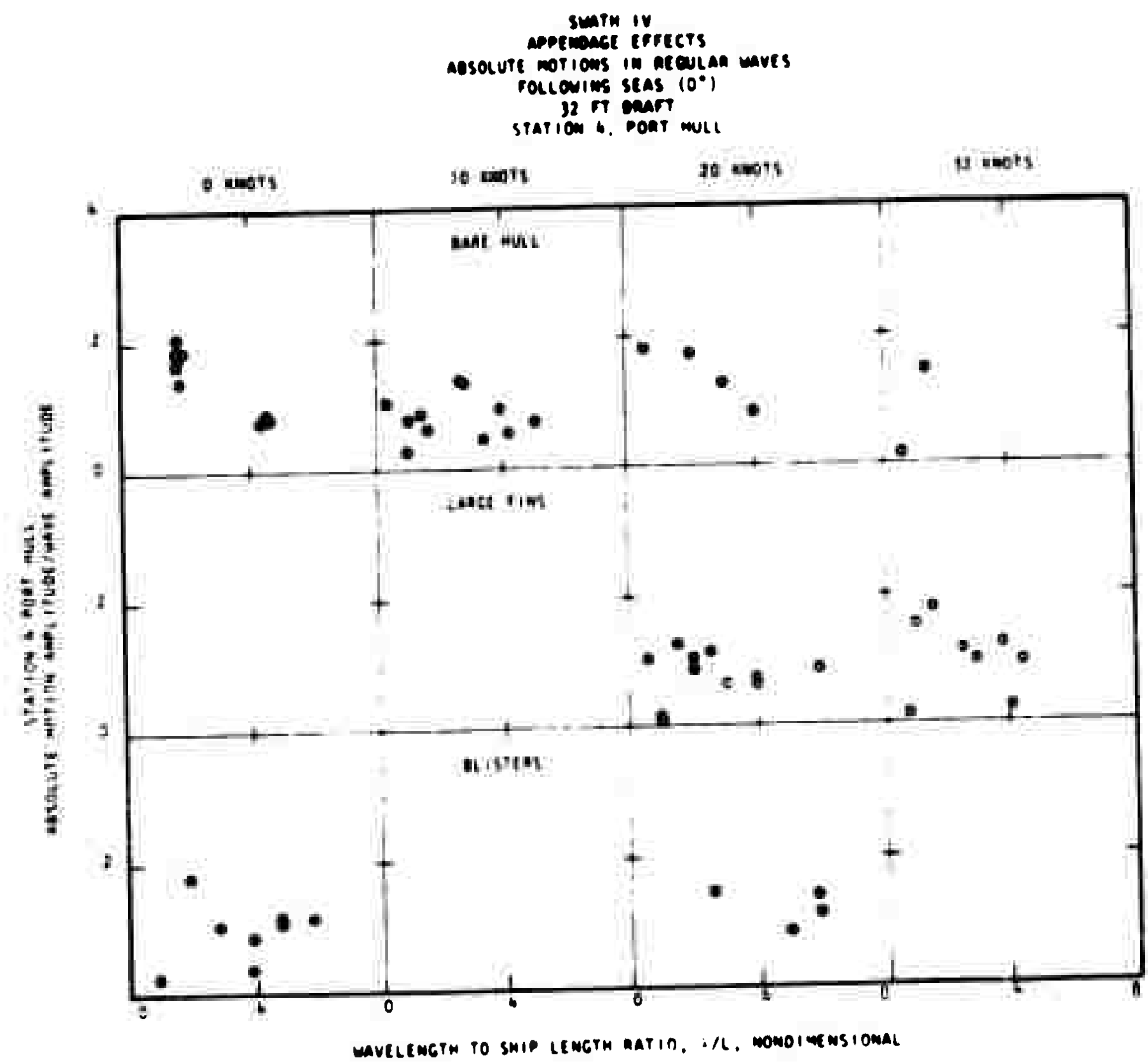

Figure 143 - Dimensionless Absolute Bow Motion in Regular Following Seas, Port Hull, 32 ft Draft, APPENDAGE EFFECT

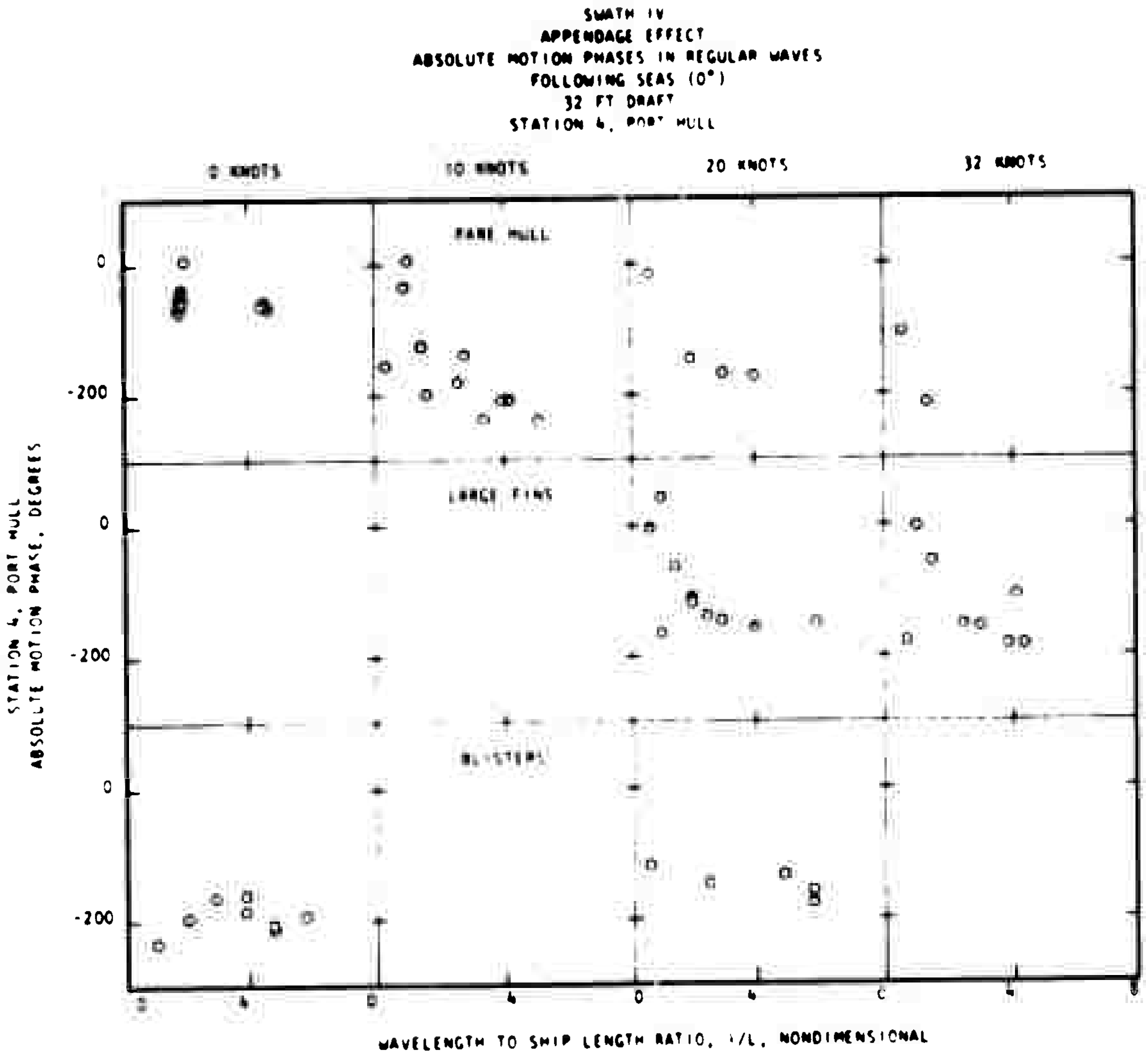

Figure 144 - Absolute Bow Motion Phase in Regular Following Seas, Port Hull, 32 ft Draft, APPENDAGE EFFECT

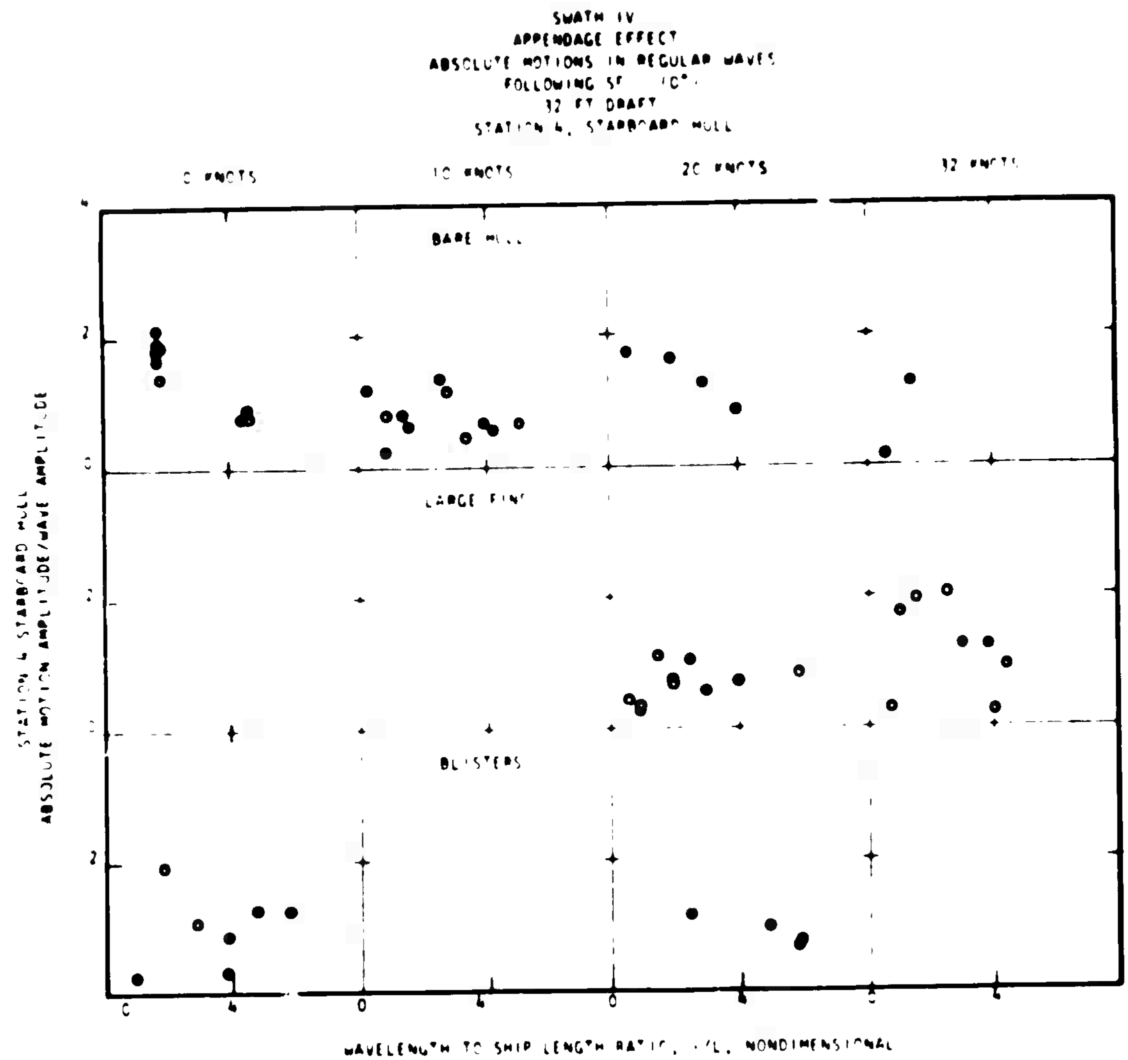

Figure 145 - Dimensionless Absolute Bow Motion in Regular Following Seas, Starboard Hull, 32 ft Draft, APPENDAGE EFFECT

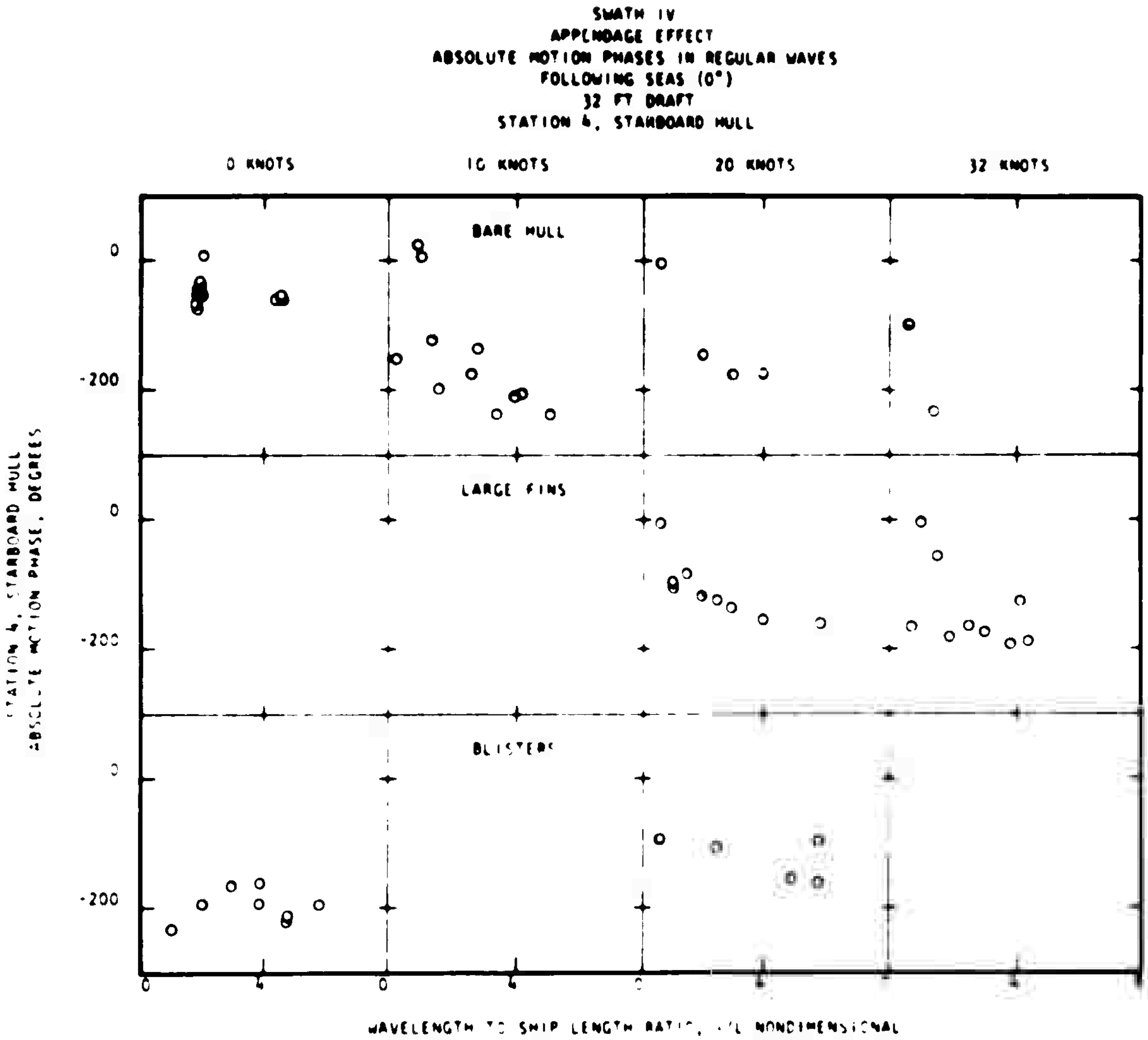

Figure 146 - Absolute Bow Motion Phase in Regular Following Seas, Starboard Hull, 32 ft Draft APPENDAGE EFFECT

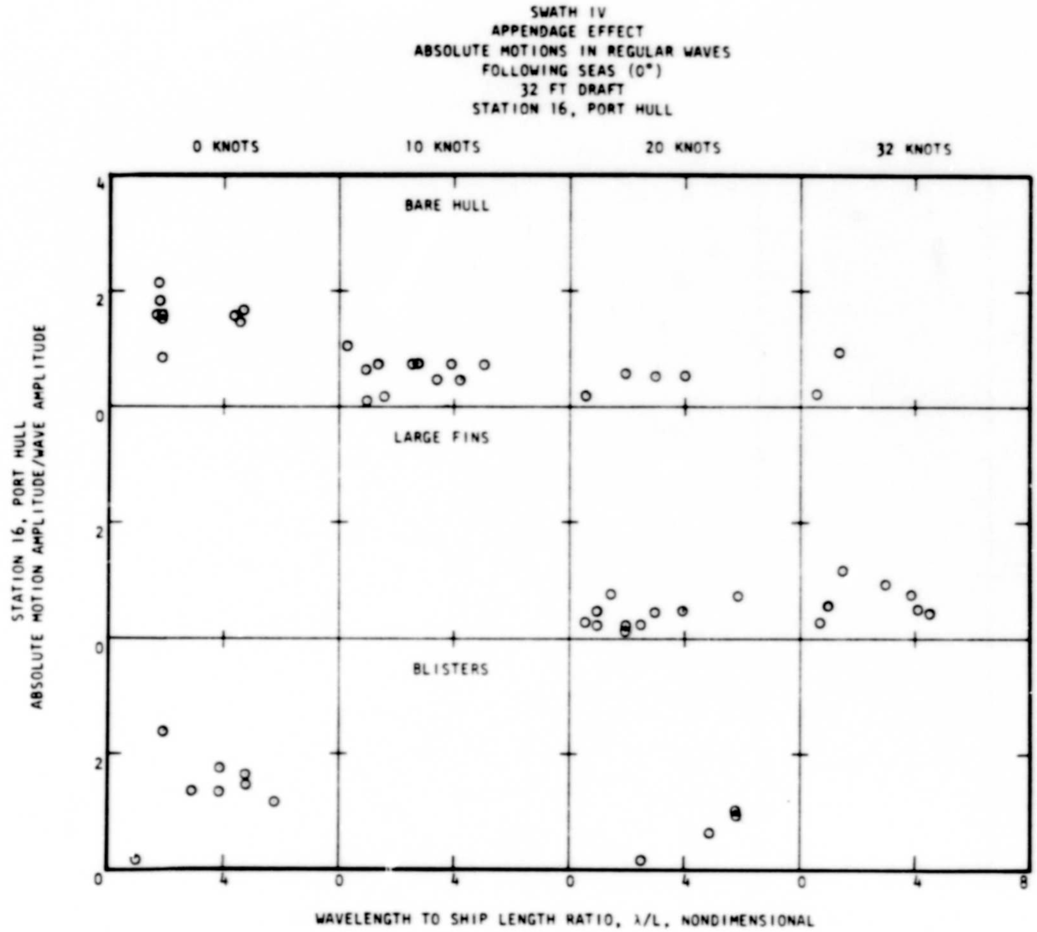

Figure 147 - Dimensionless Absolute Stern Motion in Regular Following Seas, Port Hull, 32 ft Draft , APPENDAGE EFFECT

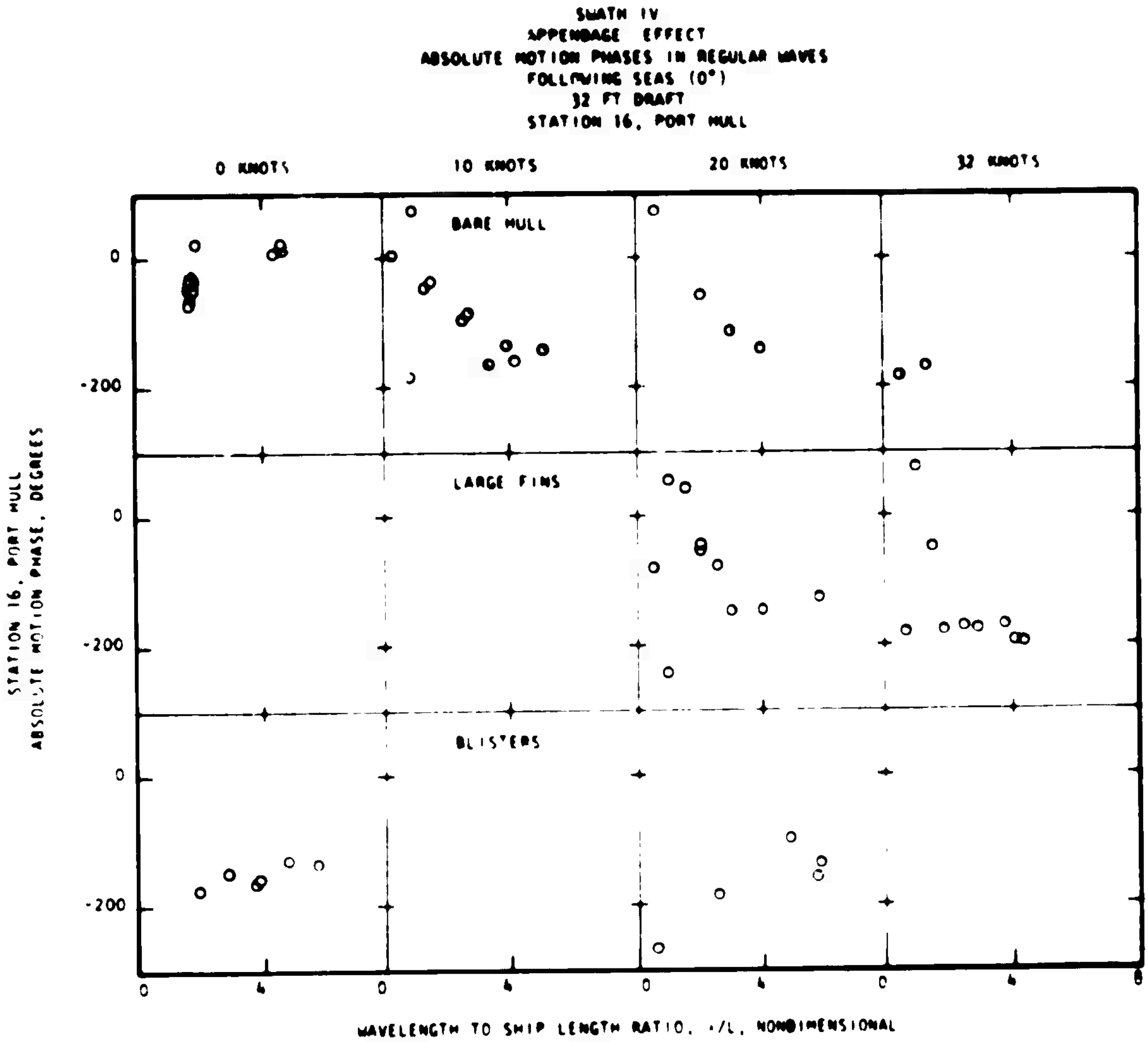

Figure 148 - Absolute Stern Motion Phase in Regular Following Seas, Port Hull, 32 ft Draft, APPENDAGE EFFECT

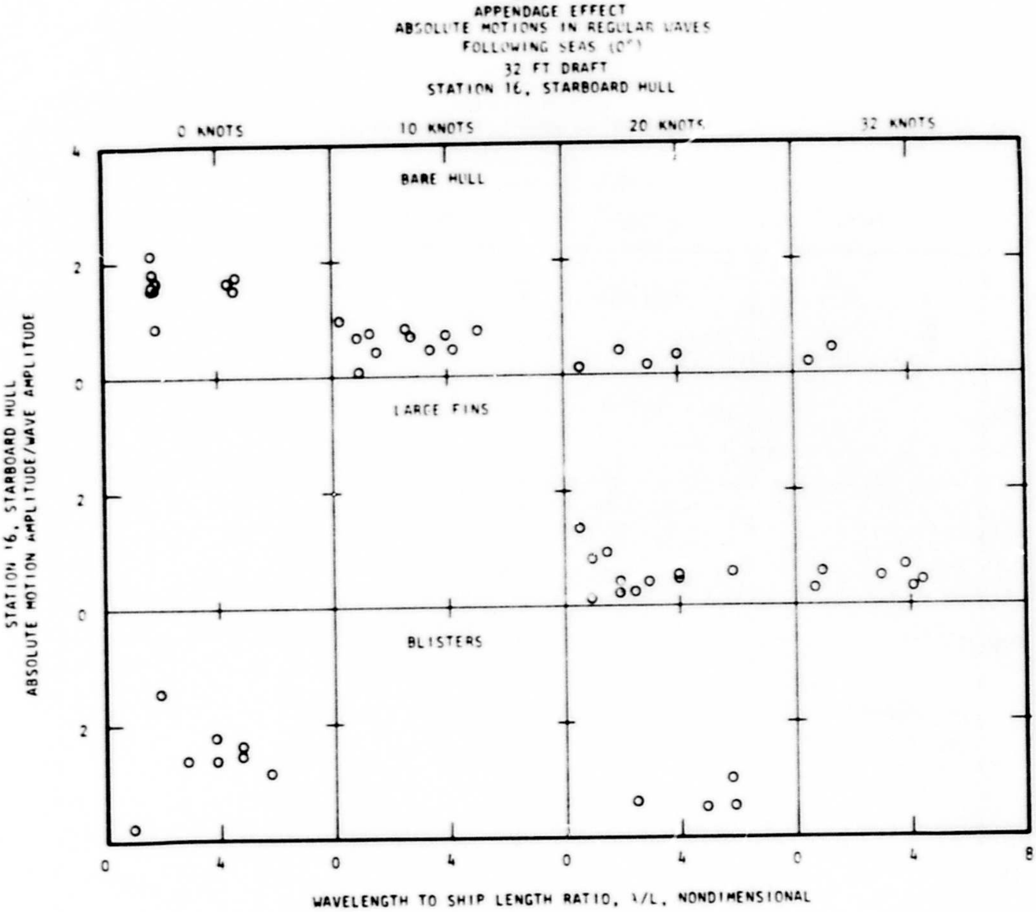

Figure 149 - Dimensionless Absolute Stern Motion In Regular Following Seas, Starboard Hull, 32 ft Draft, APPENDAGE EFFECT

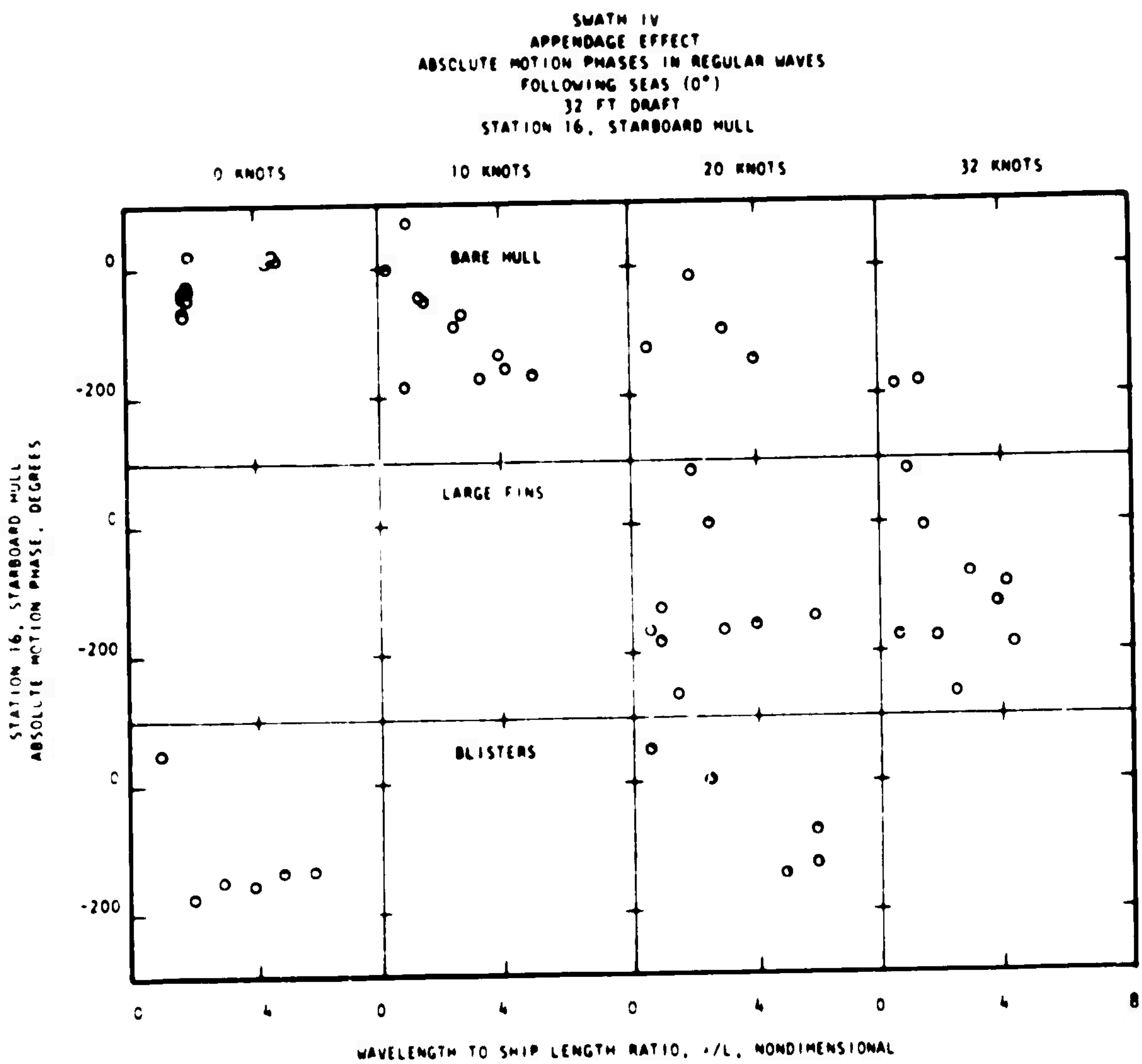

Figure 150 - Absolute Stern Motion Phase in Regular Following Seas, Starboard Hull, 32 ft Draft, APPENDAGE EFFECT

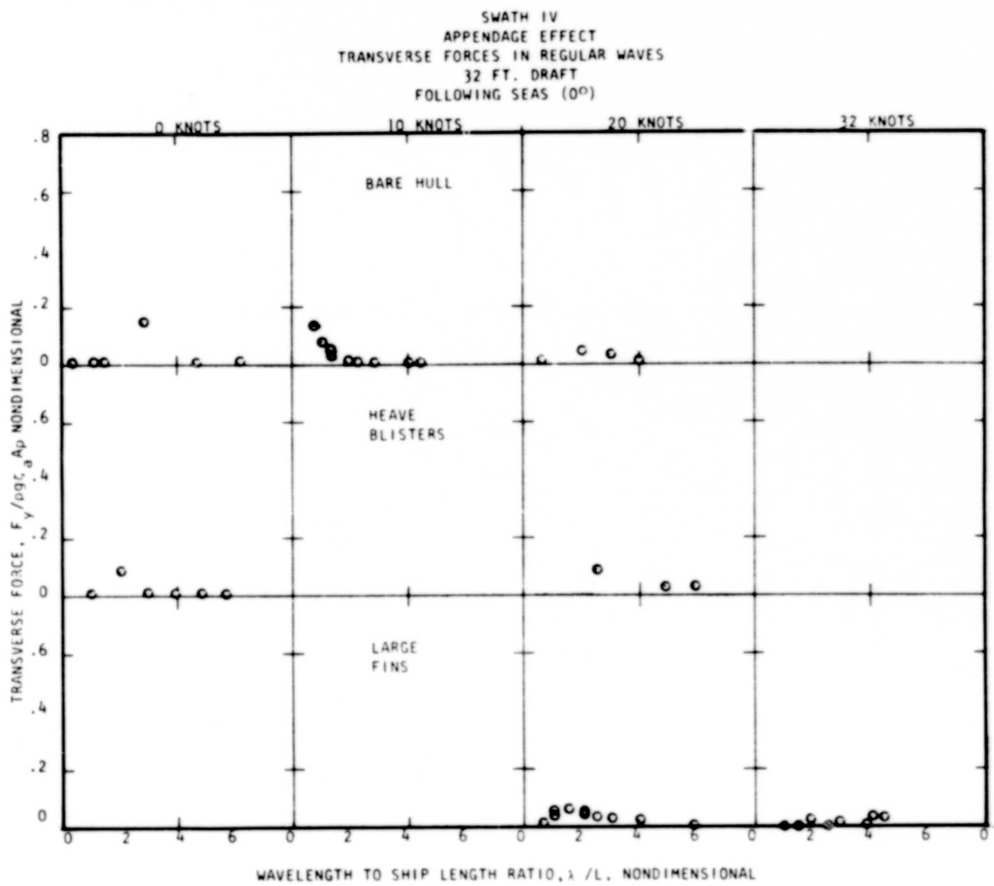

Figure 151 - Dimensionless Transverse Force in Regular Following Seas, 32 ft Draft, APPENDAGE EFFECT

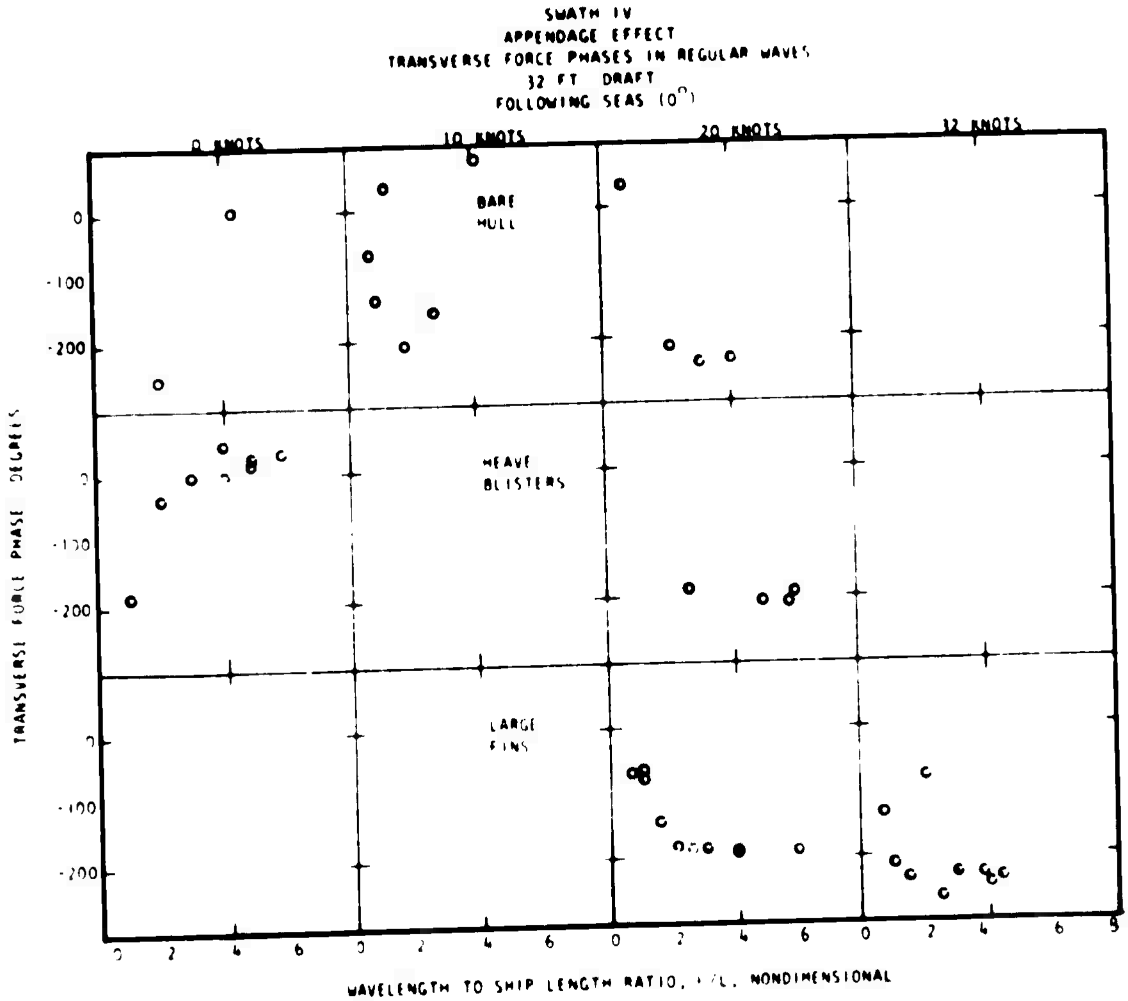

Figure 152 - Transverse Force Phase in Regular Following Seas, 32 ft Draft, APPENDAGE EFFECT

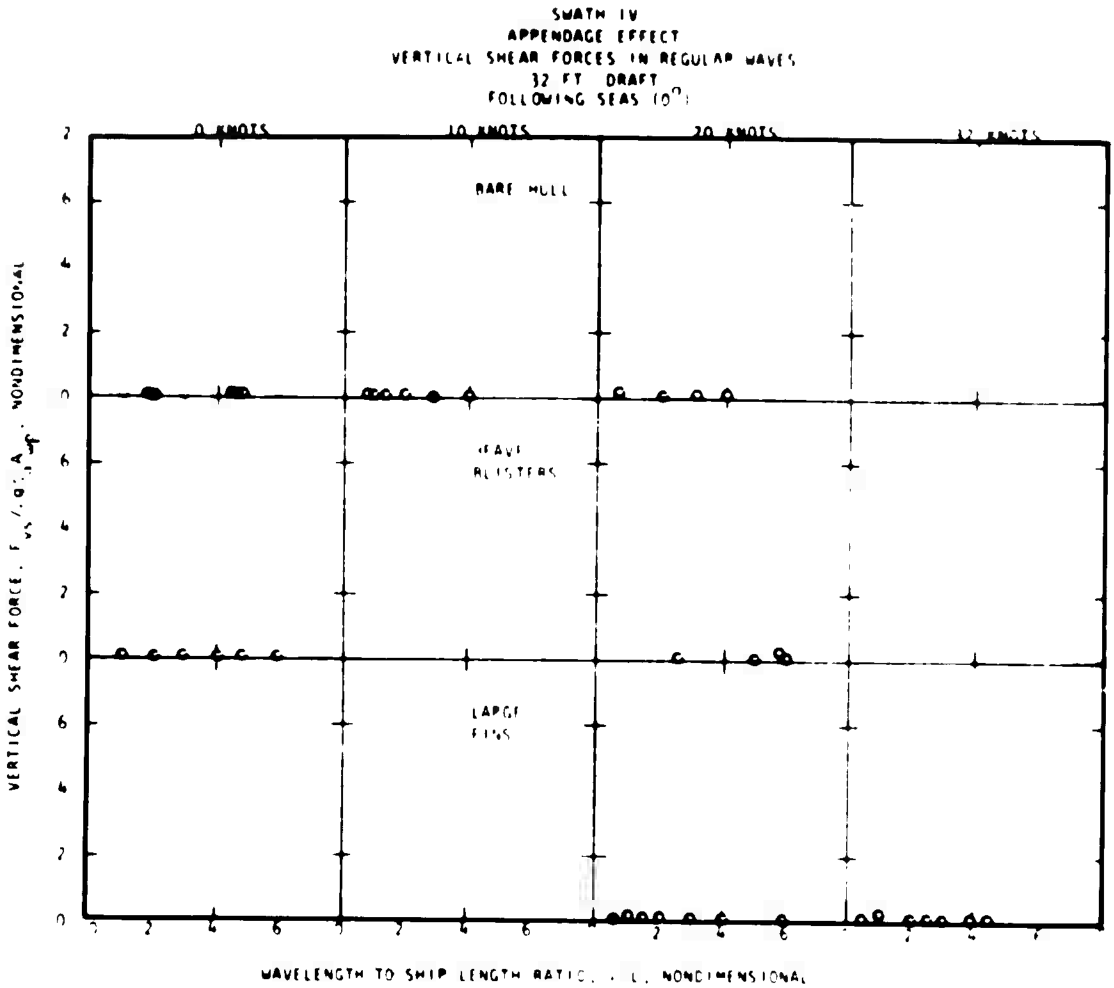

Figure 153 - Dimensionless Vertical Shear Force in Regular Following Seas, 32 ft Draft, APPENDAGE EFFECT

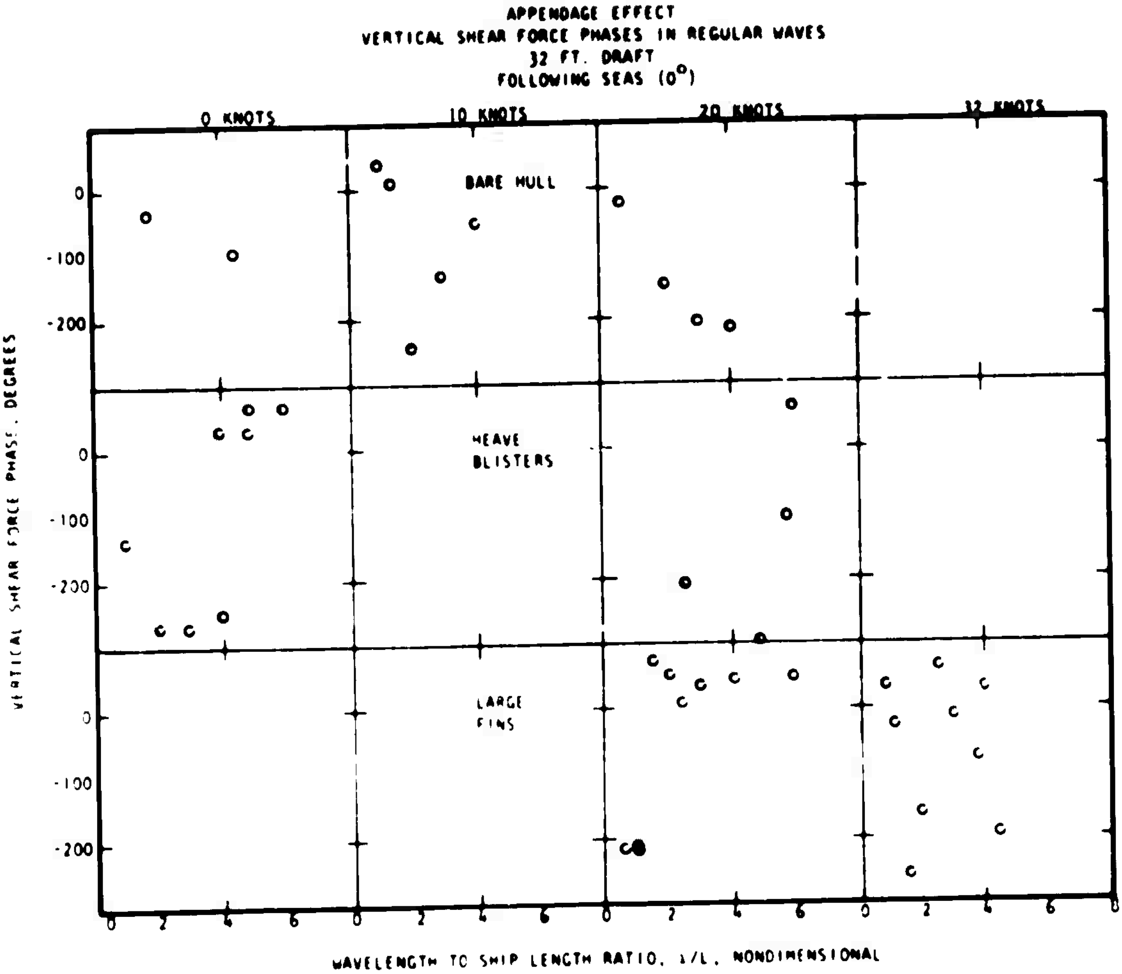

Figure 154 - Vertical Shear Force Phase in Regular Following Seas, 32 ft Draft, APPENDAGE EFFECT

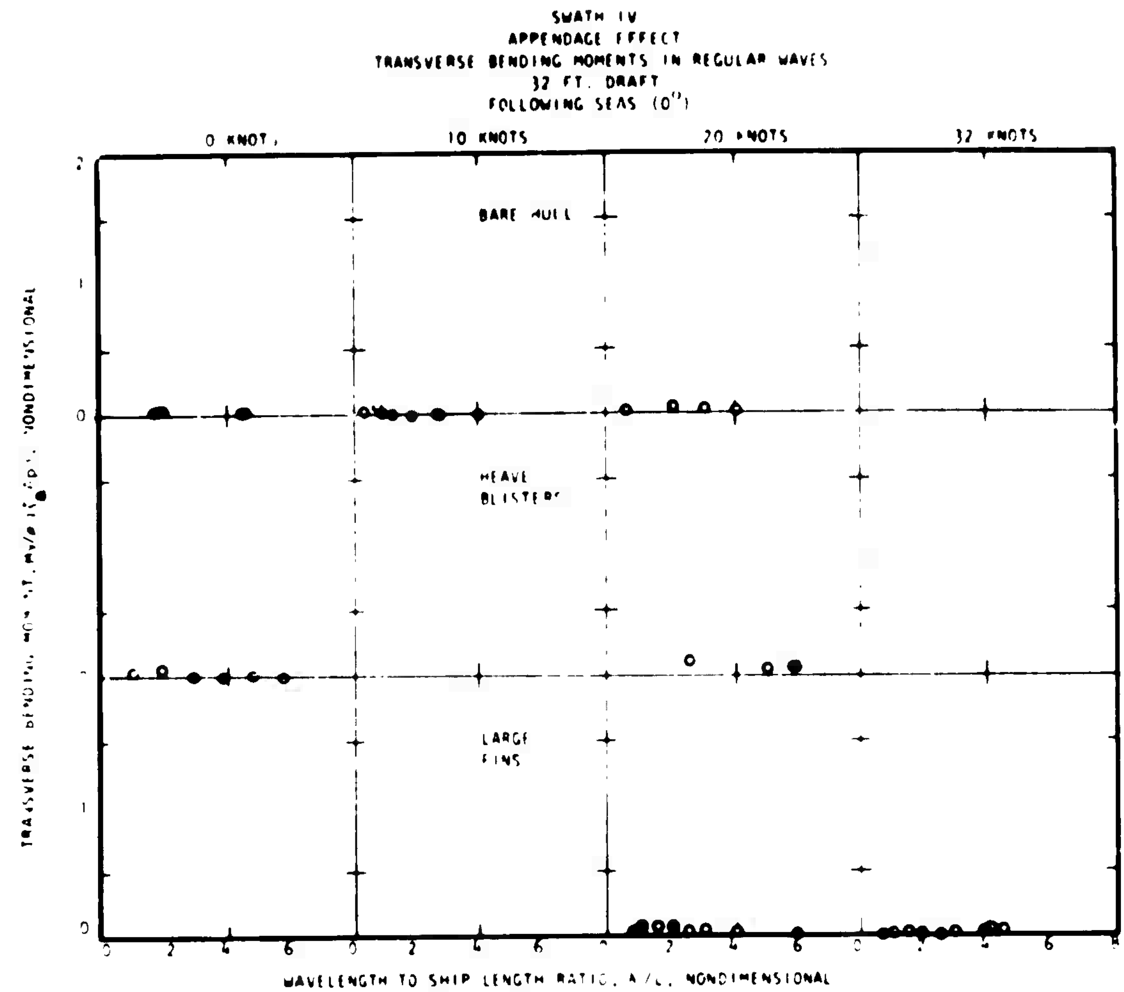

Figure 155 - Dimensionless Transverse Vertical Bending Moment in Regular Following Seas, 32 ft Draft, APPENDAGE EFFECT

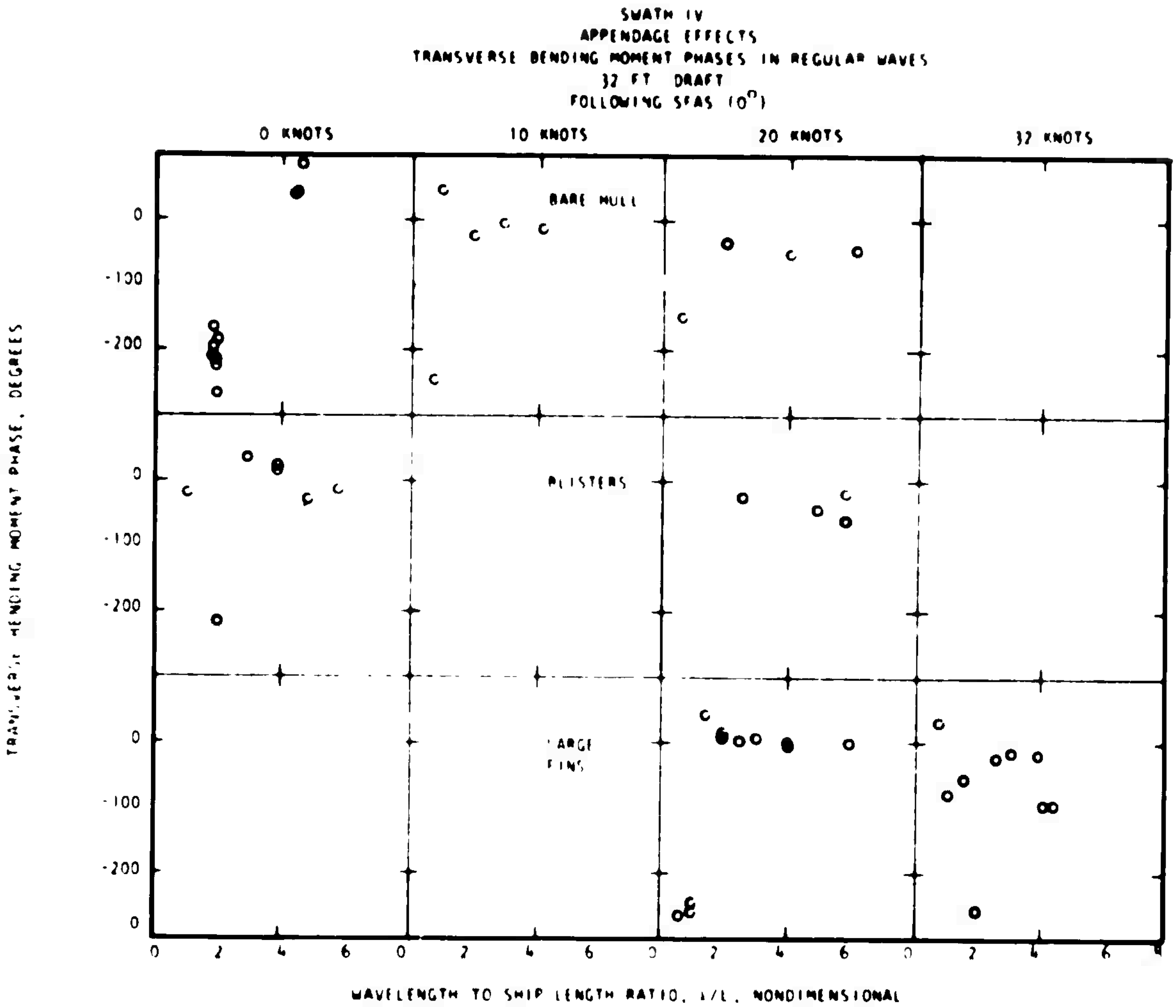

Figure 156 - Transverse Vertical Bending Moment in Regular Following Seas, 32 ft Draft, APPENDAGE EFFECT

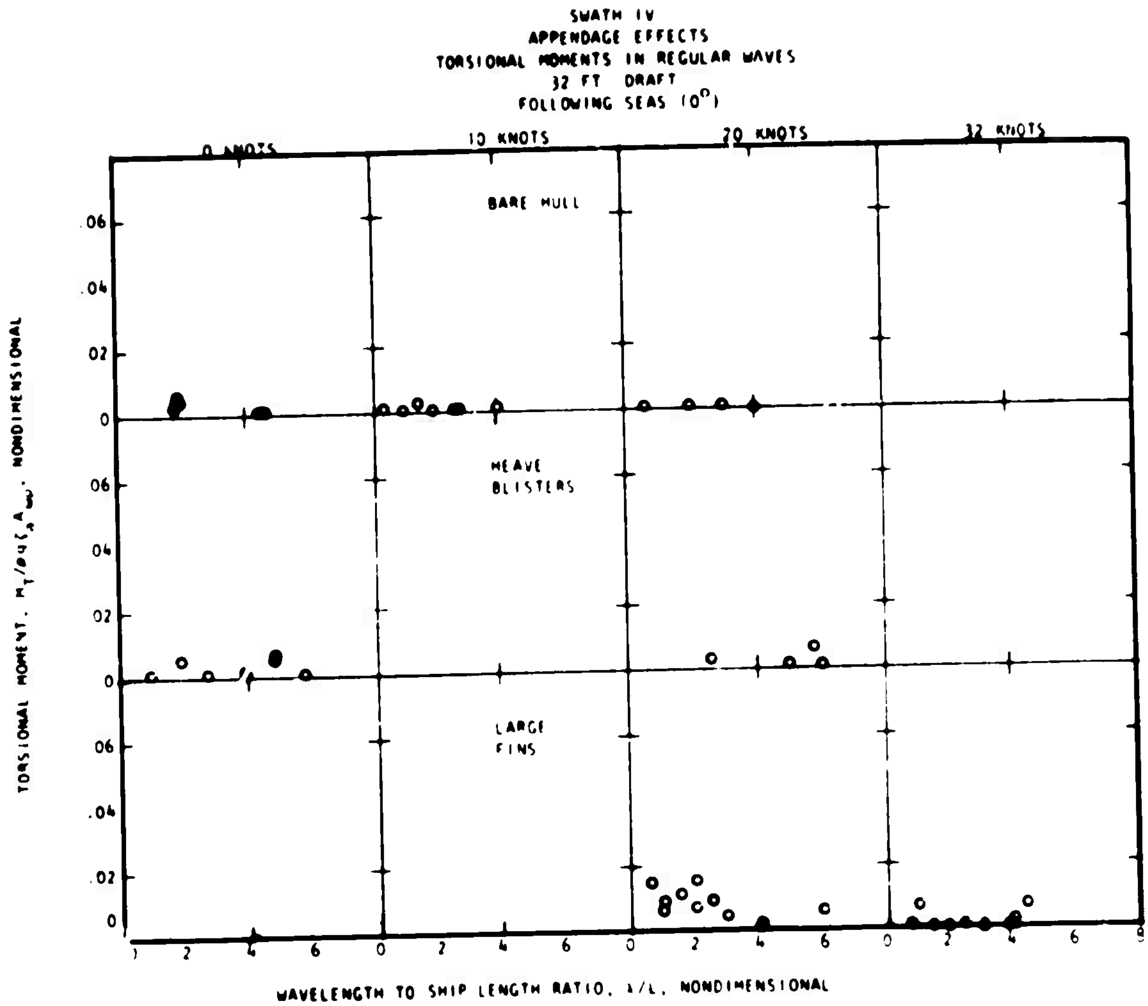

Figure 157 - Dimensionless Torsional Moment in Regular Following Seas, 32 ft Draft, APPENDAGE EFFECT

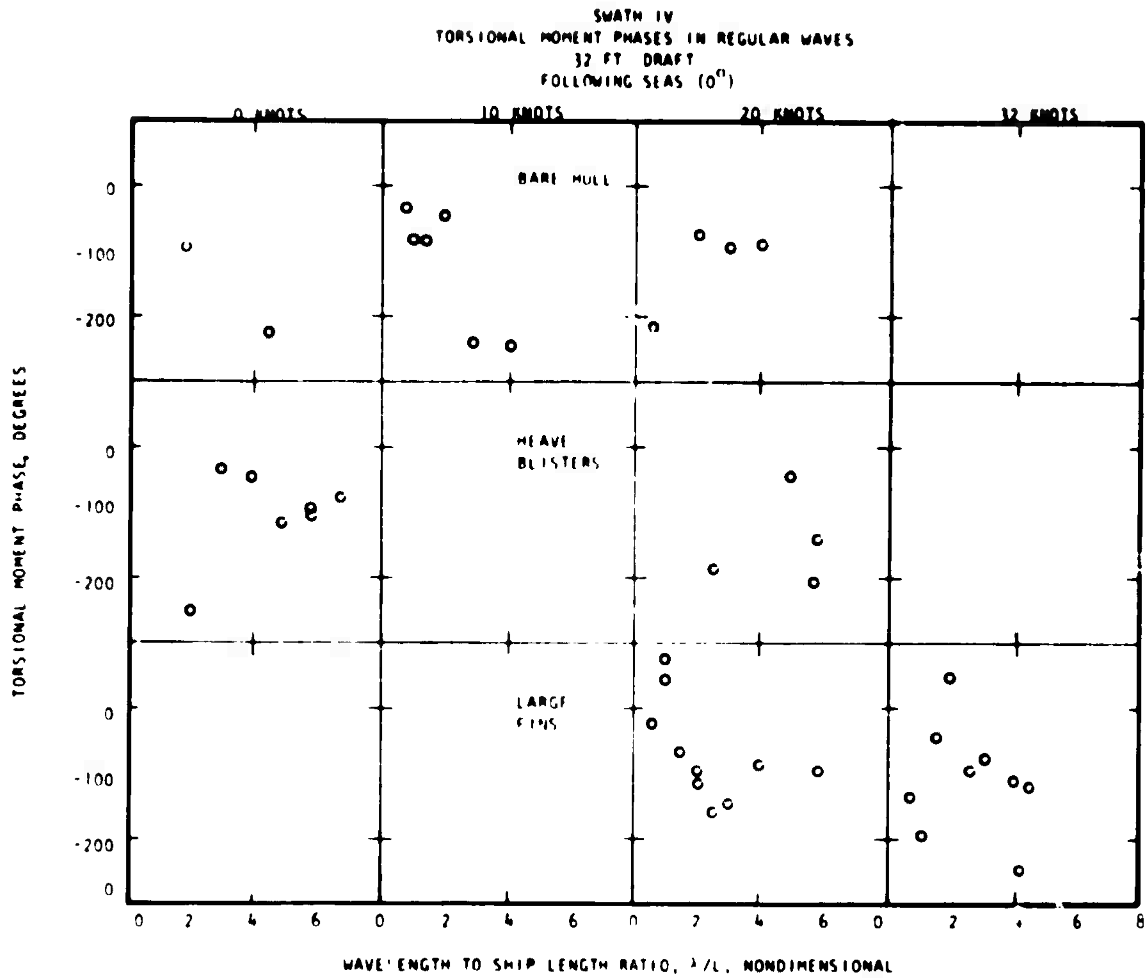

Figure 158 - Torsional Moment Phase in Regular Following Seas, 32 ft Draft, APPENDAGE EFFECT

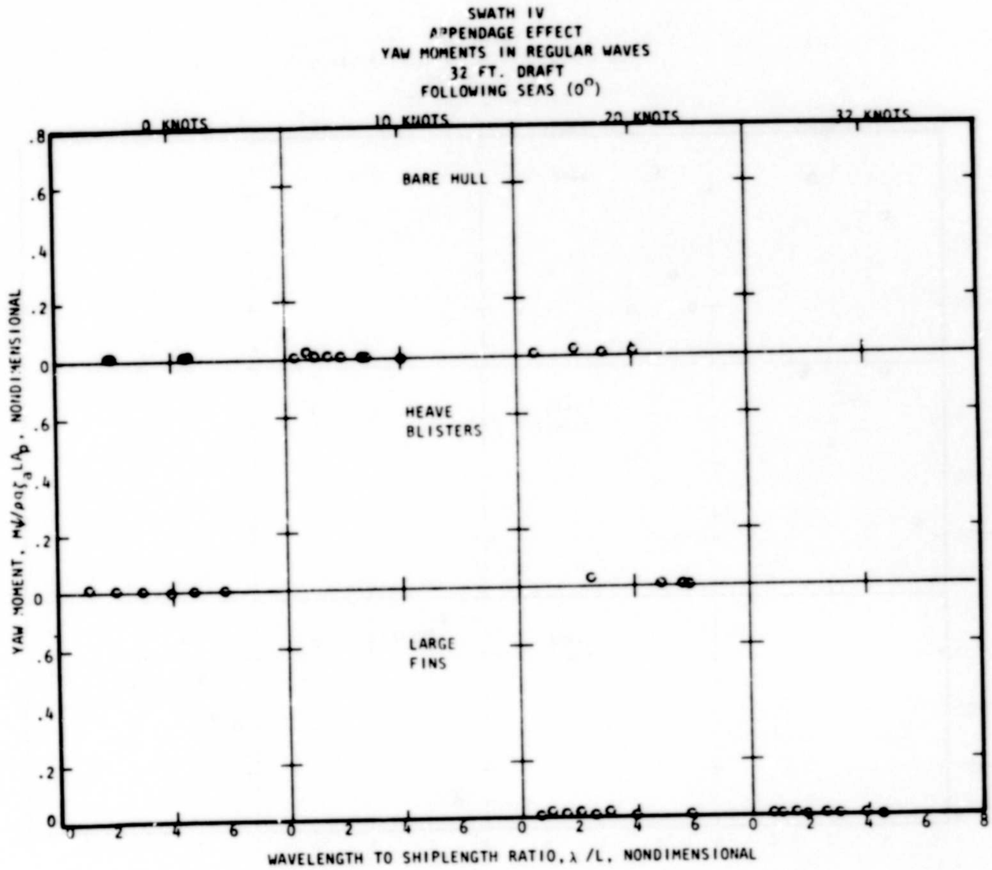

Figure 159 - Dimensionless Yaw Moment in Regular Following Seas, 32 ft Draft, APPENDAGE EFFECT

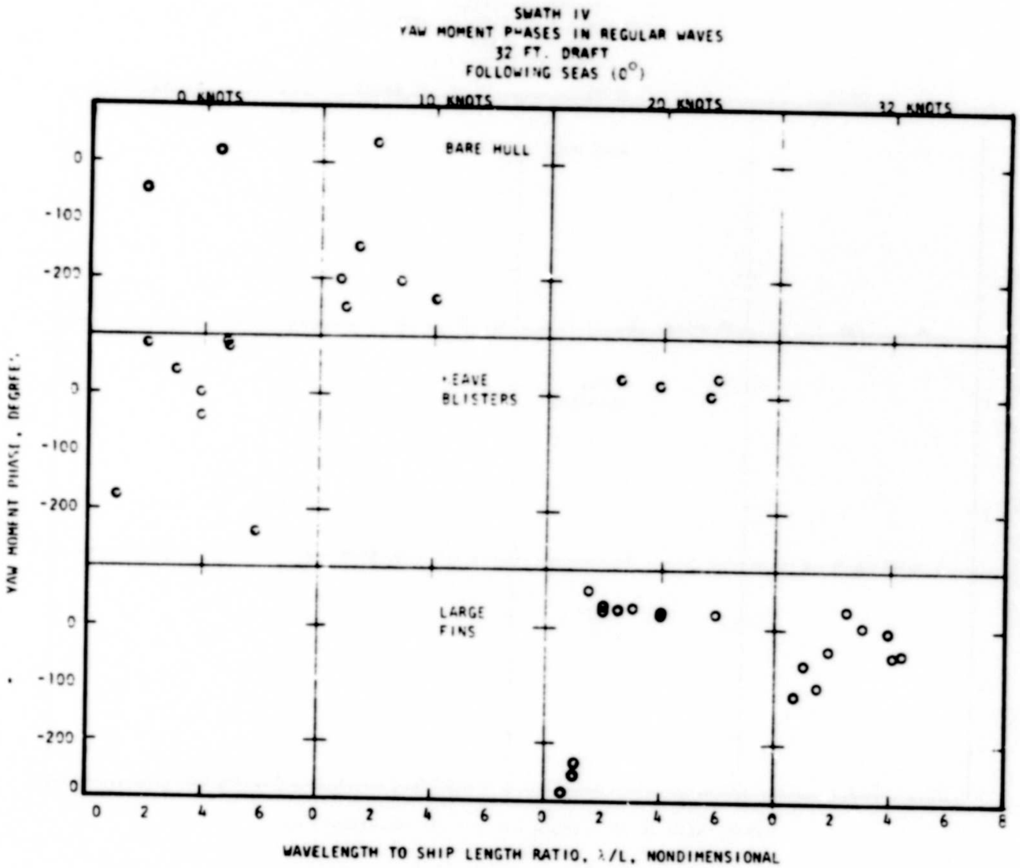

Figure 160 - Yaw Moment Phase in Regular Following Seas, 32 ft Draft, APPENDAGE EFFECT

SWATH IV

SIGNIFICANT DOUBLE AMPLITUDES OF MOTIONS IN RANDOM WAVES

APPENDAGE EFFECT, 32 ft DRAFT

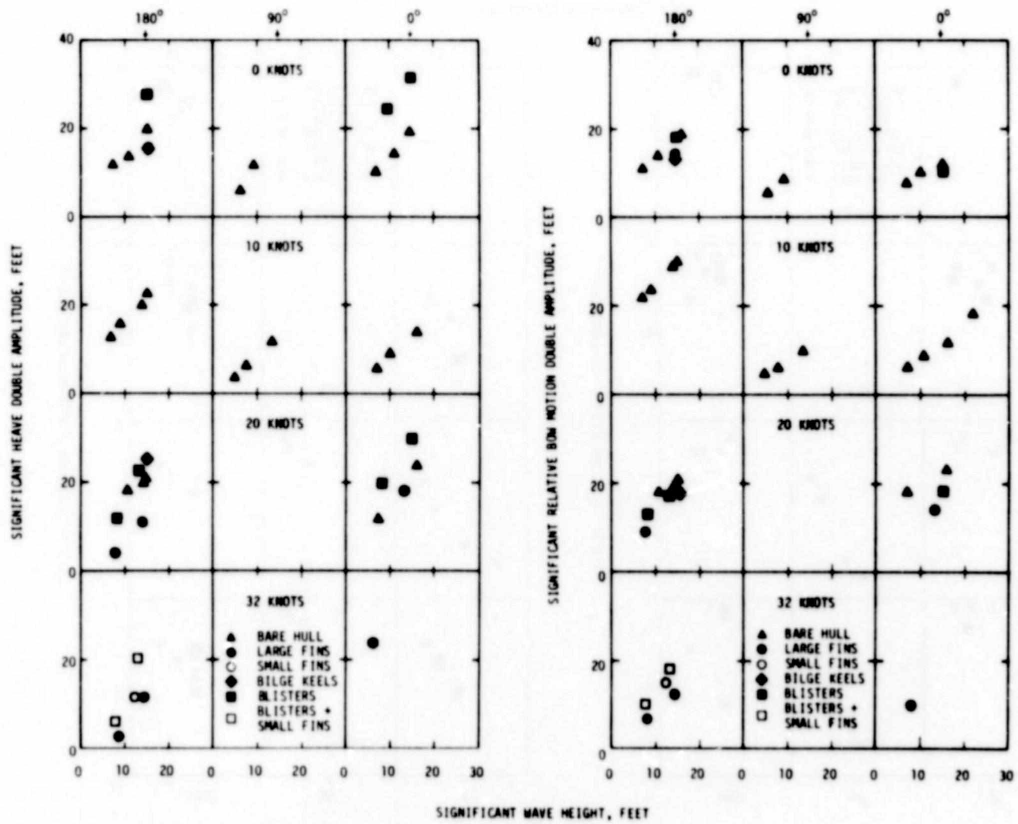

Figure 161 - Significant Double Amplitudes of Heave and Relative Bow Motion in Random Waves, 32 ft Draft, APPENDAGE EFFECT

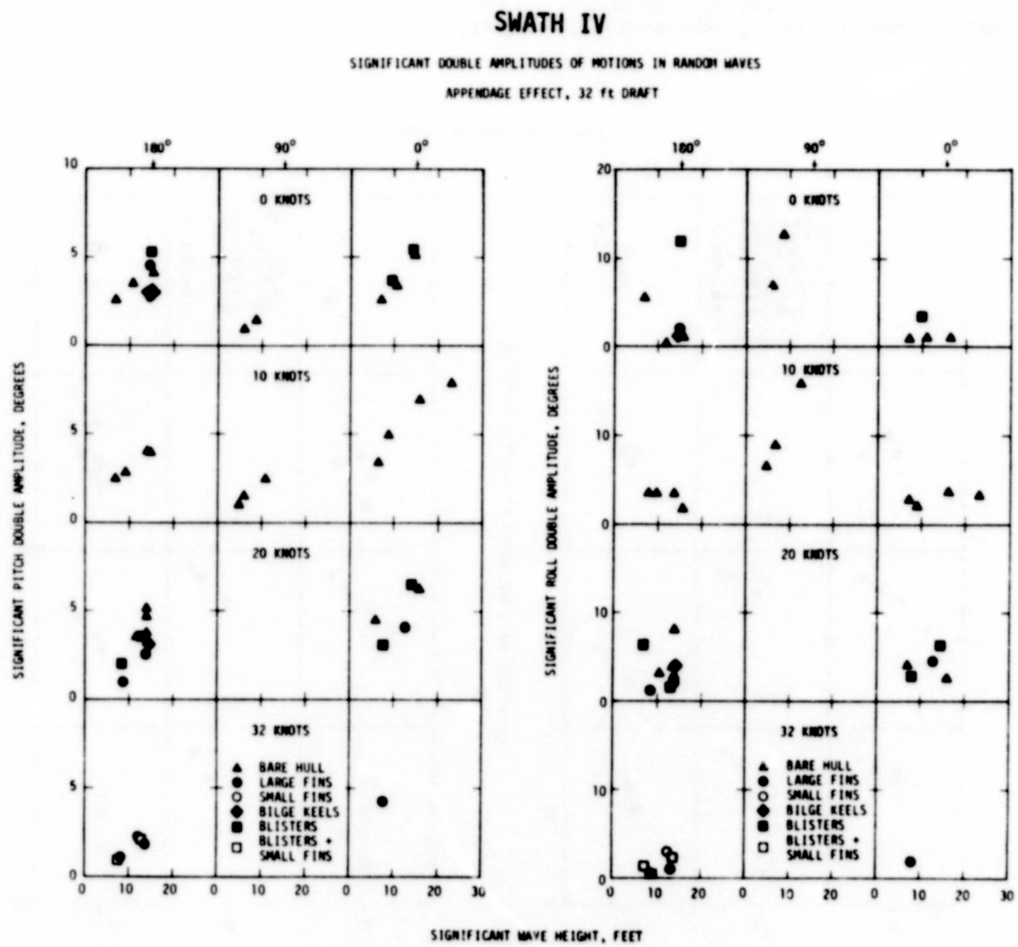

Figure 162 - Significant Double Amplitudes of Pitch and Roll in Random Waves, 32 ft Draft, APPENDAGE EFFECT

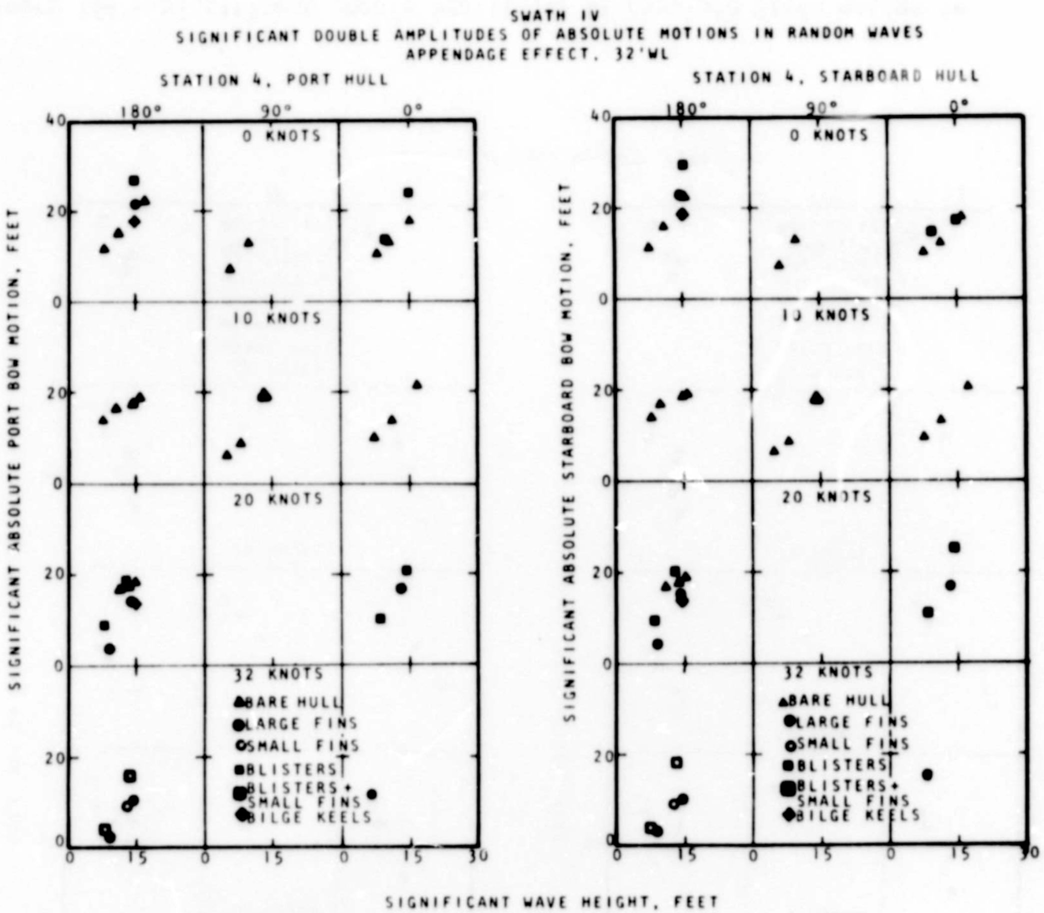

Figure 163 - Significant Double Amplitudes of Absolute Bow Motion in Random Waves, 32 ft Draft, APPENDAGE EFFECT

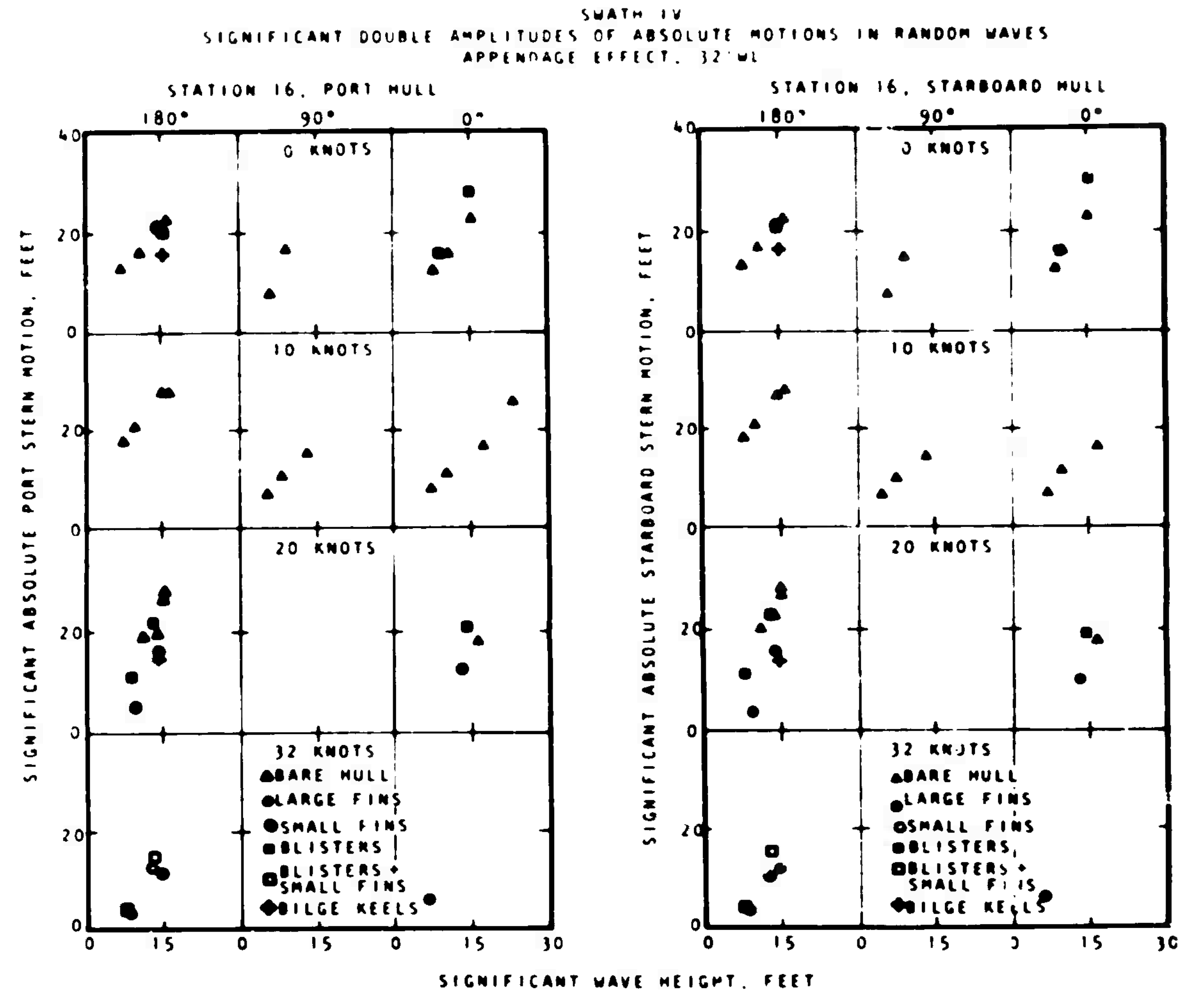

Figure 164 - Significant Double Amplitudes of Absolute Stern Motion in Random Waves, 32 ft Draft, APPENDAGE EFFECT

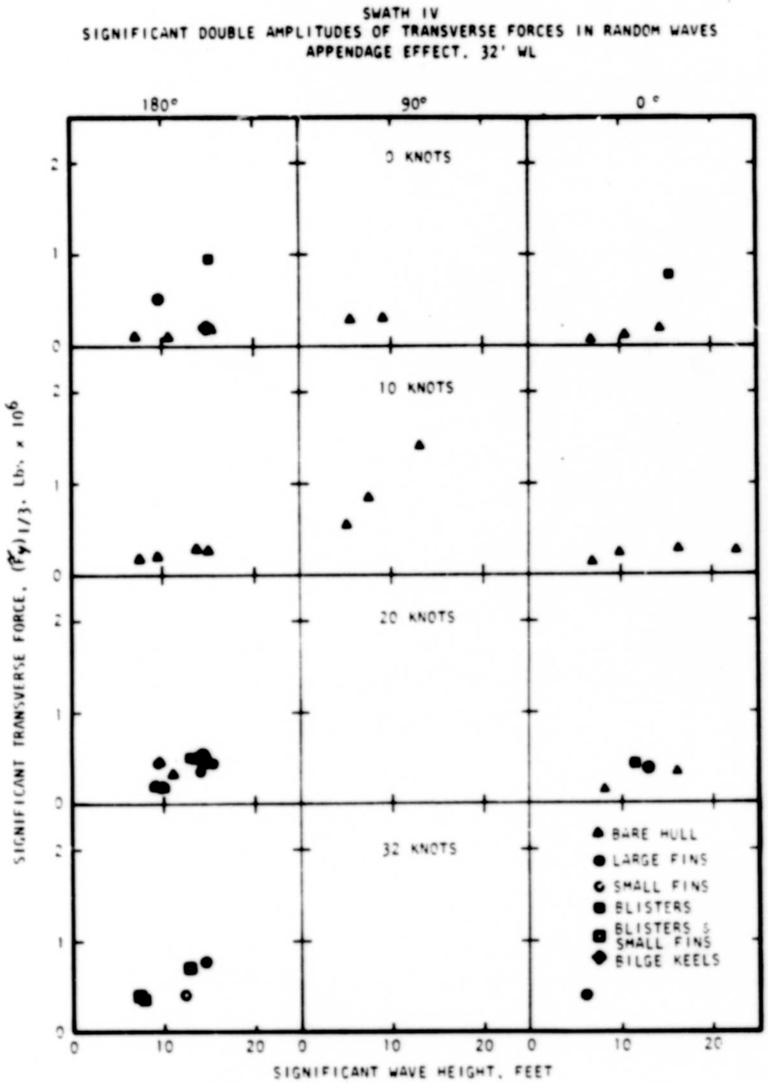

Figure 165 - Significant Double Amplitudes of Transverse Force in Random Waves, 32 ft Draft, APPENDAGE EFFECT

SWATH IV

SIGNIFICANT DOUBLE AMPLITUDES OF VERTICAL SHEAR FORCES IN RANDOM WAVES

APPENDAGE EFFECT 32 ft DRAFT

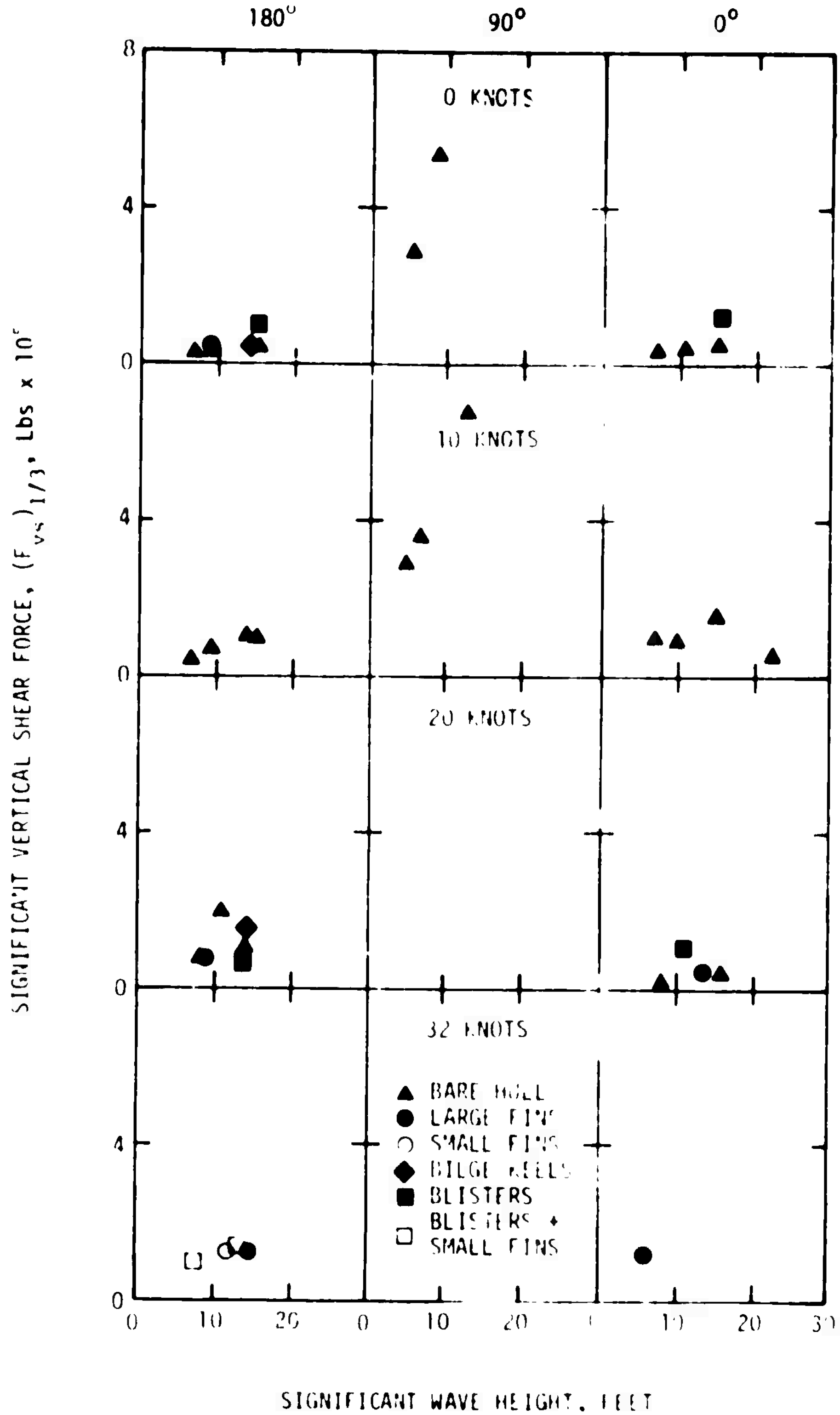

Figure 166 - Significant Double Amplitudes of Vertical Shear Force in Random Waves, 32 ft Draft, APPENDAGE EFFECT

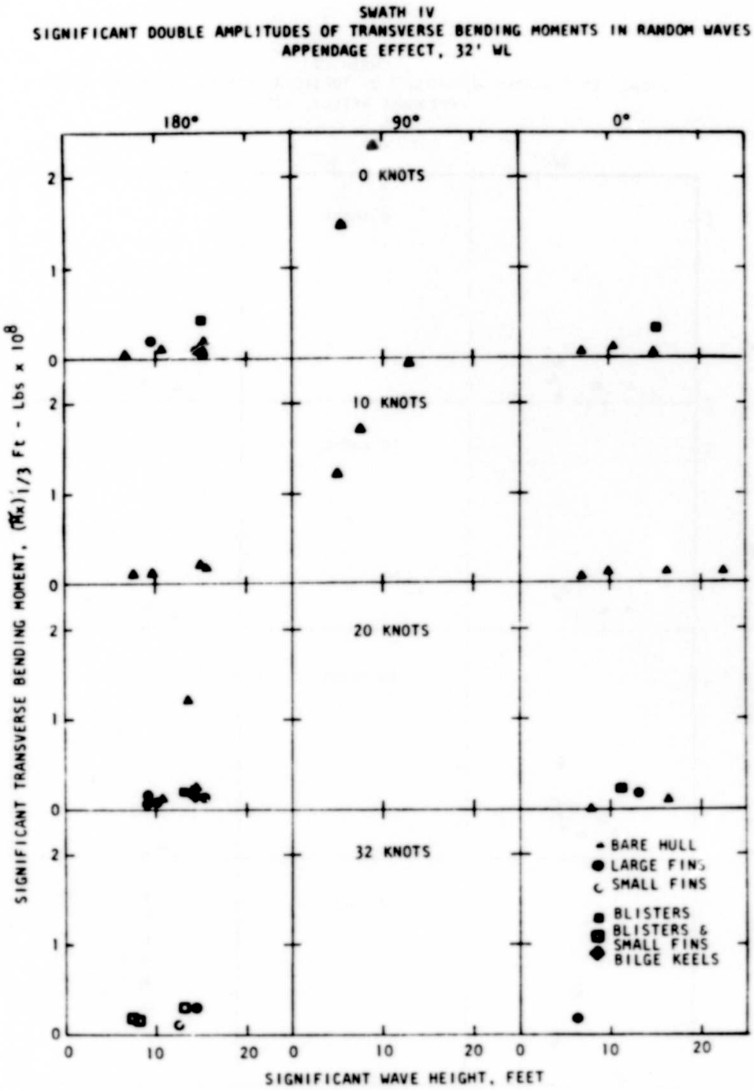

Figure 167 - Significant Double Amplitudes of Transverse Vertical Bending Moment in Random Waves, 32 ft Draft APPENDAGE EFFECT

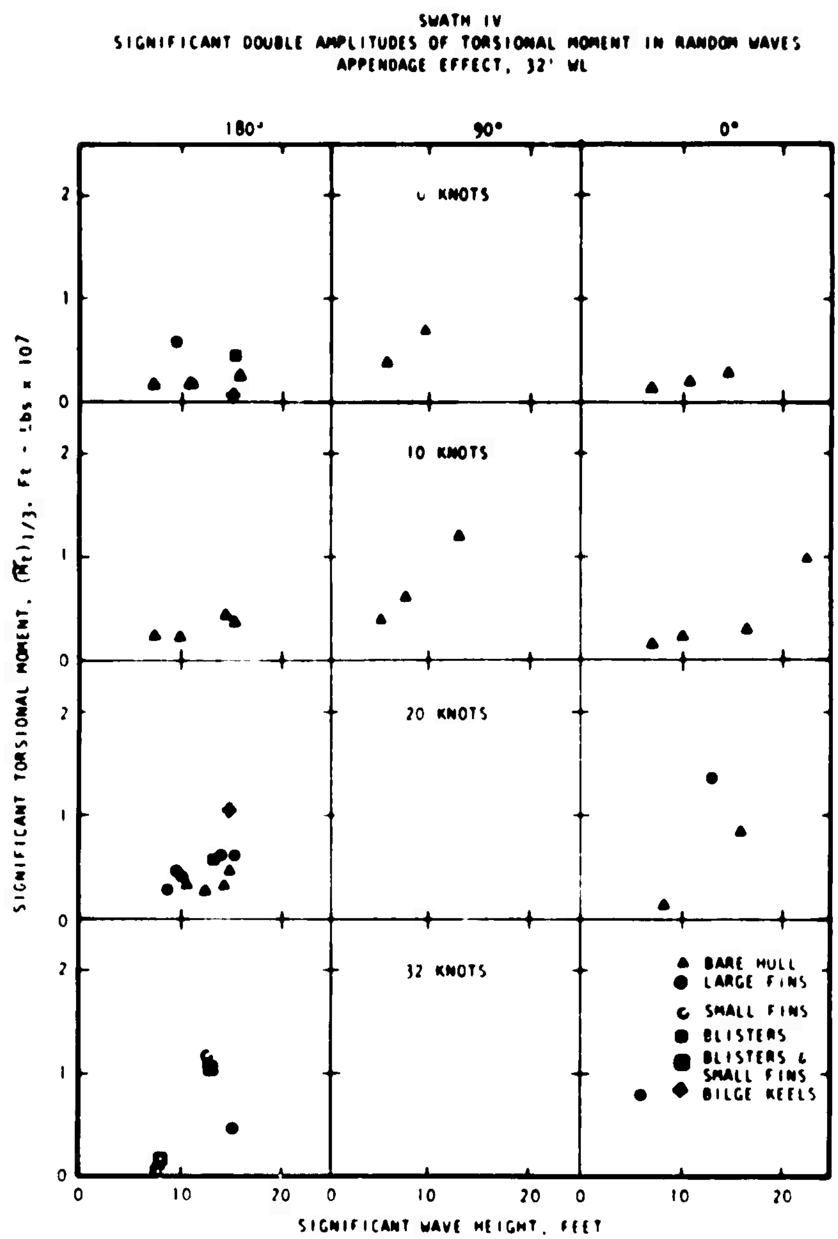

Figure 168 - Significant Double Amplitudes of Torsional Moment in Random Waves, 32 ft Draft, APPENDAGE EFFECT

SWATH IV
SIGNIFICANT DOUBLE AMPLITUDES OF YAW MOMENTS IN RANDOM WAVES
APPENDAGE EFFECT, 32' WL

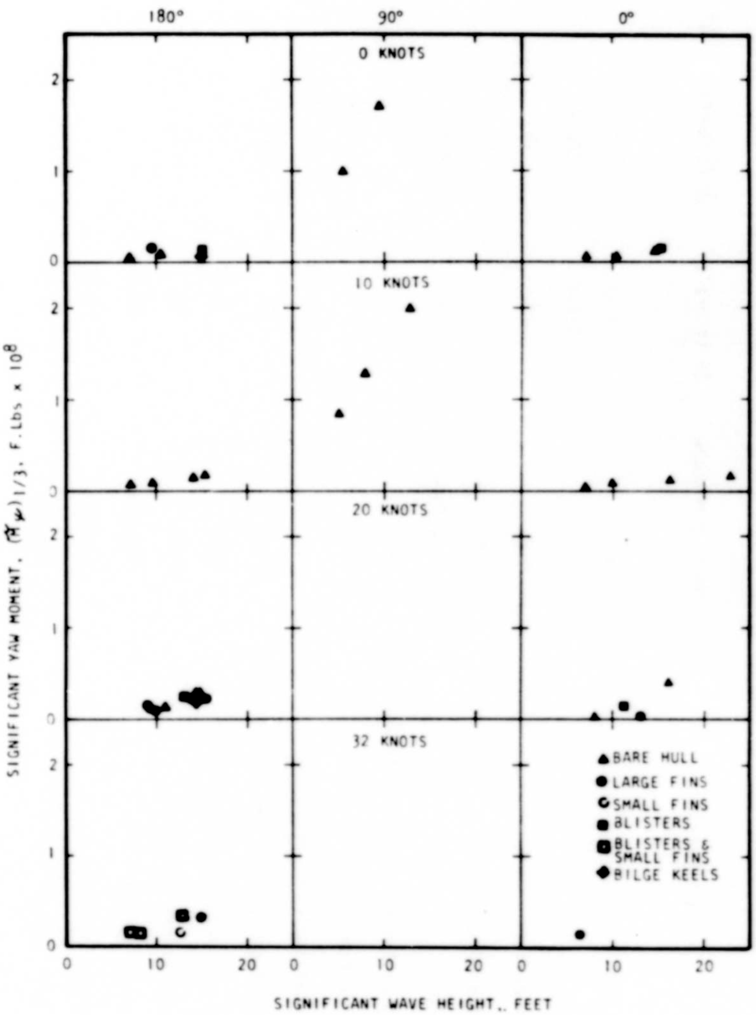

Figure 169 - Significant Double Amplitudes of Yaw Moment in Random Waves, 32 ft Draft, APPENDAGE EFFECT

TABLE 1

SWATH IV Ship Particulars - Bare Hull

Particular	Unit of Measure	28 ft Draft	30 ft Draft	32 ft Draft
Length (LOA)	Feet	287.6	287.6	287.6
Length (LWL)	Feet	226.7	226.7	226.7
Beam each Hull	Feet	18	18	18
Midship Maximum Breadth	Feet	93	93	93
Displacement	Long Tons	3960	4115	4270
Longitudinal Center of Gravity (Aft of FP)	Feet	110.5	110.9	110.7
Vertical Center of Gravity ($\overline{KG}$)	Feet	31.23	31.62	30.04
Longitudinal Radius of Gyration	-	0.233 LOA	0.237 LOA	0.226 LOA
Distance Between Centerlines at Station 10	Feet	75	75	75
Transverse Metacentric Height ($\overline{GM}_t$)	Feet	7.99	-	8.19
Bridging Structure Clearance	Feet	19	17	15
Natural Heave Period	Seconds	10.25		10.39
Natural Pitch Period	Seconds	16.21		16.21
Natural Roll Period	Seconds	17.95		18.20

TABLE 2

SWATH IV Ship Particulars - All Configurations

DRAFT Ft.	DISPLACEMENT Long Ton	CONFIGURATION	SHIP SPEED Knot	TRIM MOMENT Ft-Tons	LONGITUDINAL $\overline{CG}$ Aft of FP Ft.	VERTICAL $\overline{CG}$ Above BL Ft.	TRANSVERSE $\overline{GM}$ Ft.	LONGITUDINAL RADIUS of GYRATION Percent of LOA	NATURAL HEAVE PERIOD Sec.	NATURAL PITCH PERIOD Sec.	NATURAL ROLL PERIOD Sec.
28	3960	Bare Hull	0	0	110.5	31.23	7.99	23.3	10.25	16.21	17.95
		Nominal $\overline{GM}_t$	10	0	110.5	31.23	7.99	23.3	9.94	17.16	-
			20	1546	110.9	31.16	8.06	23.3	9.62	17.61	-
			32	5025	111.8	31.09	8.13	23.3	9.26	-	-
28	3960	Bare Hull	0	0	110.5	30.58	8.70	23.3	-	-	17.20
		Large $\overline{GM}_t$	10	0	110.5	30.58	8.70	23.3	-	-	-
			20	Not Run							
			32	Not Run							
30	4115	Bare Hull	0	Not Run							
		Nominal $\overline{GM}_t$	10	0	110.9	31.62	-	23.7	-	-	-
			20	1546	111.3	31.62	-	23.6	-	-	-
			32	5025	112.1	31.62	-	23.6	-	-	-
32	4270	Bare Hull	0	0	110.7	30.04	8.19	22.6	10.39	16.21	18.20
		Nominal $\overline{GM}_t$	10	0	110.7	30.04	8.19	22.6	10.16	17.04	-
			20	1546	111.1	30.04	8.19	22.5	-	-	-
			32	Not Run							
32	4270	Large Fin	0	0	110.7	30.04	-	22.6	10.57	16.80	20.46
			10	Not Run							
		-4° Fin Angle	20	1546	111.1	30.04	-	22.5	10.84	15.36	-
		+1.4° Fin Angle	32	5025	111.9	30.04	-	22.4	-	-	-
32	4270	Small Fin	0	Not Run					-	-	20.78
			10	Not Run							
			20	Not Run							
		+1.4° Fin Angle	32	5025	111.9	30.04	-	22.4	-	-	-
32	4270	Blisters	0	0	111.4	30.04	-	23.3	10.39	15.81	-
			10	Not Run							
			20	1546	111.8	30.26	-	23.2	9.71	18.07	-
		w/small fin	32	5025	112.6	30.26	-	23.2	-	-	-
32	4270	Bilge Keels	0	0	110.7	30.15	-	23.0	11.20	16.76	21.23
			10	Not Run							
			20	2190	111.2	30.15	-	23.0	-	-	-
			32	Not Run							

TABLE 3

Definition of SWATH IV Dimensionless Data Presentation Scheme

Motion or Load	Dimensionless Presentation
Heave	$\frac{\text{Heave Amplitude (ft)}}{\text{Wave Amplitude (ft)}}$
Relative Bow Motion (RBM)	$\frac{\text{Relative Bow Motion Amplitude (ft)}}{\text{Wave Amplitude (ft)}}$
Absolute Motion (AM)	$\frac{\text{Absolute Motion Amplitude (ft)}}{\text{Wave Amplitude (ft)}}$
Pitch	$\frac{\text{Pitch Amplitude (rad)} \times \text{Ship Length (ft)}}{2 \times \text{Wave Amplitude (ft)}}$
Roll	$\frac{\text{Roll Amplitude (radians)}}{\text{Wave Slope}}$ Wave Slope = $\frac{360 \text{ deg} \times \text{Wave Amplitude (ft)}}{\text{Wave Length (ft)}}$
Vertical Shear Force	$\frac{\text{Vertical Shear Force Amplitude (lb)}}{(\rho g)\ (A_w) \times \text{Wave Amplitude (ft)}}$
Transverse Force	$\frac{\text{Transverse Force Amplitude (lb)}}{(\rho g)\ (A_p) \times \text{Wave Amplitude (ft)}}$
Transverse Vertical Bending Moment	$\frac{\text{Transverse Vertical Bending Moment Amplitude (lb-ft)}}{(\rho g)\ (A_p)\ (d) \times \text{Wave Amplitude (ft)}}$
Torsional Moment	$\frac{\text{Torsional Moment Amplitude (lb-ft)}}{(\rho g)\ (L)\ (A_w) \times \text{Wave Amplitude (ft)}}$
Yaw Moment	$\frac{\text{Yaw Moment Amplitude (lb-ft)}}{(\rho g)\ (A_p)\ (L) \times \text{Wave Amplitude (ft)}}$

ρg = density of salt water, 64 lb/ft^3

A_w = waterplane area, 2684 ft^2

A_p = projected lateral area below the waterline
= 6760 ft^2 for 28 ft draft
7215 ft^2 for 30 ft draft
7670 ft^2 for 32 ft draft

d = distance from bending moment neutral axis to mid-draft
= 49 ft (Phase I), 46.6 ft (Phase II) for 28 ft draft
45.6 ft (Phase II) for 30 ft draft
47 ft (Phase I), 44.6 ft (Phase II) for 32 ft draft

L = Ship length, overall, 287.6 ft